DEPOSITION AND DIAGENESIS OF OLIGOCENE-LOWER MIOCENE SANDSTONES IN THE SOUTHERN MALAY BASIN

by

KHALID BIN NGAH

A thesis submitted for the degree of Doctor of Philosophy at the University of London and for the Diploma of Membership of the Imperial College of Science, Technology and Medicine.

Department of Geology,
Imperial College of Science,
Technology and Medicine,
London.

February, 1990.

ABSTRACT

This thesis describes the deposition and diagenesis of the Upper Oligocene-Lower Miocene petroleum reservoir sandstones in the southern Malay basin, Malaysia. The thesis is based on a study of 1980 line-km of seismic data, 350 metres of cores, and geological logs from 19 wells, in an area of approximately 18,600 square km. These data have been used to develop a predictive depositional and diagenetic model for the Pulai-II sandstones.

The Pulai-II sandstones were deposited in continental, transitional and marine environments during the early-stage opening of the Malay basin. Braided fluvial channel sandstones are the dominant facies and, together with near-shore barrier bar sandstones, they predominate in the northeast; whilst transitional deposits of distributary and tidal channel sandstones predominate in the southern part of the study area.

The reservoir quality is primarily the result of burial diagenesis, and is related to facies, depth of burial, temperature, hydrocarbon occurrences and structure. Dominant textural modifications are the destruction of primary porosity by the precipitation of authigenic minerals, primarily quartz and ferroan-calcite, and porosity enhancement by the dissolution of framework feldspars and chert. Up to 40 percent of the total porosity is believed to have been caused by the dissolution process, largely by percolating meteoric waters. Porosity values exceeding 45 percent have been recorded in the braided channel sandstones. Poor porosity is generally found in fine-grained sandstones, and in some medium to coarse-grained sandstones which are, or have been, buried deeper than 3000 metres.

The area which may provide the best hope for discovering additional hydrocarbons in the Pulai-II sandstones is in the northeast. The chances of finding liquid hydrocarbons in high-temperature areas are probably remote. The discontinuous nature of the sandstones in the south would additionally make the assessment of any discovery difficult.

ACKNOWLEDGEMENTS

I am very grateful to Dr. Abdul Aziz Mahmood, Vice President, E and P, PETRONAS, for allowing me to have access to the data which formed the basis of this research. I wish to thank Y. B. Dato' Dr. Abdullah Sanusi Ahmad, Vice President, HRM, PETRONAS, for granting me leave of absence to undertake this study.

I am also grateful to Mr. M. Yeldhem and Mr. M. J. Cox of BP Exploration, for arranging to use SEM and XRD facilities at BP Sunbury; to Mr. M. Hopkins for helping to run the XRD samples and to Ms. J. Huggett on the discussion of the XRD results.

I am also grateful to many people at ERICO, in particular Dr. P. Wigley, for providing many support and allowing me to use their computer facilities for log analyses and stratigraphic modelling.

To Professor R. Stoneley and Professor R. C. Selley, my supervisors, I wish to express my gratitude for their consistent guidance and constructive criticisms from the initial stage to the final phase of writting this thesis.

I wish to express thanks to all graduate students, Petroleum Geology Department for some fruitful discussions.

Finally, special thanks to my wife, Hasimah, and the four children: Jamsani, Jamsari, Jamzidi and Siti Hajar, who shared with me the best and worst of the three year stay in the United Kingdom.

CONTENTS

Chapter		*Page*
	Abstract	i
	Acknowledgements	iii
	List of illustrations	vii
1	Introduction	1
	1.1 General statement and location of study area	1
	1.2 Historical background	1
	1.3 Hydrocarbon occurrences	7
	1.4 Previous work	8
	1.5 Objectives of the study	14
2	Regional Setting	16
	2.1 The Malay basin	16
	2.2 Structures	18
	2.3 Stratigraphy	28
	2.3.1 Armitage-Viotti scheme	30
	2.3.2 Carigali scheme	30
	2.4 Age of sedimentary sequences in southern Malay basin	31
	2.5 Stratigraphic sequence under investigation	34
3	Methodology	36
	3.1 Data source	36
	3.2 Seismic data	36
	3.3 Well data	38
	3.4 Core data	40
	3.5 Methods of investigation	42
	3.6 Data treatment	43
	3.6.1 Seismics	43
	3.6.2 Geological logs	43
	3.6.3 Cores	44
	3.6.3.1 Core description	44
	3.6.3.2 Reservoir quality	44
	3.6.4 Temperature data	48
	3.7 Data analysis	49
	3.7.1 Seismics	49
	3.7.1.1 Seismic reflection-geological log correlation	50
	3.7.1.2 Seismic reflector mapping	51
	3.7.1.3 Map construction	54
	3.7.2 Facies	56
	3.7.2.1 Seismic facies	56
	3.7.2.2 Geological log motifs	61
	3.7.2.3 Log correlation	72
	3.7.2.4 Stratigraphic modelling	73

3.7.3 Pulai-II sandstones 74
3.7.3.1 Sandstone distribution 74
3.7.3.2 Sandstone quality 74
- Polarising Microscope 76
- XRD 77
- SEM 83
- Geological log 83
- Geothermal gradient 83
- Depth of burial 85

4 Facies Analysis 89

4.1 Introduction 89
4.2 Palaeontology 98
4.3 Facies of Pulai-II sandstones 98
4.3.1 Seismic facies 98
4.3.1.1 Red-Blue seismic sequence 98
4.3.1.1 Blue-Purple seismic sequence 108
4.3.2 Geological-Litholog facies 110
4.3.3 Lower Pulai Sandstone sequence 116
4.3.3.1 Characteristic features 116
4.3.3.2 Facies distribution 121
4.3.3.3 Facies and environments of deposition 121
4.3.4 Upper Pulai Sandstone sequence 125
4.3.4.1 Characteristic features 125
4.3.4.2 Facies distribution 132
4.3.4.3 Facies and environments of deposition 134
4.3.5 Lower Terengganu Shale sequence 136
4.3.5.1 Characteristic features 136
4.3.5.2 Facies distribution 139
4.3.5.3 Facies and environments of deposition 142
4.3.6 Upper Terengganu Shale sequence 147
4.3.6.1 Characteristic features 147
4.3.6.2 Facies interpretation and distribution 148
4.4 Seismic-litholog facies integration 148
4.5 Palaeogeography 150
4.5.1 Late Oligocene-Early Miocene 154
4.5.2 Early Early Miocene-late Early Miocene 155
4.6 Stratigraphic modelling 155

5 Petrography and Diagenesis 162

5.1 Introduction 162
5.2 Petrography 162
5.2.1 Sandstone composition 162
5.2.1.1 Framework quartz 163
5.2.1.2 Framework feldspar 169
5.2.1.3 Framework rock fragments 173
5.2.1.4 Other accessory framework minerals .. 173

5.2.2 Authigenic minerals 176
5.2.2.1 Authigenic quartz 188
5.2.2.2 Authigenic kaolinite 190
5.2.2.3 Authigenic illite and smectite-illite 192
5.2.2.4 Authigenic chlorite 199
5.2.2.5 Authigenic calcite and ferroan-calcite 201
5.2.2.6 Authigenic siderite and ankerite 205
5.2.2.7 Authigenic pyrite 205
5.2.2.8 Authigenic barytes 207
5.2.2.9 Authigenic albite 209
5.3 Paragenetic sequence 211
5.4 Porosity 215
5.5 Porosity distribution 226
5.5.1 East and northeastern region 228
5.5.2 South and southwestern region 230
5.6 Porosity destruction 233
5.6.1 Compaction 233
5.6.2 Cementation 239
5.7 Porosity enhancement 241

6 Findings and Conclusions 247

6.1 Findings 247
6.2 Conclusions 255
6.3 Future work 258

7 Selected Bibliography 260

List of Illustrations

Figure: *Page*

1-1 - Location map of the study area..... 2

1-2 - Map of sedimentary basins off the east coast of Peninsula Malaysia..... 3

1-3 - Location map of producing fields in the southern Malay basin..... 4

1-4 - Map of concession areas awarded to Esso and Conoco in 1968..... 5

1-5 - Tertiary basins of the northern Sunda shelf..... 9

1-6 - Stratigraphic nomenclature of Armitage-Viotti, southern Malay basin..... 11

1-7 - Alphabetical stratigraphic nomenclature of Esso, Malay basin..... 12

1-8 - Stratigraphic nomenclature of Carigali, southern Malay basin..... 13

2-1 - Basement structure map of the southern Malay basin..... 17

2-2 - Seismic section in the southern part of the study area, showing possible Gagau Group of Jurassic-Cretaceous age (J-C), which forms a part of the basement rocks..... 19

2-3 - Generalised cross-section along seismic line 68-38B.... 20

2-4 - Generalised cross-section along seismic line 68-145.... 21

2-5 - Structural map of the study area drawn on the Blue-seismic marker..... 23

2-6 - Seismic cross-section showing a fault, Fault A, believed to have been formed initially as growth fault, but which later became reverse fault..... 24

2-7 - Seismic cross-section showing anticlinal feature believed to have been related to deep-seated "shale" diapirism..... 25

2-8 - Seismic cross-section showing faulted anticlinal feature believed to have been formed by reverse fault movement..... 26

2-9 - Generalised cross-section along seismic line 68-34A.... 27

2-10 - Composite stratigraphic schemes of the study area..... 29

2-11 - Chrono-stratigraphy of five wells in the study area.... 33

2-12 - Stratigraphic nomenclature used in this study..... 35

3-1 - Seismic and well location map of the study area..... 37

3-2 - An illustration of seismic data processed at different time: a) processed in 1968, and (b) reprocessed in 1987..... 39

3-3 - Well profiles showing relative positions of cores taken in Pulai-II Formation..... 41

3-4 - Synthetic seismogram for Ophir-1 showing correlation of main stratal surfaces..... 52

3-5 - A typical correlation of seismic data with well data... 53

3-6 - Depth conversion curve used to convert TWT in seconds, to depth in metres..... 55

3-7 - A comparative illustration of seismic characters between a) original paper print and b) lateral "squeezing" of same by about 50 percent..... 58

3-8 - Type I seismic facies..... 59

3-9 - Type II seismic facies..... 60

3-10 - Type III seismic facies..... 62

3-11 - Type IV seismic facies..... 63

3-12 - Gamma-ray and S.P. logs of Belumut-1 displaying suspect gamma-ray reading in upper section of the sandstones... 64

3-13 - Gamma-ray log motifs to indicate clastic lithofacies... 65

3-14 - An illustration to determinate net sandstone in a sandstone-shale sequence..... 66

3-15 - Vertical grain size evolution in sandstones as indicators of environments of deposition..... 68

3-16 - Some examples of log motifs as indicators of facies and environments of deposition..... 69

3-17 - Three basic log motifs of sandstones..... 70

3-18 - A display of four gamma-ray log motifs of Pulai-II Formation..... 71

3-19 - An illustration of resultant stratigraphic model..... 75

3-20 - XRD spectrum of whole rock sample from Pulai-I..... 78

3-21 - XRD spectrum of whole rock sample from Besar-1..... 79

3-22 - XRD spectra of clay-sized fraction from Pulai-I..... 81

3-23 - XRD spectra of clay-sized fraction from Besar-1..... 82

3-24 - Average temperature gradient of the study area..... 84

3-25 - Shale compaction trend at Banggol-1..... 87

3-26 - An illustration to determine maximum depths of sediment burial..... 88

4-1 - Thin calcareous siltstone bed within generally shale interval..... 90

4-2 - Thin calcareous layer within generally massive sandstone unit..... 91

4-3 - Calcareous layers enveloping thick and massive sandstone unit..... 92

4-4 - Regional seismic cross-sections along line 68-26 (Section A-A') and line 68-38B (Section B-B')..... 93

4-5 - Regional seismic cross-sections along line 68-121 (Section C-C') and line 68-145 (Section D-D')..... 94

4-6 - Isopach map of B-P seismic sequence (Pulai Sandstones). 95

4-7 - Isopach map of R-B seismic sequence (Terengganu Shales)..... 96

4-8 - Map of R-B sequence showing seismic reflection configuration and distribution of seismic facies within the sequence in the study area..... 99

4-9 - Convergent seismic configuration and onlapping transgressive-regressive units of Type III within the R-B seismic sequence..... 100

4-10 - Downlapping seismic configuration, and related seismic facies of Type II within the R-B and B-P seismic sequences..... 102

4-11 - Stratigraphic cross-section along Angsi-Tapis-Palas-Banggol..... 103

4-12 - Stratigraphic cross-section along Tapis-Tiong-Bekok-Seligi-Pulai-Belanga..... 104

4-13 - Stratigraphic cross-section along Duyong-Ophir-Seligi-Tinggi-Peta..... 105

4-14 - Stratigraphic cross-section along Angsi-Besar-Duyong..... 106

4-15 - Stratigraphic cross-section along Sotong-Duyong Barat-Duyong..... 107

4-16 - Map of Blue-Purple sequence showing seismic reflection configuration and the distribution of seismic facies within the sequence in the study area..... 109

4-17 - Gamma-ray-resistivity log facies distribution map of Upper Terengganu Shales..... 111

4-18 - Gamma-ray-resistivity log facies distribution map of Lower Terengganu Shales..... 113

4-19 - Gamma-ray-resistivity log facies distribution map of Upper Pulai Sandstones..... 114

4-20 - Gamma-ray-resistivity log facies distribution map of Lower Pulai Sandstones..... 115

4-21 - Log responses and core description of facies in Lower Pulai Sandstones at Pulai-1..... 118

4-22 - Log responses and core description of facies in Lower Pulai Sandstones at Duyong 6H-32.1..... 119

4-23 - Log responses and core description of facies in Lower Pulai Sandstones at Sotong 5G-5.1..... 120

4-24 - Net sandstone map of Lower Pulai Sandstone sequence.... 122

4-25 - Log responses and core description of facies in Upper Pulai Sandstones at Seligi-3..... 127

4-26 - Log responses and core description of facies in Upper Pulai Sandstones at Pulai-1..... 128

4-27 - Log responses and core description of facies in Upper Pulai Sandstones at Besar-1..... 129

4-28 - Log responses and core description of facies in Upper

Pulai Sandstones at Angsi-1..... 130

4-29 - Log responses and core description of facies in Upper Pulai Sandstones at Sotong 5G-5.1..... 131

4-30 - Net sandstone map of Upper Pulai Sandstone sequence.... 133

4-31 - Log responses and core description of facies in Lower Terengganu Shales at Bekok-1..... 138

4-32 - Log responses and core description of facies in Lower Terengganu Shales at Seligi-3..... 140

4-33 - Log responses and core description of facies in Lower Terengganu Shales at Sotong 5G-5.1..... 141

4-34 - Net sandstone map of Lower Terengganu Shale sequence... 143

4-35 - Dipmeter log motif within sediments of Lower Terengganu Shales at Ledang-1..... 145

4-36 - Log responses and core description of facies within Lower Terengganu Shales at Tinggi-1..... 146

4-37 - Net sandstone map of Upper Terengganu Shale sequence... 149

4-38 - Geoseismic cross section along line 68-50, showing facies of Pulai-II Formation..... 151

4-39 - Geoseismic cross section along line 68-128, showing facies of Pulai-II Formation..... 152

4-40 - Generated stratigraphic model through Tapis, Palas and Banggol wells..... 156

4-41 - Generated stratigraphic model through Ophir, Bekok, Tiong and Palas wells..... 157

4-42 - Generated stratigraphic model through Bekok, Seligi, Tinggi and Belumut wells..... 158

4-43 - Comparative illustration of a section of seismic section along line 68-121, and generated seismic model along Section A..... 160

5-1 - Average sandstone composition, Pulai-II Formation..... 166

5-2 - Sandstone compositions in a) Motif A, b) Motif C and c) Motif D..... 167

5-3 - Sandstone compositions in a) Pulai Sandstone Member and b) Terengganu Shale Member..... 168

5-4 - Clay mineral compositions in Pulai II sandstones at different well locations..... 186

5-5 - Clay mineral composition in sandstones of a) Motif A, b) Motif C and c) Motif D..... 187

5-6 - EDAX spectra of ferroan-calcite showing relative intensity of Fe with respect to Ca peaks, taken at two separate locations on a "calcite" crystal..... 204

5-7 - Paragenetic sequence of authigenic minerals in Pulai-II sandstones..... 212

5-8 - Concentration of carboxylic acids in oil-field waters verses temperature..... 214

5-9 - An illustration showing relationship of total porosity with total cement..... 219

5-10 - An illustration showing relationship of total porosity with total carbonate minerals in sandstones of different textures..... 220

5-11 - An illustration showing relationship of total porosity with total clay minerals in sandstones of different textures..... 221

5-12 - An illustration showing relationship of total porosity with kaolinite/total clay minerals in sandstones of different textures..... 223

5-13 - An illustration showing relationship of total porosity with smectite-illite/total clay minerals in sandstones of different textures..... 224

5-14 - Average porosity-depth trend in Pulai-II sandstones..... 225

5-15 - Porosity distribution in Pulai-II sandstones, southern Malay basin..... 227

5-16 - Porosity-depth trend in Motif A sandstones at different well locations..... 229

5-17 - Porosity-depth relationship in Motif D sandstones at different well locations..... 231

5-18 - Porosity-depth relationship in Pulai-II sandstones at a) Tapis -2 and b) Tiong-5..... 234

5-19 - Depth-velocity plot at Tapis-2..... 235

5-20 - Depth-velocity plot at Tiong-5..... 236

5-21 - Schmetic cross-section through Tapis-2, Tiong-5, Pulai-1 and Belanga-1 illustrating present-day and palaeo settings and the relative amounts of overburden removed during late Late Oligocene to Early Miocene and Late Miocene..... 237

5-22 - Geothermal gradient map of the study area..... 238

5-23 - Depth-porosity-temperature diagram illustrating loss in porosity is related to increase in depth and temperature..... 240

5-24 - Average formation temperature map, Pulai-II sandstones. 242

5-25 - Water salinity (ppm total chloride) map in Pulai-II sandstones, incorporating temperature and structural data..... 243

Plates

5-1 - Microphotograph of thin section showing framework grain composition of the Pulai-II sandstones..... 164

5-2 - Microphotograph of thin section showing framework grains cemented by calcite (Ca)..... 164

5-3 - SEM microphotograph of pore-filling calcite (Ca), smectite-illite (SI) and overgrowth quartz (OV)..... 165

5-4 - SEM microphotograph showing well-developed quartz overgrowth (OV) and kaolinite crystals (K)..... 165

5-5 - Microphotograph of thin section showing corrugated framework quartz (FQ) virtually floating in pore spaces (PS)..... 170

5-6 - Microphotograph of thin section showing closely packed framework grains: quartz (FQ), chert (FC) and highly altered feldspar grains (F)..... 170

5-7 - SEM microphotograph showing pitted surface on framework quartz..... 171

5-8 - SEM microphotograph showing pitted surface on framework quartz..... 171

5-9 - Microphotograph of thin section showing enlarged pores (Oo) and almost completely dissolved plagioclase framework grain (AP) rimmed by brownish material..... 172

5-10 - SEM microphotograph showing albite (Al) and illite (I) as by-products of plagioclase alteration..... 172

5-11 - SEM microphotograph showing albite overgrowth (AO) on plagioclase grain..... 174

5-12 - SEM microphotograph showing partially dissolved K-feldspar framework grain..... 174

5-13 - Microphotograph of thin section showing partially dissolved chert framework grain (C), encased partially by brownish material..... 175

5-14 - Microphotograph of thin section showing drusy authigenic quartz overgrowth on lithic grain (L)..... 177

5-15 - SEM microphotograph showing quartz overgrowth (OV) on feldspar framework grain (F)..... 177

5-16 - SEM microphotograph showing barytes overgrowth (BO) on feldspar (?) framework grain..... 178

5-17 - SEM microphotograph showing kaolinite "booklets" (KB) and quartz overgrowth (OV)..... 178

5-18 - SEM microphotograph showing smectite-illite (SL) and quartz overgrowth (OV)..... 179

5-19 - SEM microphotograph showing illite (IL) and quartz overgrowth (OV)..... 179

5-20 - SEM microphotograph showing idiomorphic chlorite (Ch).. 180

5-21 - Microphotograph of thin section showing siderite rhombs (S) rimming pore walls..... 180

5-22 - Microphotograph of thin section showing ankerite clusters (AN) within generally very fine grained sandstones..... 181

5-23 - SEM microphotograph showing framboid pyrite (PY)..... 181

5-24 - SEM microphotograph showing euhedral quartz druse (QS) settling on chlorite (Ch) coated framework grain..... 189

5-25 - SEM microphotograph showing authigenic quartz (OV) overgrowing on illite (IL) coated framework grain..... 191

5-26 - SEM microphotograph showing interlocking syntaxial quartz overgrowth..... 191

5-27 - SEM microphotograph showing 1-3 micron kaolinite "booklets" (KA), in association with altered K-feldspar (AK)..... 193

5-28 - SEM microphotograph showing 5-10 micron kaolinite "booklets" (KA), on smectite-illite (SL) coated framework grain..... 193

5-29 - SEM microphotograph of accordian-like kaolinite vermicules..... 194

5-30 - SEM microphotograph of fractured framework quartz grain (FQ), showing illitic line (L) around the framework grain..... 196

5-31 - SEM microphotograph of whiskery illite (IL)..... 196

5-32 - SEM microphotograph of bridging illite (IL)..... 197

5-33 - SEM microphotograph of illite (IL)..... 197

5-34 - SEM microphotograph of illite (IL)..... 198

5-35 - SEM microphotograph of chlorite (Ch)..... 200

5-36 - Microphotograph of thin section showing calcite (Ca) within generally very fine grained sandstone..... 202

5-37 - Microphotograph of thin section showing calcite (Ca) within generally medium grained sandstone..... 202

5-38 - SEM microphotograph of intertwinning siderite (Sd)..... 203

5-39 - SEM microphotograph showing the locations on the calcite crystal, which have been determined for basic elemental compositions..... 206

5-40 - SEM microphotograph of framboid pyrite (Py) pore-filling the pore space..... 206

5-41 - SEM microphotograph of cubic pyrite (Py) pore-filling the pore space..... 208

5-42 - SEM microphotograph showing development of overgrowths: barytes (Ba) and quartz (OV)..... 208

5-43 - SEM microphotograph of albite overgrowth (Al)..... 210

5-44 - SEM microphotograph showing intergranular, primary porosity (PS)..... 217

5-45 - Microphotograph of thin section showing pores (Ps) caused by dissolution of unstable framework grains..... 217

5-46 - Microphotograph of SEM showing additional porosity to the sandstone caused by partial dissolution of framework feldspar garin (AF)..... 218

5-47 - Microphotograph of thin section showing intragranular pores caused by grain fracturing (Psf)..... 218

Table

3-1 - Depths of Red, Blue and Purple seismic markers at 18 well locations..... 56

3-2 - Selected D-spacings of some common minerals present in the Pulai-II sandstones, and their respective weightage used in semi-quantification..... 80

5-1 - Sandstone composition from XRD analyses..... 182

5-2 - Relative composition of clay and carbonate minerals in some sandstones..... 184

5-3 - Compute porosity of the Pulai-II sandstones at 18 well locations..... 230

5-4 - Pressure and temperature data in Pulai-II sandstones... 232

5-5 - Estimated maximum depths of burial of the Pulai-II sandstones at 16 well locations..... 239

1. INTRODUCTION

1.1 *GENERAL STATEMENT AND LOCATION OF STUDY AREA*

The main aim of this study is to enhance the understanding of hydrocarbon occurrences within the Upper Oligocene-Lower Miocene sandstones in the southern end of the Malay basin, Malaysia. This thesis provides a comprehensive synthesis of reservoir development in the Pulai-II sandstones in the area.

The study area is located off the east coast of Peninsular Malaysia (Fig. 1-1). It is situated some 160 km from Kuala Terengganu, a township in the state of Terengganu. The area is bounded by latitudes 4° 50' N and 6° 00' N and longitudes 104° 30' E and 105° 50' E, and has an area of about 16,800 square km. It covers partly or wholely five Production Sharing Contract (PSC) areas which are held currently by Esso, Carigali, and Japex-Taiyo Oil Company. The area is in the southeastern corner of the Malay basin (Fig. 1-2), within which are found producing oil and gas fields of the Peninsula (Fig. 1-3).

1.2 *HISTORICAL BACKGROUND*

Although exploration for hydrocarbons in Malaysia started about 100 years ago, beginning with the drilling of some land wells by Anglo-Saxon Petroleum Company in the state of Sarawak between 1888-1907, the exploration activities in the states of Peninsular Malaysia began only recently. In 1968, the government of Malaysia offered hydrocarbon exploration and exploitation rights in the offshore area of the Peninsula facing the South China Sea to two companies: Esso and Conoco (Fig. 1-4). The area to the north of 5°N latitude and extending from the

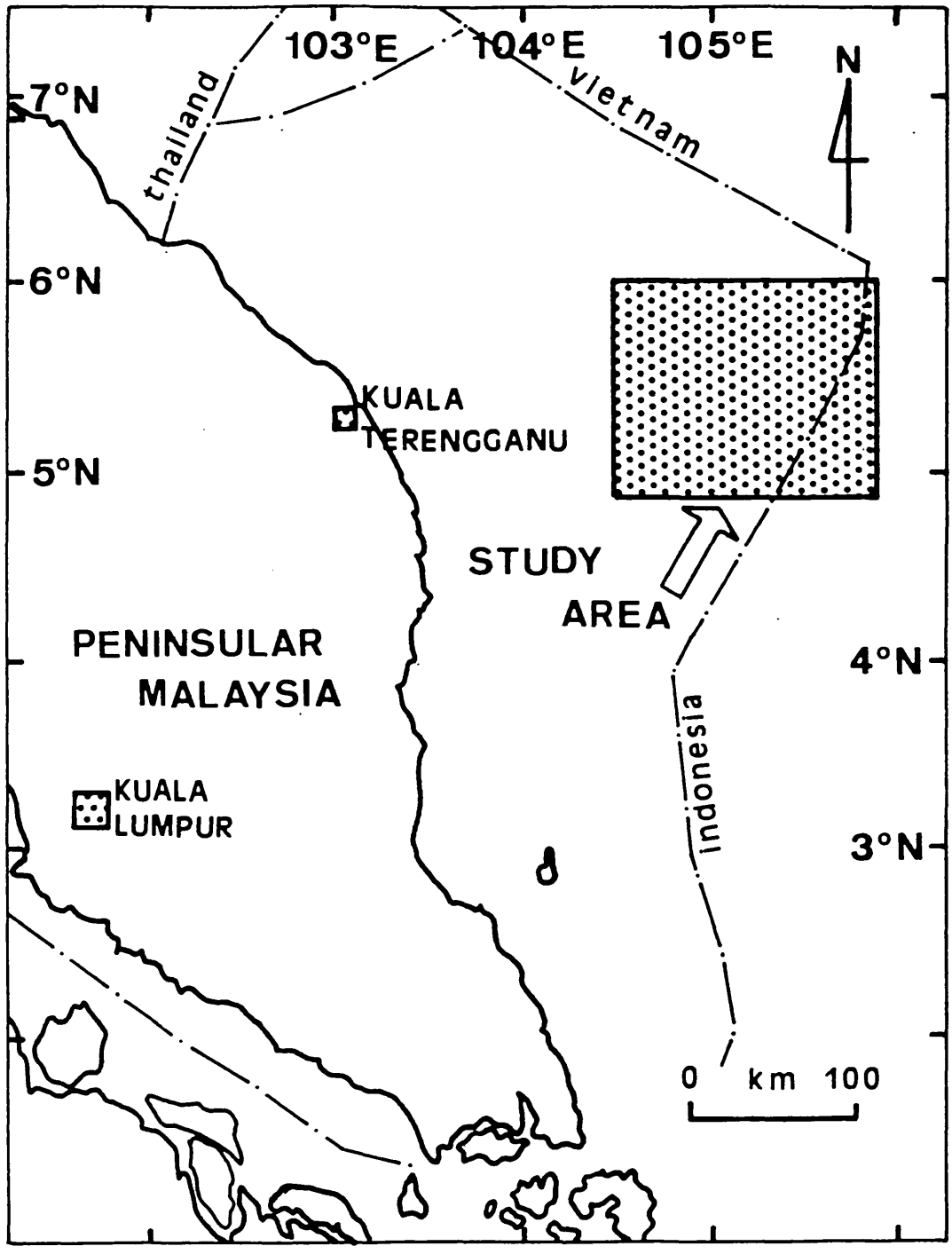


Figure 1-1 - Location map of the study area.

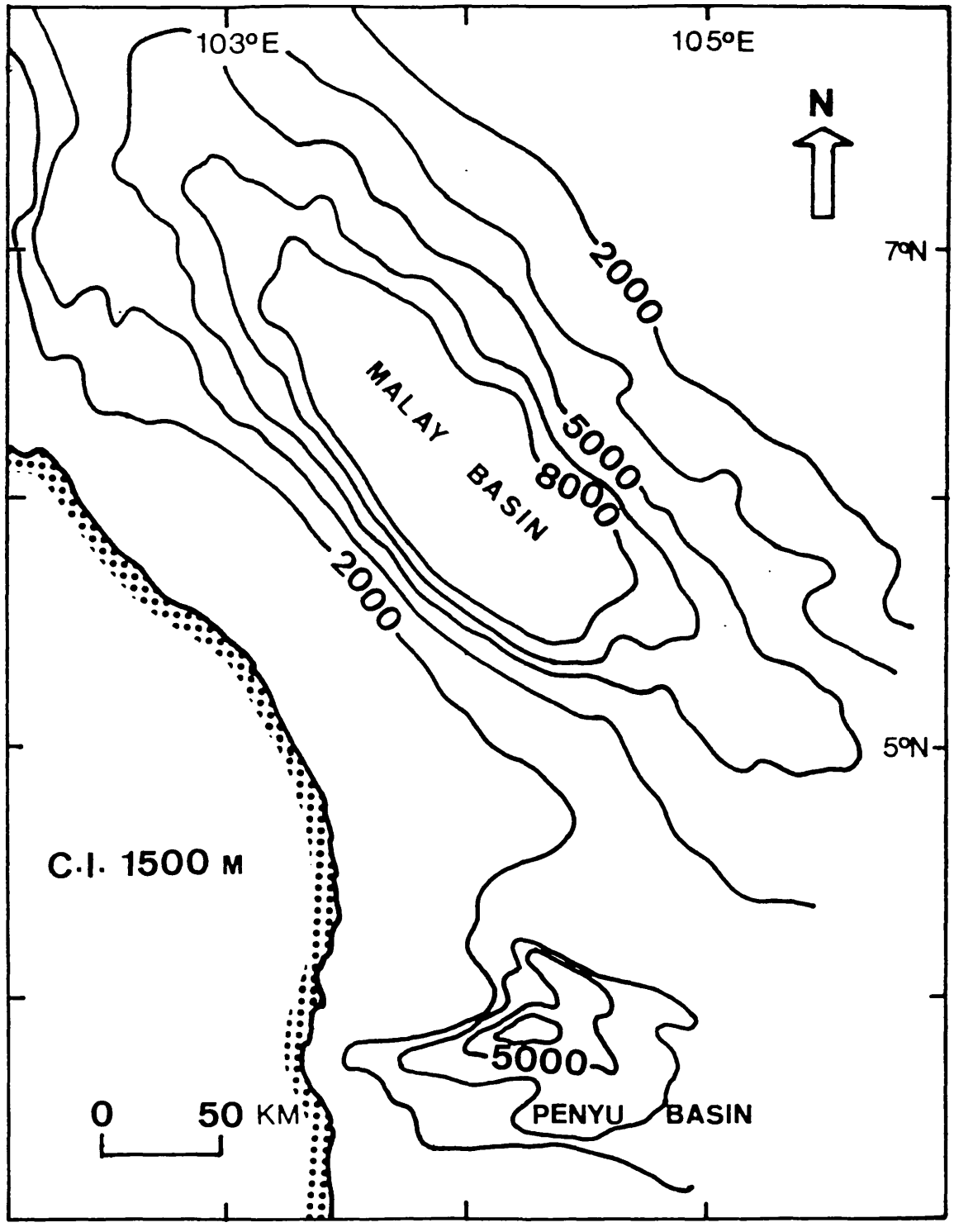


Figure 1-2 - Map of sedimentary basins off the east coast of Peninsular Malaysia, showing the Malay and Penyu basins (modified after Esso, 1976; Ngah, 1975). Contours in metres.

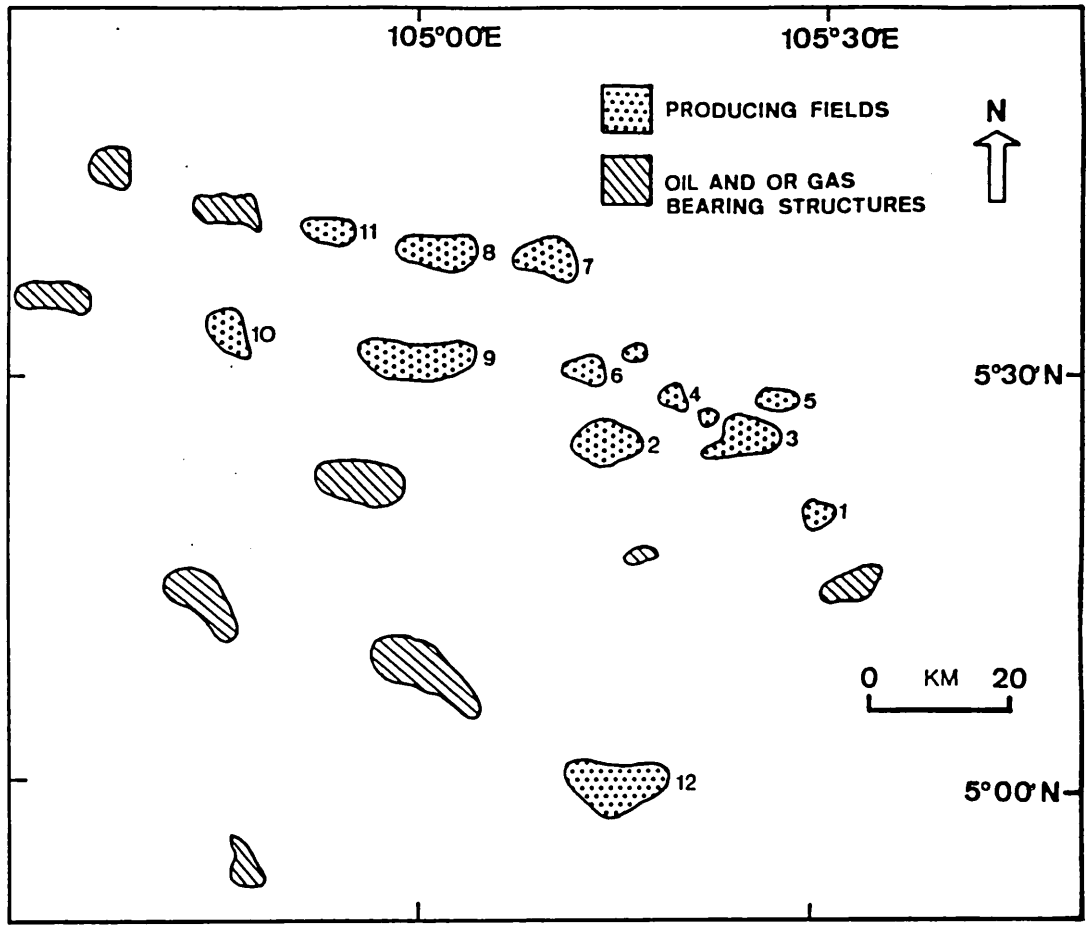


Figure 1-3 - Location map of producing fields in the southern Malay basin: 1-Pulai; 2-Bekok; 3-Seligi; 4-Kepong; 5-Tinggi; 6-Tiong; 7-Palas; 8-Guntong; 9-Tapis; 10-Irong Barat; 11-Tabu and 12-Duyong. Pulai, Bekok, Seligi, Kepong and Tinggi are producing oil and gas from Pulai and Tapis Formations; Tiong, Palas, Guntong, Tapis, Ir. Barat, Tabu and Duyong from Tapis and Bekok Formations.

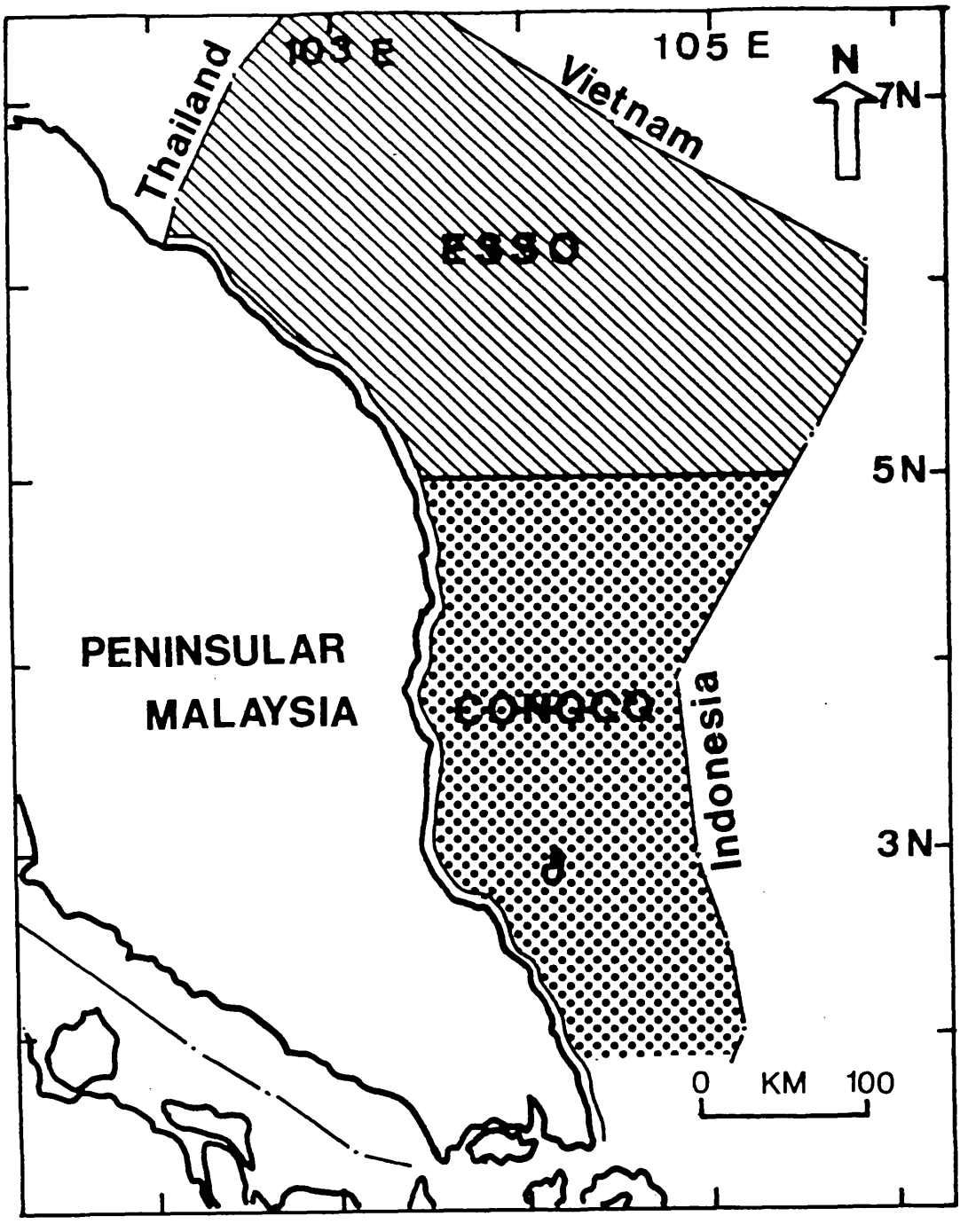


Figure 1-4 - Map of concession areas awarded to Esso and Conoco in 1968.

coast to the international boundaries between Malaysia-Indonesia and Malaysia-Vietman, was offered to Esso, and the area to the south of 5°N latitude and extending from the coast to the Malaysian-Indonesian boundary, to Conoco.

Both companies conducted active exploration campaigns, and prior to 1975 when the government introduced an oil profit sharing legislation based on the Indonesian production sharing experience, they have acquired more than 30,000 line-km of seismics and drilled a total of 47 exploration wells.

Esso signed a PSC agreement with PETRONAS, the national oil company of Malaysia, in 1976, but with Conoco, negotiations in the subsequent year failed to materialise, and in 1977, Conoco transferred its exploration and exploitation rights to Petronas Carigali Sendirian Berhad (Carigali), a wholly-owned subsidiary of PETRONAS, for an undisclosed amount.

In 1985, the government revised the terms of the PSC to encourage participation by other oil companies to explore for hydrocarbons in the country. Since the introduction of the new formula, 27 new PSCs had already been signed.

During the past 20 years of exploration in the Malay basin (Fig. 1-2), more than 60,000 line-km of seismic data have been acquired and processed, and 130 exploration wells drilled. These exploration activities have resulted in the discovery of many oil and gas fields. Although only one gas structure is currently under production, and a few others await approval, most major oil discoveries are now being developed and some are in various stages of development.

Both oil and gas are produced primarily from the sandstones of Late Oligocene to Late Miocene age. In the south and southeastern areas of the Malay basin (Fig. 1-2), oil and gas are produced primarily from the Upper Oligocene-Lower Miocene sandstones. In the north and northwestern areas, the hydrocarbon bearing reservoirs are the sandstones of Middle to Late Miocene age. The Upper Oligocene-Lower Miocene sandstones in the south and southeastern part of the basin form the subject of this investigation, the results of which are presented in this thesis.

1.3 *HYDROCARBON OCCURRENCES*

Hydrocarbons in the Malay basin have been found to occur in sandstones of the Oligocene-Miocene sequence, but primarily in the sandstones of Late Oligocene to Late Miocene age. In the study area, the primary hydrocarbon bearing sandstones are from the Bekok (Unit IVA), Tapis (Unit III) and Pulai (Unit IIB-IIA upper) Formations of Late Oligocene-Middle Miocene age. Of the twelve producing fields in the area (Fig. 1-3), only five: Pulai, Bekok, Seligi, Kepong and Tinggi are producing hydrocarbons from the Tapis (Unit III) and Pulai (Unit IIB-IIA upper) Formations at depths between 1200 and 2200 metres. The others are producing hydrocarbons from the Bekok (Unit IVA) and Tapis (Unit III) Formations at depths between 1500 to 2000 meters. Hydrocarbons have also been found in the Bekok Formation (Unit IVA) and the Seligi Formation (Unit IIA lower) at Sotong, Duyong, Besar, Angsi, Ophir and Ledang. At Sotong, a significant hydrocarbon accumulation was found in the Pulai Formation (Unit II) at depths of 2000 to 2500 metres.

1.4 *PREVIOUS WORK*

Prior to 1968 the offshore area of Peninsular Malaysia was virtually unknown, but with the participation of Esso and Conoco exploring for hydrocarbons in the region beginning in 1968, and the participation by government bodies and institutions in subsequent years, a great deal of information is now available. However, much of this information remains with the companies which hold the exploration and exploitation rights, and the government. What is now known of the area is based on selective releases by the companies of data of general interest, and on the work of international institutions.

Early work of Parke et al (1971) and Pupilli (1973) focused on the descriptions and tectonics of the South China Sea, and discussed, in general, the structural styles and tectonic evolution of the region. In the discussions, they indicated the importance of both extensional and compressional stresses in the development of the basins, and proposed that the basins were formed during Late Cretaceous-Early Eocene.

Hutchison (1973) and Hamilton (1979) considered the creation of the Gulf of Thailand (Pattani), Malay, Penyu and the West Natuna basins (Fig. 1-5), and other basins in the South China Sea, as being the results of the interaction of stresses acting on two opposite sides of the Sunda micro-plate. They believed that the stresses were caused by:

1) The collision of the Indian and Eurasian plates, and

2) The opening of the South China Sea through sea-floor spreading.

The net effect of these stresses on the Sunda plate, which was being "sandwiched" by the northward motion of the Indian plate on the west and

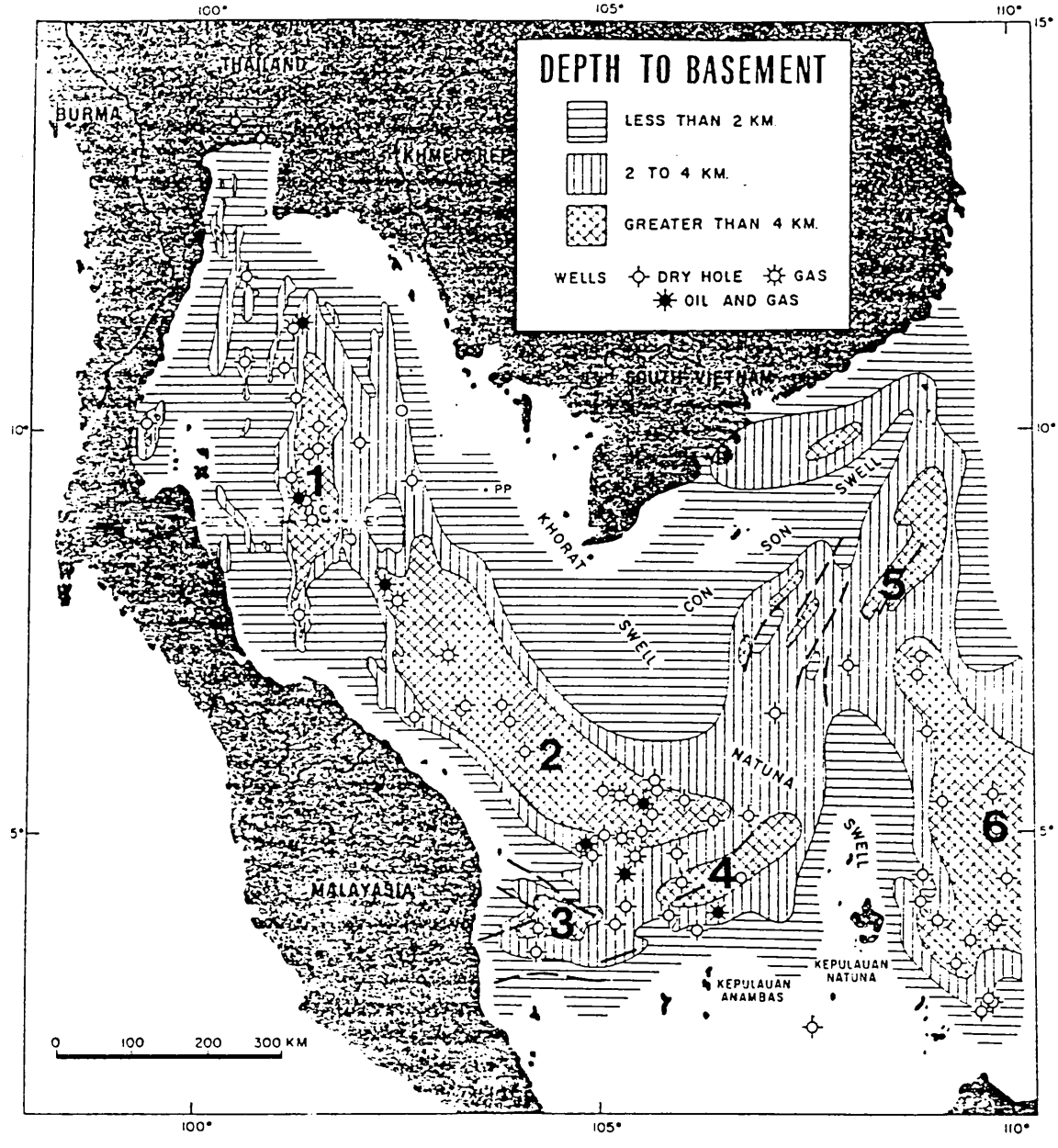


Figure 1-5 - Tertiary basins of the northern Sunda shelf: 1-Gulf of Thailand (Pattani); 2- Malay; 3-Penyu; 4-Natuna; 5-Vietnam and 6-Sarawak) (after Paul, L.,1975).

south, and on the east by the southward motion of the South China Sea sea-floor and the Borneo landmass, was that the plate was slightly rotated clockwise, elevated, arched and domed. Because arching created extensional stresses within the crustal landmass, it eventually fractured to form grabens and half-grabens.

Tapponier et al (1982) suggested an alternative mechanism for the crustal buckling and fracturing in some areas of eastern Asia. Based on the experimental work on plasticine models, they proposed that extrusive tectonics was responsible for initiating crustal buckling, arching and eventual fracturing.

On the stratigraphy of the region, Senathirajah (1969) noted the occurrences of undisturbed Jurassic-Cretaceous sediments on Peninsular Malaysia, and Haile (1970, 1973) reported on the occurrences of unmetamorphosed Tertiary sediments in the offshore islands of Anambas and Natuna. But it was Armitage and Viotti (1977) who formally proposed the stratigraphy of the Malay basin (Fig. 1-6). Prior to their work Esso used an informal alphabetical nomenclature to describe the stratigraphy of the basin (Fig. 1-7). This nomenclature, which was referred to by the ASCOPE Committee meeting at Bangkok, 1981, was developed on the basis of seismic sequence analysis.

Carigali (1986) considered that neither Armitage-Viotti's stratigraphic proposal, nor Esso's alphabetical nomenclature, was suitable for application, at least in its areas of operations. (These areas constitute parts of the concession areas held by Esso and Conoco prior to their relinquishment in 1976). Consequently, a new nomenclature was proposed (Fig. 1-8).

Figure 1-6 - Stratigraphic nomenclature of Armitage-Viotti, southern Malay basin (1977).

AGE	FORMATION	MEMBER
Recent-Pliocene	Pilong	-
Miocene	Bekok	
	Tapis	Upper Shale
		Lower Sandstone
	Pulai	Upper Shale
		Lower Sandstone
	Seligi	Upper Shale
		Lower Sandstone
	Ledang	Upper Shale
		Lower Sandstone
	Telukbutan	Upper Shale
		Lower Sandstone
Oligocene	Semala	Upper Shale
		Lower Sandstone
	Sambas and Undifferentiated Complex	
Cretaceous and Older	Metasediments and igneous rocks	

Figure 1-7 - Alphabetical stratigraphic nomenclature of Esso, Malay basin (1976).

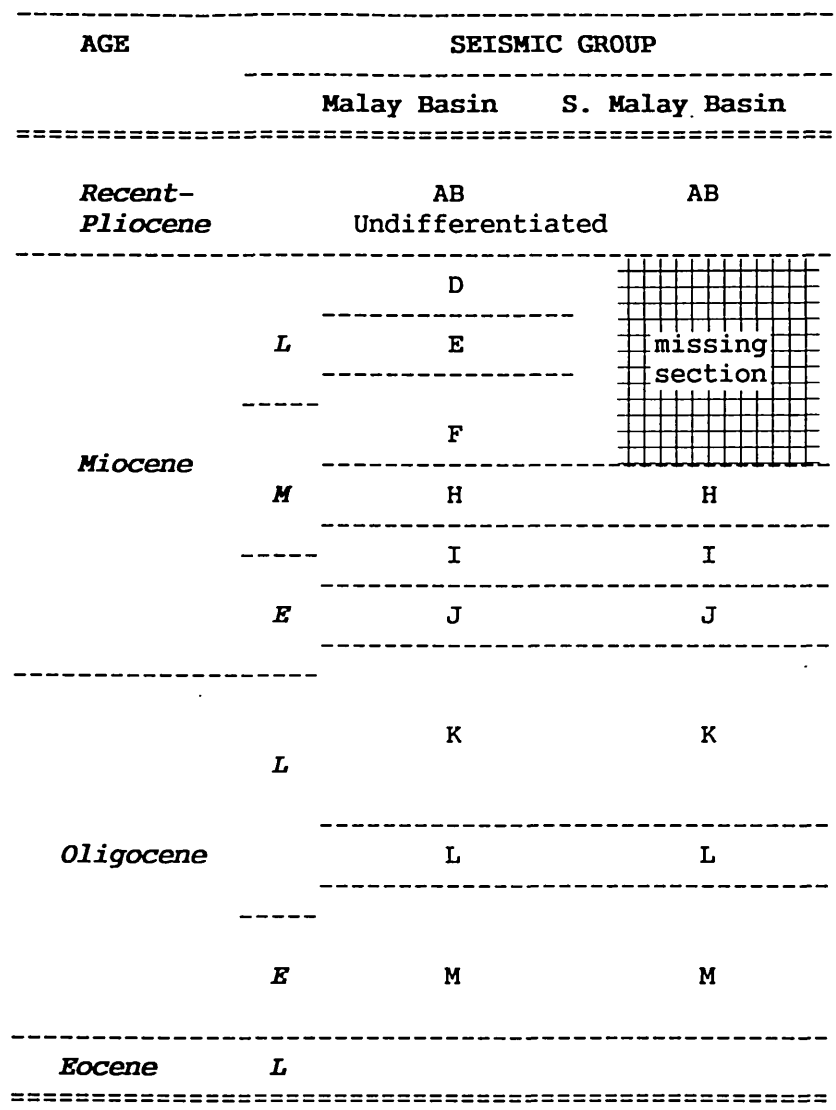
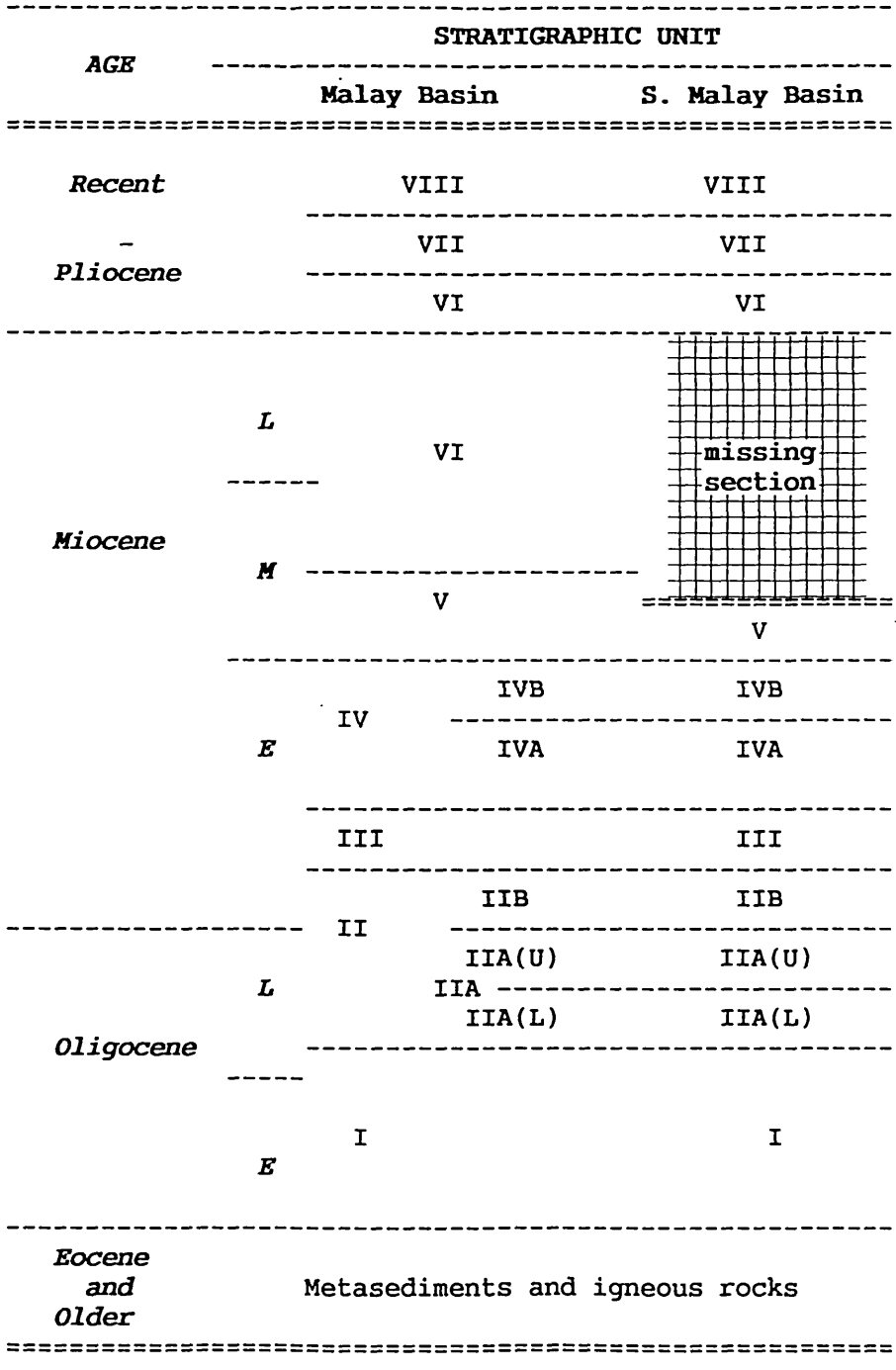


Figure 1-8 - Stratigraphic nomenclature of Carigali, southern Malay basin (1986).



Nik Ramli (1988) conducted some study of the Oligocene-Miocene sandstones in some parts of the study area, and concluded that the sandstones were deposited on fan delta systems.

Rashidah et al (1988) discussed the general significance of foraminifera assemblages found in the wells in the southern part of the basin, and indicated their limitations in the chrono-stratigraphic subdivision of the sedimentary sequence in the basin. They used instead nannofossils and palynomorphs as tools for their chronological work.

1.5 *OBJECTIVES OF THE STUDY*

Limited information is available on the characterization of the sandstones of the study area. Although Nik Ramli (1988) had studied the productive Pulai and Tapis sandstones at some selected localities in the area in some detail, much is yet to be learnt of their regional distribution, reservoir quality and, most importantly, their additional potential to contain hydrocarbons.

When examining the distribution of the commercially significant occurrences of the hydrocarbon accumulations in the Pulai Formation (Unit IIB-IIA upper) (Fig. 1-3), two general questions emerged:

1) Why accumulations of significant sizes were found to be concentrated in a relatively small area of the northeast of the study area, and

2) Could significant hydrocarbon accumulations be present elsewhere in the study area and in the deeper parts of the basin?

This study attempts to unravel these mysteries. In order to achieve this objective, it was necessary to examine and evaluate the sandstones on a regional scale by undertaking the following investigations:

1) To map the Pulai Formation (Unit IIB-IIA upper) and to determine its stratigraphic framework,

2) To predict its regional distribution and to determine its reservoir quality, and

3) To investigate the factors which influenced the sandstone quality development.

It is hoped that through the understanding of the distribution and quality of the sandstones, areas which have potential to contain hydrocarbons could be delineated.

Investigation of the source rocks and their potential to generate hydrocarbons was not attempted. In this study, it was assumed that source rocks are present within the basin, and that they have been subjected to appropriate temperature regimes and depth of burial for the generation of hydrocarbons. These assumptions were made on the premise that the hydrocarbons occurring throughout much of the Upper Oligocene-Upper Miocene sandstones must have been derived from some sources somewhere within the basin.

2. REGIONAL SETTING

2.1 *THE MALAY BASIN*

The Malay basin trends generally northwest-southeast, and, as defined by the 5000-metre total sediment isopach, measures roughly 500 km in length and 100 km in width (Fig. 1-2). On the basis of the 2000-metre contour, the basin measures more than 800 km in length and 250 km in width, and extends into the Gulf of Thailand in the northwest, and to Indonesia in the southeast (Fig. 1-5). Seismic data quality generally deteriorates below 2.5 seconds two-way-time (TWT), and due to this and the accumulation of a very thick sedimentary pile towards the centre of the basin, basement has not properly been recognised. Esso (1976) believed that the total sediment thickness exceeds 13,000 metres in the deepest parts of the basin. In the study area, the thickest sedimentary section is in the northwest, which exceeds 10,000 metres (Fig. 2-1).

The Malay basin is an intra-cratonic basin or interior fracture trough (Kingston et al, 1982), within a relatively stable complex of the Sunda Shelf (Fig. 1-5). The work of the Geological Survey of Malaysia (1968), Haile (1970, 1973), and Achalabhuti (1974) on the geology of Peninsular Malaysia, the offshore islands of the Sunda Shelf, and the Gulf of Thailand respectively, suggest that this crustal Sunda landmass consists essentially of igneous and metamorphic rocks and sediments of pre-Cretaceous age. Sediments of the Gagau Group of Late Jurassic-Late Cretaceous in age on the Peninsula (Senathirajah, 1969; Rishworth, 1974), probably extend offshore and constitute, in part, the basement of the Tertiary basin. The most recent seismic which was acquired in 1988, in the southern region of the study area illustrates truncation and

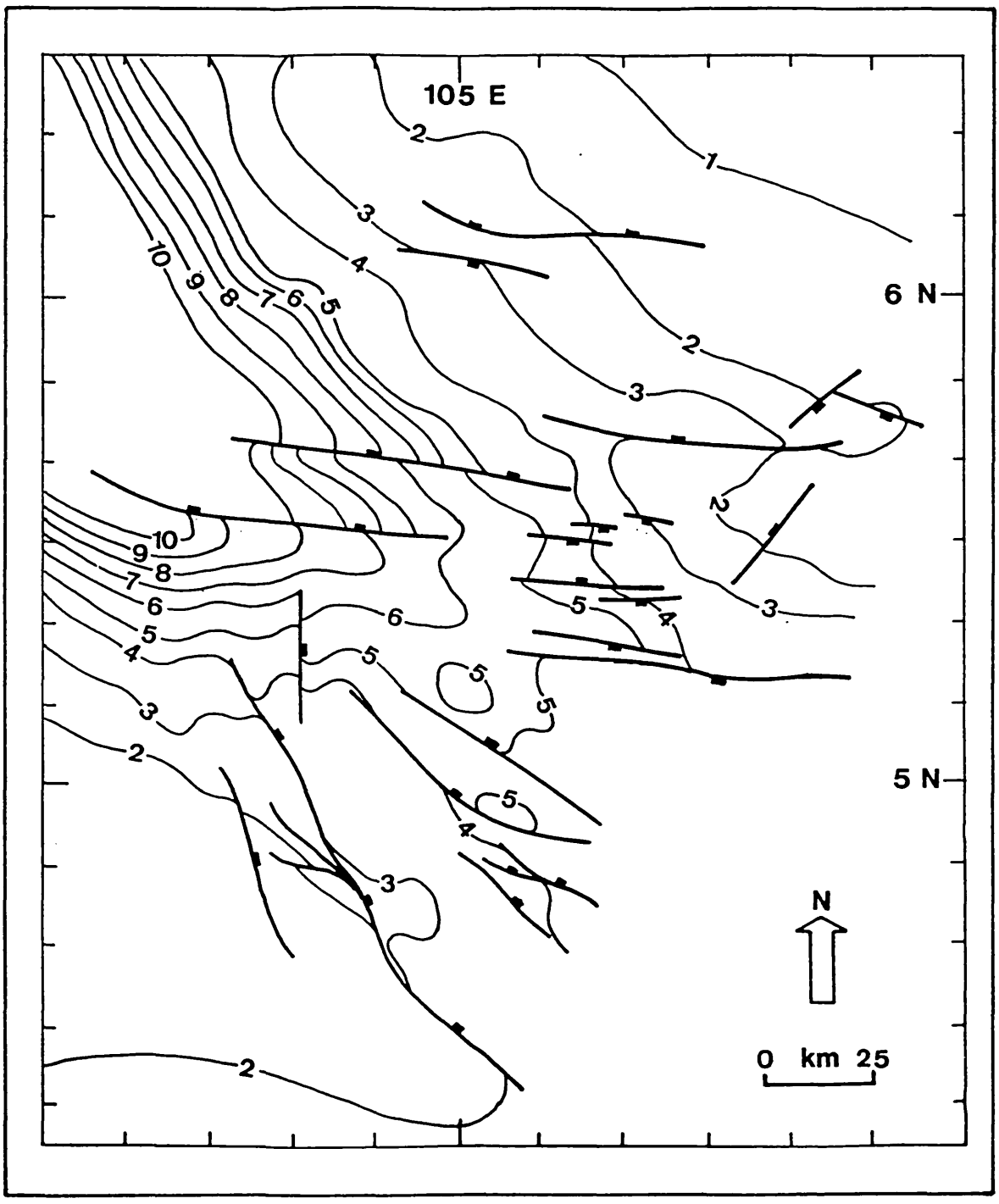


Figure 2-1 - Basement structure map, southern Malay basin (modified after Esso, 1976 and Carigali, 1985). Contours in km.

steeply dipping sediments which are believed to be part of the Gagau Group which constitute the basement (Fig. 2-2).

Three wells in the study area, Belumut-1, Peta-1 and Sotong 5G-5.1, were drilled into the basement and encountered granites at Belumut-1 at a depth of 1480 metres and at Sotong 5G-5.1 at a depth of 2675 metres, and metasediments at Peta-1 at a depth of 1550 metres. Two other wells outside the area, Tok Bidan-1 in the northwestern tip of the basin, and Malong-1 in the south on the Tenggol Arch, also encountered metasediments and granites respectively.

2.2 *STRUCTURES*

The basin has a steeper southwest flank than the northeast flank (Fig. 1-2). Although faults have not been detected seismically at depth, this steep basinal flank probably indicates the occurrence of some deep seated northwest trending faults dipping to the northeast, supporting the general description of the basin by some workers as being a half-graben.

Three primary lineaments (fold and fault) have been mapped by Esso (1976). In the northern one-third of the basin, these lineaments generally trend north-south, but in the southern two-thirds, eastwest and northwest-southeast trending lineaments are more predominant. Esso (1976) suggested that these lineaments were related to three phases of tectonism:

1) Extensional phase which represents the period of basin opening and rapid sediment accumulation, commencing from Late Cretaceous-Late Eocene to Late Miocene. Basin subsidence occurred through block faulting (Figs. 2-3 and 2-4). Some of the major east-west faults

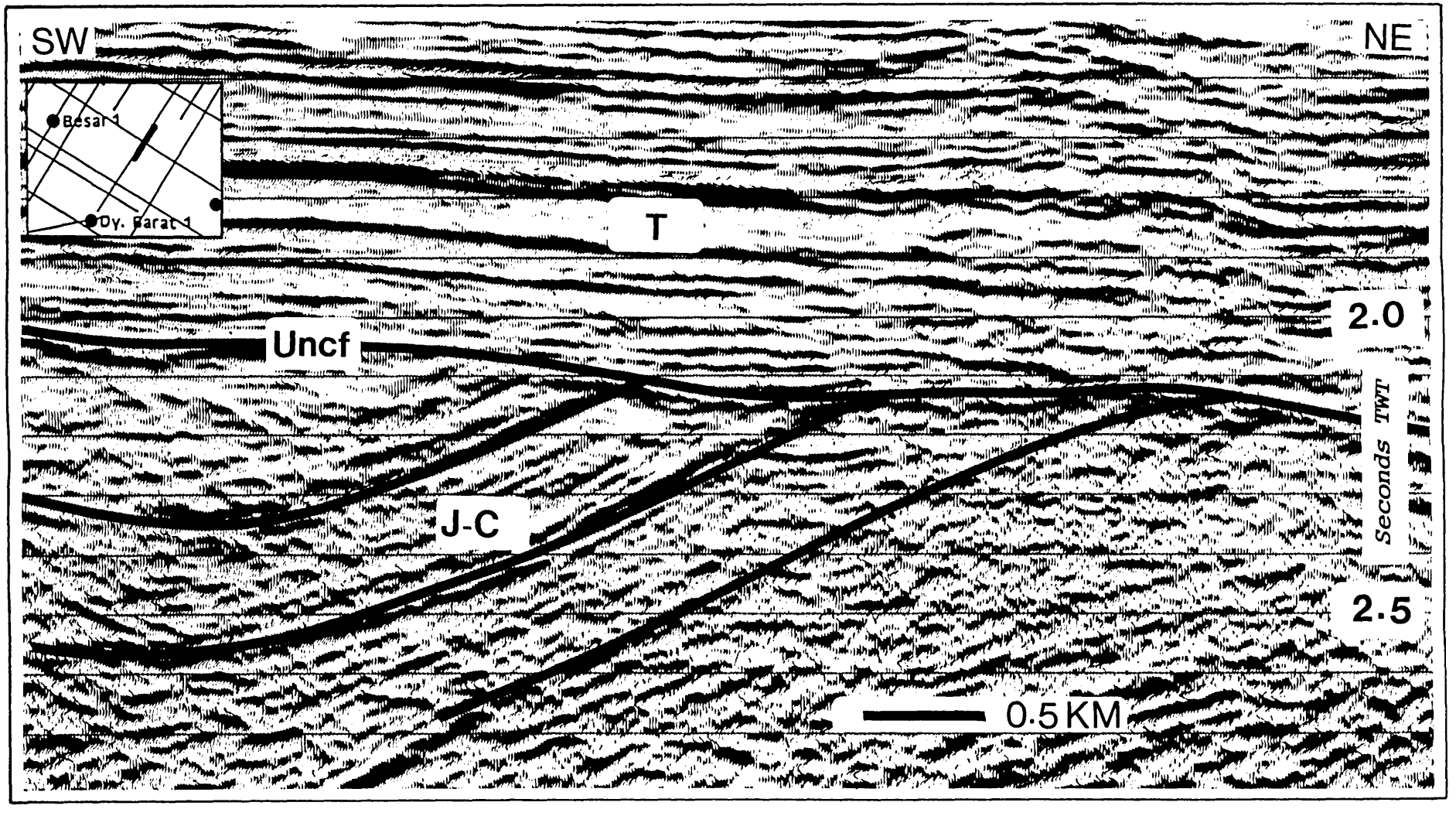


Figure 2-2 - Seismic section in the southern part of the study area, showing possible Gagau Group of Jurassic-Cretaceous age (J-C), which forms a part of the basement rocks. Tertiary (T) sediments lie unconformably over it. Inset map shows location of the section.

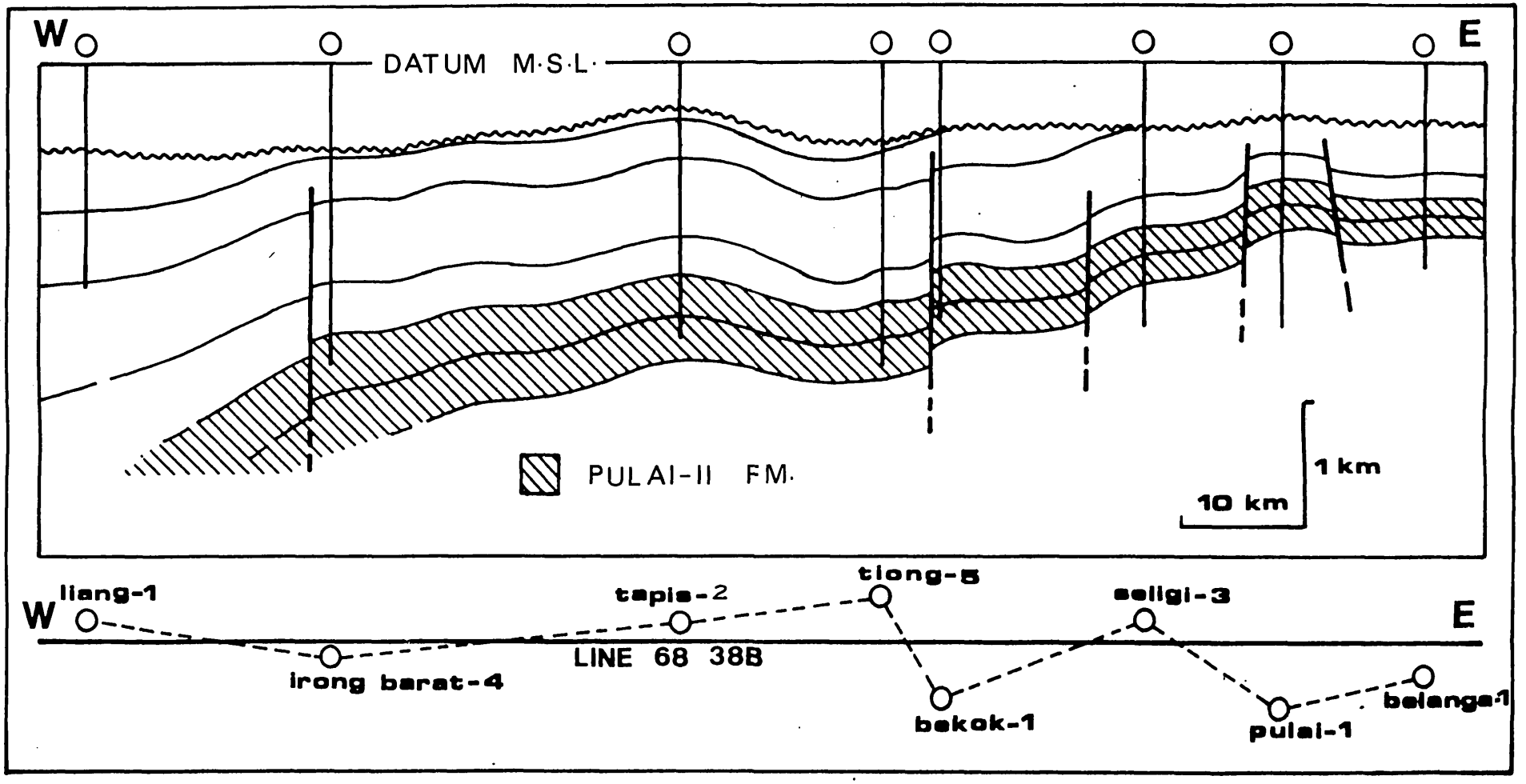


Figure 2-3 - Generalised cross-section along seismic line 68-38B, showing down-step block faulting which is common in the northeastern part of the study area (see Fig. 4-4, Section B-B' for details). Datum m.s.l.

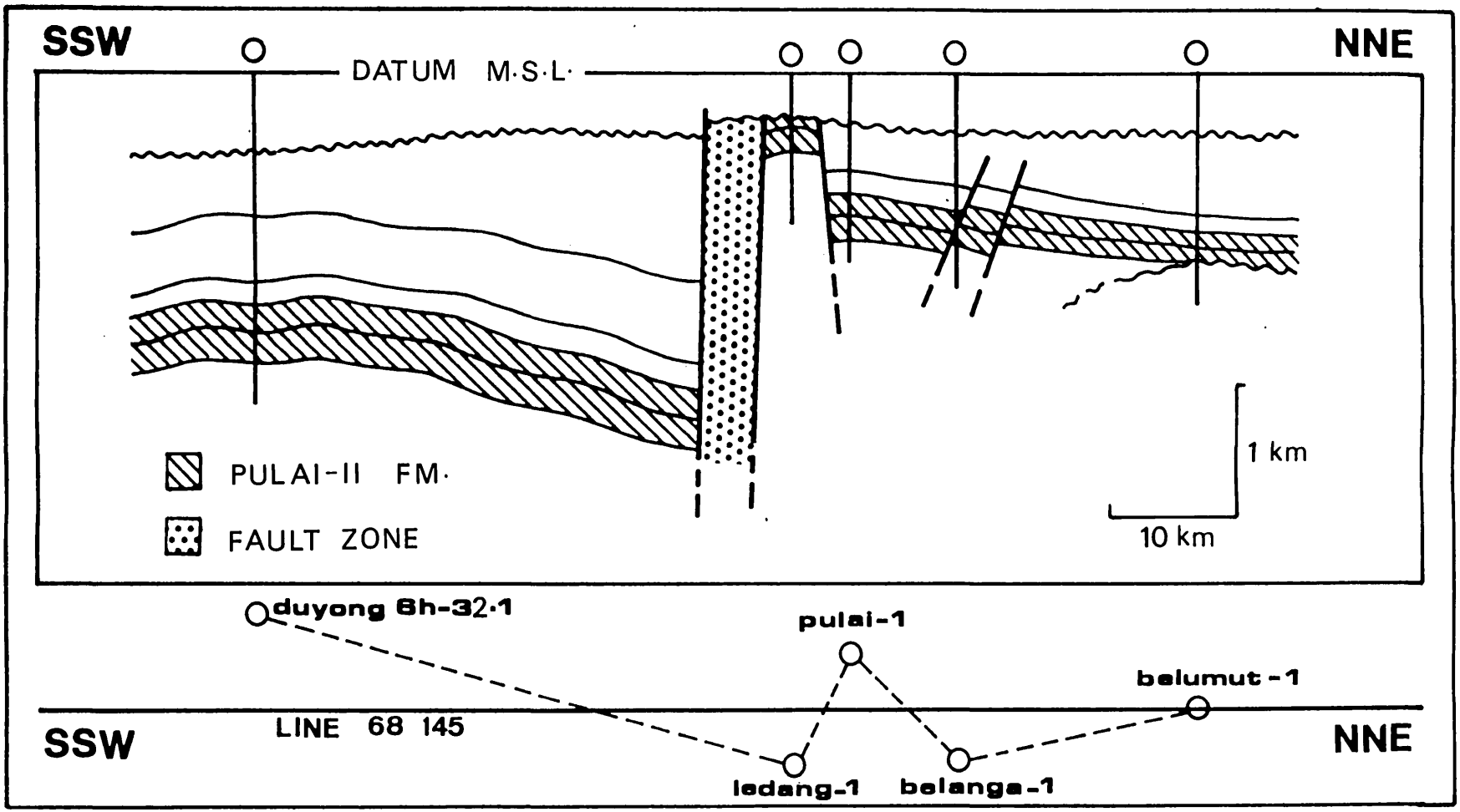


Figure 2-4 - Generalised cross-section along seismic line 68-145, showing steeply dipping normal (reverse ?) fault trending in east-west direction. Throw exceeds 1.5 km. This fault in the east (Fig. 2-5), shows a reverse fault movement (Fig. 2-8) (see Fig. 4-5, Section D-D' for details). Datum m.s.l.

observed in the study area are believed to have been related to this initial phase of basin formation (Figs. 2-1 and 2-5),

2) A compressional phase in Late Miocene-Pliocene, which formed most of the domal and anticlinal features, many of which trapped hydrocarbons. Some of these features and faults in the area are believed to be associated with re-adjustments of fault blocks and shale(?) pillow and/or diapirism(?) (Figs. 2-6 to 2-8). Many of the anticlinal folds appeared to be in en echelon patterns and, although wrench faults have not been mapped, or are difficult to prove on seismic sections, the occurrence of en echelon features probably indicate deep-seated wrench movements. The re-adjustment of the fault blocks in the south and southeast, which led to uplifting, tilting and subsequent erosion (Fig. 2-9), is manifested in the basement being relatively shallow. This study indicates that at least some 800 metres of sediments in some areas of the study area have been eroded (see Section 5.3). While in the east, as the basement was being elevated and subjected to erosion (Fig. 2-9), in the western part of the area, it appears to suggest that the deposition of the sediments was uninterrupted. This phase was followed by:

3) An extensional phase of basin re-juvenation, with extensive marine incursion and sedimentation during Pliocene-Recent. It would appear locally, however, that some of the domal and/or anticlinal features continued to grow for sometime during this period, and it is believed that this persistant structural growth was caused by basement re-adjustments which triggered the more ductile sediments, probably shale, to "flow" (Fig. 2-7).

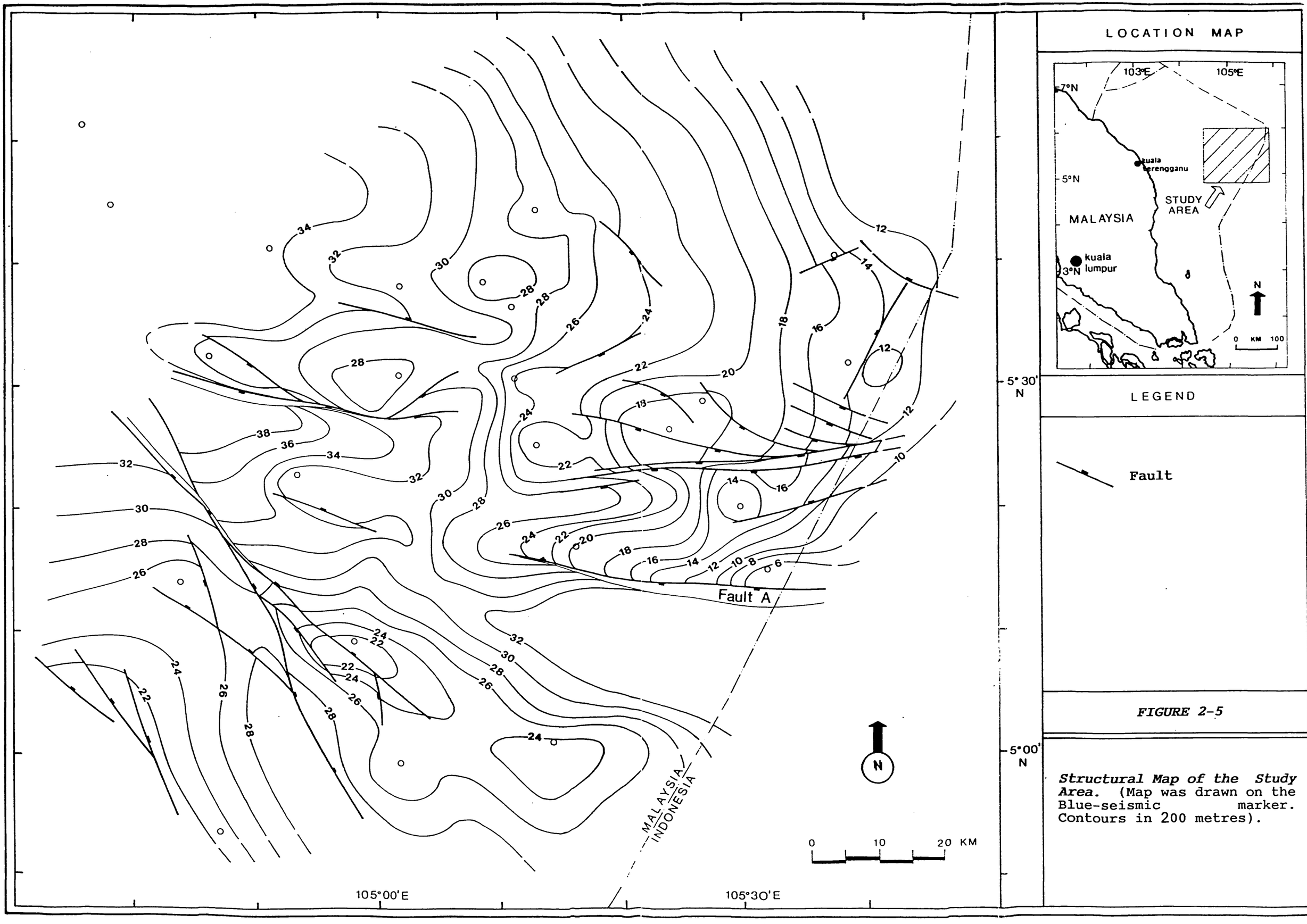


FIGURE 2-5

Structural Map of the Study Area. (Map was drawn on the Blue-seismic marker. Contours in 200 metres).

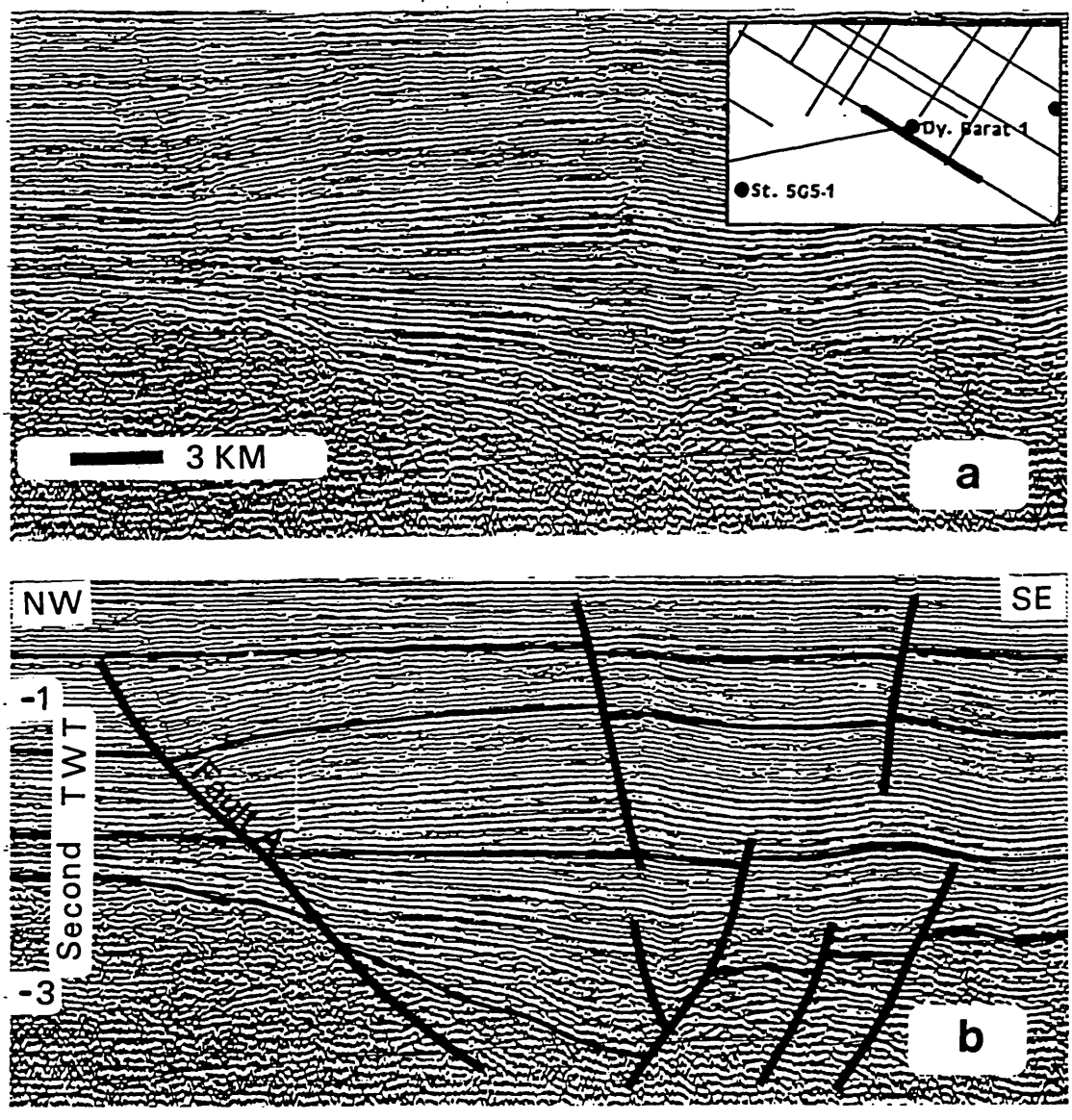


Figure 2-6 - Seismic cross-section showing several faults believed to have been formed during Late Miocene-Pliocene tectonic movement. Fault A is interpreted as a growth fault; reverse movement might have occurred along the fault during this compressive tectonic period. The anticlinal feature could have been resulted from this movement. a) uninterpreted section; b) interpreted section. Inset map shows location of the section.

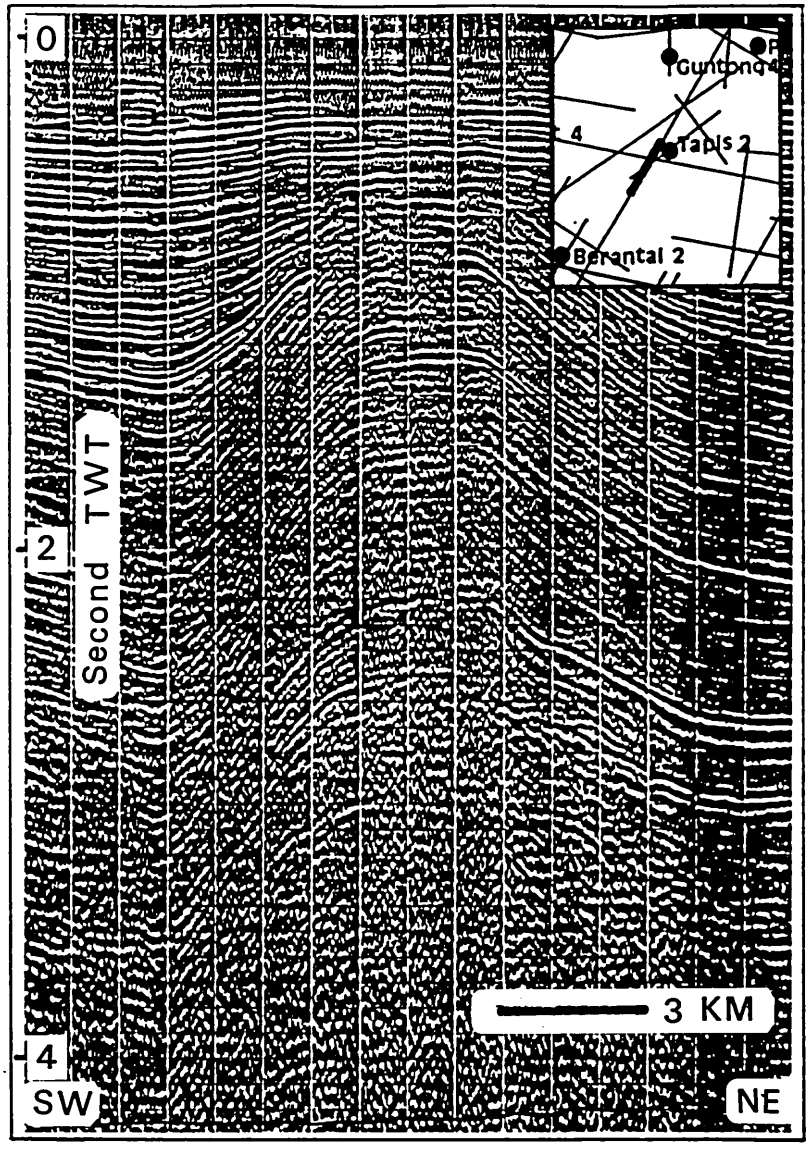


Figure 2-7 - Seismic cross-section showing anticlinal feature believed to have been related to deep-seated "shale" pillow (diapir ?). Inset map shows location of the section.

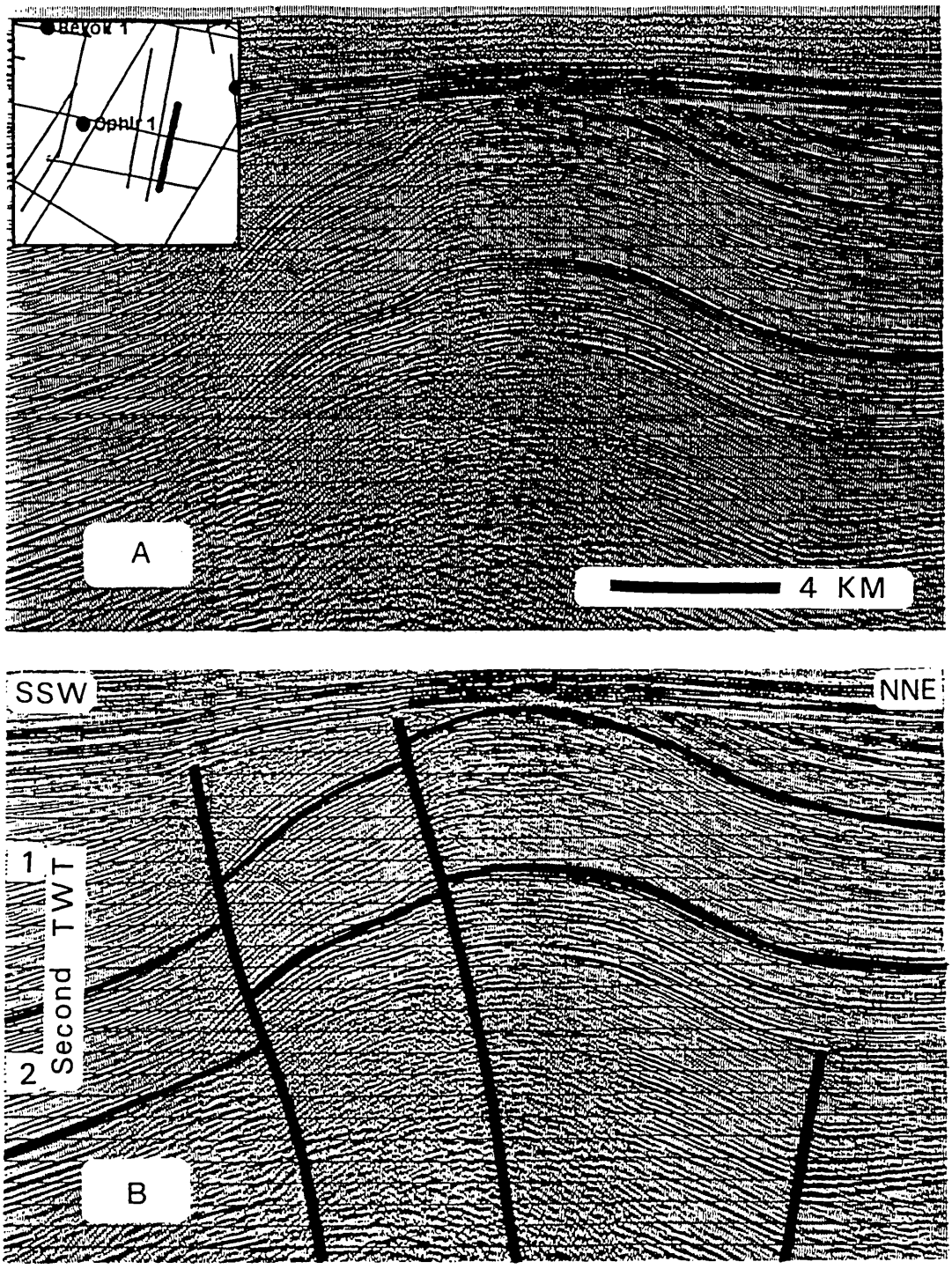


Figure 2-8 - Seismic cross-section showing faulted anticlinal feature believed to have been formed by reverse (upthrust) fault movement. Since the faults constitute the western end of the east-west trending Fault A (Fig. 2-5), and Fault A in the east shows normal fault movement, Fault A could be a wrench fault. a) uninterpreted section; b) interpreted section. Inset map shows location of the section.

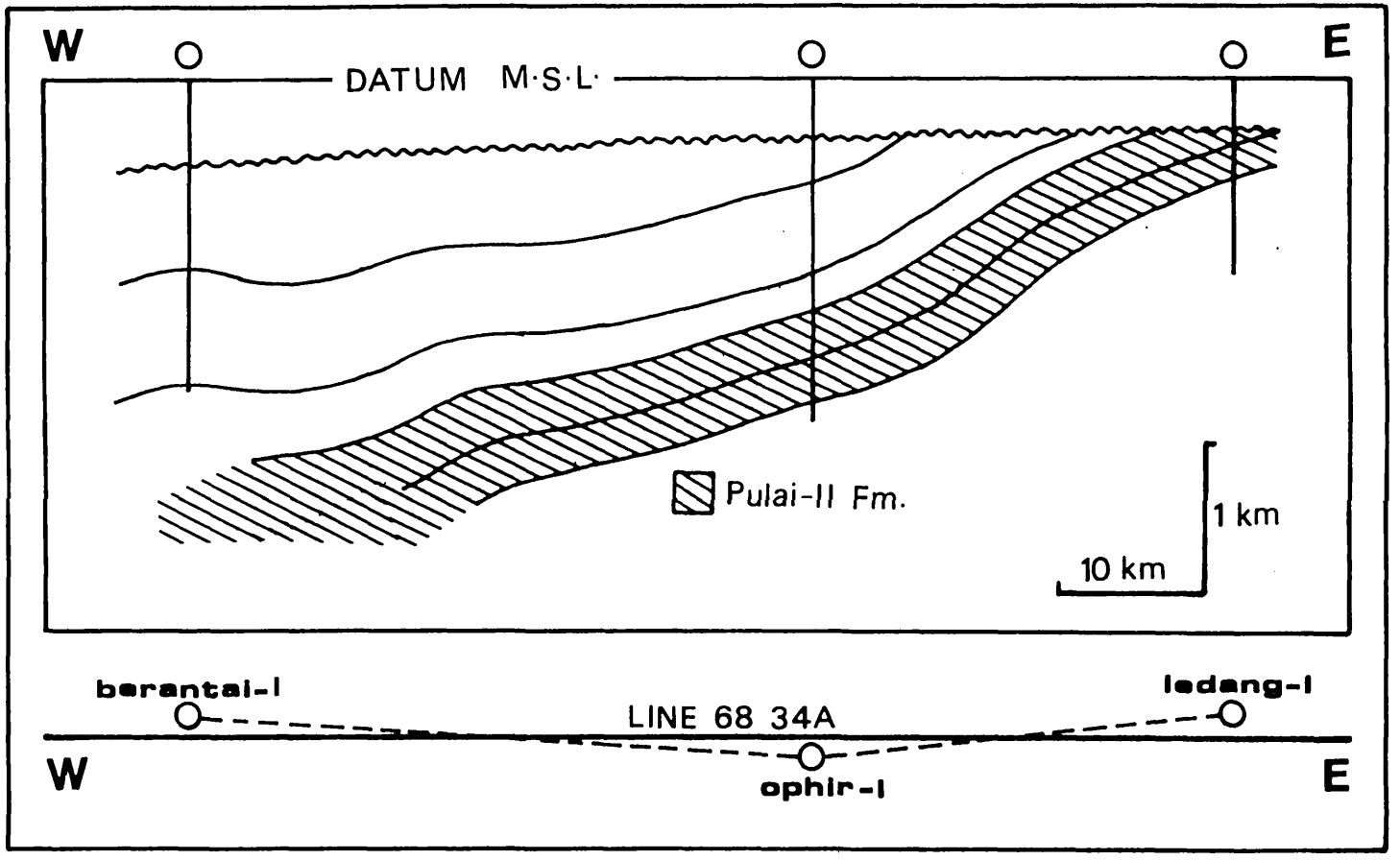


Figure 2-9 - Generalised cross-section along seismic line 68-34A, showing extensive truncation in the eastern part of the study area (see Fig. 3-5 for details). Datum m.s.l.

2.3 *STRATIGRAPHY*

Most wells in the Malay basin terminated below 3000 metres m.s.l.. A few wells reached the basement. Some of the wells drilled towards the centre of the basin were terminated prematurely due to over-pressures. Based on these drilling data, it is now known in part, that the sediments of the Malay basin consist of thick sequences of interbedded sandstones and shales. Although significant carbonate sequences have not been found in drilling anywhere in the basin, occurrences of thin lenses of calcareous clastic rocks were encountered. Most sandstones are massive and in places very thick, exceeding 100 metres. Well records indicate that the sandstones are well-developed in the south and southeast of the basin. Reddish-brown sandstones, which some workers believed to be of volcanic origin, were also reported in some wells in the southern area of the basin (A. O. Beall, personal communication, 1975).

Our knowledge and understanding of the stratigraphy of the basin, particularly of its southern area where it is relatively more petroliferous, are based on the work of Esso, Conoco and Carigali between 1970-86. Four stratigraphic nomenclatures have been developed (Fig. 2-10), but only three were used regularly (Figs. 1-6 to 1-8). The nomenclature developed by Conoco on the basis of lithology, has localised application, and was not widely used. Highlighted below are the premises on which two of the stratigraphic schemes, Armitage-Viotti and Carigali, were developed. The alphabetical stratigraphic scheme of Esso was developed on the basis of seismic sequence analysis, and no further elaboration was thought necessary.

Figure 2-10 - Composite stratigraphic schemes of the study area, southern Malay basin (after Conoco, 1973, Esso, 1976, Armitage-Viotti, 1977 and Carigali, 1986).

AGE		CONOCO Formation	ARMITAGE *	ESSO Seismic	CARIGALI Unit
Recent - Pliocene		Pilong	Pilong	AB	VIII-VI
Miocene	*L*	Sand and Coal		D	
				E	VI
				F	
				H	V
	M		Bekok	I	IV
			Tapis	J	III
	E	T'ganu Sh	Pulai	K	IIB
					II IIA(U)
Oligocene		Tapis			
	L		Seligi	L	
			Ledang	M	
				?-	I
	E	Sotong	T'bukun and Older Fm		
Eocene - U. Jurassic		Sediments, metasediments and igneous rocks			

* age re-adjusted

▦ *missing section in the Study Area*

2.3.1 Armitage-Viotti Scheme

The Armitage-Viotti nomenclature was based on lithology and wireline log characterization of rock units and their seismic signatures. Fauna and/or floral assemblages present in the sediments were used to determine the ages of the units and their environments of deposition.

Armitage-Viotti chose two wells, Pulai-1 on the Malaysian side and AQ-4X in Indonesia, as the type wells representing the sedimentary pile in the southern part of the basin. This sedimentary pile consists of alternating sandstone and shale sequences, and these sequences are often separated by well developed shale intervals. The bases of these sandstone sequences correspond to seismic markers which are mappable throughout the area. Based on this observation and the study of lithologies from wireline log characteristics, they recognised eight regionally significant litho-seismic sequences. These sequences have been named accordingly, with the youngest sequence represented by the Pilong Formation, and the oldest the Sambas and the Undifferentiated Complex (Fig. 1-6).

2.3.2 Carigali Scheme

Carigali's stratigraphic scheme developed for the southern Malay basin was based primarily on the recognition of the widespread occurrence of shale markers and marine transgressive pulses. Carigali observed that these shale markers and transgressive pulses are correlateable and traceable seismically throughout its areas of operations. With good palaeontological control, primarily using nanno-planktonics and palynomorphs to date the pulses, seven stratigraphic breaks were recognised; and the intervals between them are designated as

Units I to VIII, with Unit VIII being the youngest (Fig. 1-8).

2.4 *AGE OF SEDIMENTARY SEQUENCES IN SOUTHERN MALAY BASIN*

Since the work of Armitage-Viotti (1977), many palaeontological studies of the southern Malay basin were carried out independently by Esso and Carigali and recently by PETRONAS (Rashidah et al, 1988). The result of the palaeontological study by Esso on Palas-1 well, and the results of a similar study undertaken by Carigali, on most of its exploration wells in the basin, and that of the study which PETRONAS conducted on Banggol-1, Seligi-3 and Angsi-1 in 1988, have highlighted that:

1) The ages of the stratigraphically equivalent Pilong, Bekok and Tapis Formations at Palas-1, Banggol-1, Seligi-3, Angsi-1 and Duyong Barat-1 are in agreement with that suggested by Armitage-Viotti, although they differ in the interpretation of the environments of deposition. Esso and PETRONAS believed that the presence of *Globorotalia fohsi lobata* in the Bekok Formation, and *Globorotalia mayeri* in the Tapis Formation, indicate that the environments of deposition were more marine than coastal plain, as was suggested by Armitage-Viotti. Glauconite has been reported in ditch cuttings and cores within this interval, and its presence is one strong evidence of a marine setting (Selley, 1985).

2) A similar discrepancy existed in case of the stratigraphic sequence of the Pulai Formation. Armitage-Viotti dated this formation as Middle Miocene in age based on the presence of *Milliammina sp.*, and *Thecamoebians*. Esso, Carigali and PETRONAS disputed this

determination, and have suggested that its age is more likely to be Late Oligocene-Early Miocene. This suggestion was based on:

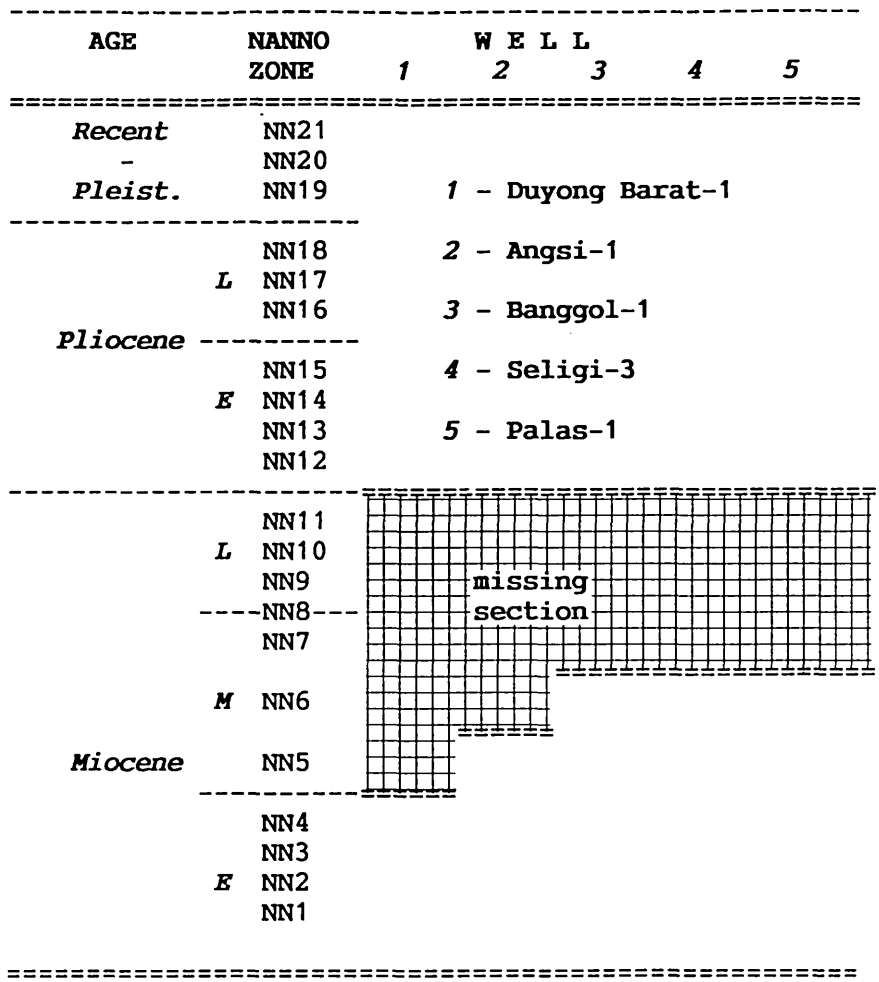
i) The presence of *Milliammina fusca*, *Cicatricosporites* and *Florscheutzia trilobata* at Duyong Barat-1, and *F. trilobata* and *Milliammina fusca* at Palas-1, and

ii) The Middle Miocene section which is represented by NN5 - NN11 nannopkanktonic zonation, is missing in the wells that they have studied (Fig. 2-11).

3) Angsi-1, Palas-1 and Duyong Barat-1 terminated in the stratigraphically equivalent Seligi Formation. Within this stratigraphic interval no diagnostic floras or faunas were detected. However, *Magnastriatites howardi* was a common constituent in samples at Palas-1. At Duyong Barat-1, there was an abundance of *Pinuspollenites sp.* and *Piceapollenites sp.*, and these were correlated with the *Gemmamonoletes (Cyclophorous)* Assemblage Zone of Oligocene age. At Palas-1, the interval was placed in the *F. trilobata* Zone, of Oligocene age because of the occurrences of *M. howardi*, and also because the floral assemblage in the interval was almost similar to the overlying Pulai Formation.

No palaeontological data were made available on the older formations of the study area. If the recent work of Esso, Carigali and PETRONAS are to be regarded as more reliable, then the ages assigned to the Ledang, Telukbutun, Semala, and Sambas Formations and the "Undifferentiated Complex" by Armitage-Viotti are probably dubious.

Figure 2-11 - Chrono-stratigraphy of five wells in the study area. (Data from Carigali (1), Petronas (2,3 and 4) and Esso (5)).



2.5 *STRATIGRAPHIC SEQUENCE UNDER INVESTIGATION*

This study focuses on the Upper Oligocene-Lower Miocene sequence which consists of the Pulai Formation and its lateral equivalent, Unit IIB-IIA upper (Fig. 2-10). Since the main objective of the study was to investigate the sandstones of the sequence, for convenience the following simplified terminologies have been used:

1) The stratigraphic sequence which contains the Pulai Formation and its lateral equivalent of Unit IIB-A IIA upper, is herein referred to as the Pulai-II Formation (Fig. 2-12), and

2) All the sandstone units of the Pulai-II Formation are herein named as the Pulai-II sandstones.

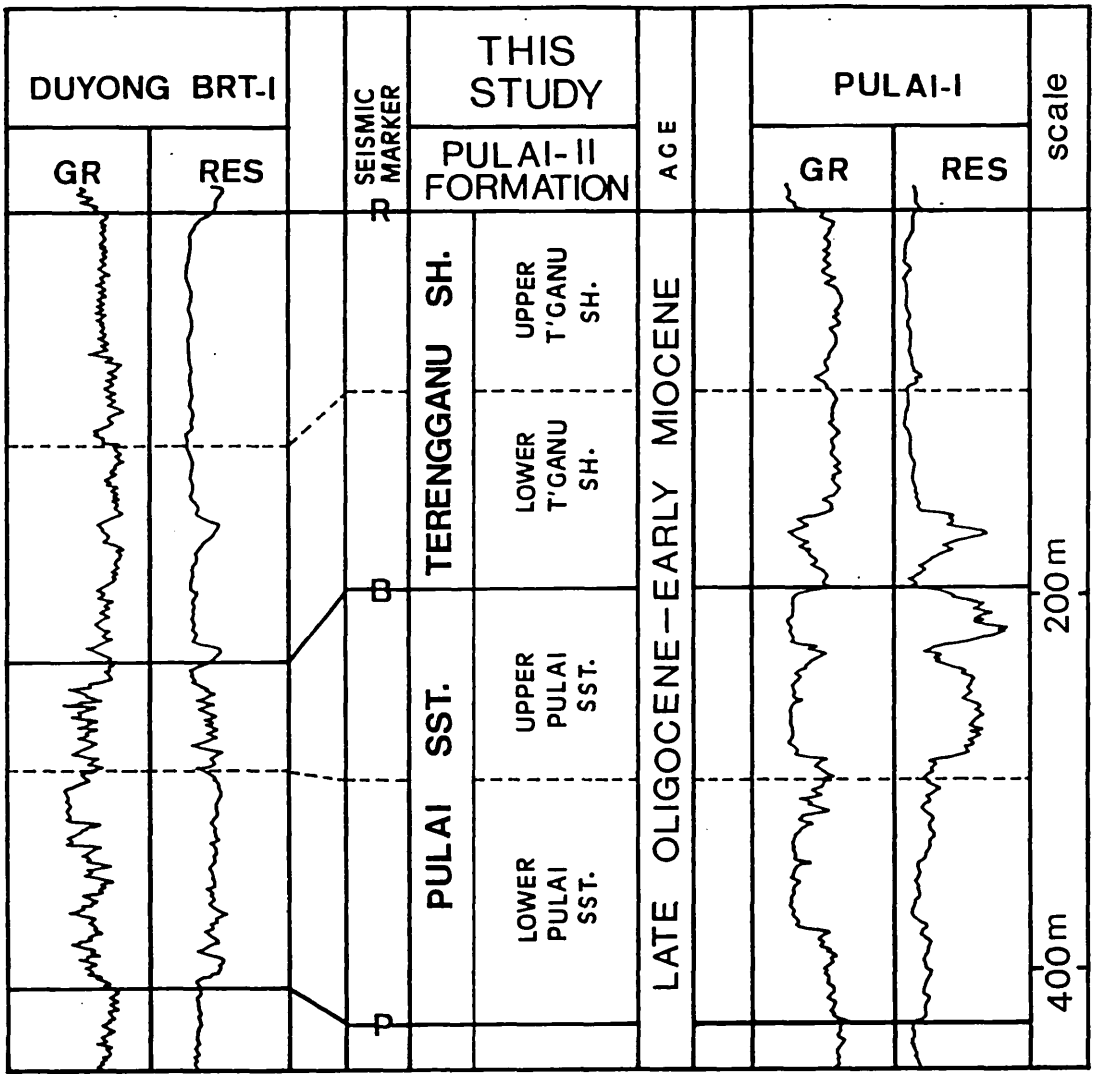


Figure 2-12 - Stratigraphic nomenclature used in this study.

3. METHODOLOGY

3.1 *DATA SOURCE*

Both seismic and well data and cores were used in this study. Drilling and well completion reports, and core analysis reports have also been used. All these data and reports were made available by PETRONAS.

3.2 *SEISMIC DATA*

A total of 1980 line-km of seismic data was used. This seismic data set consisted of the following:

1) 1400 km acquired and processed in 1968-69. About 300 km of these were reprocessed in 1987,

2) 200 km acquired and processed in 1974-75,

3) 200 km acquired and processed in 1978-79,

4) 30 km acquired and processed in 1984, and

5) 150 km acquired and processed in 1987.

The 1968-69 data are reconnaissance seismics which were acquired on a grid of 10 by 20 km (Fig. 3-1). The 1974-75 and 1978-79 seismics are either infill or delineation/development surveys and the grids are much denser. The 1984 and 1987 seismics are both regional and infill seismics.

The 1968 to 1984 data consisted of full scale negative prints with a vertical time scale of 9.5 cm per second TWT. The horizontal scale

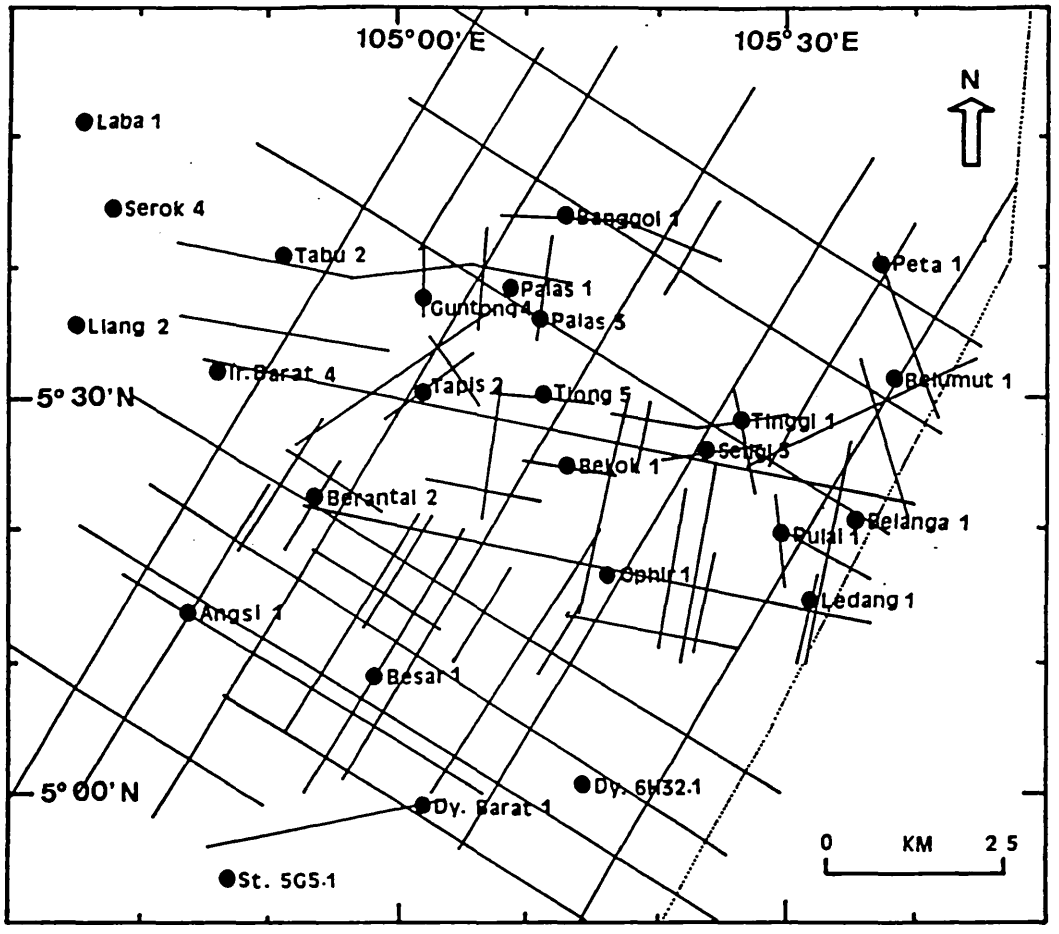


Figure 3-1 - Seismic and well location map of the study area.

however varies, with the 1968-69, 1974-75 and 1984 data sets having a scale of 10 cm for every 7 km, and the 1978-79 set having a scale of 10 cm for every 2.5 km. The 1987 data consisted of prints with a vertical time scale of 10 cm per second TWT and a horizontal scale of 10 cm for every 2.5 km.

The quality of the seismic data is generally fair to good for shallower strata (up to 2.5 seconds TWT), but resolution for deeper strata and the basement in certain parts of the study area, is poor to fair. A slight improvement is shown in the 1968-69 seismics reprocessed in 1987 (Fig. 3-2).

The new 1987 seismics are generally of good quality. Like the 1968-69 data, the resolutions are much improved and well-defined in the shallower strata (top 2.5 seconds TWT), but are generally less well-defined below this depth. Nevertheless, these data are generally much superior to most data acquired previously (Fig. 2-2), and although they were processed purely for structural mapping, some of the stratigraphic features are discernable.

3.3 *WELL DATA*

As at December 1987, a total of 118 exploration wells (34 wildcats and 84 appraisals) had been drilled within the study area. Twenty-six of these wells, each drilled on a separate seismic anomaly, were selected for this study (Fig. 3-1). The selection of the wells was based on one or several of the following criteria:

1) The wells should be situated in close proximity to the selected seismic lines,

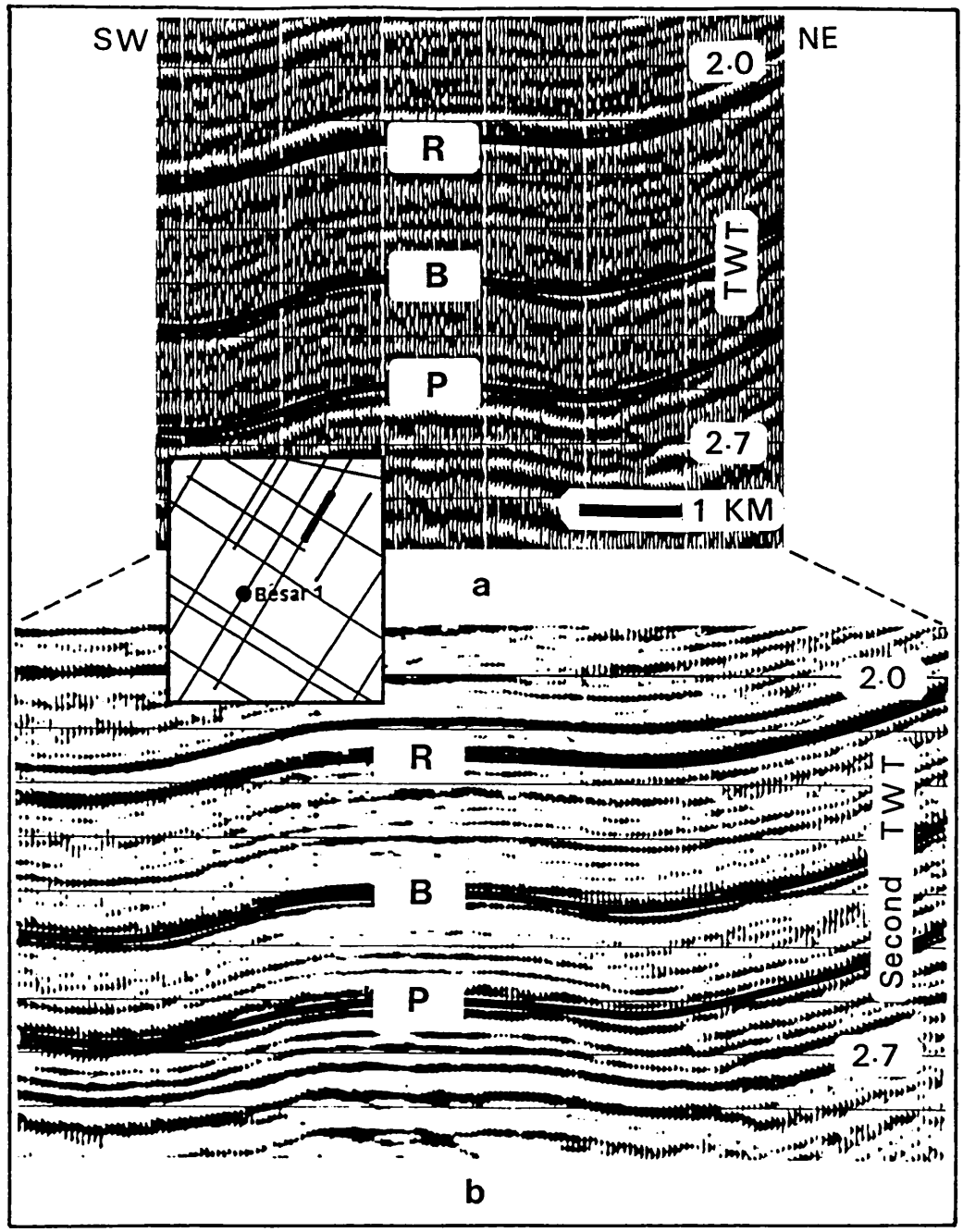


Figure 3-2 - An illustration of seismic data processed at different time: a) processed in 1968, and (b) reprocessed in 1987. Note an overall improvement in resolution in (b). Inset map shows location of the section. (R, B and P represent top, mid and bottom of the Pulai-II Formation respectively.)

2) They should preferrably penetrate the Pulai-II Formation,

3) The cores cut at the appropriate depths of the formation should preferrably be available for the study,

4) The wells should be located adequately and, where possible, ideally spaced for control purposes, and

5) The wells should have adequate temperature data for temperature analysis, and also checkshot and well velocity survey data for sonic log calibration purposes.

In addition, it would be advantageous if these wells had palaeontological data.

Seven of the wells did not reach the Pulai-II Formation, and were selected purely for the temperature data. Three others terminated within the formation and were chosen purely for the same reason. The remaining sixteen wells penetrated the formation, and three of these terminated in the basement. Of the twenty-six wells, twelve have cores (Fig. 3-3).

3.4 *CORE DATA*

A total of 350 metres of the cores had been studied. The majority of these cores was cut within the sandstone intervals. Seligi-3 provides a near-complete representation of the Pulai-II sandstone section. Corrections of core depths were made by a constant correlation with geological (gamma-ray) logs of the wells.

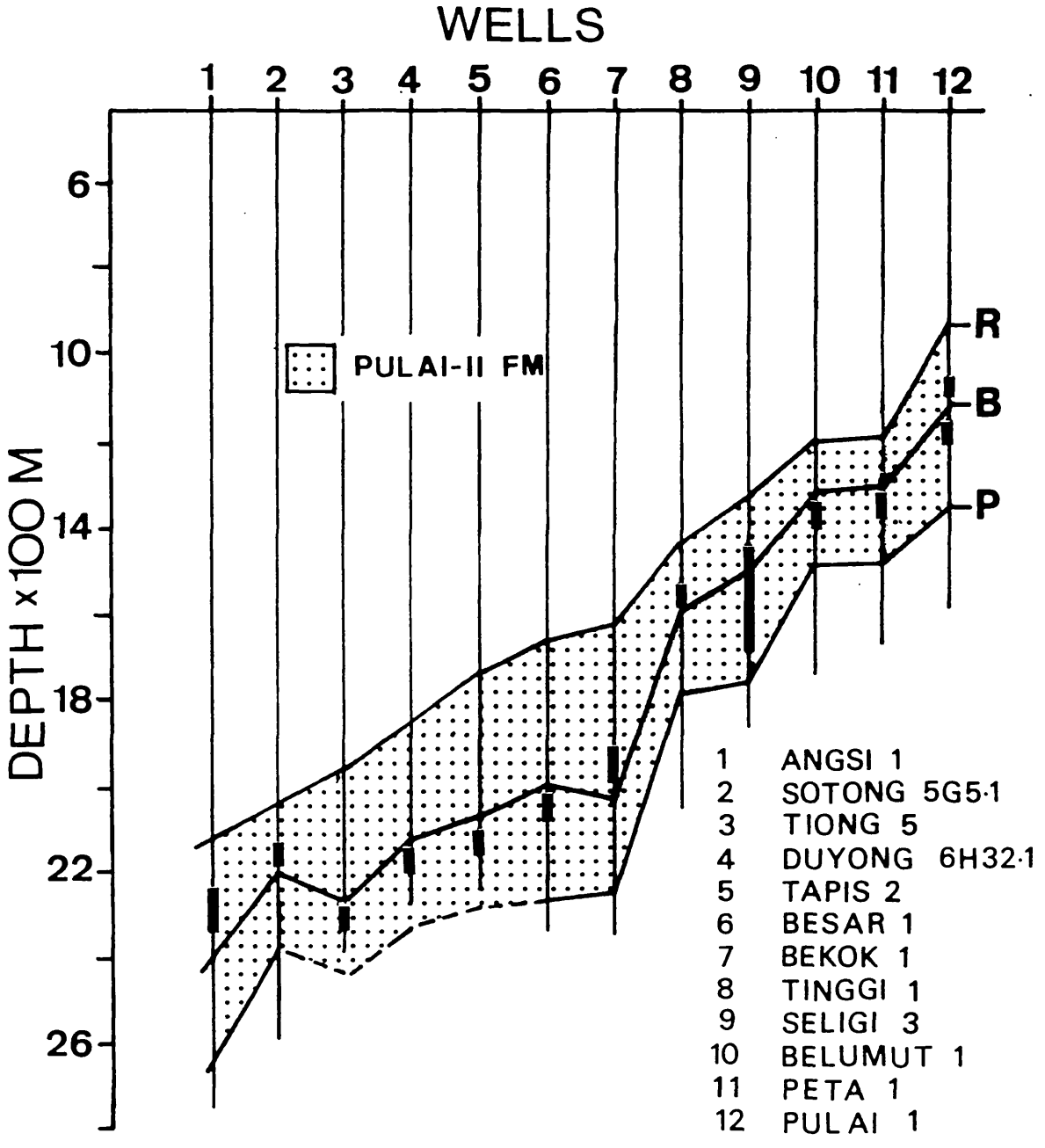


Figure 3-3 - Well profiles showing relative positions of cores taken in the Pulai-II Formation.

3.5 *METHODS OF INVESTIGATION*

The procedures of investigation and interpretation consisted of integration of geophysical and geological methods to determine structural and stratigraphic settings, and computer, geological and laboratory-cum-analytical methods for the reservoir quality analysis. The study examined the current problem in four broad scopes, within which various techniques were employed. These four scopes are:

1) The use of the geophysical seismic data to interprete structural and stratigraphic settings and facies of the Pulai-II Formation,

2) The use of geological wireline logs to:

   i) Identify sandstone facies and their geometry, and to interprete their environments of deposition,

   ii) Generate synthetic seismograms and stratigraphic models,

   iii) Determine porosity of the Pulai-II sandstones, and

   iv) Determine maximum depth of sediment burial,

3) The use of cores to:

   i) Identify and interprete sandstone facies and their environments of deposition, and

   ii) Determine sandstone diagenesis, and

4) The use of temperature-depth data to predict porosity.

3.6 *DATA TREATMENT*

3.6.1 Seismics

Two regional seismic lines, 68-50 and 68-129, have been squeezed horizontally to a horizontal scale of 1 cm to 1.4 km. The vertical scale was kept at 9.5 cm to 1.0 second TWT. The objective of this squeezing was two-fold:

1) To present a display of the relationship of observed seismic reflection characters with synthesised well log characters, and

2) To examine if subtle stratigraphic features could be better discerned through data squeezing technique.

The remaining seismic data were untreated, and the interpretation of the data was based on the original paper prints.

3.6.2 Geological Logs

The geological logs (caliper, gamma-ray, sonic, spontaneous potential (SP), resistivity (ILD, ILS and MSFL), and neutron-density (FDC-CNL)) of the twenty-six wells were digitised. This log digitization was made purely for:

1) The generation of synthetic seismograms and for stratigraphic modelling, and

2) The determination of the porosity by means of a personal computer, PC.

But otherwise, interpretation of the sandstone facies, facies boundaries

and their environments of deposition was based on the integration of the original, undigitised logs and other geological data. Beside using them to create synthetic seismograms and generate stratigraphic models, sonic logs have also been used to determine possible maximum sediment burial depths.

3.6.3 Cores

3.6.3.1 *Core Description*

The majority of the 350 metres of cores of the Pulai-II Formation was slabbed cores. In describing the cores, core description technique of Selley (1980) was adopted. A graphic scale of 1 cm to represent 3.197 metres of core was used. Photographs were taken of some cores to illustrate some of the more important sedimentological features.

3.6.3.2 *Reservoir Quality*

A total of 135 sandstone samples were selected to determine sandstone quality: texture (grain size, grain inter-relationship and pore throat condition) and mineralogy (framework minerals and cement, and their relative composition). Texture of the sandstones formed the basis for sample selection. The selected samples, each about 3 cm-cube in size, were sliced for thin section study, and each of the remaining portions were divided into two parts, one part each for SEM and XRD analyses. It would be ideal to study the thin sections made from core plugs, where porosity and permeability data are known, but such plugs were not available.

1) Thin Section

A total of 135 thin sections were made. The objective of thin section study was three-fold:

i) To identify the framework's basic mineral composition, and authigenic mineral constituents,

ii) To examine pores and pore throat conditions, and

iii) To recognise porosity-type and to estimate porosity.

In making the thin sections, the samples were sliced perpendicular to the depositional surfaces. Prepared in Canada balsam, the samples were impregnated with blue epoxy, the objective of which was to provide an easy recognition of porosity. Estimation of the porosity was undertaken visually by using an A.P.I. No. 6 comparison Chart (Terry et al, 1955).

2) X-Ray Diffractometry (XRD)

This study was designed to determine:

i) Clay minerals and their relative composition in the sandstones, and

ii) All minerals which may be present in the samples, particularly those other minerals other than the clay minerals which were not observed during the petrographic analysis.

About 10 grammes of each of the samples were taken for XRD analysis. Each sample was divided into two portions: one portion of 135 samples, was for the identification and determination of the clay

minerals and their relative compositions in the clay-sized (less than 5 microns) fractions, and the other portion of 78 samples, was for the identification and the determination of mineral constituents of the whole rock samples. Texture of the samples formed the basis of selection for the whole rock analysis. The following standard techniques of BP Research Centre, Sunbury, were used to prepare the sample for analyses:

i) Preparation For Clay-sized Fraction

About 5 grammes of each sample were disaggregated gently in a pestle and mortar. The disaggregated powder was then placed in a calgon solution in an ultrasonic bath for about 5 minutes to release the maximum amount of the clay minerals into suspension. The clay suspensions were centrifuged for about 2 minutes to allow greater-than-5-micron fraction to settle. The remaining clay fractions in suspension were decanted and filtered. A little distilled water was added to the filtered clay residues to make them into a slurry, and was pippetted onto an unglazed ceramic tile to dry. Clay mineral identifications were run on XRD machine using the following specifications:

- Radiation tube - Fe-filtered Co-K alpha
- Receiving slit size - 0.03 mm
- Scanning speed - 5 seconds per 0.02°
- Scanning angle - 4° to 16° two-theta

In identifying clay minerals present in the samples, four sets of XRD scannings were carried out:

a) first was for the air-dried, untreated samples,

b) second was for the samples sprayed with ethylene glycol,

c) third was for the samples heat-treated at 350° C for about 4 hours, and

d) fourth was for the samples heat-treated at 550° C.

ii) Preparation For Whole Rock Fraction

The 78 samples, each about 5 grammes, were gently crushed and later ground in an acetone medium in a micronising mill for about 5 minutes to form slurries. These slurries were filtered and the residues left to dry. Each powder was then packed firmly into a powder mount for the whole rock XRD analysis. Unlike the clay-sized samples, the whole rock samples were untreated and were scanned air-dried. In obtaining XRD data, the following specifications were used:

- Radiation tube - Fe-filtered Co-K alpha
- Scanning speed - 60 seconds per 5.0°
- Dectector size - 5° slit and step width of 0.02°
- Scanning angle - 5° to 65° two-theta.

The prepared clay-sized and whole rock samples were scanned in batches of 35, on a fully automated Siemens D500 X-Ray diffractometer at the BP centre.

3) Scanning Electron Microscopy (SEM)

This analysis was designed:

i) To evaluate sandstone diagenesis through examination in 3 dimensions of framework grain relationship and inter-granular pore structures, and

ii) To reconfirm the identification of a) minerals detected in petrographic and XRD analyses, through simultaneous detection of emitted energy dispersive X-Ray (EDAX), and b) porosity type.

Thirty-five samples were selected for the SEM analysis. Each sample was carefully chipped perpendicular to the bedding surfaces to a size of about 5 by 10 by 10 mm, large enough for it to be mounted on a 1-cm diameter SEM specimen plug. Carbon paste was used to mount the specimen onto the plug. A similar liquid carbon was used to gently paint the edges of the sample. The samples were ready for examination after they have been coated with gold in an evaporative chamber.

3.6.4 Temperature Data

The objective of this analysis was to examine whether diagenetic advancement or modification observed in the sandstones was, among others, a function of:

1) Temperature,

2) Depth of sediment burial, and

3) Presence of hydrocarbons.

In the study of subsurface temperature it was essential that the data are reliable. Much of this reliability depends on the way in which the data were acquired. In most cases, the data, if acquired during normal drilling, are inaccurate or distorted. Data distortion is usually caused by the effect of drilling and cementing of casing. Such data distortion must be corrected. The temperature data used in this study were acquired during shut-in periods when production tests were being carried out. Unfortunately, only one temperature reading was taken at each tested interval, and it was not possible to undertake data corrections. However, according to Gretener (1981), the data obtained by this method are usually reliable and they represent close-to-true or static temperature of the interval under investigation. Since it was not possible to confirm the validity of this statement, such temperature data obtained from the tests were assumed to represent the minimum temperatures and/or best approximations of the temperatures of the intervals.

3.7 *DATA ANALYSIS*

3.7.1 Seismics

Three basic concepts used for stratal mapping of seismic sequences which contained the Pulai-II Formation are:

1) That seismic reflectors are generated at the boundaries of rock layers having contrasting acoustic impedence, and that these reflectors in most cases, follow geologic time-lines (Bally, 1987). Exceptions are those reflectors created within same rock units of

different diagenetic fronts, and of different fluid contents, and are therefore time-diachronous,

2) That mostly, only primary seismic reflections correspond to stratal surfaces, and these stratal surfaces may occasionally represent a significant chronostratigraphic gap (Hubbard et al, 1985), and

3) That a seismic sequence is a depositional sequence, which is bounded by mappable sequence boundaries. The sequence boundaries are primary seismic reflections which represent unconformities (angular, non-conformities or disconformities) (Bally, 1987).

3.7.1.1 *Seismic Reflection-Geological Log Correlation*

Before the mapping exercise was carried out, it was necessary to determine which of the many regionally significant seismic reflectors on the seismic sections correspond to or correlate with the stratal surfaces of the Pulai-II Formation. The determination of these seismic reflectors on the seismic sections was carried out by:

1) Selecting the Ophir-1 well which was located on the seismic section 68-34A which exhibited a fair to good seismic reflectivity throughout (Fig. 3-1),

2) Correlating the geological logs of Ophir-1 with the logs of Pulai-1, one of two type wells of the Malay basin, and with the logs of near-by wells. A combination of the gamma-ray, resistivity and sonic logs was used in the correlation exercise. In correlating these logs, a technique of pattern correlation which carries a group of stratal interfaces rather than one or two large "kicks" on the geological log curves, was employed, and

3) Generating a synthetic seismogram for Ophir-1 to tie-in with the seismic reflectors of the seismic section 68-34A (Fig. 3-4). GMA Stratigraphic Modelling System, a computer software package developed by QC Calgary and adaptable for PC, was used to generate synthetic seismograms. Similarly, synthetic seismograms were generated for the other wells in the study area. These synthetic seismograms were used in mapping of the seismic markers.

3.7.1.2 *Seismic Reflector Mapping*

Three signatures of the resultant synthetic seismogram of Ophir-1, which corresponded to the top, middle and base of the Pulai-II Formation were identified. They were arbitrarily named as Red, Blue and Purple markers (Fig. 3-4). By matching the synthetic markers with the seismic reflectors, it was possible to recognise the stratigraphic sequence of the formation on the seismic section (Fig. 3-5).

Undoubtedly, mapping of the three markers of this scale had introduced some misties. Fortunately, these misties were minor and not more than one-half of a cycle. Misties happened probably because of lateral changes of facies, faulting and intense folding. Attempts were made to reduce the misties by ensuring that the markers were seismically looped at cross lines. In fact well log correlation was performed concurrently with the mapping of the seismics in order to provide mapping confidence and to ensure the pick of the right stratigraphic interval.

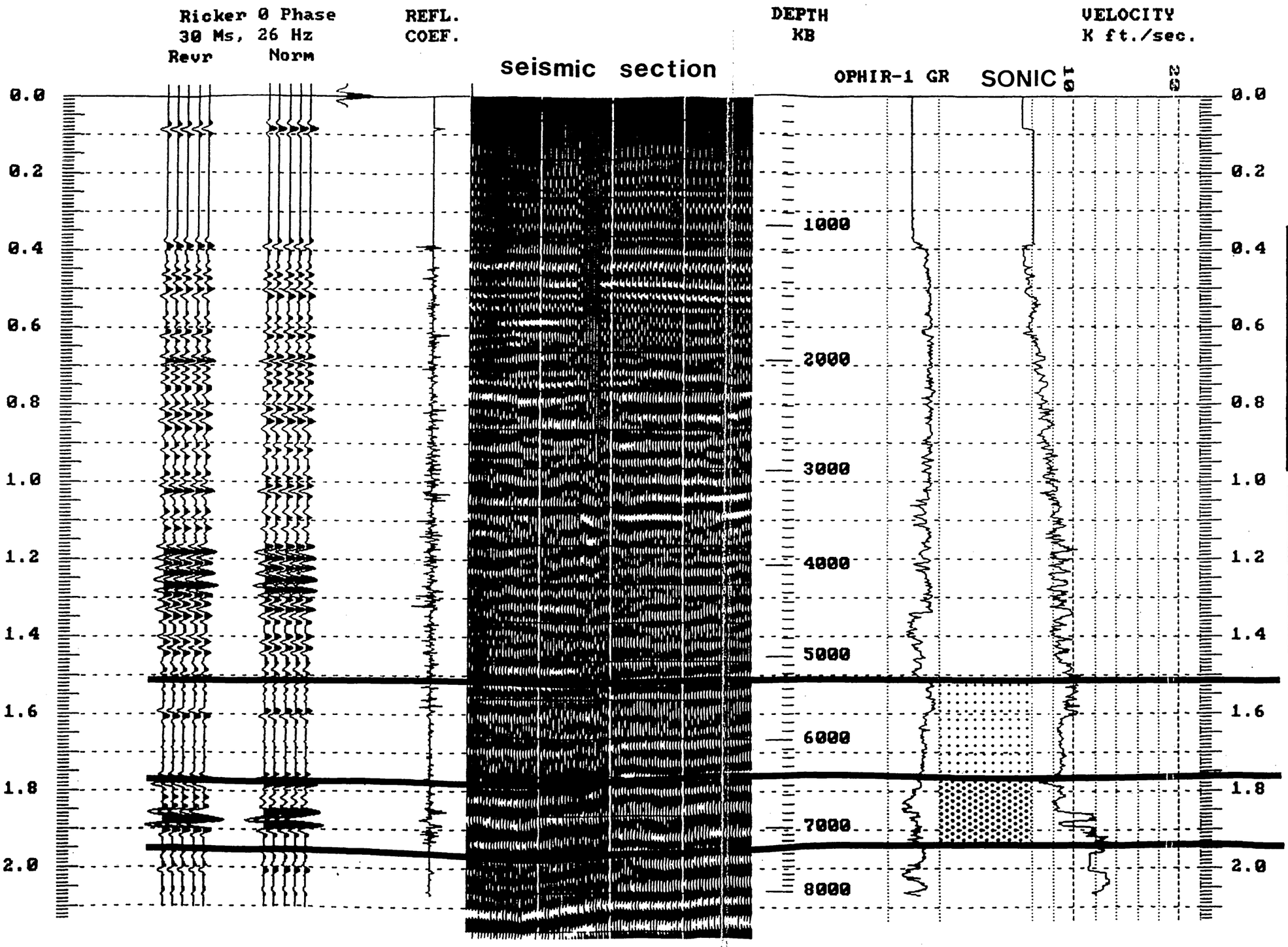


FIGURE 3-4

Synthetic Seismogram For Ophir-1 Showing Correlation Of Main Strata Surfaces. (Top, middle and base of the Pulai-II Formation correlate with Red(R), Blue(B) and Purple(P) seismic markers respectively)

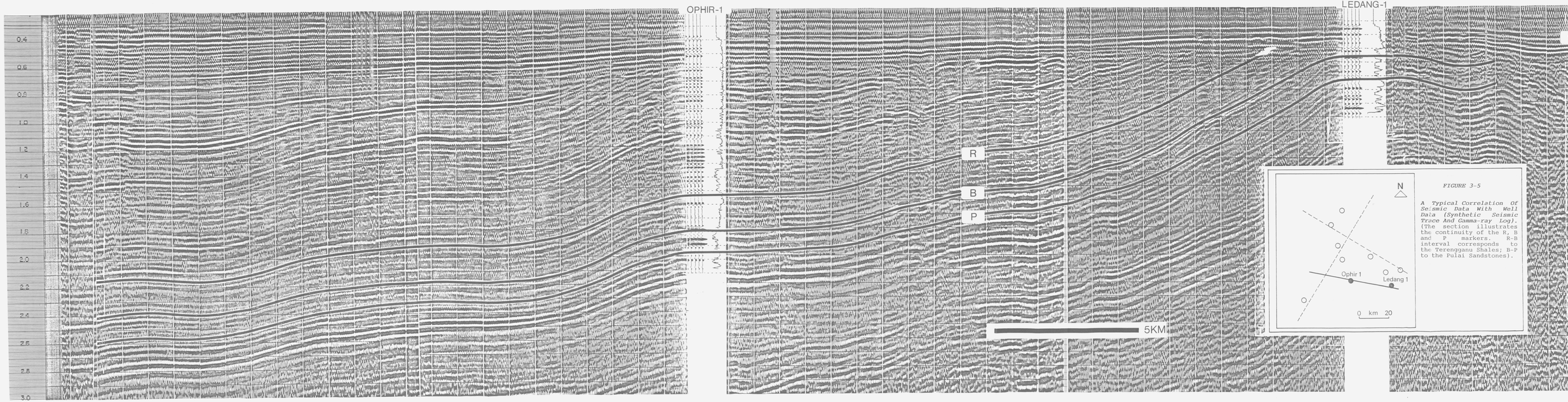


FIGURE 3-5

A Typical Correlation Of Seismic Data With Well Data (Synthetic Seismic Trace And Gamma-ray Log). (The section illustrates the continuity of the R, B and P markers. R-B interval corresponds to the Terengganu Shales; B-P to the Pulai Sandstones).

3.7.1.3 *Map Construction*

The depth sampling of the three seismic markers along a particular seismic section was made at every 1.5 to 3.0 km distance. Considering the grid density of the seismics used in this study (Fig. 3-1), and the observed structuring along a particular seismic section, the depth sampling in TWT at these distances was considered adequate.

Depth conversion of the seismic markers from TWT in seconds to metres was accomplished through the extrapolation from an average velocity-depth curve (Fig. 3-6). This velocity curve was obtained by plotting the checkshot well velocity survey data of Angsi-1, Duyong Barat-1, Ophir-1, Tinggi-1, Banggol-1, and Palas-1. These wells were chosen to represent the south, the central, the east and the northwestern parts of the study area. This method of depth conversion, and subsequently of determining the thickness of the formation, was recognised to have inherent inaccuracies, and as indicated earlier, inaccuracies were expected for the study of this scale. Fortunately, adequate well coverage enabled depths of the markers to be determined to check consistancy and accuracy of the conversion (Table 3-1).

Because this study was focused only on the Pulai-II Formation, only one structure map was constructed. This map was drawn on top of the Blue seismic marker (Fig. 2-5). Two isopach maps for the Red-Blue and Blue-Purple sequences were also constructed. These maps were used to predict:

1) The basinal setting at the time of the deposition of the Pulai-II sandstones, and

2) The sandstone provenance.

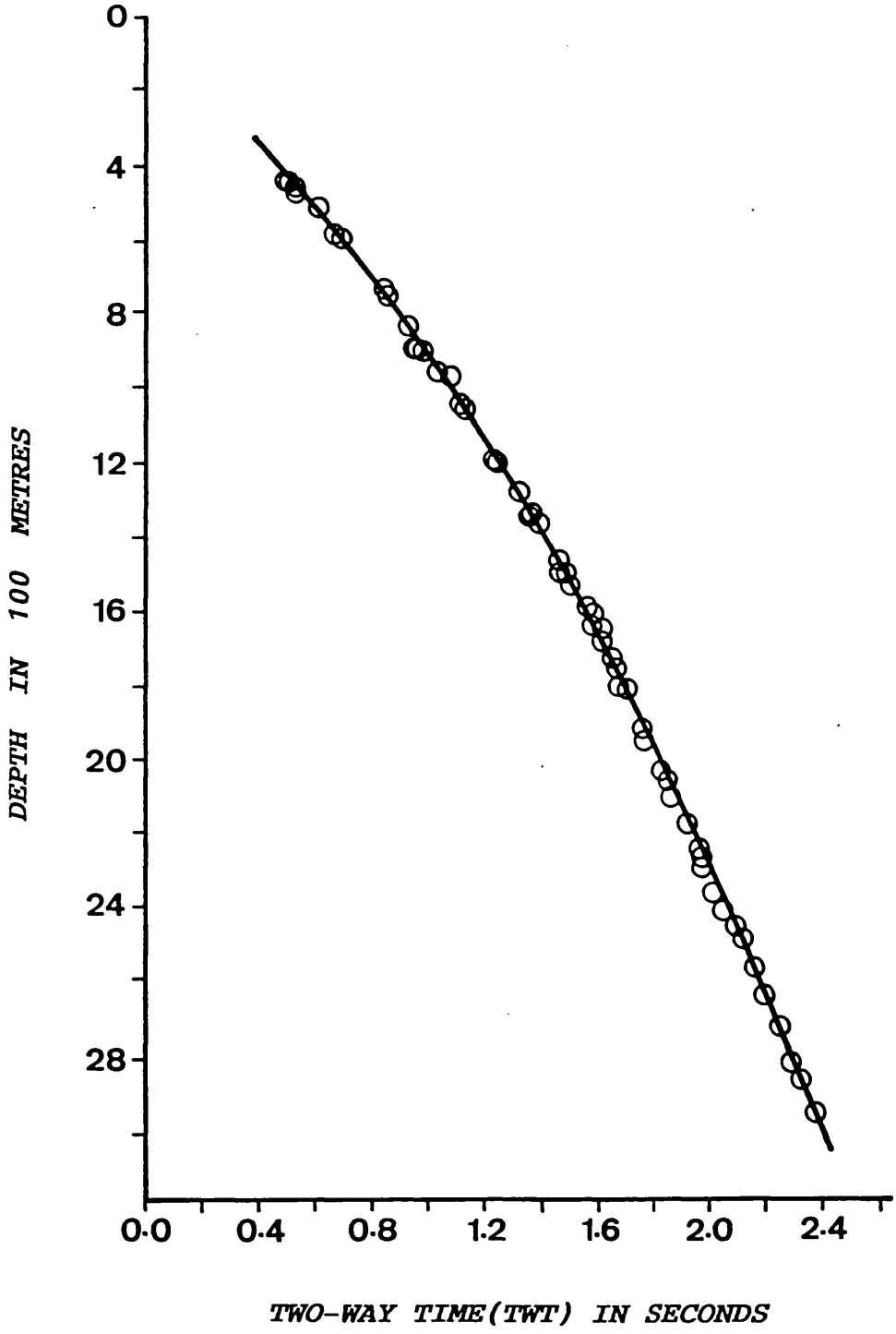


Figure 3-6 - Depth conversion curve used to convert TWT in seconds, to depth in metres. Curve was derived from five wells: Palas-1, Seligi-3, Ophir-1; Angsi-1 and Sotong 5G-5.1 from the north, northeast, centre and southern part of the study area.

Table 3-1 - Depths of Red, Blue and Purple seismic markers at various well locations in the study area. Measurement in metres from m.s.l.

Well Name	Red	Blue	Purple
Ledang-1	...	0480	0699
Belanga-1	1040	1199	1341
Belumut-1	1207	1308	1430
Peta-1	1213	1308	1414
Tiong-5	1955	2263	2581+
Seligi-3	1317	1506	1762
Tinggi-1	1416	1586	1787
Duyong 6H-32.1	1823	2088	2302
Dy. Barat-1	2862	2398	2566
Besar-1	1664	2015	2266
Ophir-1	1586	1937	2220
Pulai-1	0936	1129	1356
Angsi-1	2064	2384	2625
Bekok-1	1596	1922	2230
Banggol-1	2491	2690	2866+
Sotong 5G-5.1	2012	2277	2311
Palas-1	2358	2617	2928
Tapis-2	1688	2048	2378+

\+ estimated depth

3.7.2 Facies

The facies of the Pulai-II Formation were analysed by means of seismic, geological log and core data.

3.7.2.1 *Seismic Facies*

The techniques employed by Mitchum et al, (1977) and by Shell Oil Company (1987) were used:

1) To study seismic facies units,

2) To predict the seismic facies unit distribution, and

3) To interpret their environments of deposition.

These involved the recognition and differentiation of seismic facies units within the Red-Blue and Blue-Purple depositional sequences of the Pulai-II Formation. However, because:

1) The majority of the seismic data used in this study are old,

2) The geophysical parameters employed in acquisition and processing of the seismics are also old, reflecting state-of-the-art technology of 1968-75, and

3) The primary objective of processing at that time was aimed at detecting structural anomalies,

Much of subtle stratigraphic features on the seismic sections could not be discerned. Steep dips produced by folding and intense faulting in some areas made the interpretation more difficult. Squeezing of the seismic sections did not facilitate much in the recognition seismic characters (Fig. 3-7). However, based on the available data, it was possible to distinguish and map four types of seismic facies within the formation. These are:

1) Type I - discontinuous high and low amplitude seismic signatures in generally low amplitude seismic background (Fig. 3-8),

2) Type II - continuous low amplitude signatures in generally low amplitude seismic background, but with occasional occurrences of continuous and high amplitude signatures (Fig. 3-9),

3) Type III - one- and occasionally two-cycle, high amplitude signatures which diffuse laterally into low amplitude medium at one end, and at the other either terminate against high amplitude

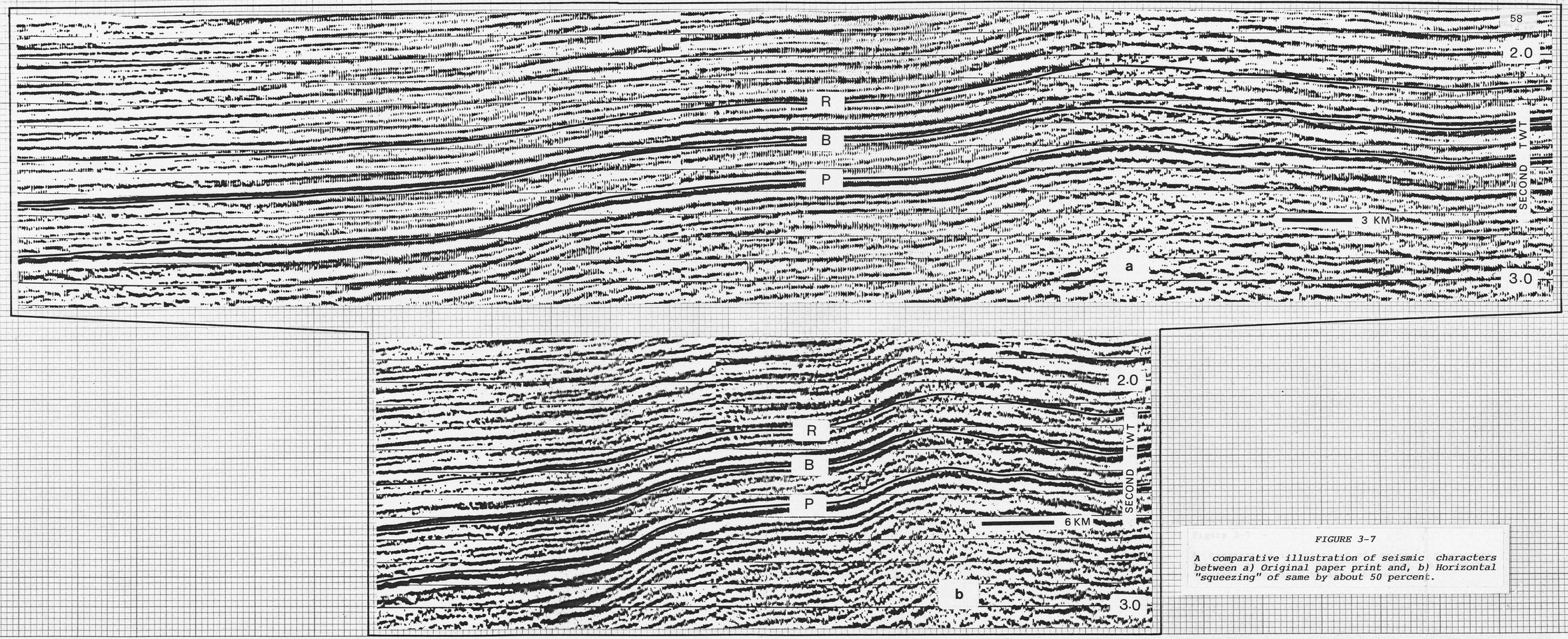


FIGURE 3-7

A comparative illustration of seismic characters between a) Original paper print and, b) Horizontal "squeezing" of same by about 50 percent.

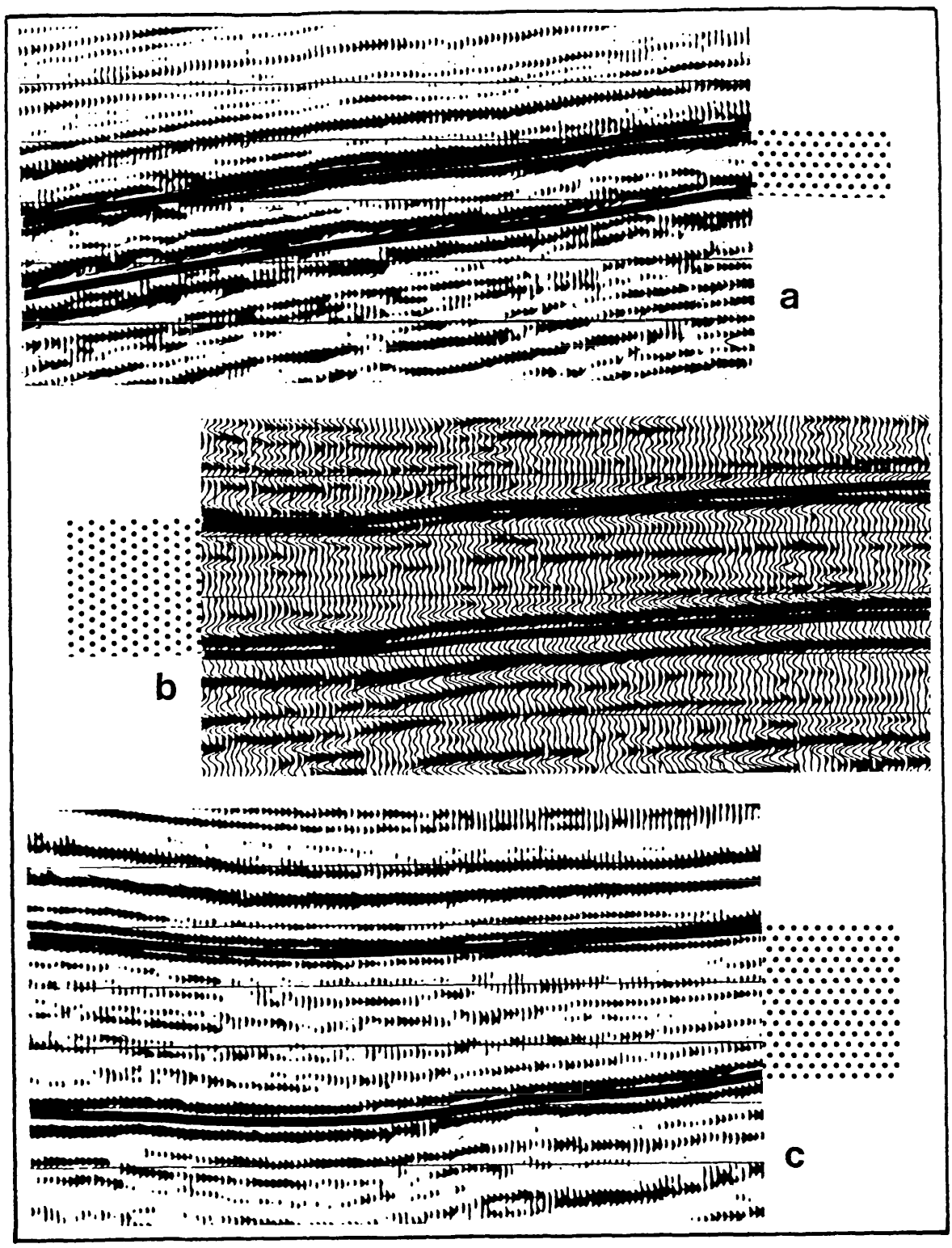


Figure 3-8 - Type I seismic facies. Note the discontinuity of characters within marked interval in a), b) and c).

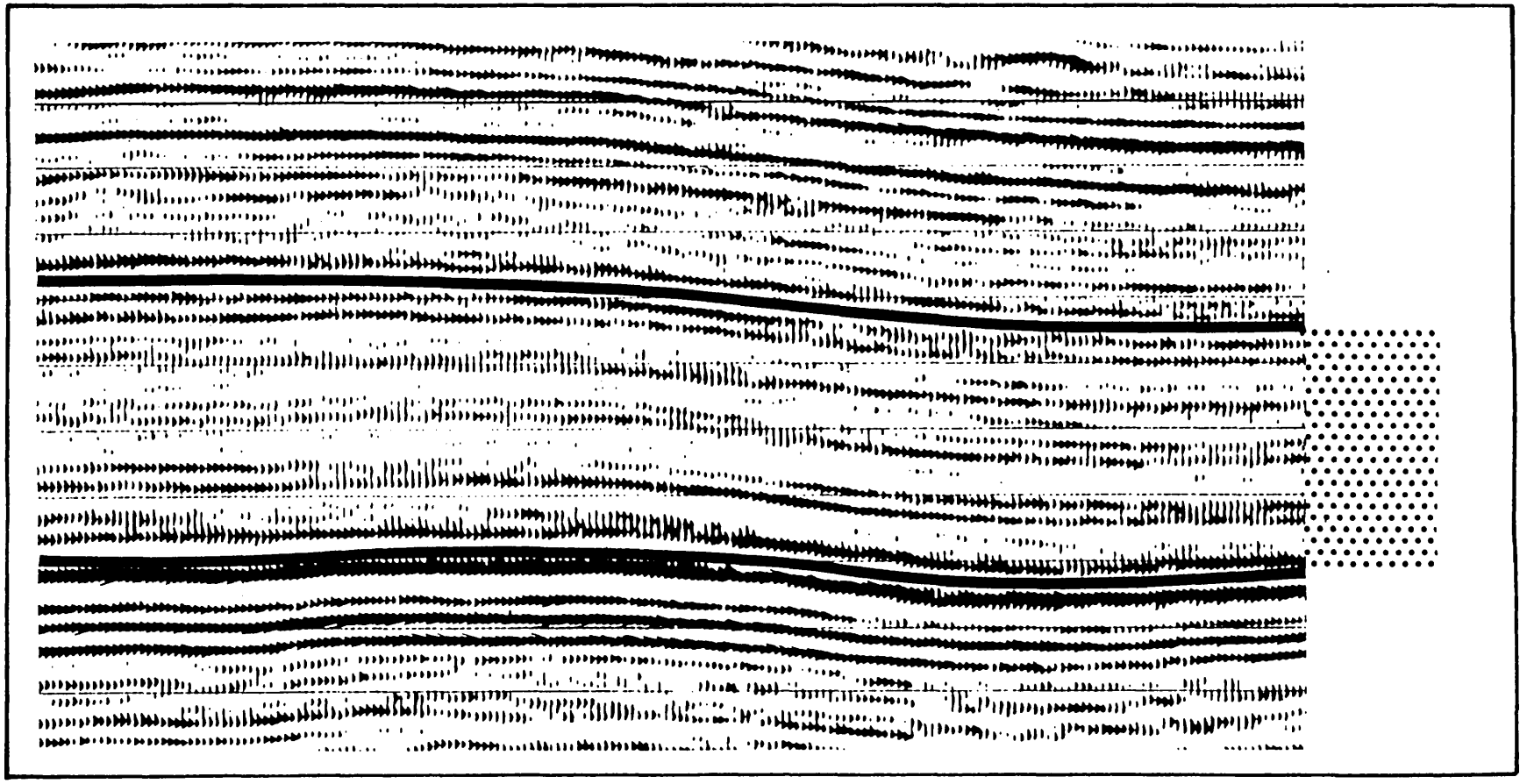


Figure 3-9 - Type II seismic facies. Note the generally low amplitude and continuity of characters within marked interval.

signatures or diffuse laterally into low amplitude medium (Fig. 3-10), and

4) Type IV - discontinuous low and continuous high amplitude signatures (Fig. 3-11).

3.7.2.2 *Geological Log Motifs*

The cores have been most useful in identifying facies and in interpreting environments of deposition. Sidewall cores and ditch cuttings have provided additional information on lithology and mineralogy of the sequence. But where cores were not available, facies and facies boundaries and subsequently their environments of deposition, were interpreted from geological log motifs. The gamma-ray logs, in conjunction with the resistivity logs, were used extensively for this purpose, although SP logs were also used where it was thought that the gamma-ray curves were suspect (Fig. 3-12).

In the determination of sandstone and shale bodies from the gamma-ray log, maximum deflection of the curve, which is conventionally to the left, was taken to consist essentially of sandstones, and likewise, the maximum deflection to the right was taken to indicate shales (Selley, 1985) (Fig. 3-13). Where the curve was suspect due possibly to high content of radioactive minerals (mica, zircon or glauconite) or clay pebbles (Figs. 3-12 and 3-13), the SP log was used along with the gamma-ray log. Where the demarcation for the sand-shale boundary was not clear, cores were used to calibrate the boundary, but where cores were not available, a 50-percentile sand-shale median-line was drawn to distinguish and identify these boundaries (Fig. 3-14). This technique was used to determine net sand thicknesses (see Section 3.7.3.1).

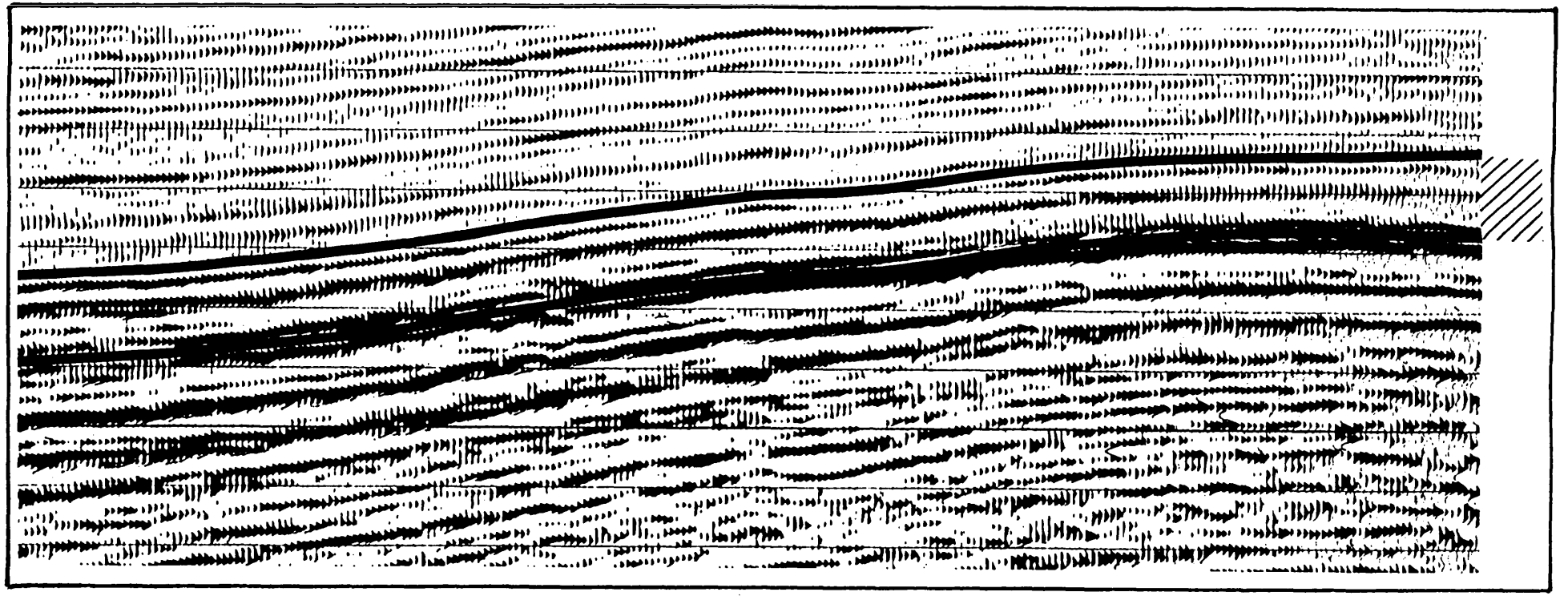


Figure 3-10 - Type III seismic facies. Note the gradual change of amplitude intensity within marked interval towards the left of the section.

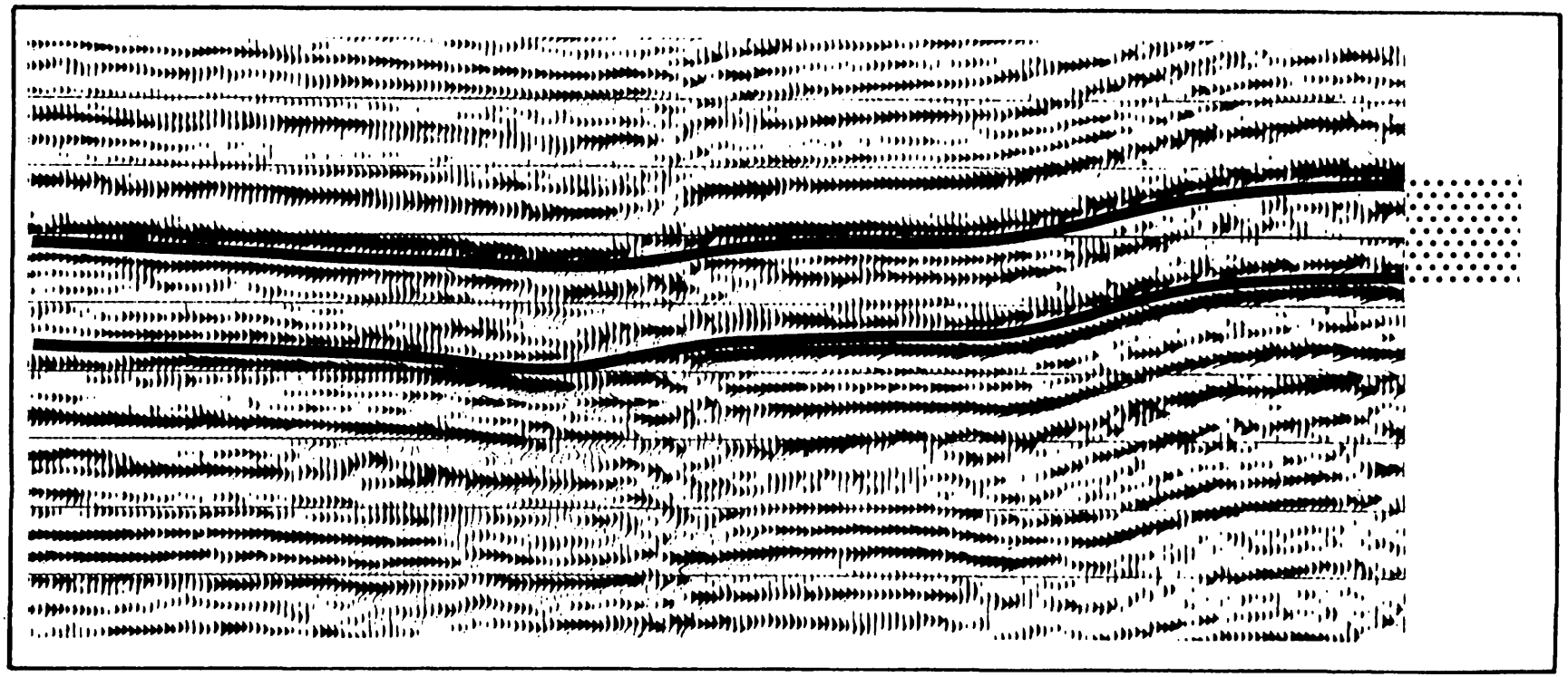


Figure 3-11 - Type IV seismic facies. Note the occurrence of concordant and discordant characters within marked interval.

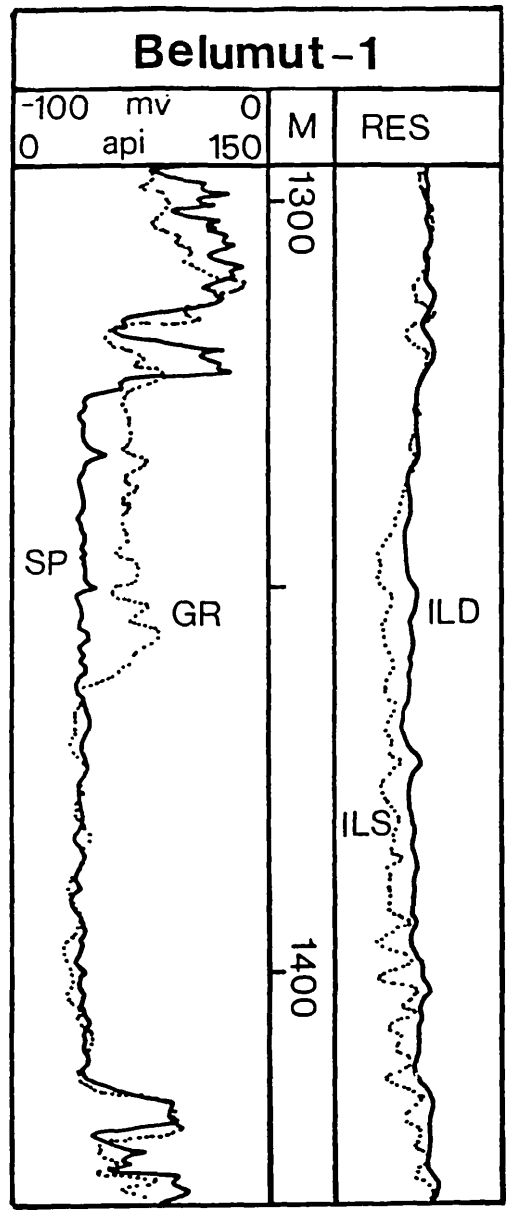


Figure 3-12 - Gamma-ray and S.P. logs of Belumut-1 displaying suspect gamma-ray reading in upper section of the sandstones.

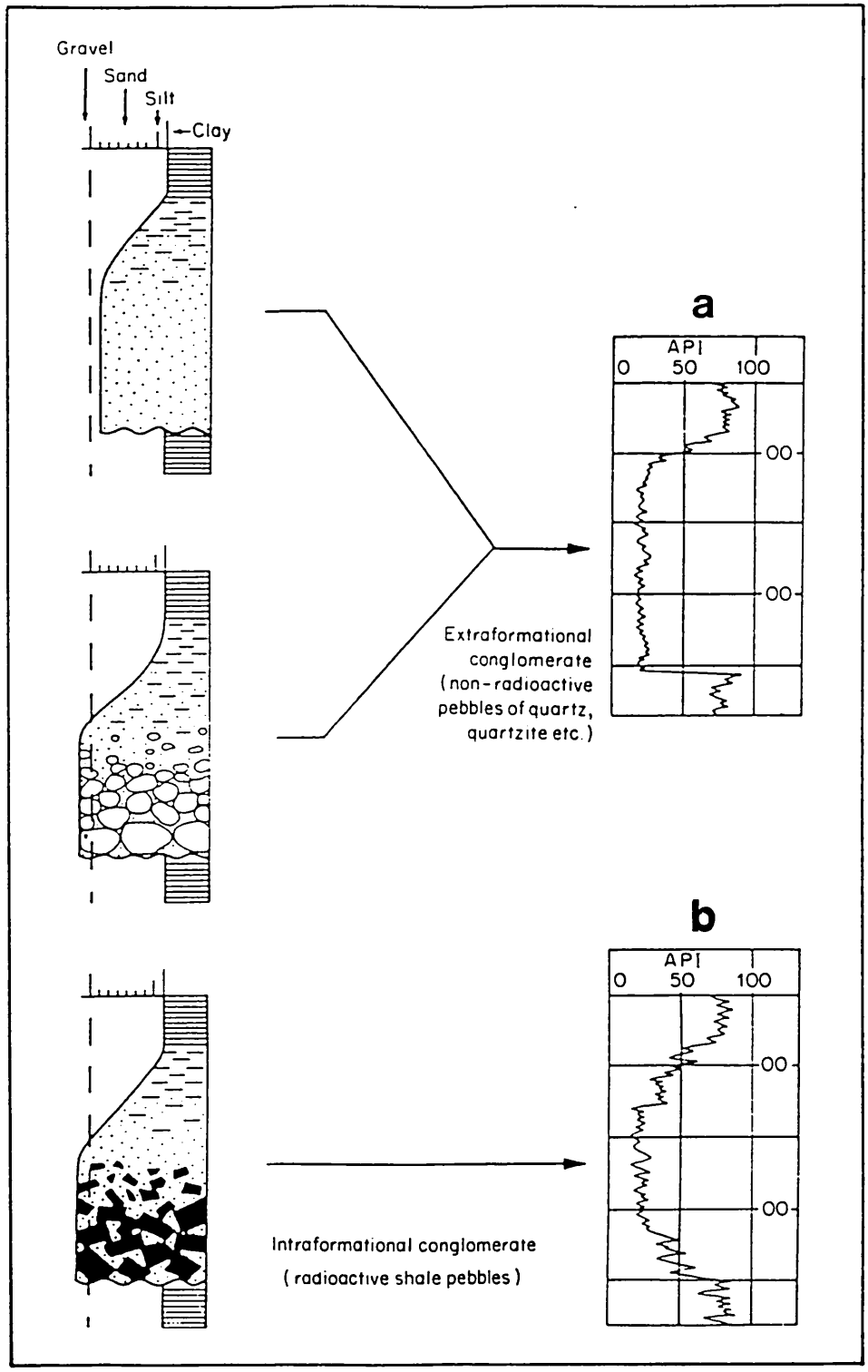


Figure 3-13 - Gamma-ray log motifs to indicate clastic lithofacies (from Selley, 1985).

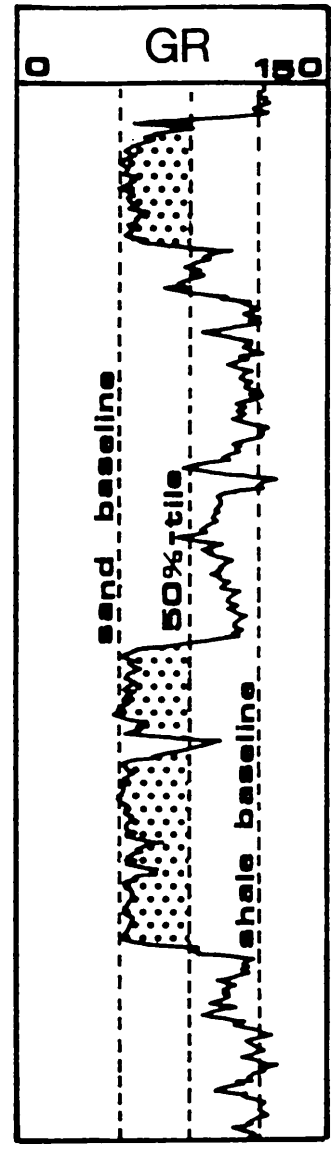


Figure 3-14 - An illustration to determine net sandstones in sand-shale sequence. A 50-percentile median baseline was drawn to demarcade sand interval from shale interval in a sandstone-shale sequence.

In studying the facies and interpreting their environments of deposition, references were made to:

1) The availability of cores,

2) The studies of facies thickness and their vertical grain size evolution by Selley (1985) (Fig. 3-15) and

3) The studies of log motifs principally by Coleman and Prior (1982) and Galloway and Hobday (1983) (Fig. 3-16).

Geological log motifs have three basic log shapes (Fig. 3-17):

1) Cylindrical-shaped profile which generally indicates either thick homogeneous sequence bounded above and below by argillaceous sediments or channel fill with abrupt top and base, such as tidal and braided channel fills,

2) Bell-shaped profile which normally indicates an upward fining sequence and relates to channel fills, and

3) Funnel-shaped profile which normally indicates an upward coarsening sequence, and which is normally associated with progradation of deltas, regressive shallow marine bars, and barrier bars.

Modifications to these general log shapes are common, reflecting the changing circumstances of the environments within which the sediments were being deposited.

Within the Pulai-II Formation, four different log motifs or log facies are apparent (Fig. 3-18):

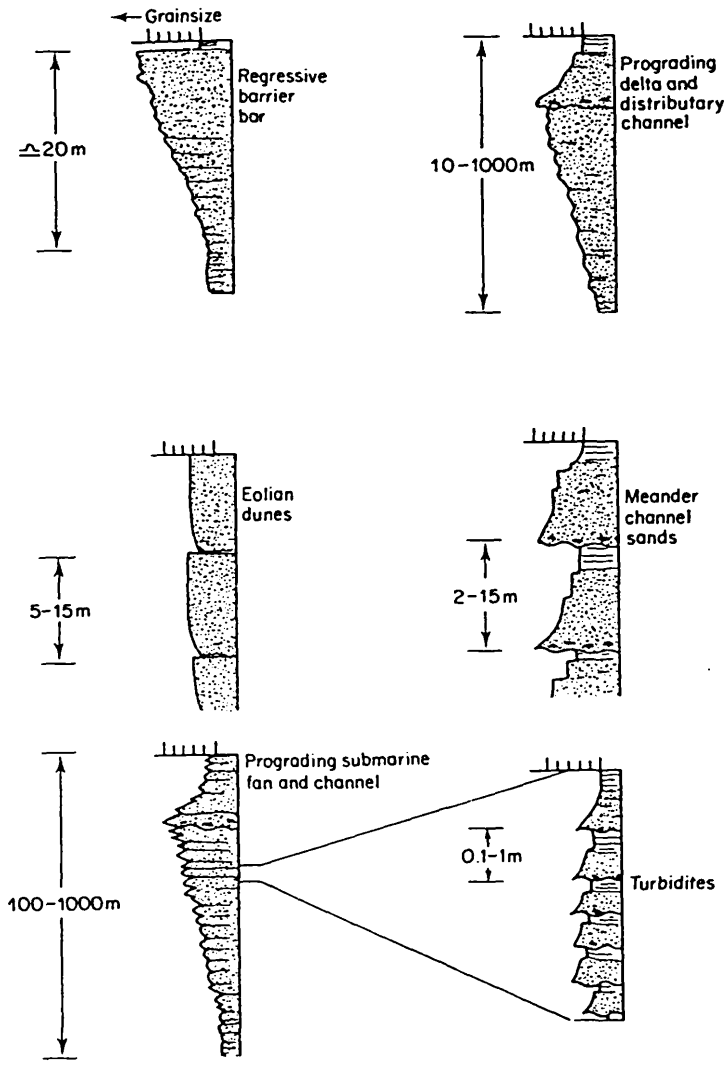


Figure 3-15 - Vertical grain size evolution in sandstones as indicators of environments of deposition (from Selley, 1985).

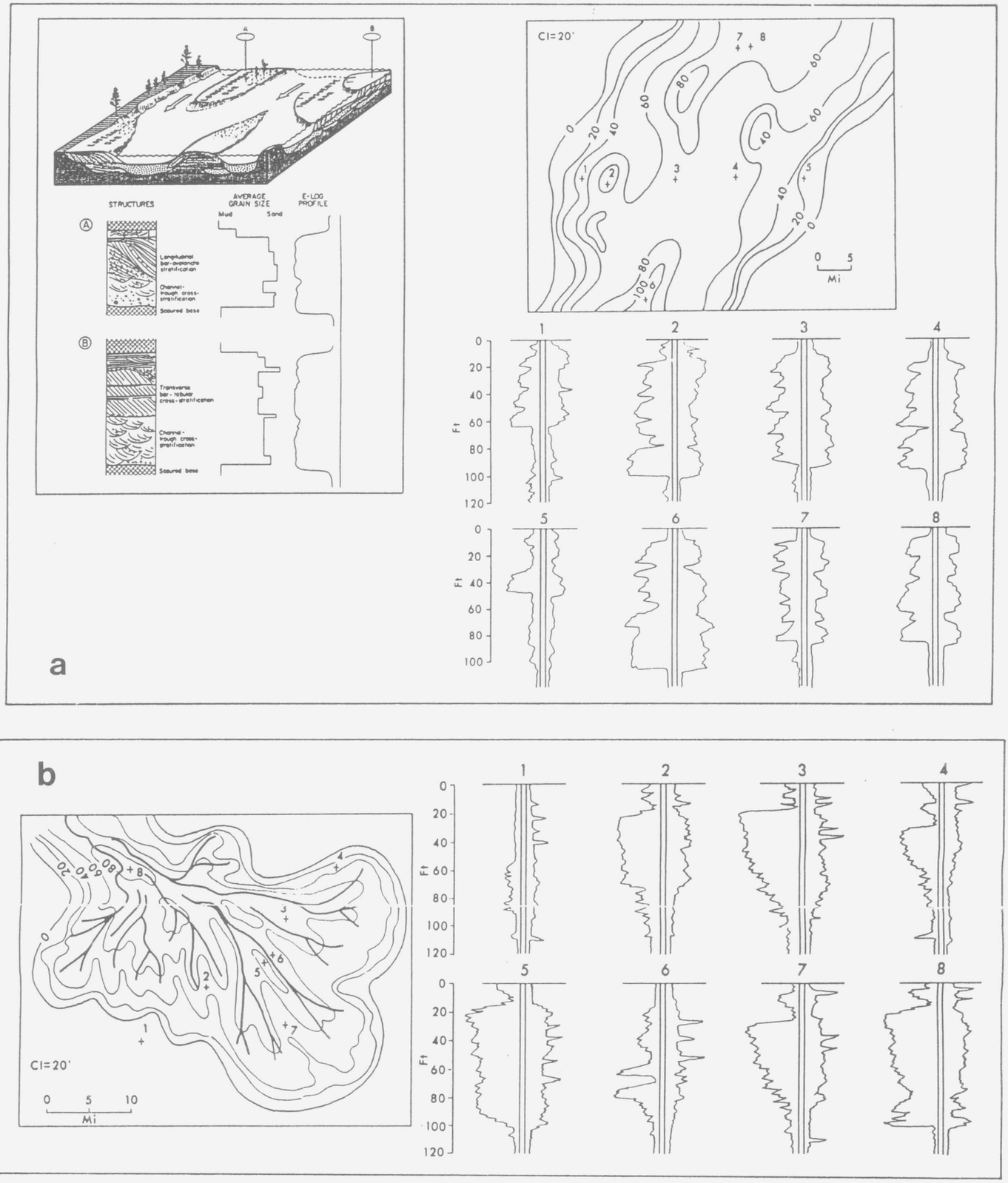


Figure 3-16 - Some examples of log motifs as indicators of facies and environments of deposition typically within: a) braided channel systems in upper deltaic/alluvial plain setting; b) lower coastal/deltaic setting (from Coleman et al, 1982; and Galloway et al, 1983).

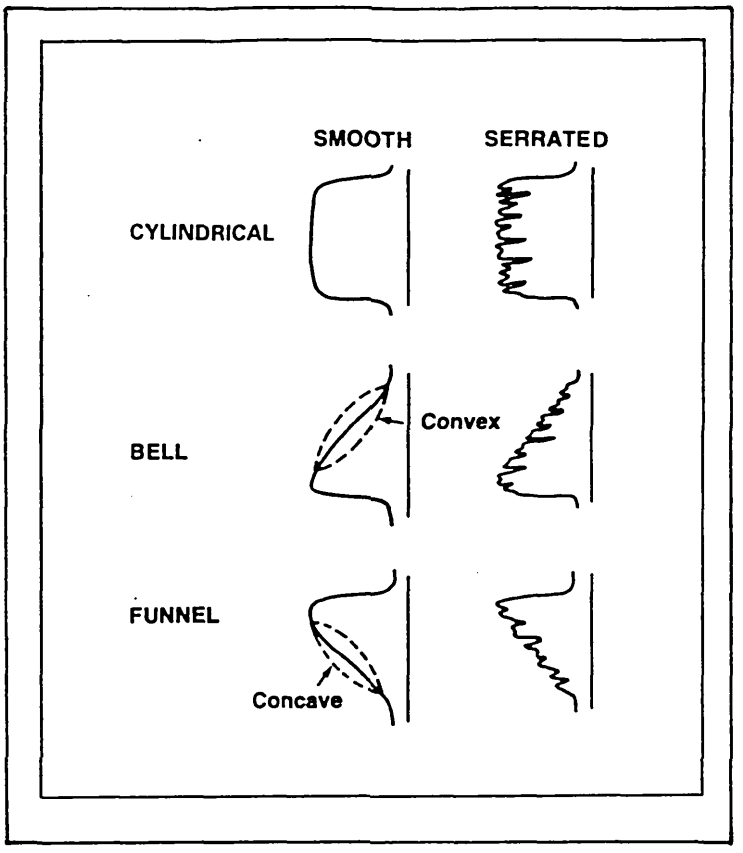


Figure 3-17 - Three basic log motifs of sandstones.

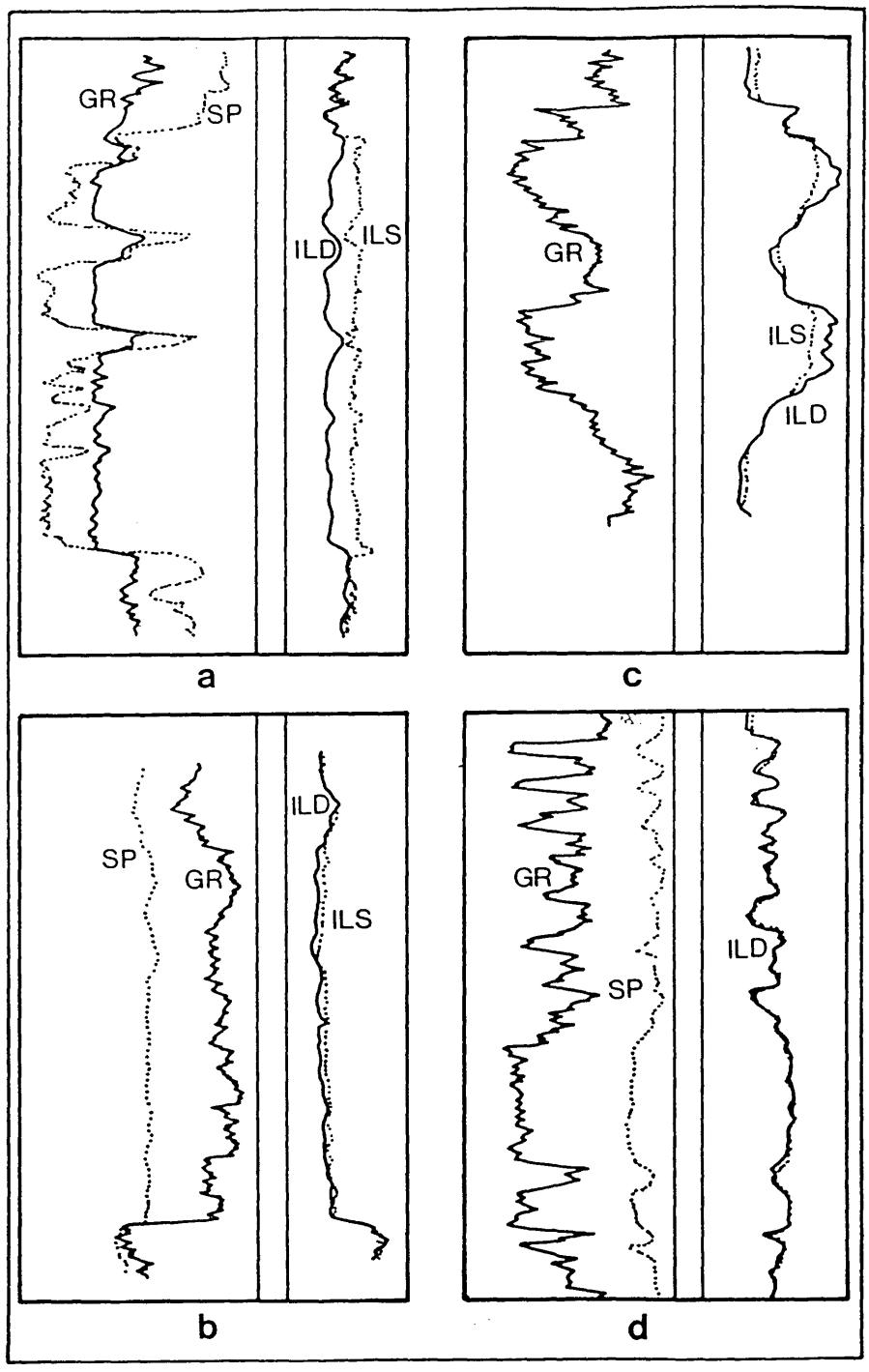


Figure 3-18 - A display of four gamma-ray log motifs of the Pulai-II Formation: a) Motif A which is predominantly blocky motif; b) Motif B which is essentially "flat", but occasionally serrated motif; c) Motif C displying a funnel-shaped motif and d) Motif D displaying serrated and blocky motif.

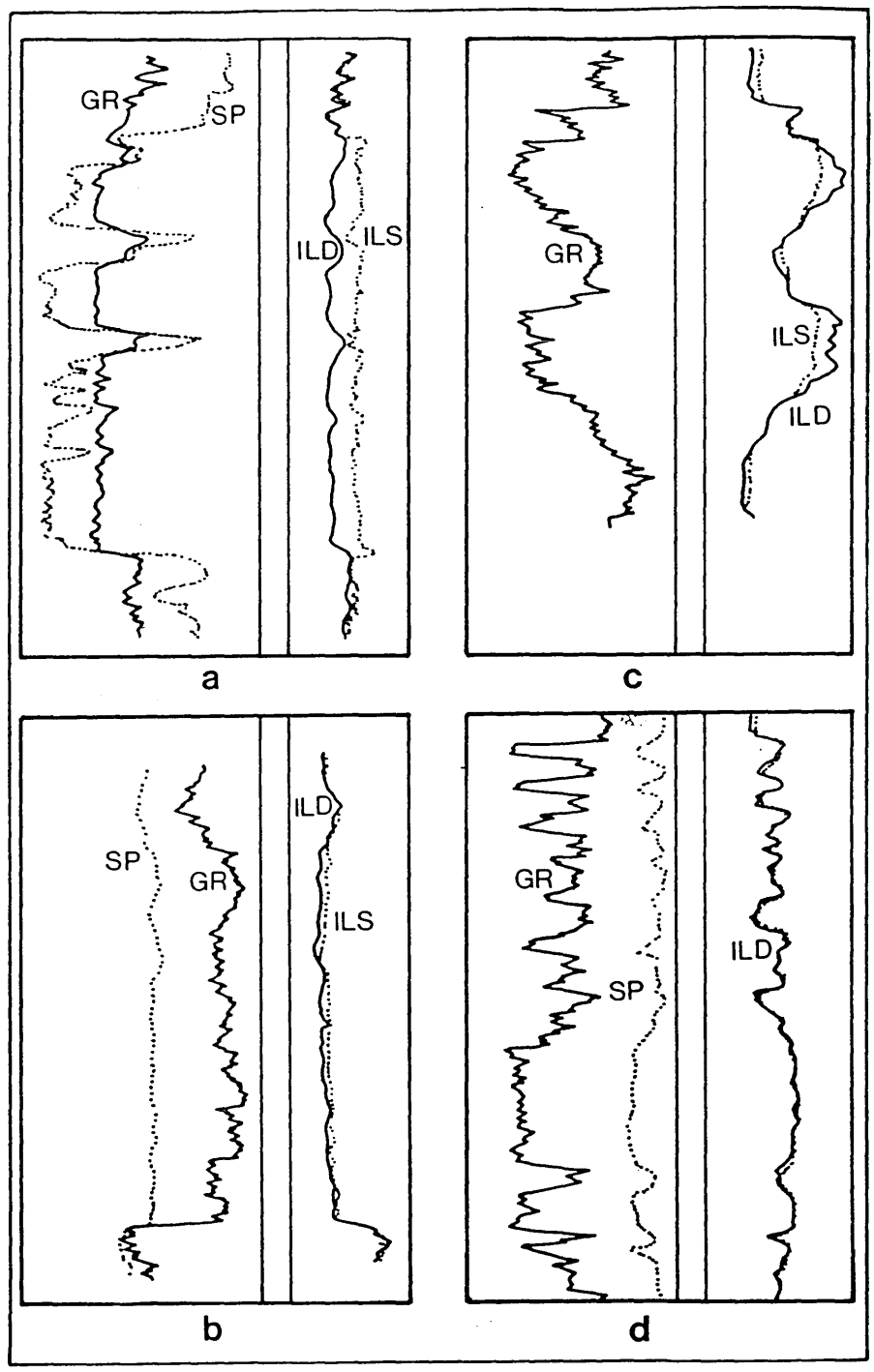


Figure 3-18 - A display of four gamma-ray log motifs of the Pulai-II Formation: a) Motif A which is predominantly blocky motif; b) Motif B which is essentially "flat", but occasionally serrated motif; c) Motif C displying a funnel-shaped motif and d) Motif D displaying serrated and blocky motif.

1) Motif A - a generally sandstone-rich sequence normally characterised by blocky gamma-ray log facies, with sharp bases and either sharp top deflections or upward-fining tops. Each unit measures up to 130 metres thick,

2) Motif B - a shale-rich sequence normally characterised by flat, occasionally serrated gamma-ray log,

3) Motif C - a funnel-shaped, upward-coarsening sandstone sequence, with the thickness of each sequence normally not exceeding 30 metres, and

4) Motif D - a sequence of interbedded sandstones, siltstones and shales or mudstones, and massive sandstones of blocky log pattern. Generally, the interbedded sequence exhibits an upward-coarsening profiling, but within each of the sandstone units in the sequence, an upward-fining pattern is apparent. The sequence of interbedded sandstones, siltstones and shales often appears cyclic, with each cycle generally not greater than 50 metres.

3.7.2.3 *Log Correlation*

In correlating the stratigraphic units of the formation, emphasis was placed on the recognition of the overall stratal geometry in cross-sections, rather than the positions of a few litho-stratigraphic tops. This correlation involved the following:

1) Marking on each log profiles the depositional boundaries which represent the Red, Blue and Purple seismic markers. (The Red-Blue depositional sequence represents the Terengganu Shales (Unit IIB) and the Blue-Purple sequence represents the Pulai Sandstones (Unit

IIA upper)),

2) Performing group stratal character matching, taking into consideration lateral facies variations. This process allowed further subdivision of the depositional sequences each into two parasequences or sub-members, Figure 2-12, consisting of the following:

   a) Upper Terengganu Shales,

   b) Lower Terengganu Shales,

   c) Upper Pulai Sandstones, and

   d) Lower Pulai Sandstones.

3.7.2.4 *Stratigraphic Modelling*

The main objective of stratigraphic modelling was two-fold:

1) To examine whether the generated stratigraphic model resembles the major characters of the seismic sections, and

2) To test and refine the concept of the stratigraphic framework developed for the Pulai-II Formation.

In the modelling exercise, three stratigraphic cross-sections were selected for the test:

1) Section A which contains Banggol-1, Palas-1 and Tapis-2. This section roughly parallels the regional seismic line 68-121,

2) Section B which contains Palas-1, Tiong-5, Bekok-1 and Ophir-1, and

3) Section C which contains Belumut-1, Tinggi-1, Seligi-3 and Bekok-1.

The GMA modelling package was used to generate synthetic seismic cross-sections (see Section 3.7.1.1). Figure 3-19 illustrates a typical resultant cross-sectional stratigraphic model. The section was displayed in two versions: sonic log traces and seismic traces, for easy recognition of the formation.

3.7.3 Pulai-II Sandstones

The study of the sandstones includes construction of facies and net sandstone maps, examination of cores by XRD and SEM, and determination of porosity through thin section and wireline logs (neutron-density and/or sonic).

3.7.3.1 *Sandstone Distribution*

The prediction of sandstone distribution within the Pulai-II depositional parasequences was made primarily by integrating seismic facies maps with log facies maps and by constructing net sandstone maps. Facies map intergration was by way of superimposing the seismic facies map with the log facies map for each sequence. With the known net sandstones at each of the sixteen wells (Table 3-1), these maps help to delineate areas likely to contain good sandstone development.

3.7.3.2 *Sandstone Quality*

The quality of the Pulai-II sandstones was determined directly from the cores and indirectly from the wireline logs. Burial profiles were constructed to determine if overburden (and subsequently temperature)

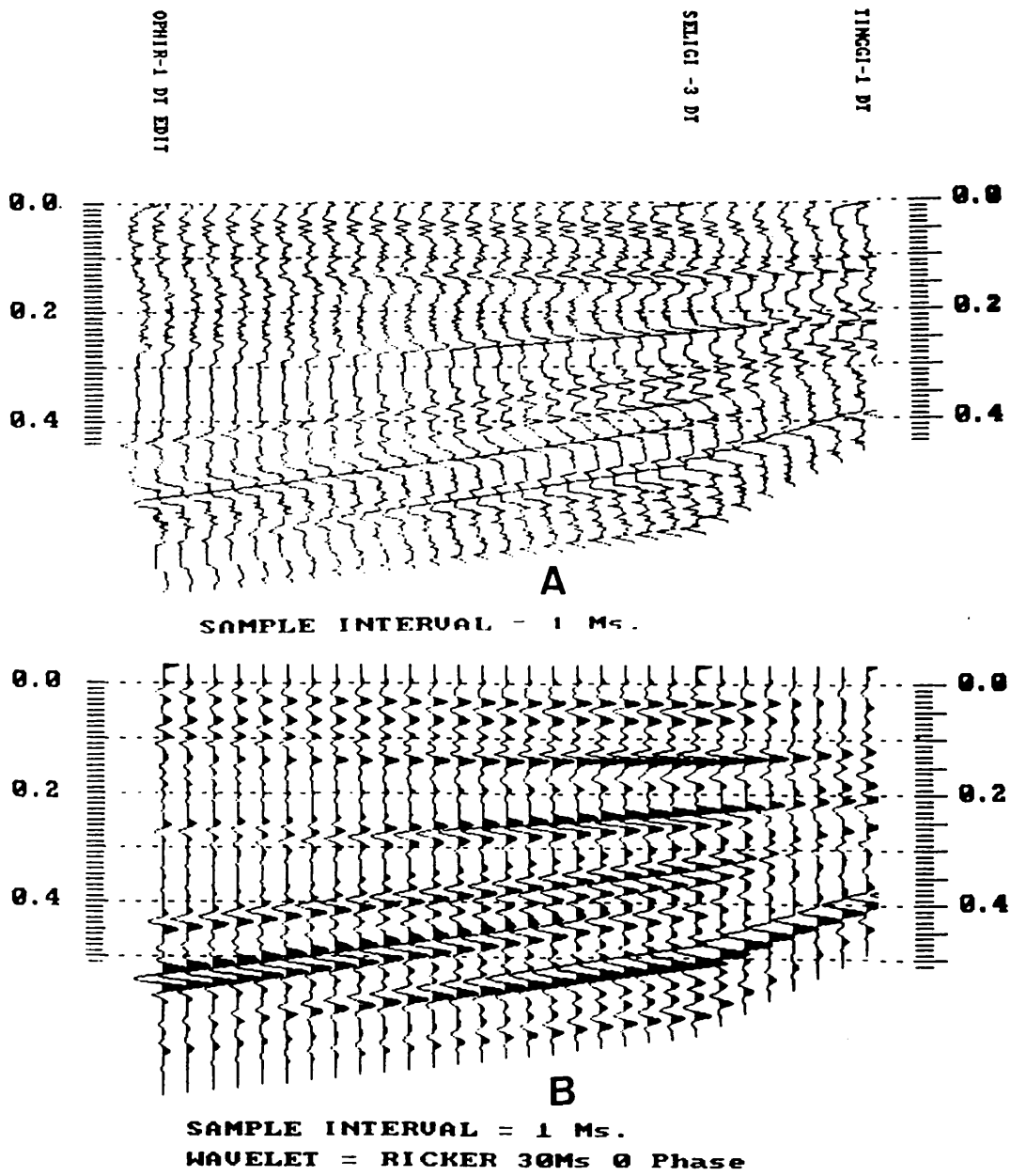


Figure 3-19 - An illustration of a typical resultant stratigraphic model displayed in two versions: A) sonic log trace, and B) seismic trace.

significantly determined the porosity development in the sandstones. In this study the following techniques were used to determine the sandstone quality:

1) Examination of cores under polarising microscope and SEM, to estimate porosity and to determine minerology,

2) Determination of clay and other authigenic minerals through XRD,

3) Determination of total porosity from wireline logs using PEP II computer programme, and

4) Construction of burial profiles at each well to determine maximum depths of burial.

- **Polarising Microscope**

The preliminary examination of some thin sections indicated numerous occurrences of oversized pores, molds with remnant, dark brown rims, and highly altered framework grains. Because:

1) There was no way to account for the types of framework grains loss through dissolution, and

2) The difficulty to identify the origin of some highly altered framework grains,

It was decided that determination of sandstone compositions was to be based on visual estimation. Therefore when estimating the composition of the sandstones, the following assumptions were made:

1) That altered framework grains with disseminated tiny aggregates of

microcrystalline quartz were considered as originally being chert. (Shanmugam et al, 1988). All other altered grains which did not give any indication of their origin, were considered as the grains of feldspars, because relatively, feldspars are more prone to alteration than chert (Schmidt et al, 1979), and

2) That no grains of any mineralogy were assigned to oversized pores.

- **XRD**

In the analysis, a set of 35 XRD spectra for the whole rock samples and a total of four sets, each of 78 XRD spectra, for the clay-sized samples, were obtained. The approach to the analysis of the XRD spectra was as follows:

1) For the whole rock samples:

   i) Spectra of the standard minerals were obtained for comparison and calibration purposes. These are the spectra for quartz, K-feldspar, plagioclase, kaolinite, chlorite, illite, smectite, calcite, ankerite, siderite, baryte, apatite, pyrite, and limonite,

   ii) The minerals present in each of the samples were identified by matching the spectra of the samples (Figs. 3-20 and 3-21), with the spectra of the standard minerals,

   iii) The relative abundance of the minerals in the samples were determined by measuring the relative intensities and by applying appropriate weightages of one selected peak for each mineral (Table 3-2) (J. Huggett, personal communication, 1988).

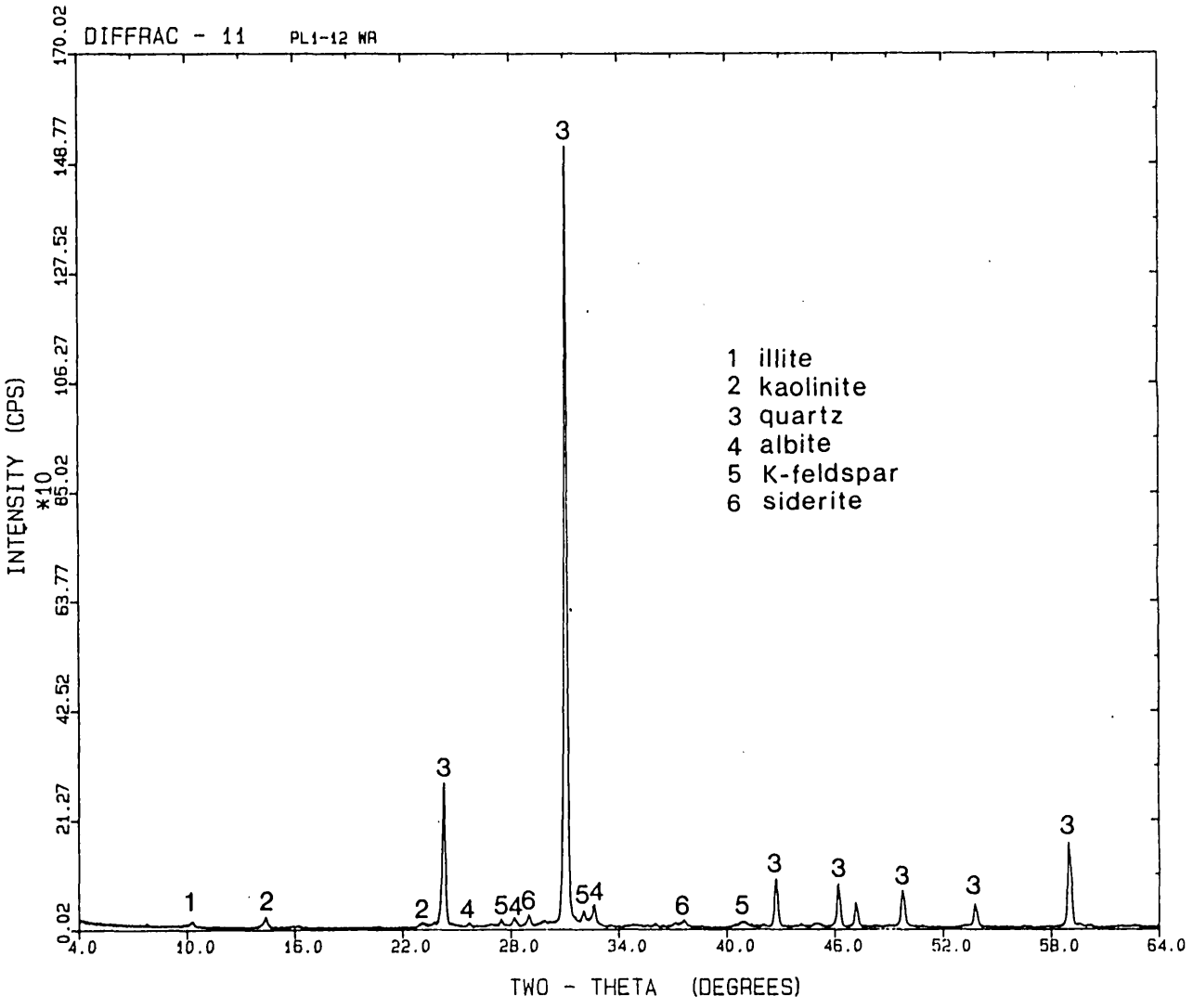


Figure 3-20 - A typical XRD spectrum of whole rock sample from the Pulai-II sandstones. Sample from Pulai-1 at depth of 1191.2 metres.

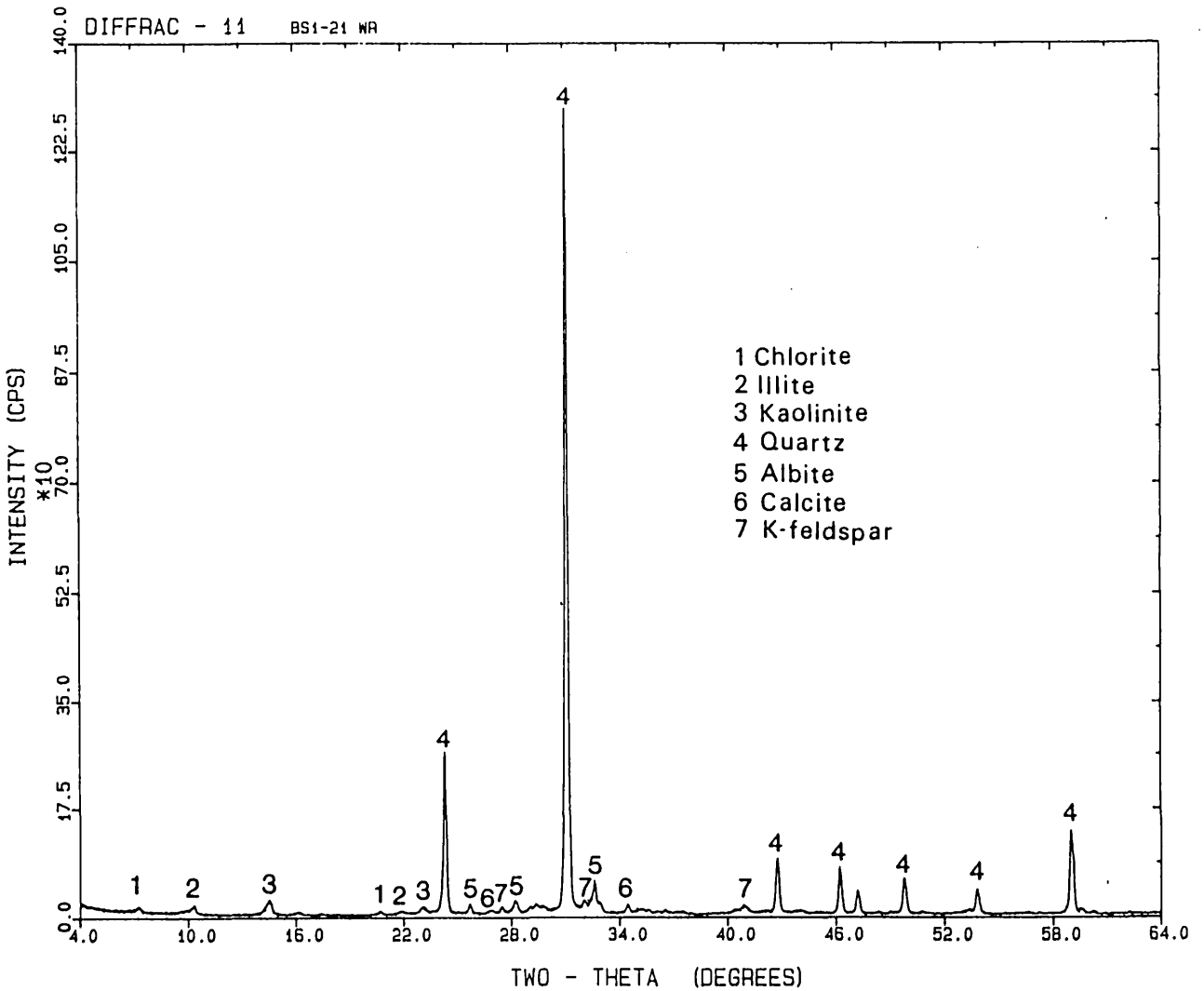


Figure 3-21 - A typical XRD spectrum of whole rock sample from the Pulai-II sandstones. Sample from Besar-1 at depth of 2128.1 metres.

Table 3-2 - Selected D-spacings of the minerals and their respective weightages for semi-quantification.

Mineral	D-spacing Angstron	Weightage*
Chlorite	14.00	1.0
Smectite-Illite	10-14.00	1.0
Illite	10.00	1.0
Apatite	8.13	1.0
Kaolinite	7.10	0.5
Quartz	4.26	1.0
K-feldspar	3.24	0.2
Plagioclase	3.19	0.2
Baryte	3.10	0.5
Calcite	3.03	0.5
Ankerite	2.89	0.5
Siderite	2.79	0.5
Geothite	2.75	1.0
Pyrite	2.71	0.4

* From J. Huggett, BP Research, Sunbury.

2) For the clay-sized fractions:

i) D-spacings for most of the commonly known clay minerals were searched (Table 3-2),

ii) The spectra were analysed, and based on the responses of the clay minerals to glycolation and heat treatments, corresponding clay minerals were identified (Figs. 3-22 and 3-23), and

iii) The relative amounts of the minerals in the samples were determined using the same approach as that for the whole rock samples.

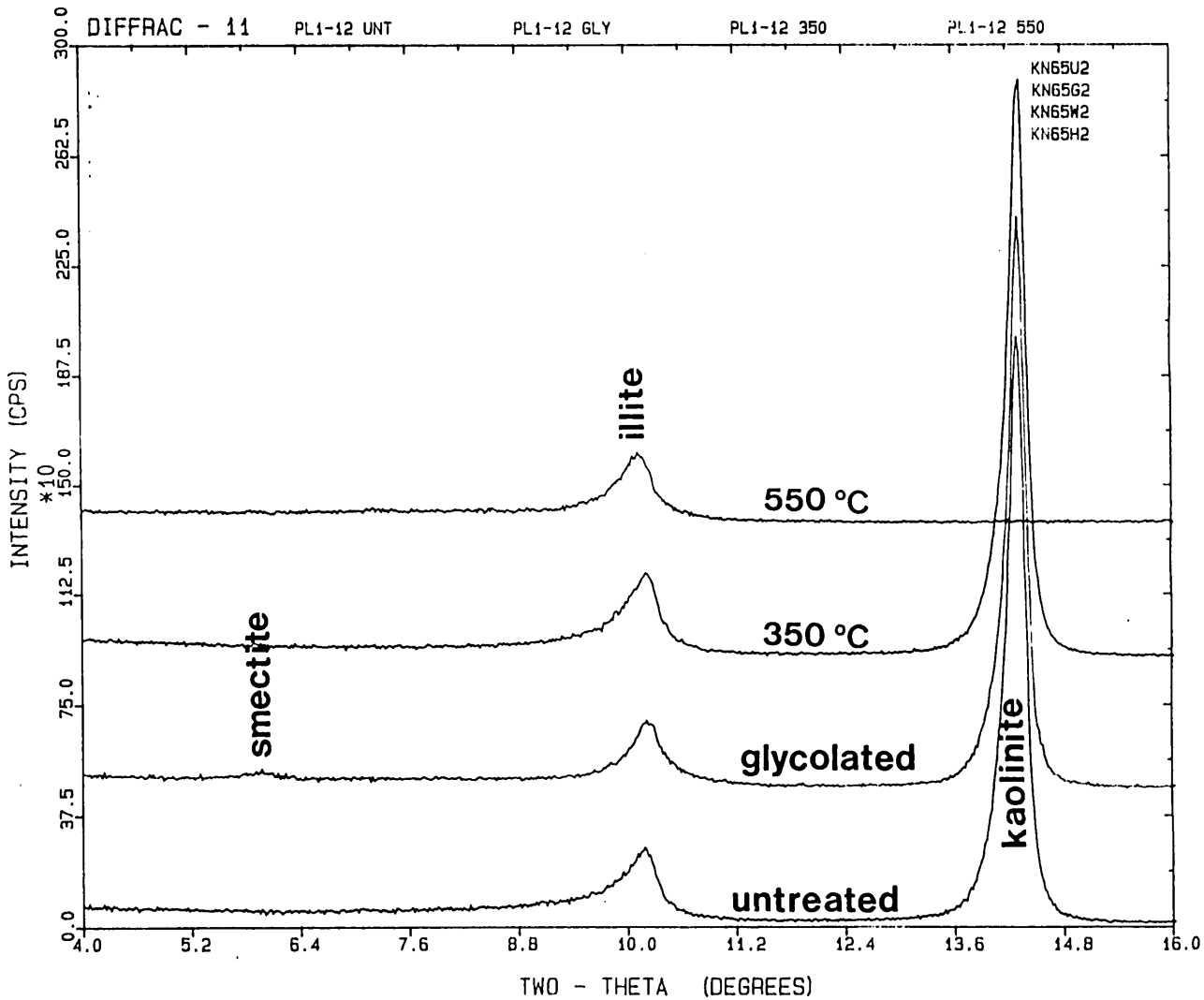


Figure 3-22 - A typical XRD spectra of clay-sized fraction of the Pulai-II sandstones under various treatments: untreated or air-dried at room temperature; glycolated; and heat-treated at 350°C and at 550° C. Sample from Pulai-1 at depth of 1191.2 metres.

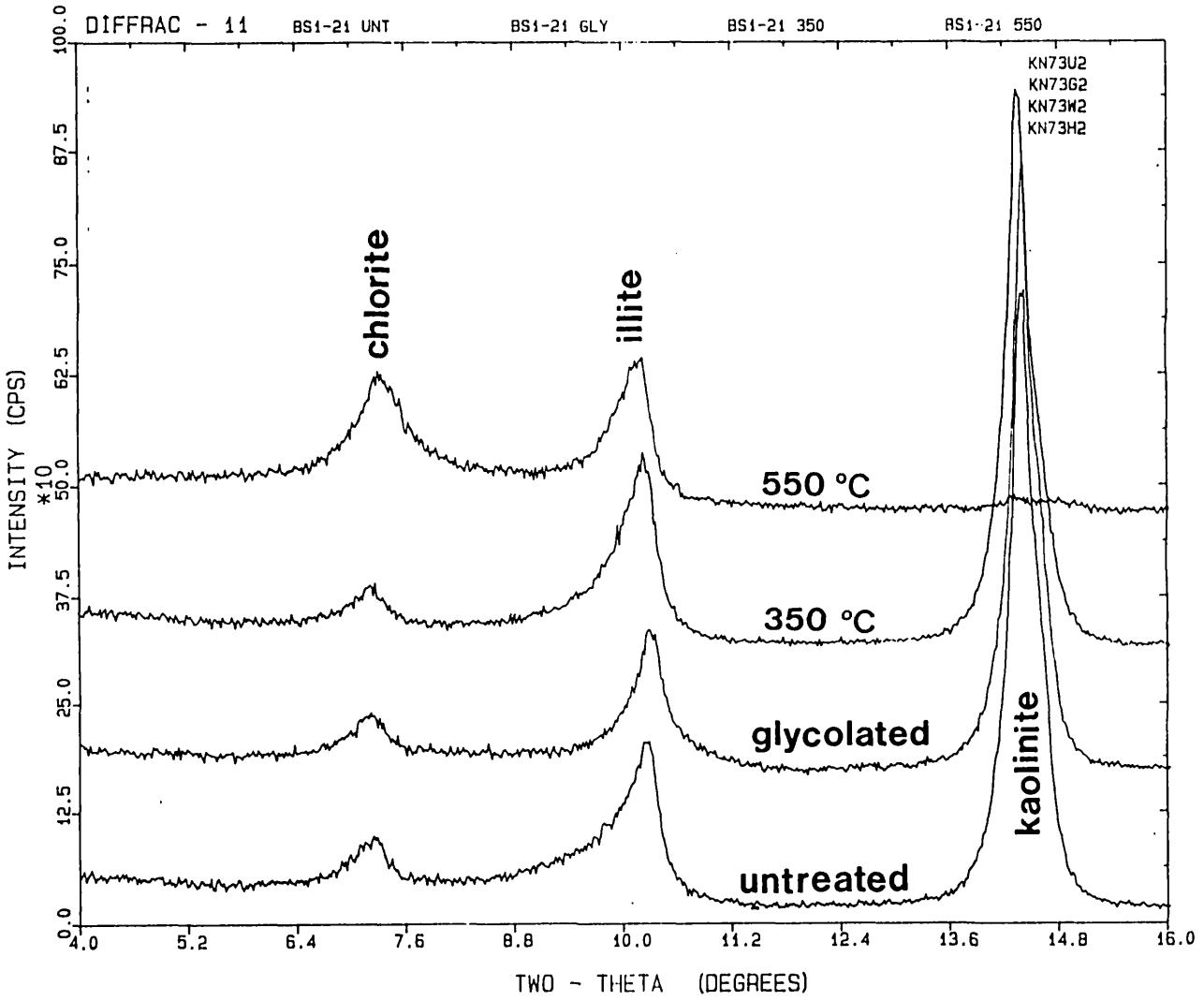


Figure 3-23 - A typical XRD spectra of clay-sized fraction of the Pulai-II sandstones under various treatments: untreated or air-dried at room temperature; glycolated; and heat-treated at 350°C and at 550° C. Sample from Besar-1 at depth of 2128.1 metres.

- **SEM**

This technique was used to study the diagenetic development of the sandstones. Recognition of minerals was made through examination of crystal morphologies and EDAX patterns. More than 200 SEM microphotographs were taken for the study.

- **Geological Log**

Neutron-density logs were used to determine porosity of the sandstones. Porosity was also obtained from sonic logs where neutron-density logs were not available. Prior to running the analysis, necessary log-curve corrections were made to account for the effects of mudcake, salinity, temperature, bit (borehole) size, and occurrences of gas.

- **Geothermal Gradient**

The static reservoir temperatures obtained during the production test period were used:

1) To determine the average sea-bottom or surface temperature and the average geothermal gradient of the study area, and

2) To construct the geothermal gradient and formation temperature maps of the study area.

The temperature-depth data for the twenty-six wells were plotted. An eyeball best-fit curve was established. The gradient of the line was taken as the average temperature gradient of the study area (Fig. 3-24). The point at which the line intersected the surface was considered as

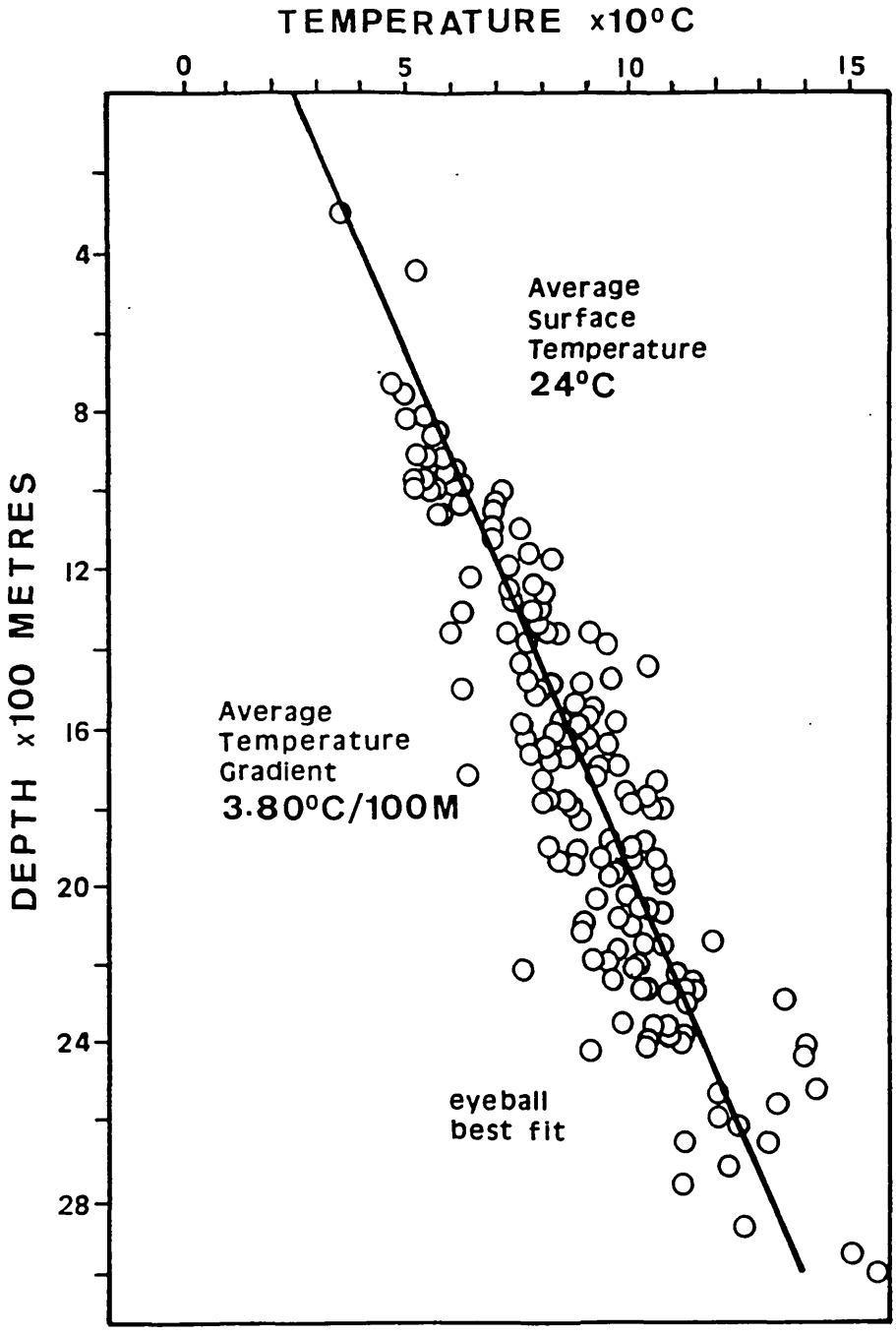


Figure 3-24 - Average temperature gradient of the study area. Data are from production tests acquired during shut-in periods and, according to Gretener (1981), represent static formation temperatures. As such these were not corrected.

the average surface temperature. To determine geothermal gradient of a location, temperature-depth profile was constructed by projecting a straight line through the average surface temperature as a fixed reference point at the surface, passing downward through temperature points. A gradient for the line was taken as the geothermal gradient at that locality. The stratigraphic boundaries of the Pulai-II Formation were marked in, and the average reservoir (formation) temperatures extrapolated. In the determination of geothermal gradient, two general assumptions were made:

1) That the temperature increases linearly with depth, and

2) That the stratigraphic sequence within the vicinity of the well borehole consisted of a homogeneous layer of rocks of similar thermal conductivity.

- **Depth of Burial**

The technique to determine maximum depth of sediment burial was based on the concept that the degree of compaction in shale beds, unless otherwise affected by over-pressures, is related to the depth of burial (Magara, 1976). Because the velocity in these beds is approximately a direct function of compaction, sonic log was used to measure the degree of compaction. Ideally, the determination of compaction trend is best achieved in an area known to have undergone normal compaction burial, little or no tectonism and no history of over-pressuring.

The occurrences of unconformities, faults and folds suggest that the study area was tectonically unstable, and therefore it was very difficult to obtain a reasonable shale compaction trend, and

subsequently to predict the maximum depths of burial. It was felt that the best approach was to determine these depths with reference to a point in the study area, which is believed to have undergone relatively little tectonic uplift. The seismic data indicate that the vicinity of the Banggol-1 well was relatively stable , and Banggol-1 was chosen as a reference point. Subsequently, a shale compaction curve was generated for the well by plotting the shale transit time with depth (Fig. 3-25). Similarly, shale compaction curves were generated for other wells in the study area. In generating the compaction curves, an assumption was made that the sequence penetrated by the wells was normally pressured. However, this assumption is not generally true, as many drilling hazards in the study area have been associated with overpressuring in shales. In depth-transit time plot, it was considered therefore, that any points to the right of the compaction curve denotes overpressuring.

In estimating depths of burial, a simple overlaying technique and curve off-set was used (Fig. 3-26). The compaction curves of different wells were compared with the reference curve of Banggol-1, and any off-sets in the trend were noted. The displacement of the curve to the left of the reference curve indicates that the stratigraphic interval in question was buried at some point deeper than its present-day depth. A break in the compaction curve signifies a possible unconformity. The fragmented curve was then synchronised with the reference curve, and the depth of burial and amount of section lost due to erosion, if any, determined. Where the resultant compaction curve superimposes onto the reference curve, it was considered that the stratigraphic interval at that locality was never being buried deeper than its present-day depth.

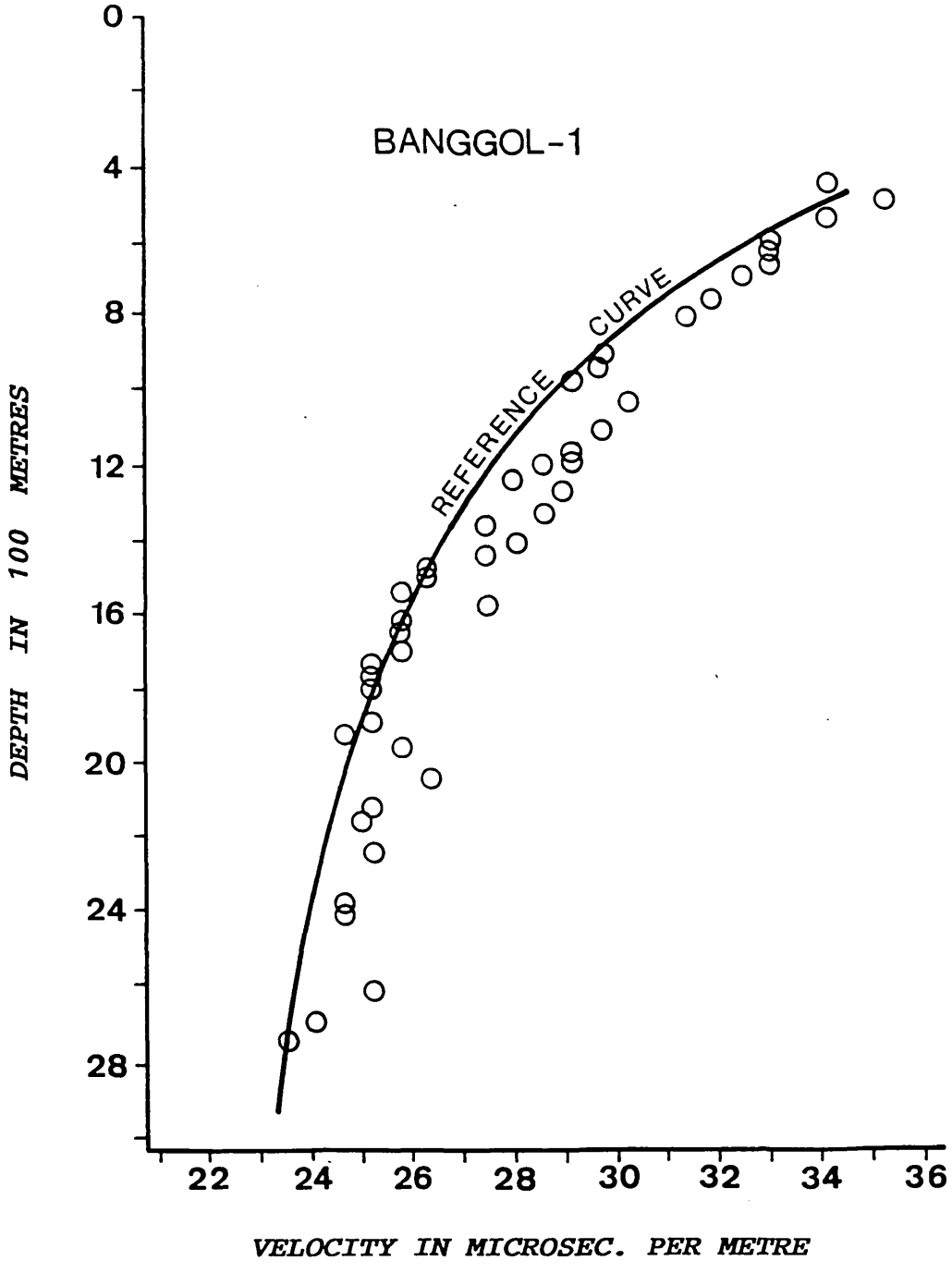


Figure 3-25 - Shale compaction trend at Banggol-1. Compaction curve at Banggol-1 was used as a reference curve for determining maximum depths of burial at other well locations.

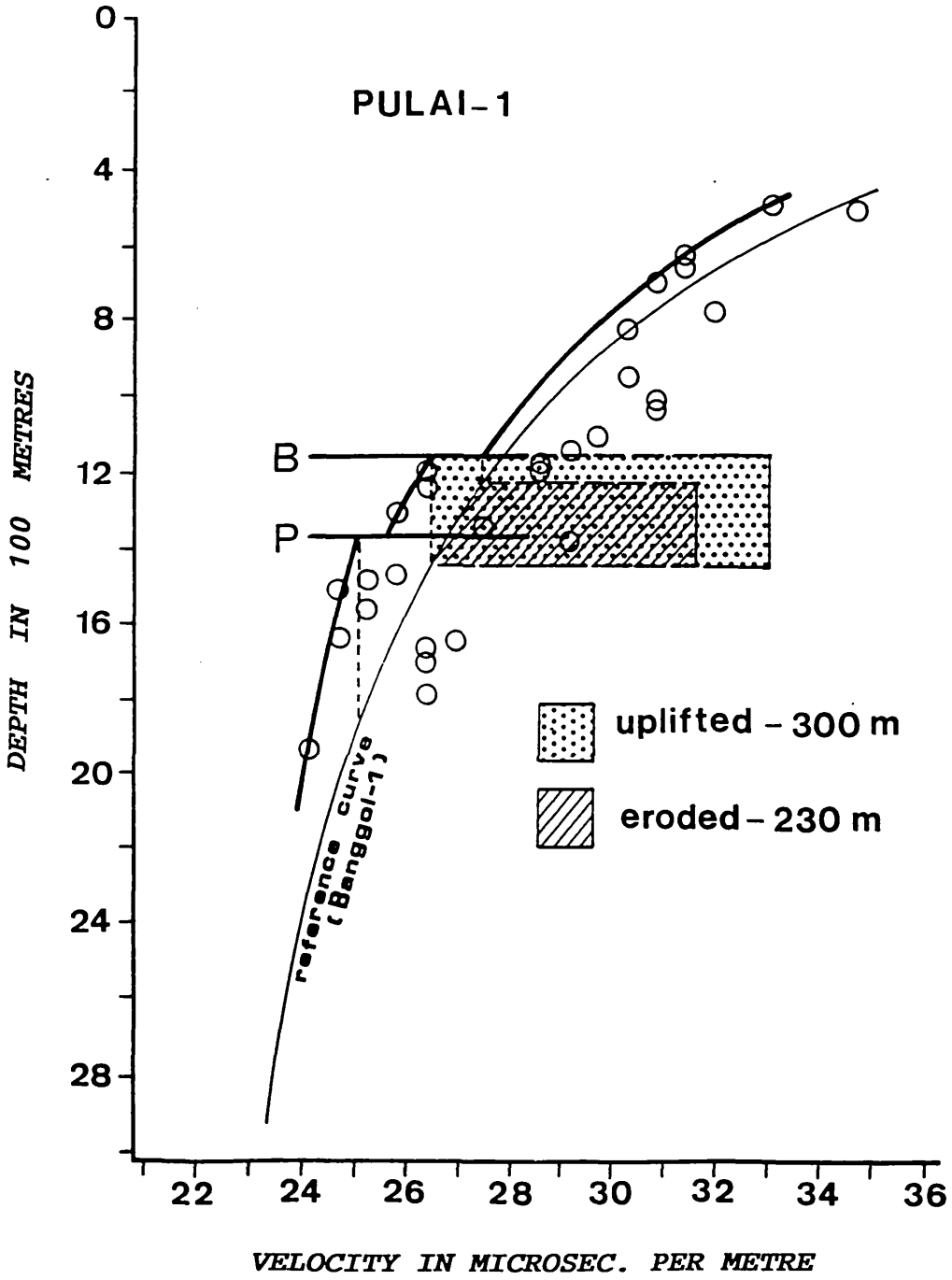


Figure 3-26 - An illustration to determine maximum depths of sediment burial by superimposition of reference curve at Banggol-1 onto compaction curve of a typical well (Pulai-1) in the study area.

4. FACIES ANALYSIS

4.1 *INTRODUCTION*

The Pulai-II Formation is a sequence of sandstones and shales. However, thin and characteristically hard calcareous layers have been found occasionally:

1) Within generally thin sandstone beds in predominantly shale intervals (Figs. 4-1),

2) Within massive sandstone bodies (Fig. 4-2), and

3) Enveloping massive sandstone bodies (Fig. 4-3).

On seismic sections this formation appears to be distributed widely throughout the study area, displaying clear upper, middle and lower seismic boundaries, corresponding respectively to the Red (R), Blue (B) and Purple (P) seismic markers (Figs. 3-5, 4-4 and 4-5). The well-defined B-marker marks the boundary between the Terengganu Shales at the top and the Pulai Sandstones in the bottom. Based on isopach maps (Figs. 4-6 and 4-7), it appears that the Pulai-II Formation is best developed in the west and central parts of the study area. The Pulai Sandstone sequence is thickest in the west, with total sequence thickness exceeding 500 metres (Fig. 4-6). It thins out to the northeast, east and south to less than 200 metres, where in the northeast, it onlaps onto the basement. A much closer contour grid to the northwest indicates flexuring, and this is well exhibited in Figure 4-4. A similar sediment development appears to have occurred within the overlying Terengganu Shale sequence (Fig. 4-7), but with some differences:

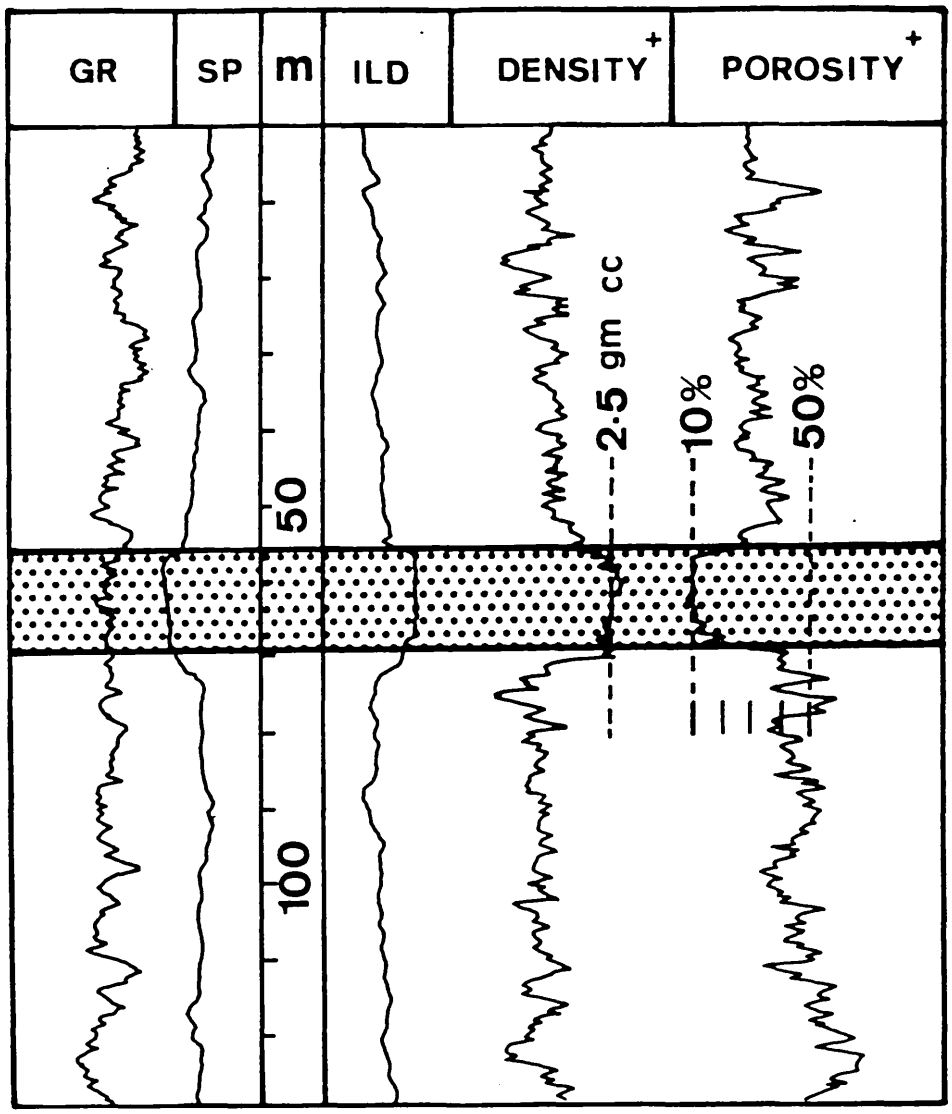


Figure 4-1 - Calcareous siltstone bed within shaly interval. Example from Seligi-3.

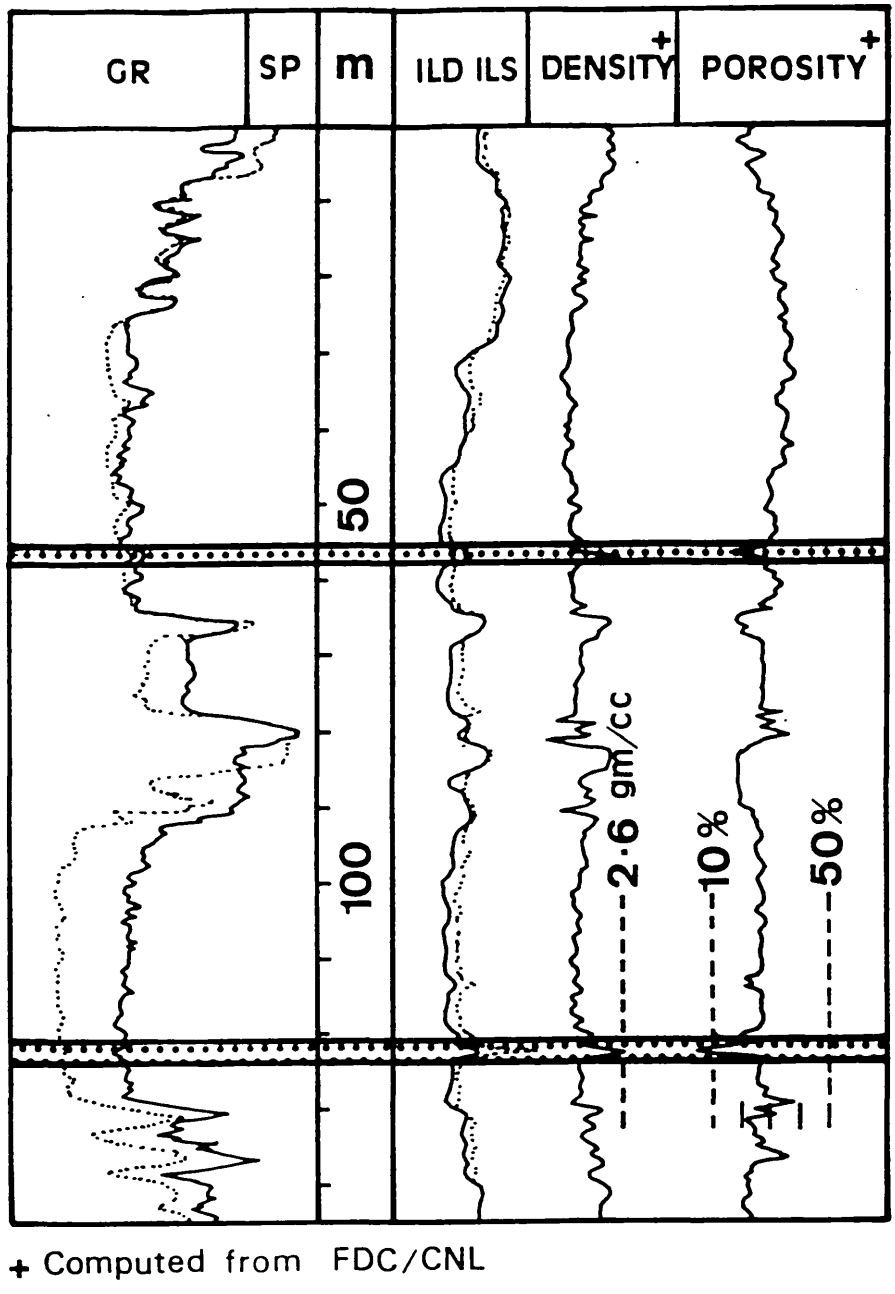


Figure 4-2 - Thin calcareous layers within generally massive sandstone units. Example from Tinggi-1.

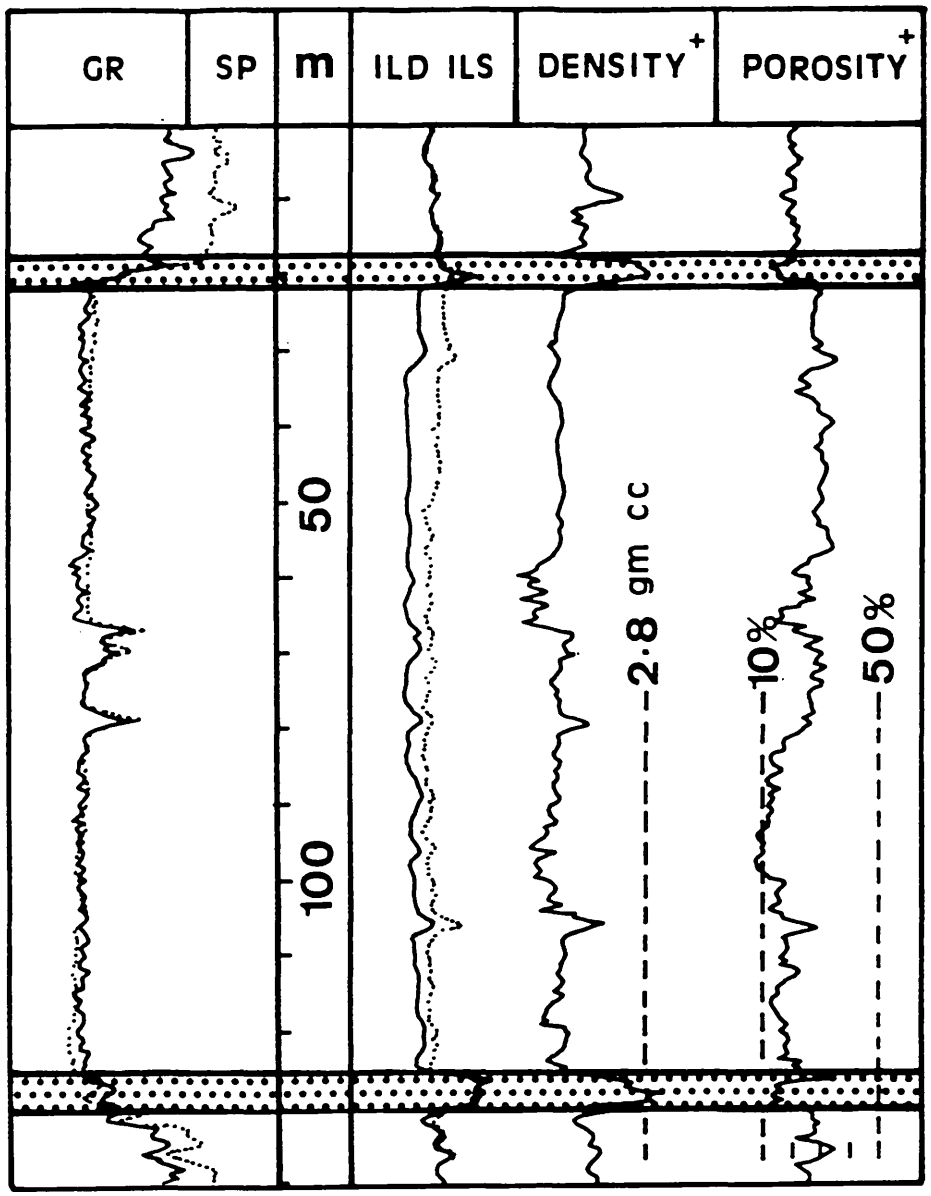
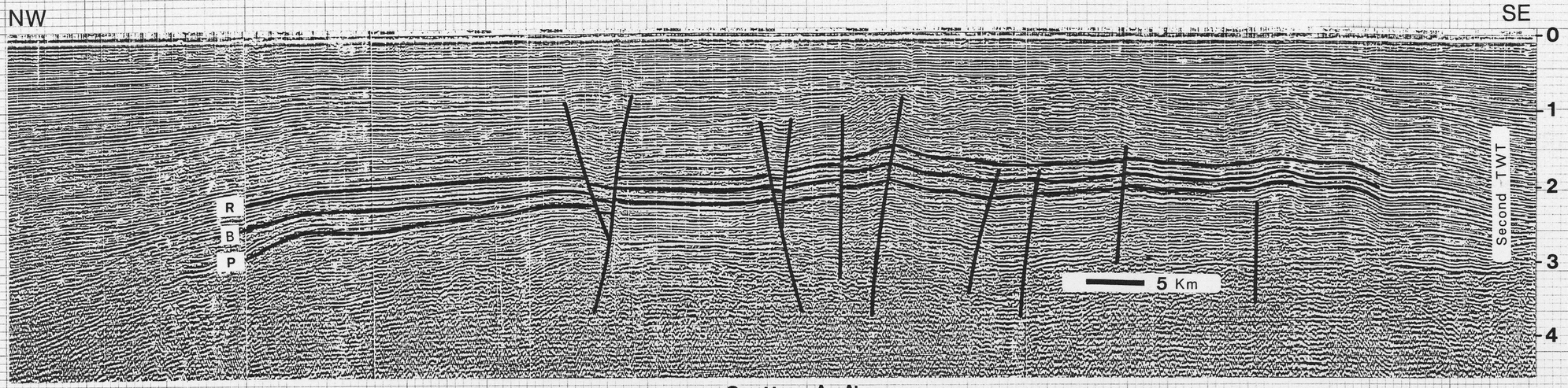
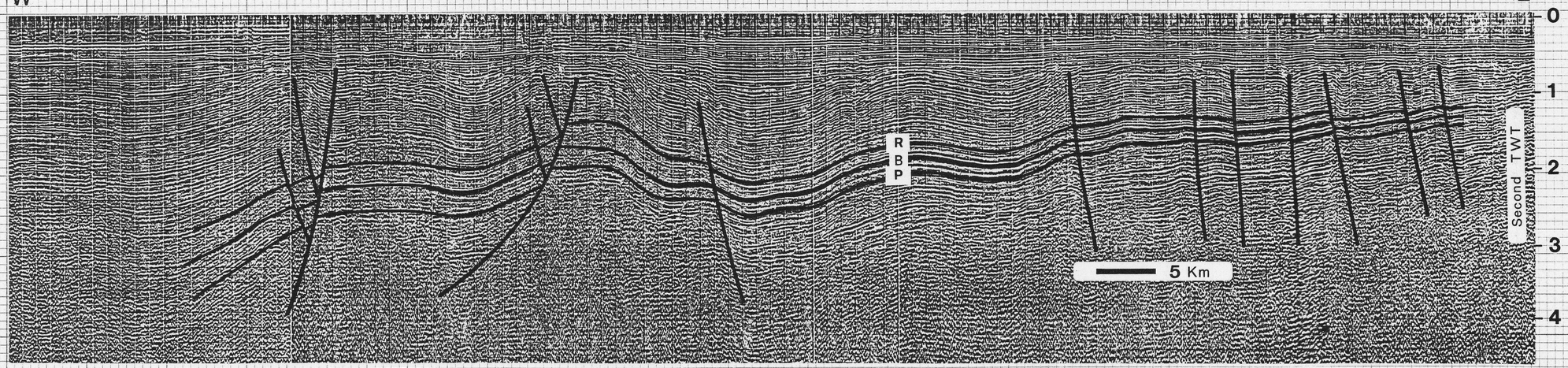


Figure 4-3 - Calcareous layers enveloping thick and massive sandstone unit. Example from Peta-1.



Section A-A'



Section B-B'

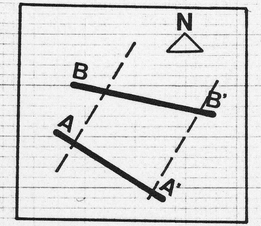
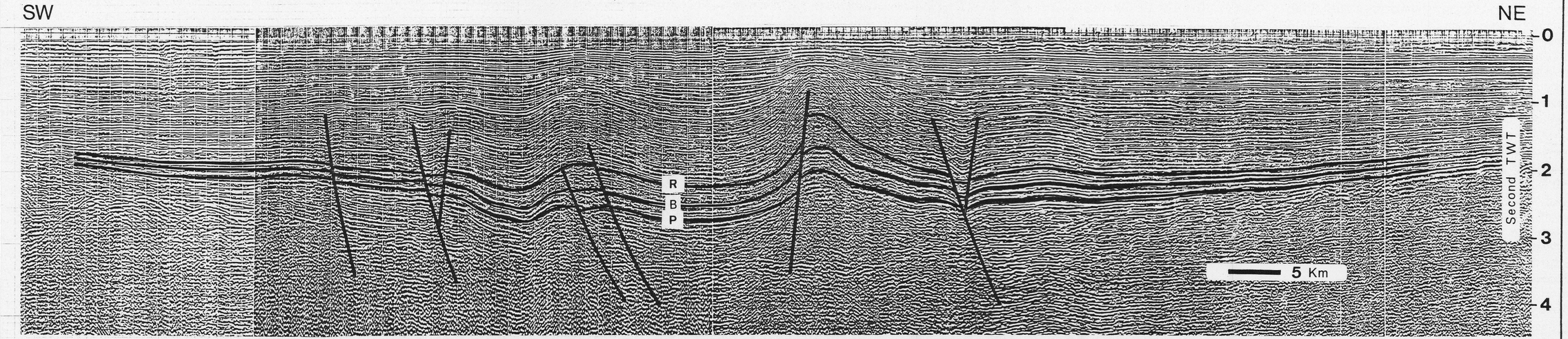
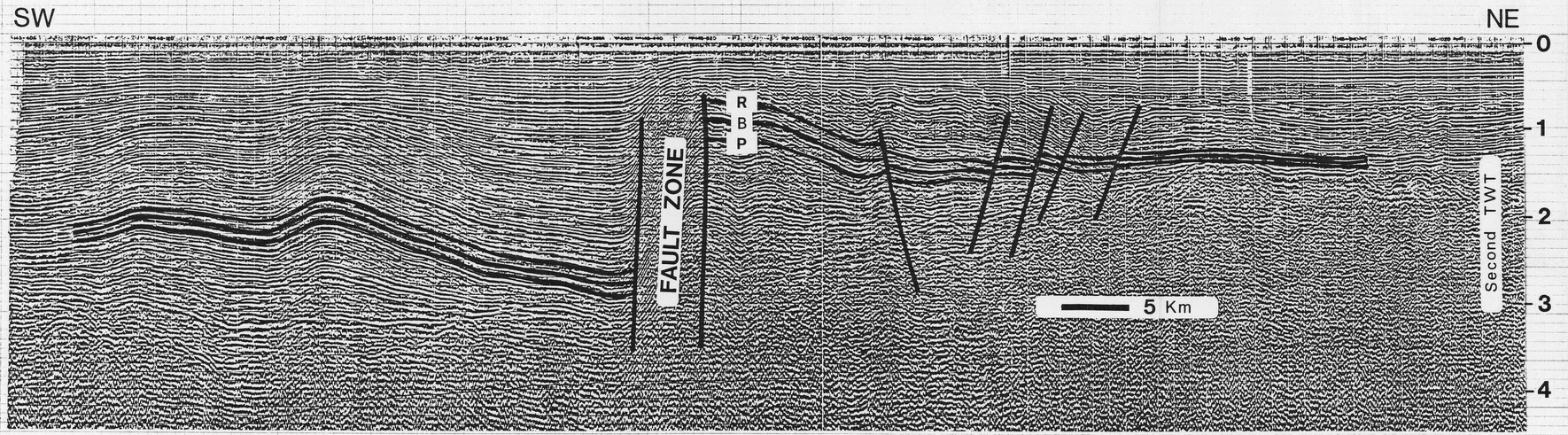


FIGURE 4-4

Regional seismic cross-sections along line 68-26 (Section A-A') and line 68-38B (Section B-B'), showing R, B and P markers. The R and P markers mark the top and bottom of the Pulai-II Formation, respectively. (Note the thickening of the formation towards the west and northwest. Zone of flexuring is towards the left of the sections).



Section C-C'



Section D-D'

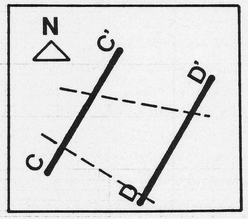
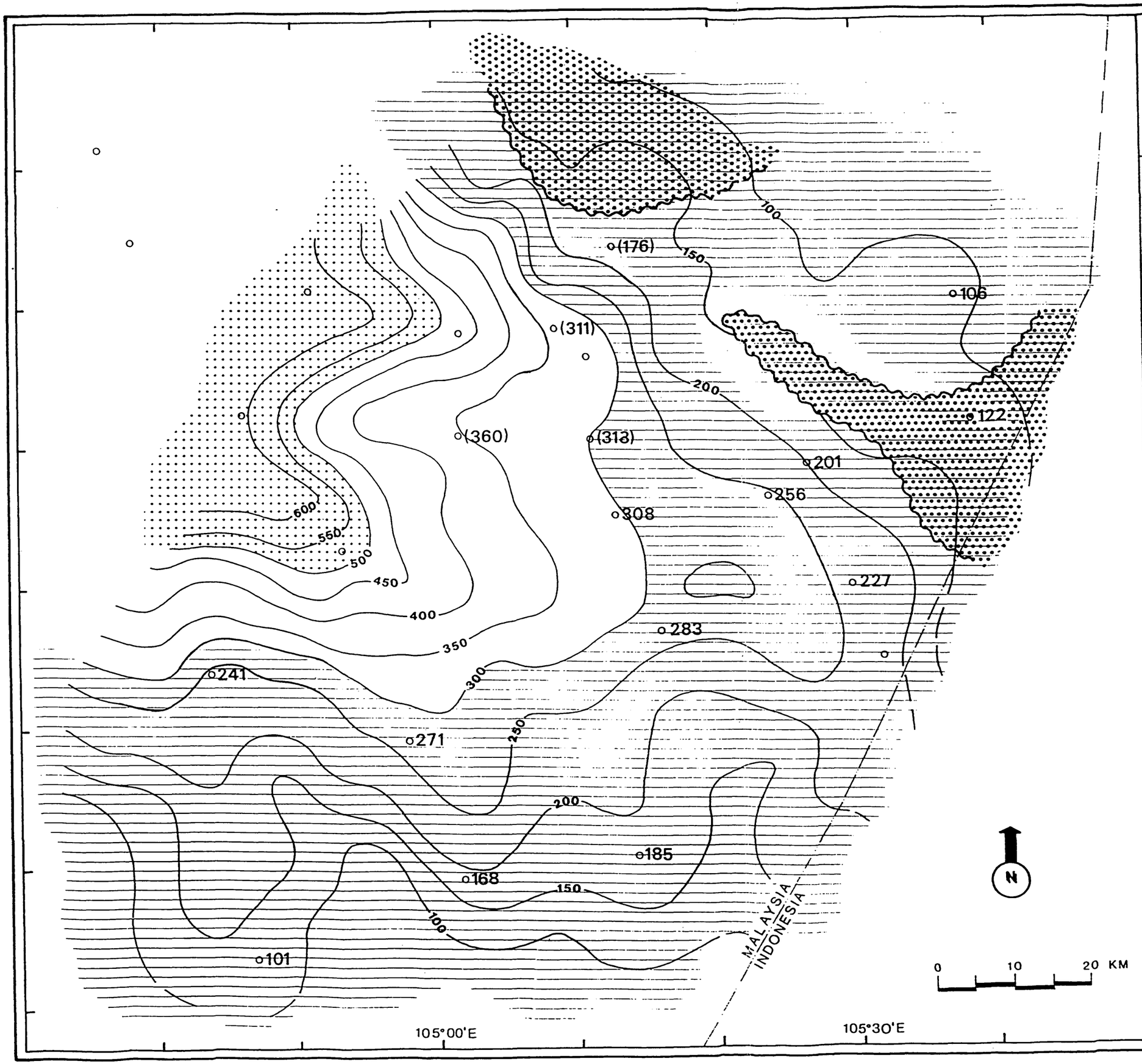
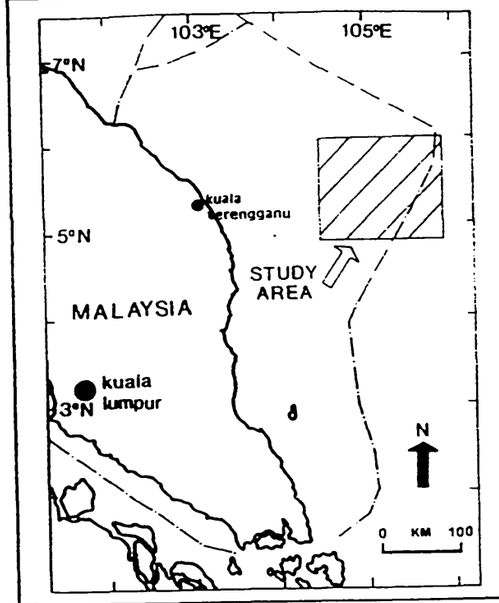


FIGURE 4-5

Regional seismic cross-sections along line 68-121 (Section C-C') and line 68-145 (Section D-D'), showing R, B and P markers. The R and P markers mark the top and bottom of the Pulai-II Formation, respectively. (Note the occurrence of shale(?) pillow/diapir(?), towards the centre of Section C-C'. The east-west Fault A in Fig. 2-5, is shown in the centre of Section D-D'). Fig. 2-4 was drawn parallel to line 68-145.



LOCATION MAP



LEGEND

Less than 300 metres

300 - 500 metres

Thicker than 500 metres

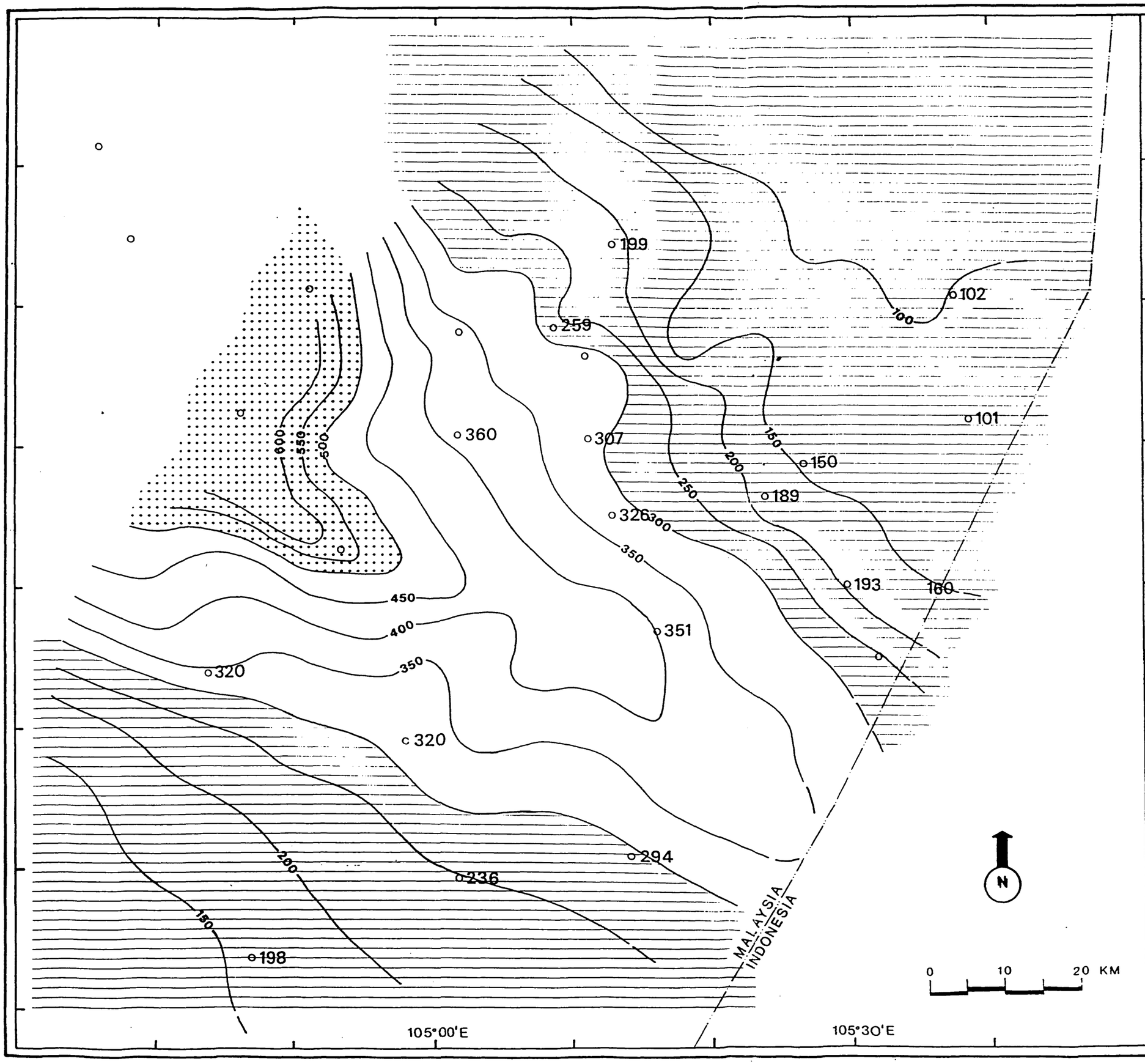
Truncation

o 345 -- control point

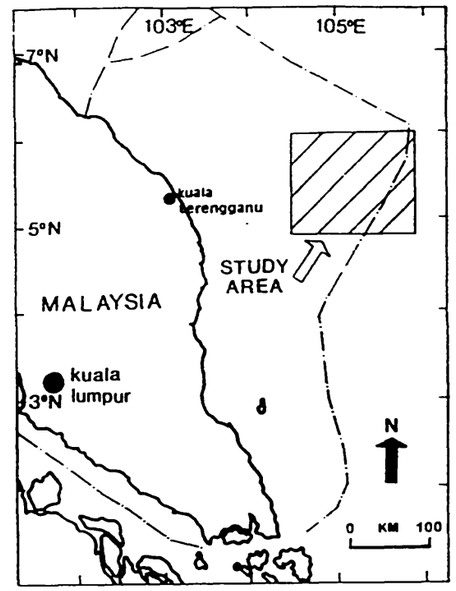
C. I. = 50 metres

FIGURE 4-6

Isopach Map of the Pulai Sandstones (B-P Seismic Sequence).



LOCATION MAP



LEGEND

Less than 300 metres

300 - 500 metres

Thicker than 500 metres

o 345 -- control point

C. I. = 50 metres

FIGURE 4-7

Isopach Map of the Terengganu Shales (R-B Seismic Sequence).

1) Although thick development of sediments is found within the overlying Terengganu Shale sequence, the 300-metre thickness contour indicate to "channel" through the area, dividing it into three regions: northeast, southwest and central regions, with the northeast and southwestern regions having lesser sediment development. In contrast, in the underlying Pulai Sandstone sequence, the 300-metre thickness contour forms a division line between the relatively thicker sediments in the northwest and than the rest of the area.

2) The depositional axis of the overlying Terengganu Shales appears to shift to the south relative to that of the underlying Pulai Sandstones.

The differences in sediment distribution within each member of the Pulai-II Formation suggest that:

1) Sediments were derived from the northeast, east and south at the time of deposition of the Pulai Sandstones, and from the northeast and southwest during the deposition of the Terengganu Shales,

2) The Upper Terengganu Shales probably marked the beginning of marine transgression, and thicker sediments in the central region indicate a "strait" which linked two bodies of waters in the northwest and southeast, and

3) The major east-west fault, Fault A (Fig. 2-5), probably was initiated during Late Oligocene-Early Miocene, and marked the general boundary between the relatively more stable area in the north and the less stable area in the south.

4.2. *PALAEONTOLOGY*

Studies of selected cores and ditch cuttings from five wells: Palas-1, Duyong Barat-1, Seligi-3, Banggol-1 and Angsi-1 have been carried out by Esso (1978), Carigali (1986) and Rashidah et al (1988). The results indicate that:

1) The Pulai Sandstone sequence is barren of foraminifera and nannofossils. In the northeastern part of the study area, only *Pediastrum,* a freshwater alga, was detected in the samples. In the southern area, in addition to the occasional occurrences of *Pediastrum*, spores of *Casuarina, Palmae* and *Rhizoporaceae,* belonging to coastal and mangrove plant species, are in abundance, and

2) Benthonic foraminiferal remains of *Milliamina fusca,* a brackish water fauna, are common within the Terengganu Shale sequence, and were found in most of the wells. Spores of *Casuarina, Palmae* and *Rhizoporaceae* have also been found within the interval.

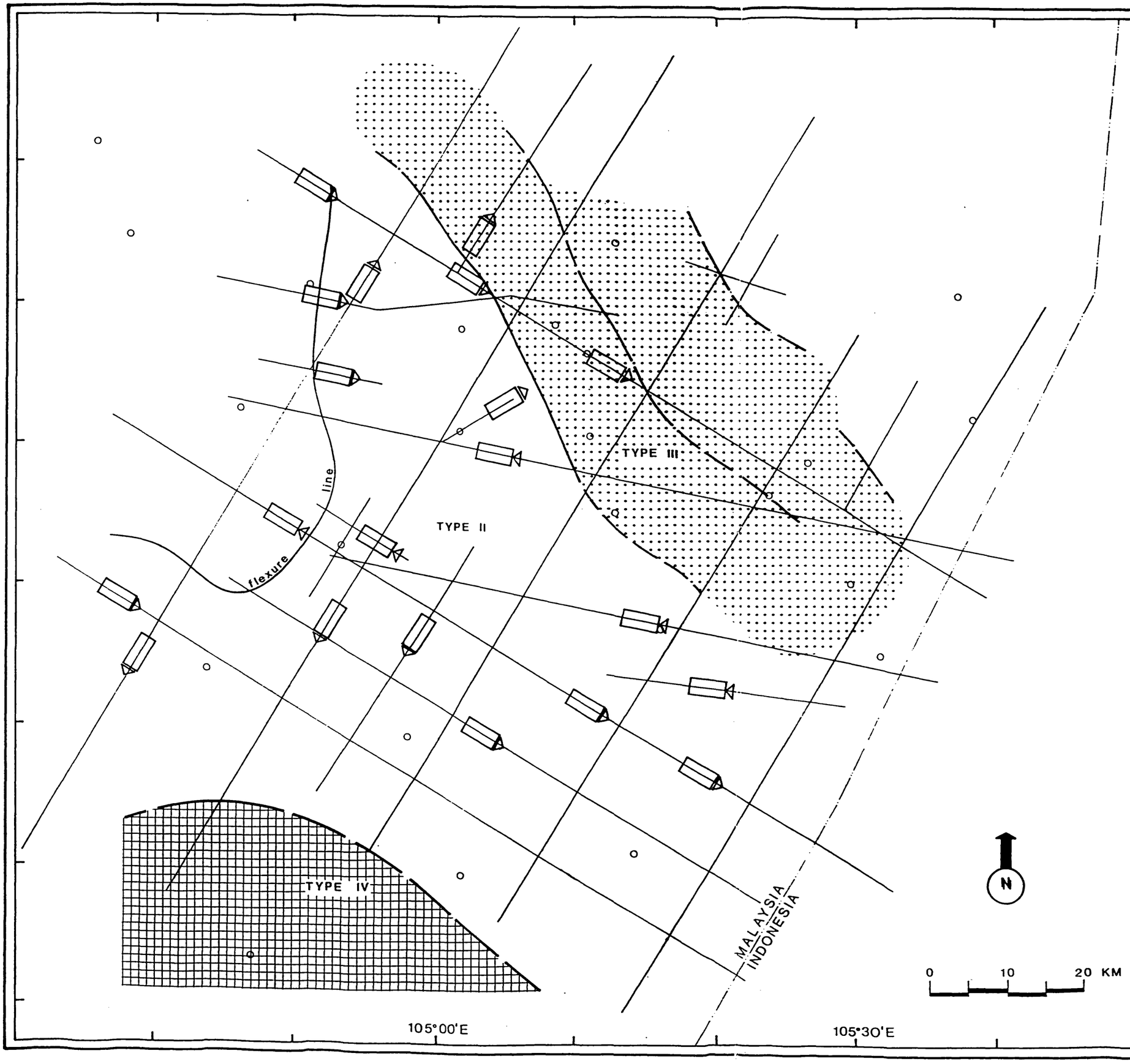
4.3 *FACIES OF PULAI-II FORMATION*

4.3.1 Seismic Facies

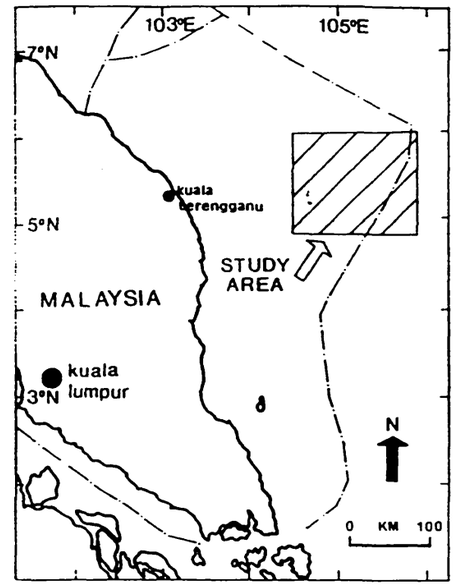
4.3.1.1 *Red-Blue Seismic Sequence*

The R-B seismic sequence, Figure 4-8, is characterised generally by:

1) Convergent reflection configurations and associated onlapping feature. These seismic signatures appear to be more common on the north, northeast and central parts of the study area (Fig. 4-5 (Section C-C') and 4-9),



LOCATION MAP



LEGEND

Type II Facies

Type III Facies

Type IV Facies

Onlap

Downlap

FIGURE 4-8

Map of the R-B sequence showing seismic reflection configurations and distribution of seismic facies.

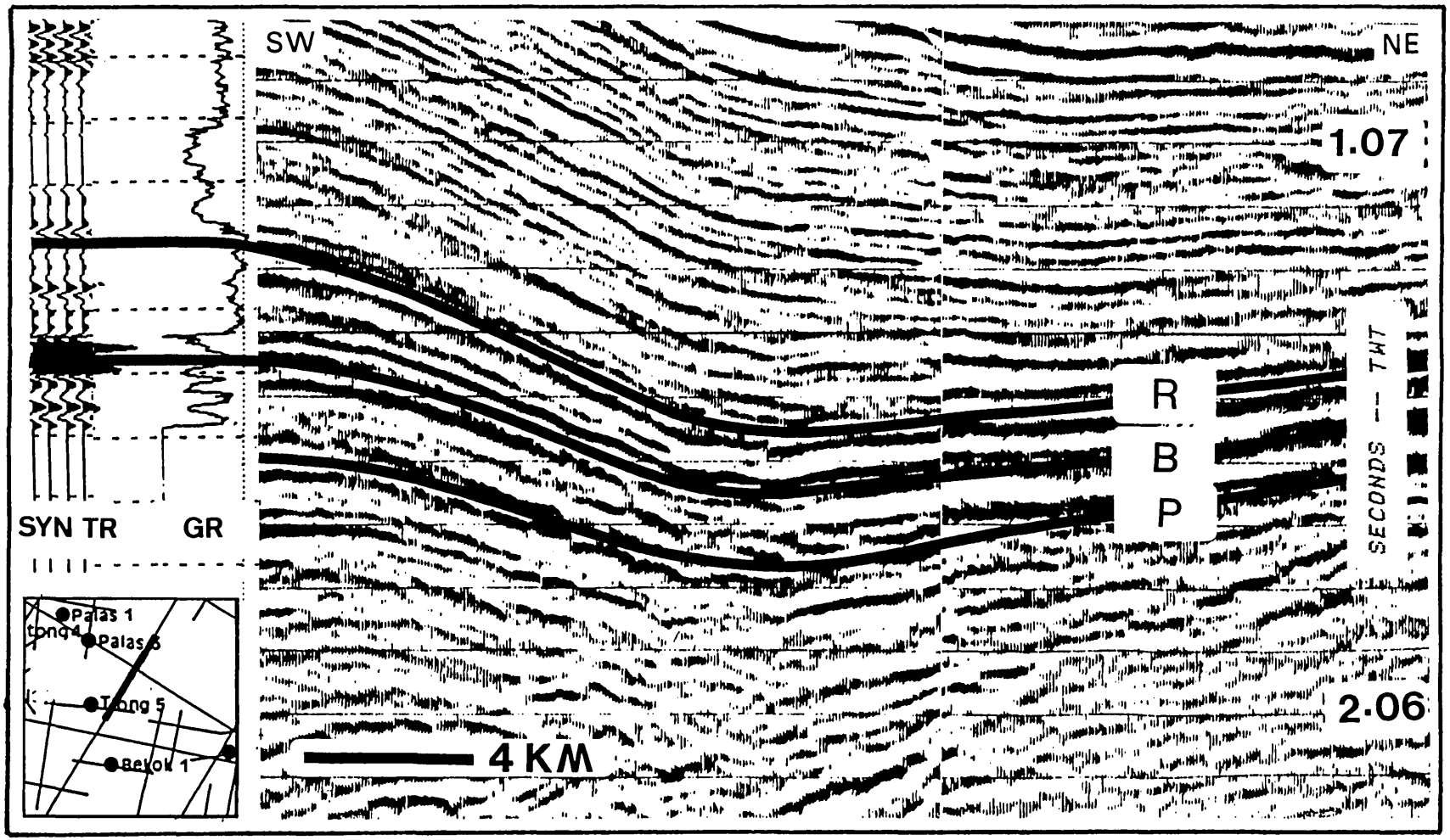


Figure 4-9 - Convergent seismic configuration and onlapping transgressive-regressive units of Type III within the R-B seismic sequence. This facies appeared to have occurred in the northeast of the study area. Inset map shows location of the section.

2.) Downlapping terminations which are more common in the centre and extreme west of the area (Fig. 4-10), and

3) Type II, Type III and Type IV seismic facies. Type II is generally common in the centre of the study area, with Type III more common in the northeast and Type IV in the south and southwest of the area.

Seismic data show that seismic facies of Type III in the northeastern area occur as transgressive-regressive couplets onlapping onto high amplitude B-seismic marker (Fig. 4-5, Section C-C'). Within this area, using the seismic data, it would appear possible to delineate trangressive-regressive couplets, in the northeastern part of the study area (Fig. 4-8), and the well data in the area indicate that these seismic couplets consist of upward-coarsening sandstone sequences (Figs. 4-11 to 4-13). The distribution and extent of occurrence of this facies around Pulai-Seligi-Bekok-Ledang-Belumut area, was however difficult to establish because of faulting (Fig. 2-5), but based on the well data, it was inferred that the facies extends to the southeast. The occurrence of similar facies in the south was difficult to establish for similar reasons. The well data do not indicate its occurrence (Figs. 4-14 and 4-15).

The seismic facies of Type II are confined generally to the centre of the study area. The wells at Ophir, Tapis, Angsi, Besar, Duyong Barat and Duyong, which penetrated the sequence indicate that the facies of Type II correspond to a predominant shale interval (Figs. 4-11 to 4-15).

The seismic facies of Type IV are found generally in the extreme southwest of the study area. Seismically, it was very difficult to map the distribution of these facies because of the poor seismic data. It

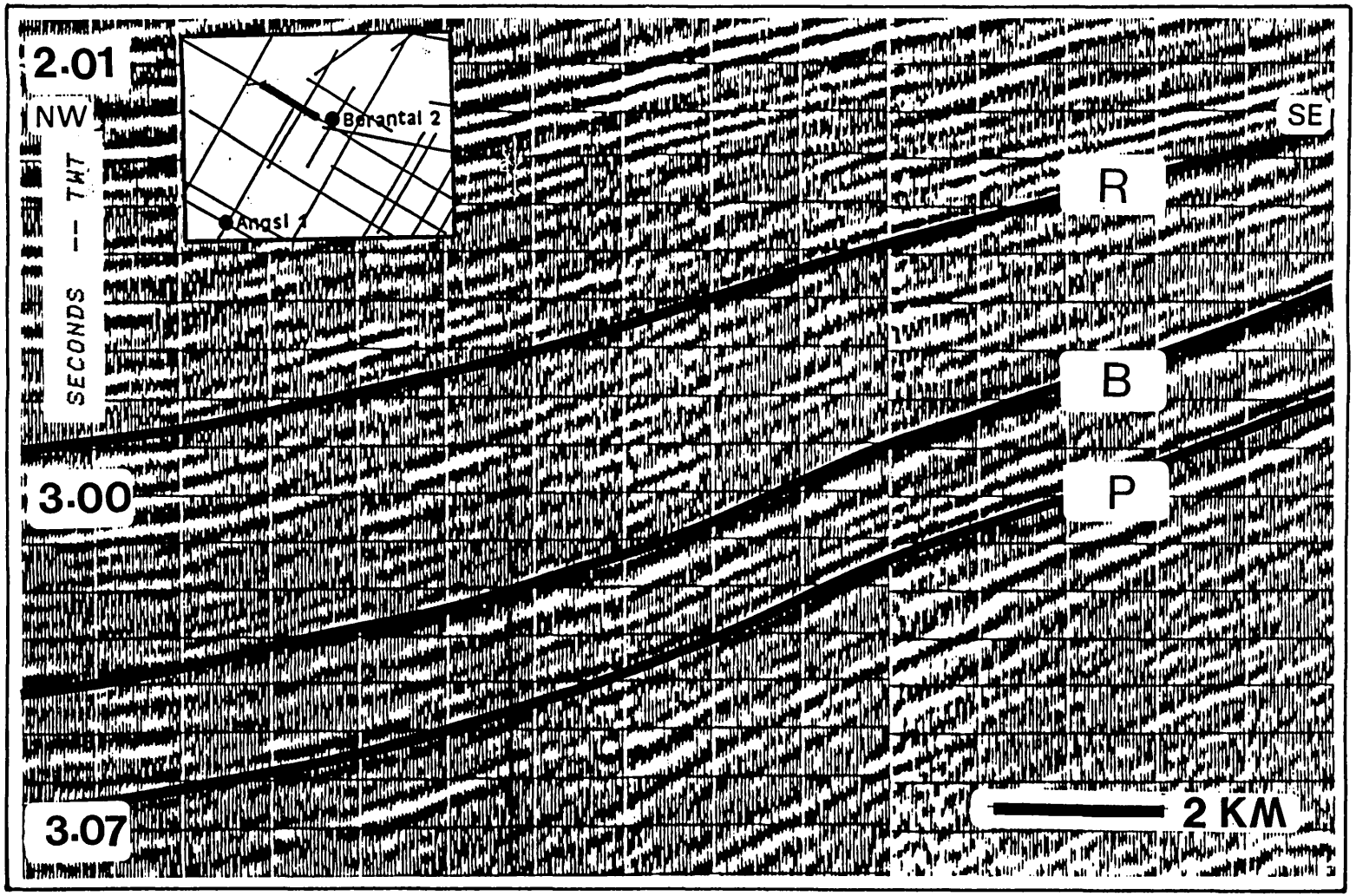
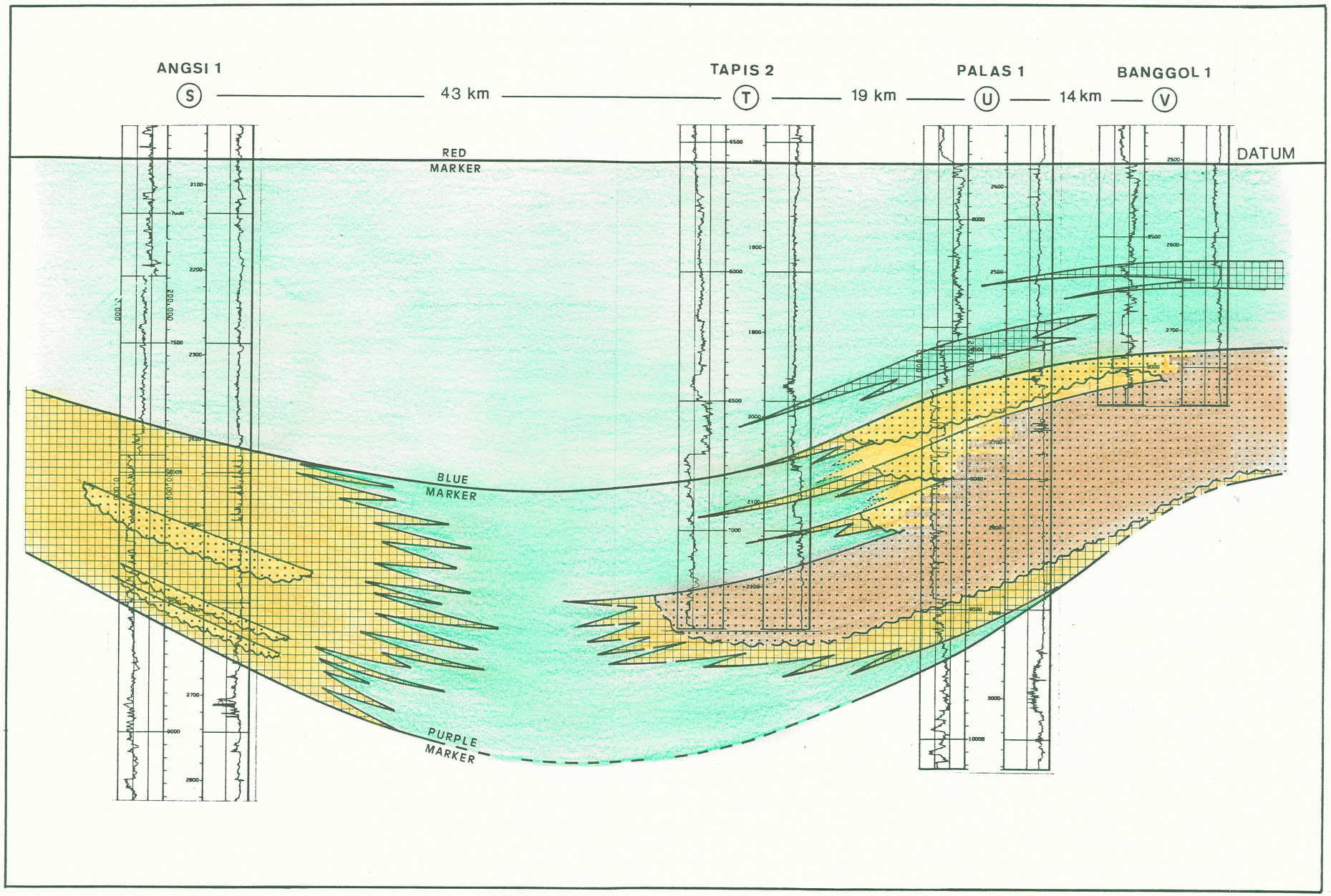
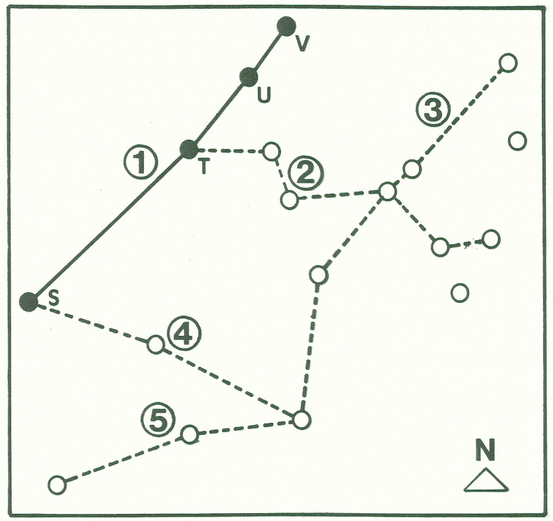


Figure 4-10 - Downlapping seismic configuration, and related seismic facies of Type II within the R-B and B-P seismic sequences. This facies type is common in the west of the study area. Inset map shows location of the section.





Alluvial Outwash Plain Deposits - braided channel sandstones and siltstones

Lower Coastal/Delta Plain Deposits -distributary and tidal channel sandstones, crevasse splay, interdistributary, lagoonal and tidal flat sandstones, siltstones and shales

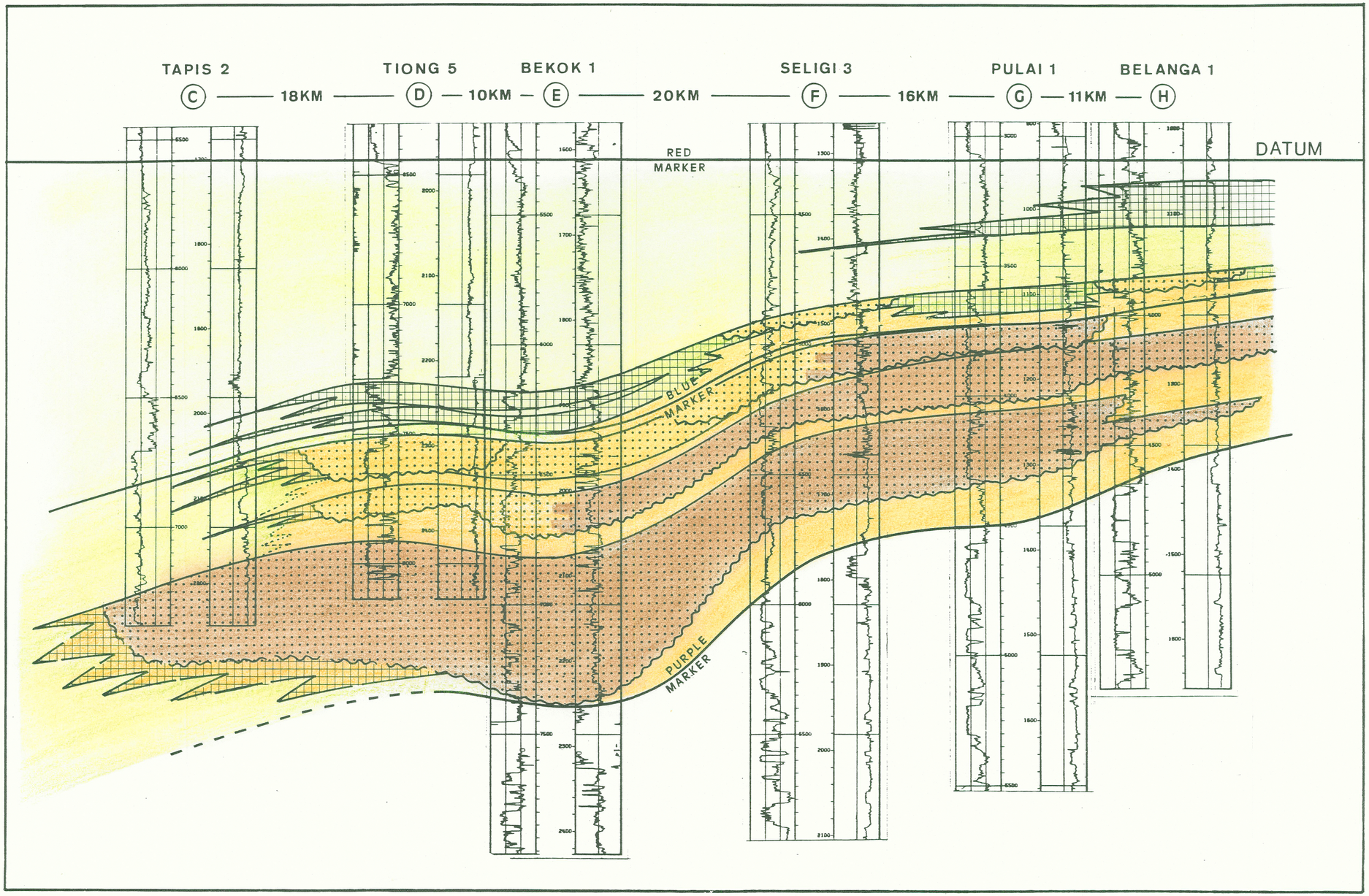
Shelfal Deposits - barrier bar sandstones and offshore shales

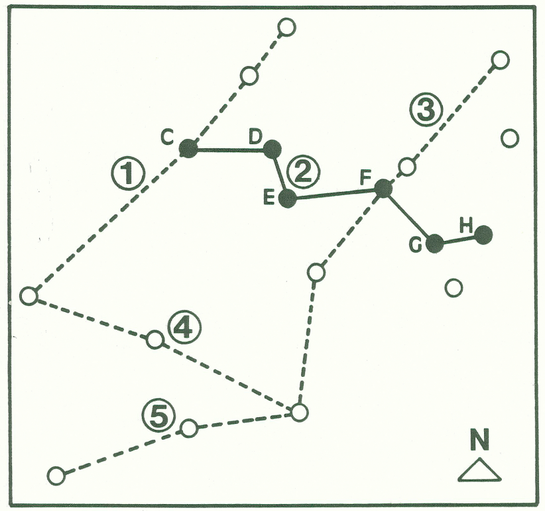
Generally massive sandstones

Interbedded sandstones, siltstones and shales

FIGURE 4-11

Stratigraphic cross-section along Tapis-Angsi-Palas-Banggol, showing correlative intervals, major environments of deposition and sandstone developments within the Pulai-II Formation.





Alluvial Outwash Plain Deposits - braided channel sandstones and siltstones

Lower Coastal/Delta Plain Deposits -distributary and tidal channel sandstones, crevasse splay, interdistributary, lagoonal and tidal flat sandstones, siltstones and shales

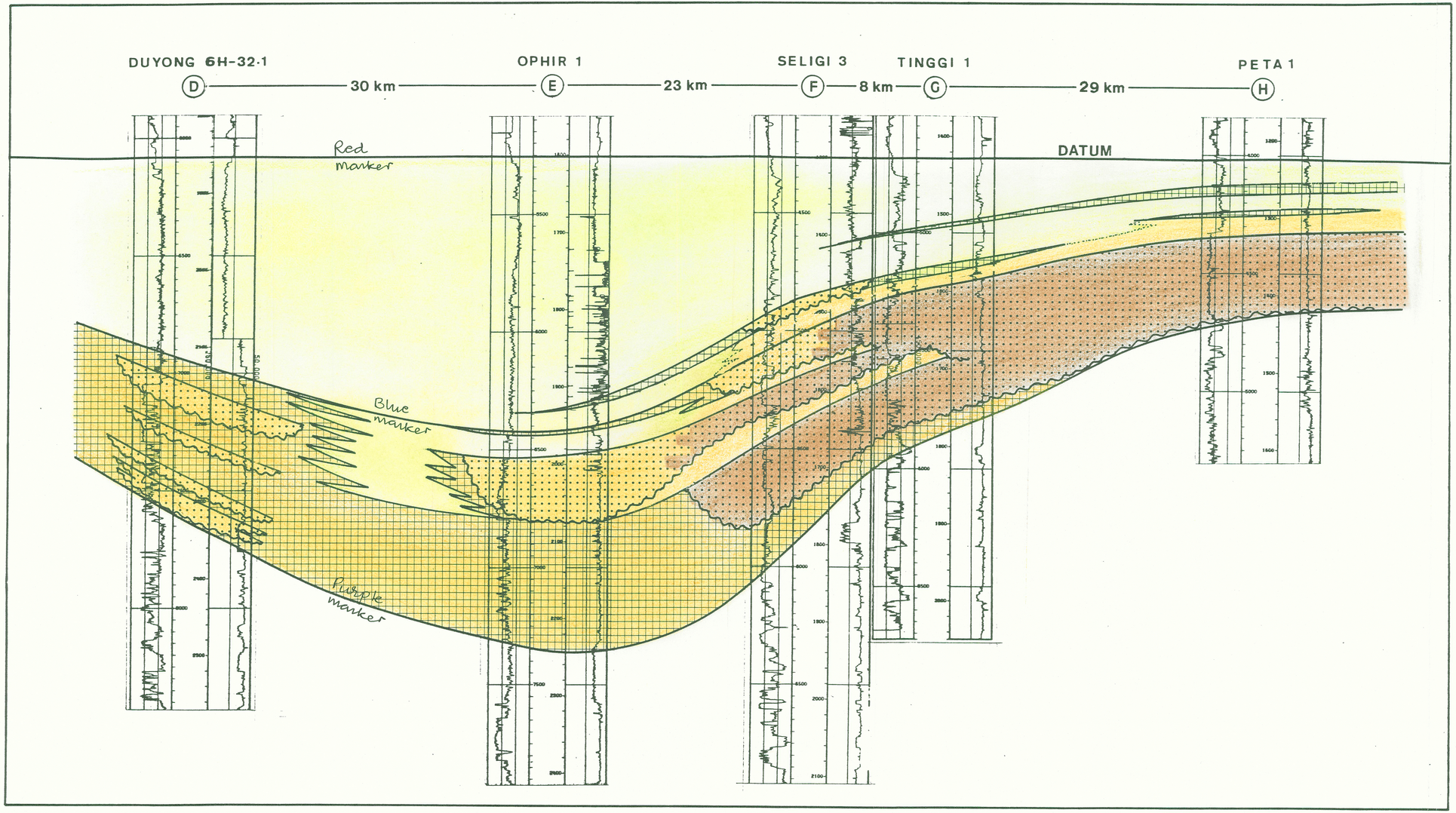
Shelfal Deposits - barrier bar sandstones and offshore shales

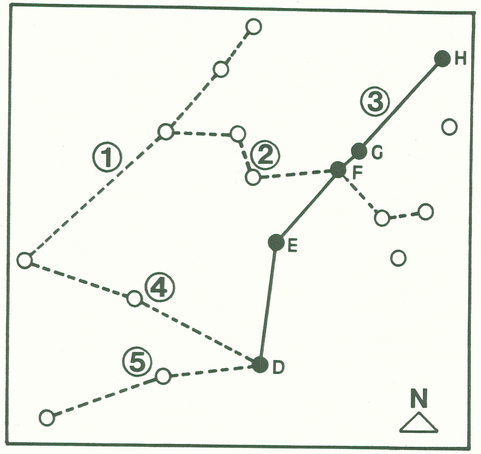
Generally massive sandstones

Interbedded sandstones, siltstones and shales

FIGURE 4-12

Stratigraphic cross-section along Tapis-Tiong-Bekok-Seligi-Pulai-Belanga showing correlative intervals, major environments of deposition and sandstone developments within the Pulai-II Formation.





Alluvial Outwash Plain Deposits - braided channel sandstones and siltstones

Lower Coastal/Delta Plain Deposits -distributary and tidal channel sandstones, crevasse splay, interdistributary, lagoonal and tidal flat sandstones, siltstones and shales

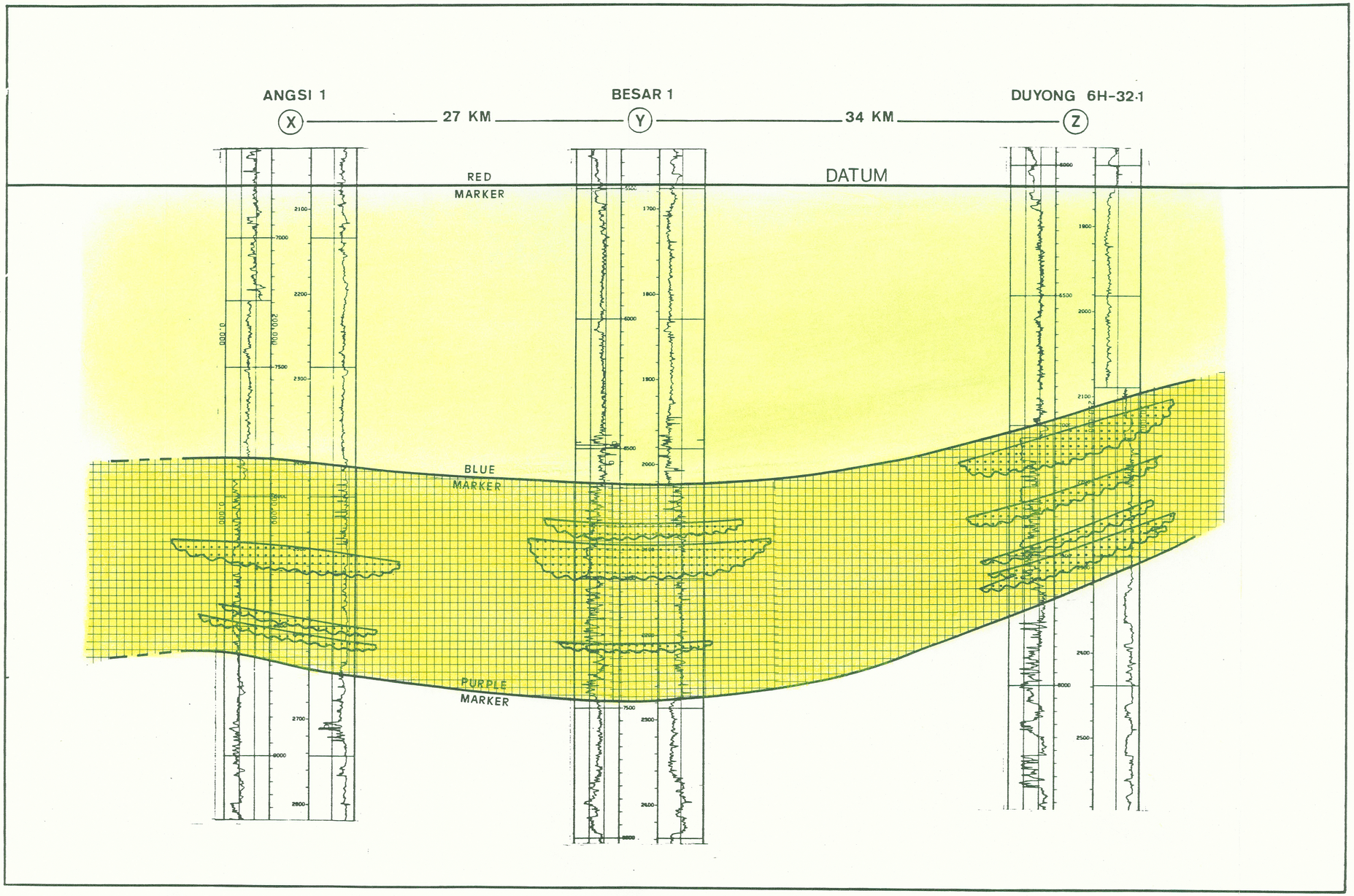
Shelfal Deposits - barrier bar sandstones and offshore shales

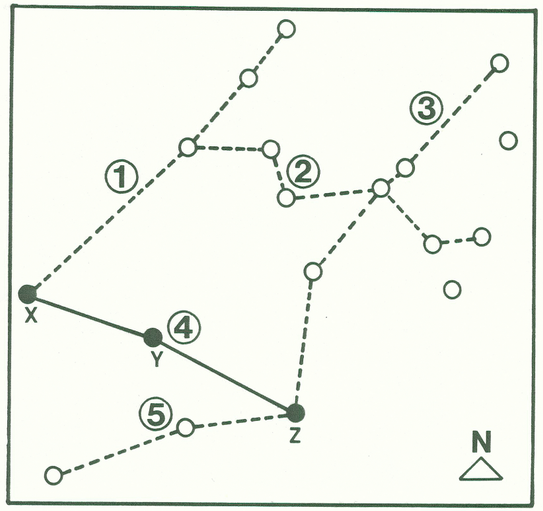
Generally massive sandstones

Interbedded sandstones, siltstones and shales

FIGURE 4-13

Stratigraphic cross-section along Duyong-Ophir-Seligi-Tinggi-Peta showing correlative intervals, major environments of deposition and sandstone developments within the Pulai-II Formation.





Lower Coastal/Delta Plain Deposits -distributary and tidal channel sandstones, crevasse splay, interdistributary, lagoonal and tidal flat sandstones, siltstones and shales

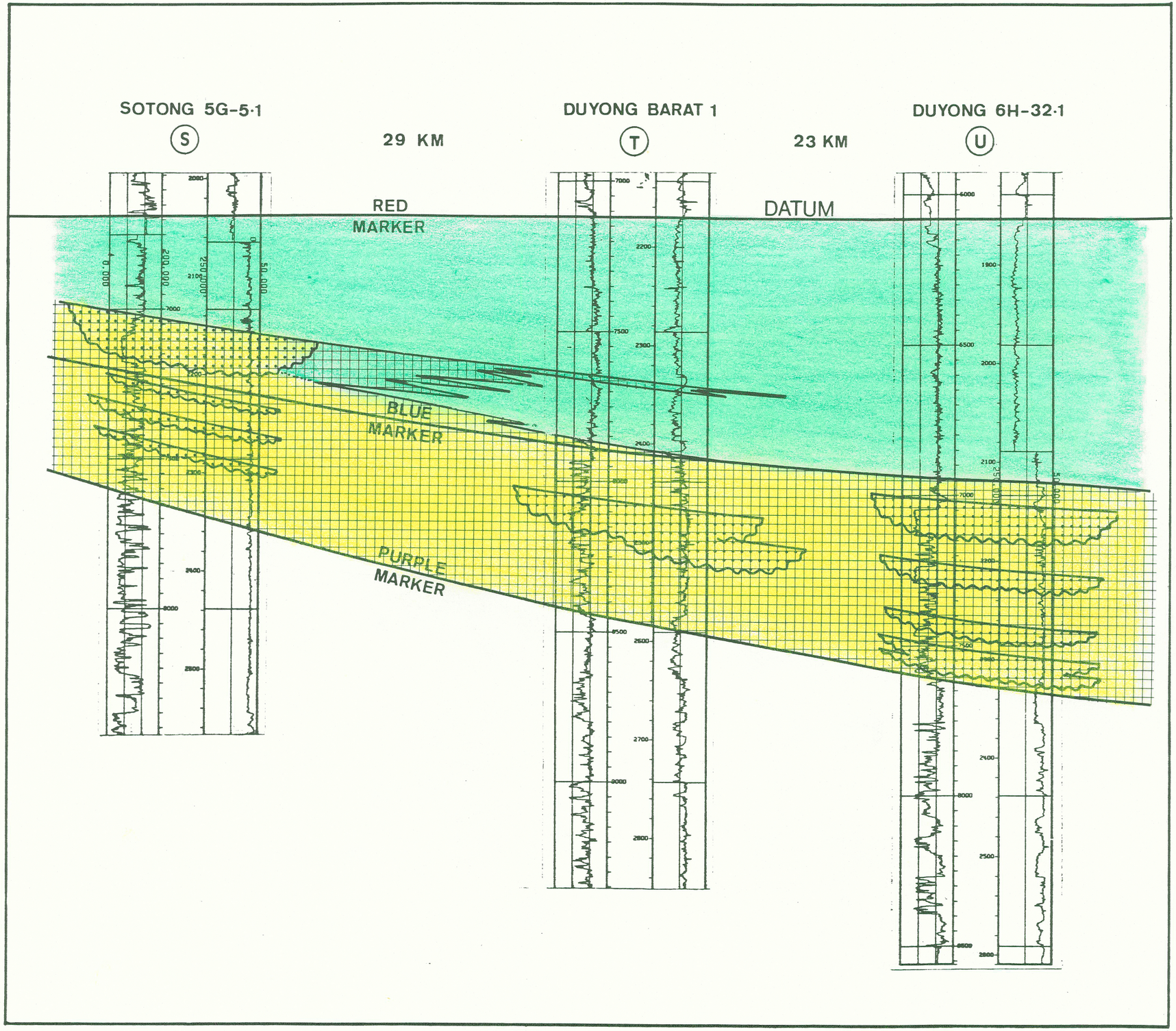
Shelfal Deposits - barrier bar sandstones and offshore shales

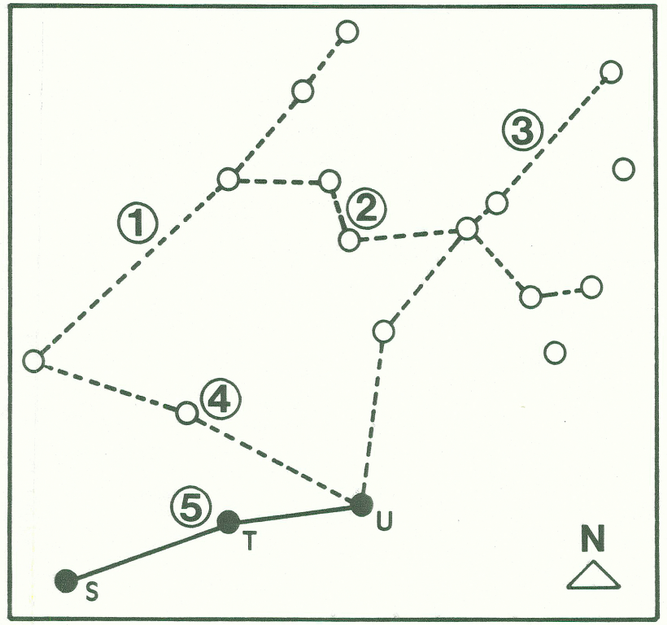
Generally massive sandstones

Interbedded sandstones, siltstones and shales

FIGURE 4-14

Stratigraphic cross-section along Angsi-Besar-Duyong showing correlative intervals, major environments of deposition and sandstone developments within the Pulai-II Formation.





Lower Coastal/Delta Plain Deposits -distributary and tidal channel sandstones, crevasse splay, interdistributary, lagoonal and tidal flat sandstones, siltstones and shales

Shelfal Deposits - barrier bar sandstones and offshore shales

Generally massive sandstones

Interbedded sandstones, siltstones and shales

Figure 4-15

Stratigraphic cross-section along Sotong-Duyong Barat-Duyong showing correlative intervals, major environments of deposition and sandstone developments within the Pulai-II Formation.

would appear that the well data at Sotong, indicate that the lithologic facies of Type IV are interbedded sandstones and shales (Fig. 4-15).

4.3.1.2 *Blue-Purple Seismic Sequence*

The B-P seismic sequence, Figure 4-16, is characterised by:

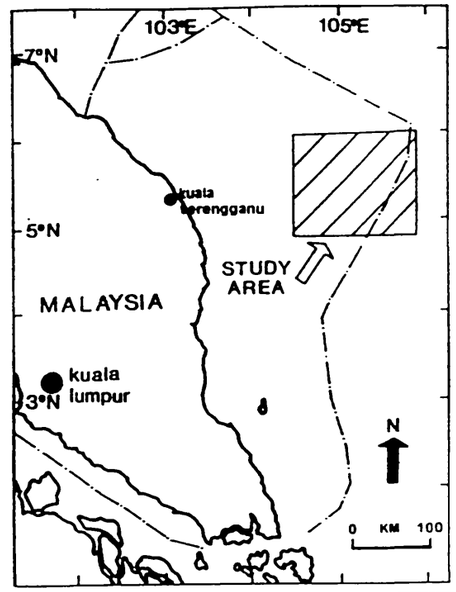
1) Diverging reflection configuration in the west (Fig. 4-4, Section A-A') and converging configuration in the north, northeast and southwest (Figs. 4-4 and 4-5, Sections A-A', B-B' and C-C'). Whereas no specific feature could be resolved within the converging seismic configuration, the diverging configuration is associated with less common downlapping features, and these are confined generally to the west and in the vicinity of the flexure zone (Fig. 4-4 (Section A-A')), and

2) Type I, Type II and Type IV seismic facies, with Type I generally more common in the north and northeast, Type II in the west and centre, and Type IV in the south of the study area.

The seismic facies of Type I appear to occur generally as "stretched lenses" which measure several tens of km in length, and in many cases have definitive boundaries. Often, these "lenses" coalesce into a continuous sheet. Based on the distribution of the facies, Figure 4-16, it would appear possible that the sheet comprises of several complexly developed delta lobe systems which overlapped, superimposed and coalesced with one another to form a blanket. The general areal configuration of this sheet is arcuate and fan-like, with the apex in the northeast. Correlation with geological logs indicates that the lithology within the sheet is predominantly sandstones (Figs. 4-11 to 4-



LOCATION MAP



LEGEND

- Type I Facies
- Type II Facies
- Type IV Facies
- Truncation
- Onlap
- Downlap

FIGURE 4-16

Map of the B-P sequence showing seismic reflection configurations and distribution of seismic facies.

13).

The seismic facies of Type II is generally confined to the west and central part of the study area. Downlapping reflection configuration is common in the west. On the map, Figure 4-16, this facies appears to be flanked by Type I facies in the north and northeast, and Type IV facies in the south. No wells in the west and the central area have penetrated the B-P sequence, but based on the generally low amplitude and concordant seismic reflectivity, Figure 3-9, which is similar to the seismic character as in Type II of R-B sequence, the Type II facies of the B-P sequence could well be shales (Vail et al, 1977).

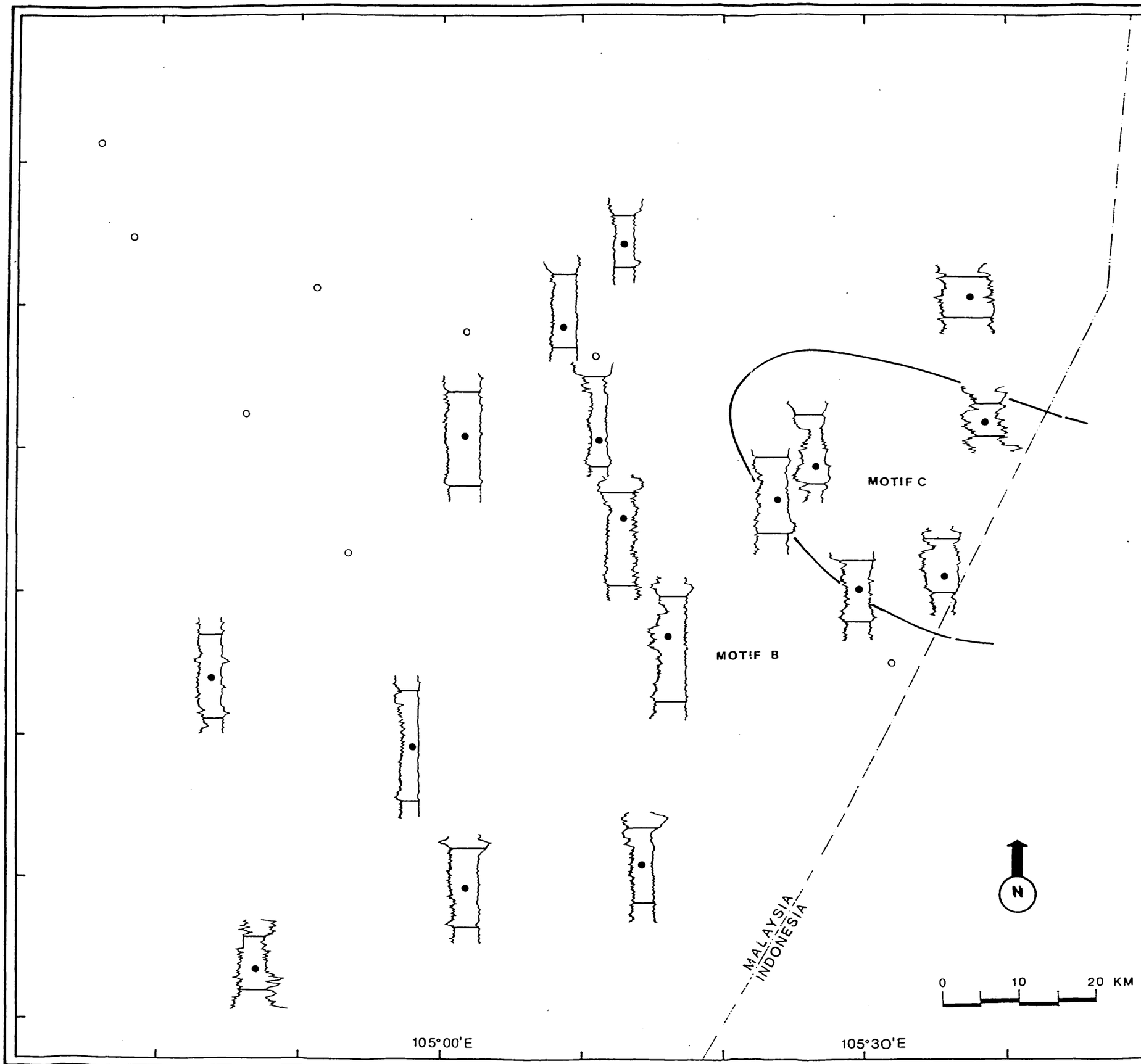
Facies of Type IV appears to be widespread in the southern regions. This facies, on correlation with the wireline logs, are seen to consist of interbedded sandstones and shales (Figs. 4-14 and 4-15).

4.3.2 Geological-Litholog Facies

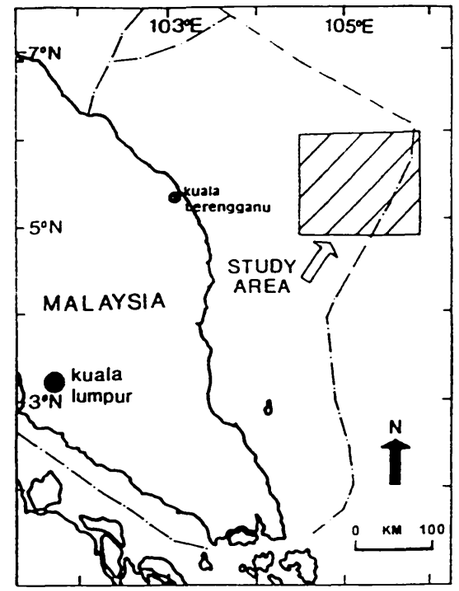
Detailed examination of the wireline logs indicates that four stratigraphic sequences can be distinguished within the Pulai-II Formation (see Section 3.7.2.3). From top to bottom (Fig. 2-12), these four stratigraphic sequences are:

1) Upper Terengganu Shale sequence which correspond to the upper half of the R-B seismic sequence. Log motifs indicate that this sequence consists predominantly of shales, and minor sandstone units (Figs. 3-18 and 4-17),

2) Lower Terengganu Shale sequence which correspond to the lower half of the R-B seismic sequence. Log motifs indicate that this sequence



LOCATION MAP



LEGEND

Motif B - shelf muds.

Motif C - barrier bar sandstones.

FIGURE 4-17

GR-Resistivity Log Facies Distribution Map of the Upper Terengganu Shales. (Note that Motif B is the dominant facies of the sequence).

consists generally of shales towards the centre, and sandstones and shales towards the edges of the study area (Figs. 3-18 and 4-18). The sandstones exhibit an upward-coarsening profile,

3) Upper Pulai Sandstone sequence which correspond to the upper half of the B-P seismic sequence. This sequence consists of:

   i) Cyclindrically-shaped or blocky log motifs of massive sandstones. In places, these sandstones are interbedded with shales, and in others, only minor shale lenses are present within the units, and

   ii) Interbedded sandstone, siltstone and shale sequence which exhibits apparent upward-coarsening log profiles. Frequently found within this sequence are generally thick, often massive sandstones with blocky log motifs (Figs. 3-18 and 4-19), and

4) Lower Pulai Sandstone sequence which correspond to the lower half of the B-P seismic sequence. This sequence consists of:

   i) Massive, occasionally stacked, blocky sandstones with minor shale beds and lenses, and

   ii) Interbedded sandstone, siltstone and shale sequence with an apparent upward-coarsening log profile. Commonly associated with this log motif are massive sandstones with blocky log pattern (Figs. 3-18 and 4-20).

MOTIF C

MOTIF D

MOTIF B

MOTIF D

MALAYSIA
INDONESIA

105°00'E

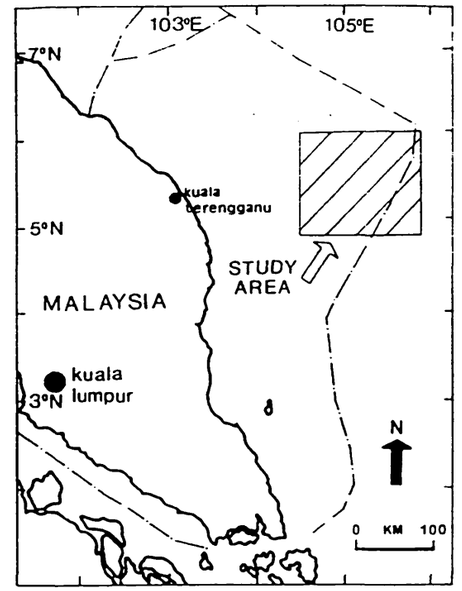
105°30'E

5° 30' N

5°00' N

0 10 20 KM

LOCATION MAP



LEGEND

Motif B - shelf muds.

Motif C - barrier bar sandstones.

Motif D - distributary and tidal channel sands, and tidal flat, crevasse splay, lagoonal and interdistributary sands, silts and muds.

FIGURE 4-18

GR-Resistivity Log Facies Distribution Map of the Lower Terengganu Shales. (Note that Motif B is dominant north of Sotong and west and southwest of Tiong-Bekok-Ledang. Motif C occurs in the northeast, and Motif D in northeast and southwest of the study area).

MOTIF A

MOTIF B

MOTIF D

MALAYSIA
INDONESIA

105°00'E

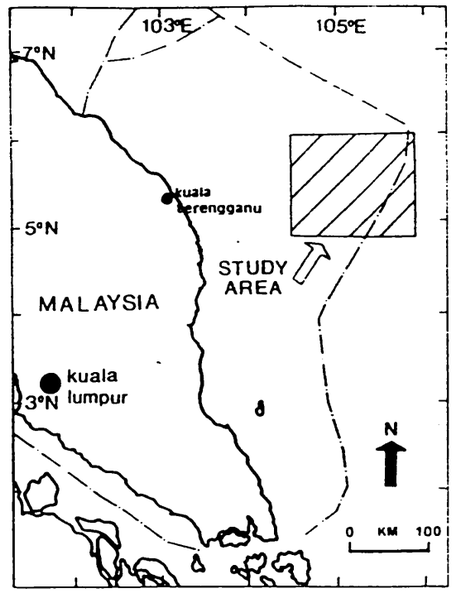
105°30'E

5° 30' N

5°00' N

0 10 20 KM

LOCATION MAP



LEGEND

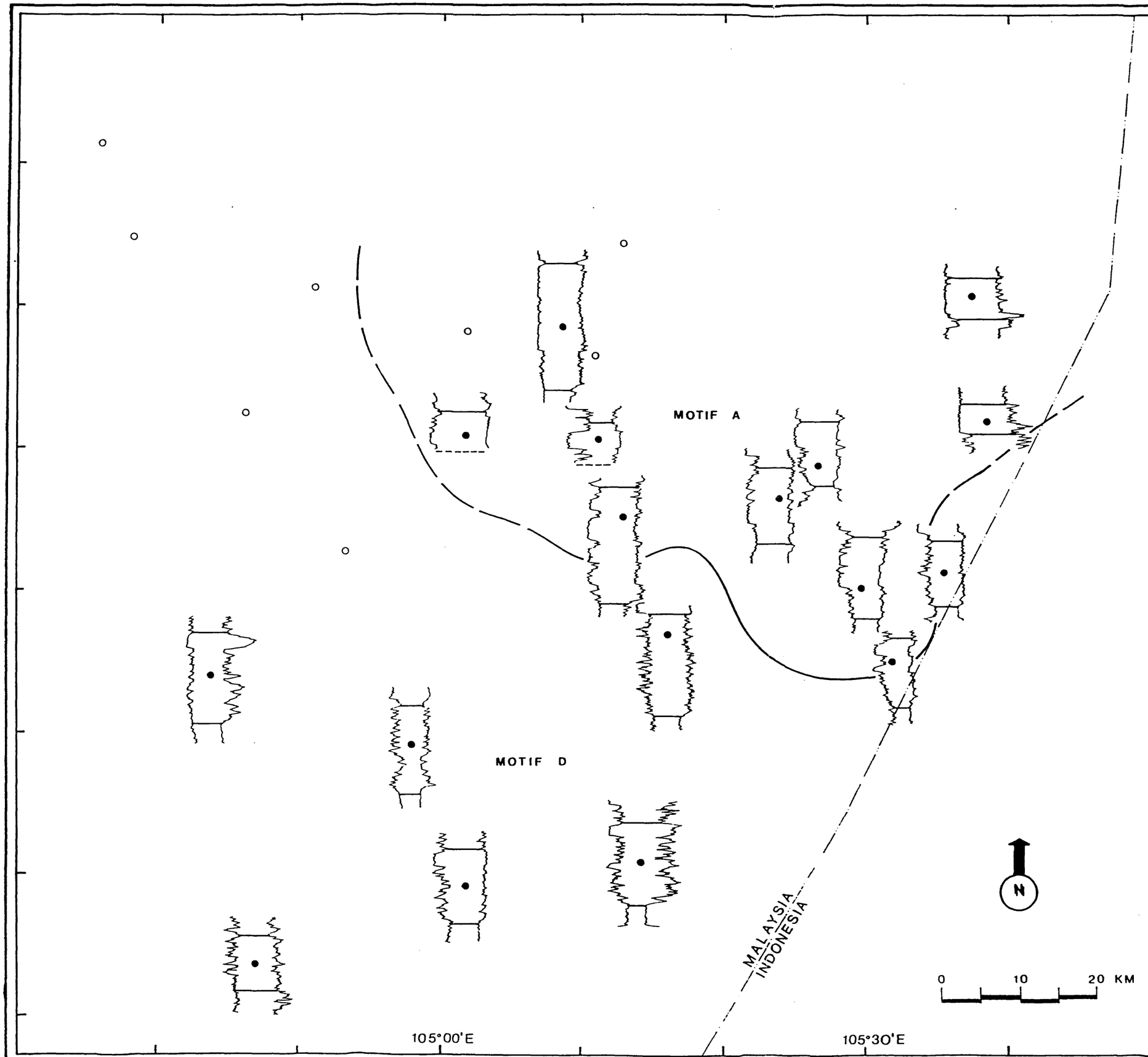
Motif A - braided channel sands and flood plain silts.

Motif B - shelf muds.

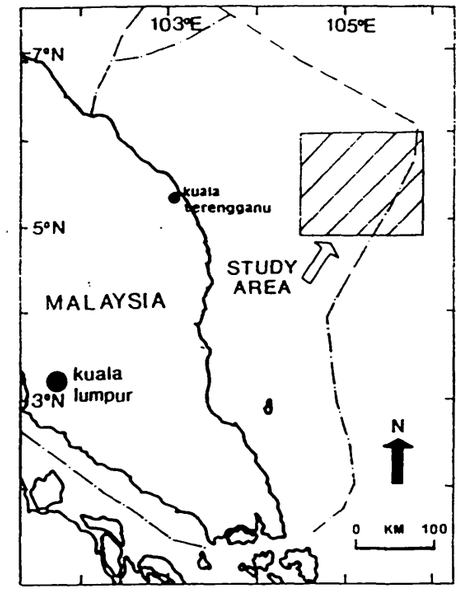
Motif D - distributary and tidal channel sands, and tidal flat, crevasse splay, lagoonal and interdistributary sands, silts and muds.

FIGURE 4-19

GR-Resistivity Log Facies Distribution Map of the Upper Pulai Sandstones. (Note that Motifs A and D are the dominant facies of the sequence. Motif B occurs primarily to the northwest of the study area).



LOCATION MAP



LEGEND

Motif A - braided channel sands and flood plain silts

Motif D - distributary and tidal channel sands, and tidal flat, crevasse splay, lagoonal and interdistributary sands, silts and muds.

FIGURE 4-20

GR-Resistivity Log Facies Distribution Map of the Lower Pulai Sandstones. (Note that only Motif A and Motif D facies have been encountered within the sequence in the study area. Motif A is dominant in the northeast; Motif D in the south and southwest).

4.3.3 Lower Pulai Sandstone Sequence

4.3.3.1 *Characteristic Features*

The Lower Pulai Sandstone sequence consists predominantly of very thick and massive sandstones, and sandstones interbedded with mudstones and shales. These sandstones are fine to very coarse grained, light to dark grey, occasionally carbonaceous. Glauconite was observed in the core at Duyong 6H-32.1 and was reported to be present in ditch cuttings at Ledang-1 (Ledang-1 Drilling Report). Associated shales are firm, and have variable colours: light to dark grey, tan/buff to greyish brown, and sometime olive green.

Two types of gamma-ray log facies have been mapped within this sequence (Figs. 3-18 and 4-20). These are:

1) Motif A which consists essentially of stacked, blocky log facies, with occasional occurrences of generally thin, 1 to 8 metre thick shale interbeds. Individually stacked sandstone units measure from 25 to 130 metres thick. At Palas-1 these sandstones are found scouring into the underlying upward-coarsening facies of Motif C, but at other places, it is commonly associated with facies of Motif D. The sandstones of this motif are more dominant in the north and north-east of the study area, and

2) Motif D which consists generally of interbedded shales, siltstones and sandstones of general upward-coarsening log pattern, with occasional individual sandstone bodies having blocky log pattern. Generally individual sandstone and siltstone units of the upward-coarsening sequence vary in thickness from 1 to 10 metres, but the sandstones of the blocky sequence are generally about 20 to 25

metres thick. These facies appear to typify the southern part of the study area.

Examination of cores and ditch cuttings of the Lower Pulai Sandstone sequence indicates that:

1) Facies of Motif A are generally massive sandstones, light grey, very fine to coarse grained, generally very clean and well sorted (Fig. 4-21). Micaceous partings are however, not uncommon. Subtle parallel laminations and medium to large scale cross-stratifications are common sedimentary structures. The sandstones are normally firm but occasionally highly friable. Occasional occurrences of shales within the sandstone interval are generally thin, medium to dark grey and in places, grey to light grey and red brown.

2) Facies of Motif D are interbedded sandstones, siltstones and mudstones of general upward-coarsening sequence. Some of these sandstones are thick and massive. The massive sandstones are generally very fine to medium-grained, light to medium grey in colour, carbonaceous and calcareous in parts, and contain traces of glauconite (Fig. 4-22). Parallel and medium scale cross laminations are faintly visible within the generally massive section. Minor rip up shale clasts are common. The sandstones within the interbedded sequence are generally very fine to medium grained, generally grey to dark grey, and contain occasional carbonaceous laminae (Fig. 4-23). The sandstones exhibit both upward-fining and upward-coarsening patterns. The upward-fining unit has a sharp erosional bases, and rip up clay clasts are common.

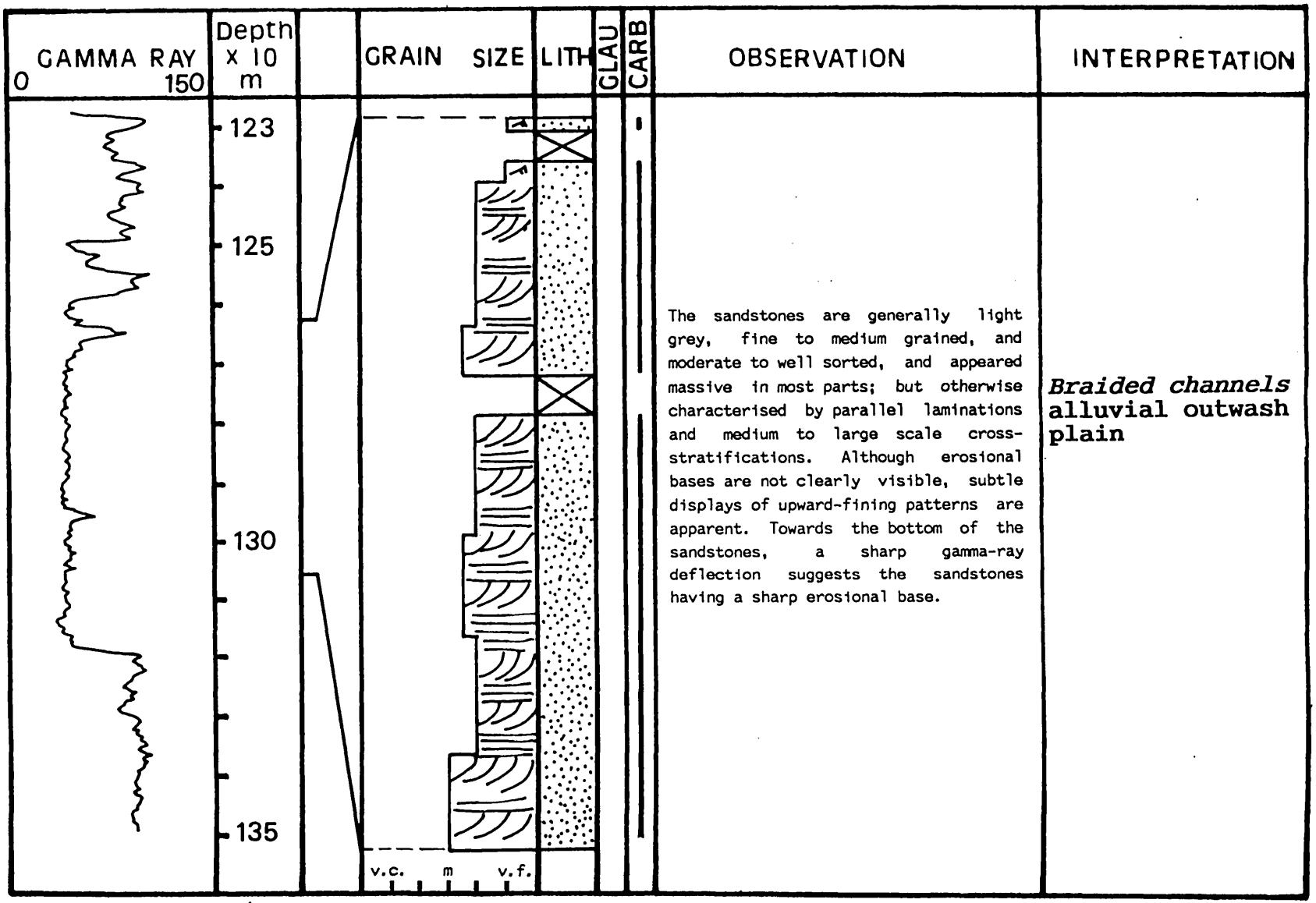


Figure 4-21 - Gamma-ray-Resistivity log responses and core description of facies in the Lower Pulai Sandstones at Pulai-1.

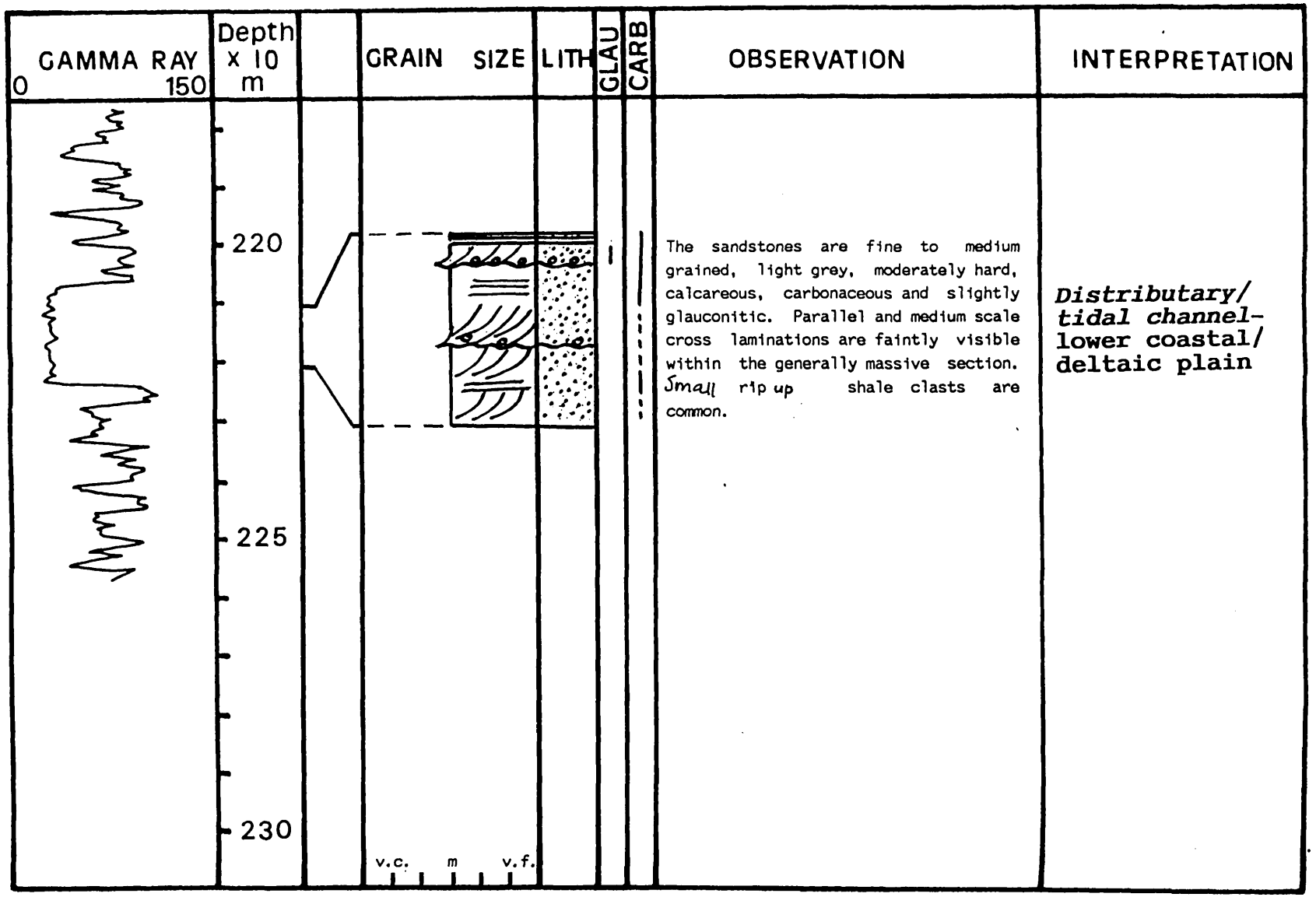


Figure 4-22 - Log responses and core description of facies in the Lower Pulai Sandstones at Duyong 6H-32.1.

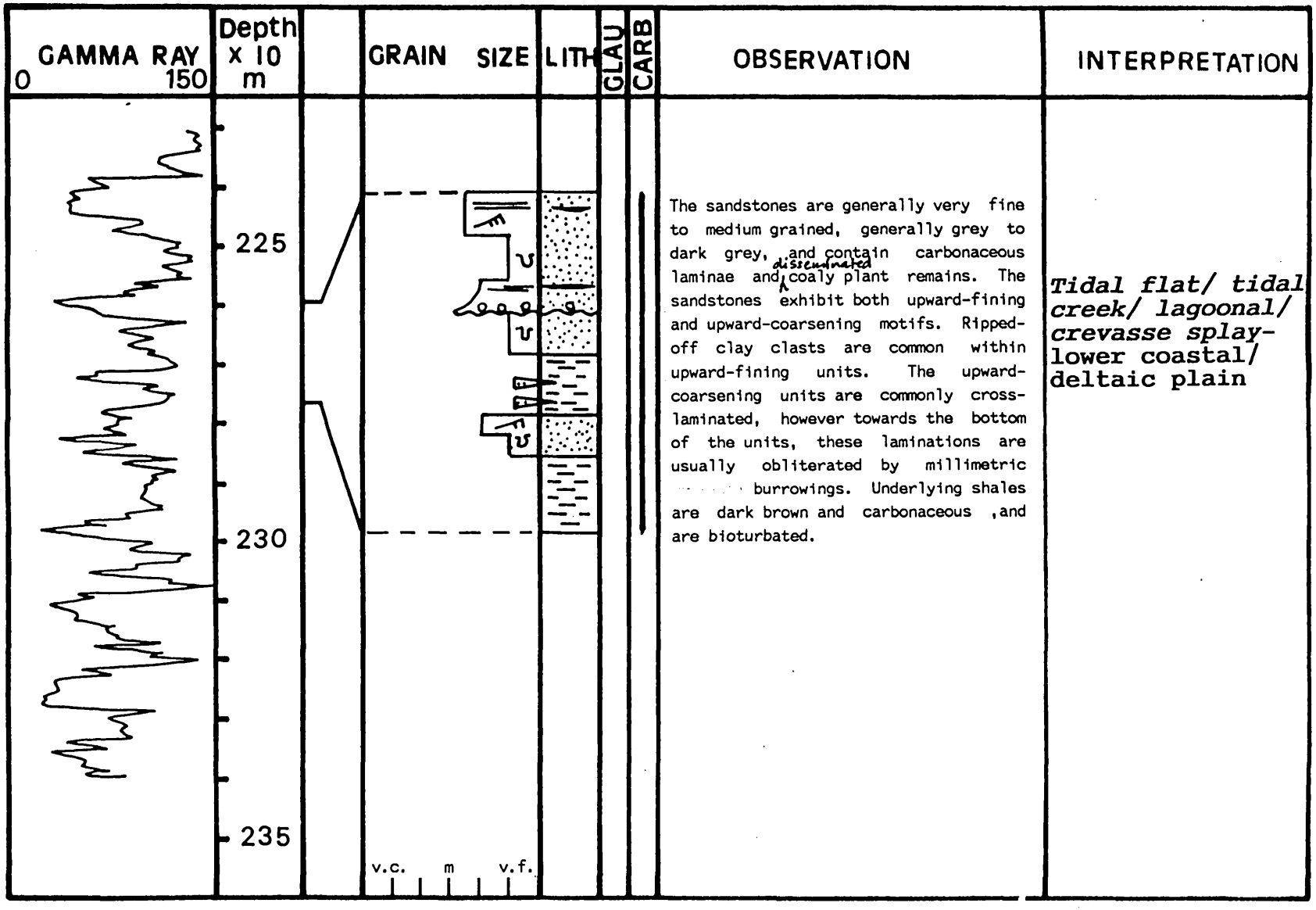


Figure 4-23 - Log responses and core description of facies in the Lower Pulai Sandstones at Sotong 5G-5.1.

4.3.3.2. *Facies Distribution*

A net percent sandstone map of the Lower Pulai Sandstone sequence, Figure 4-24, indicates:

1) A zone of relatively low sand content, less than 30 percent, in the central part of the study area. This zone, about 10-40 km in width, separates two regions of high sand contents. The region to the north and northeast is relatively more sand-prone, with sand content exceeding 50 percent. The sand content in southern region is relatively moderate, with about 30 to 50 percent, and

2) A possible occurrence of an area of low sand to the east of Ledang-Belanga region. The percent sand at Ledang-1 and Belanga-1 is less than 40 percent.

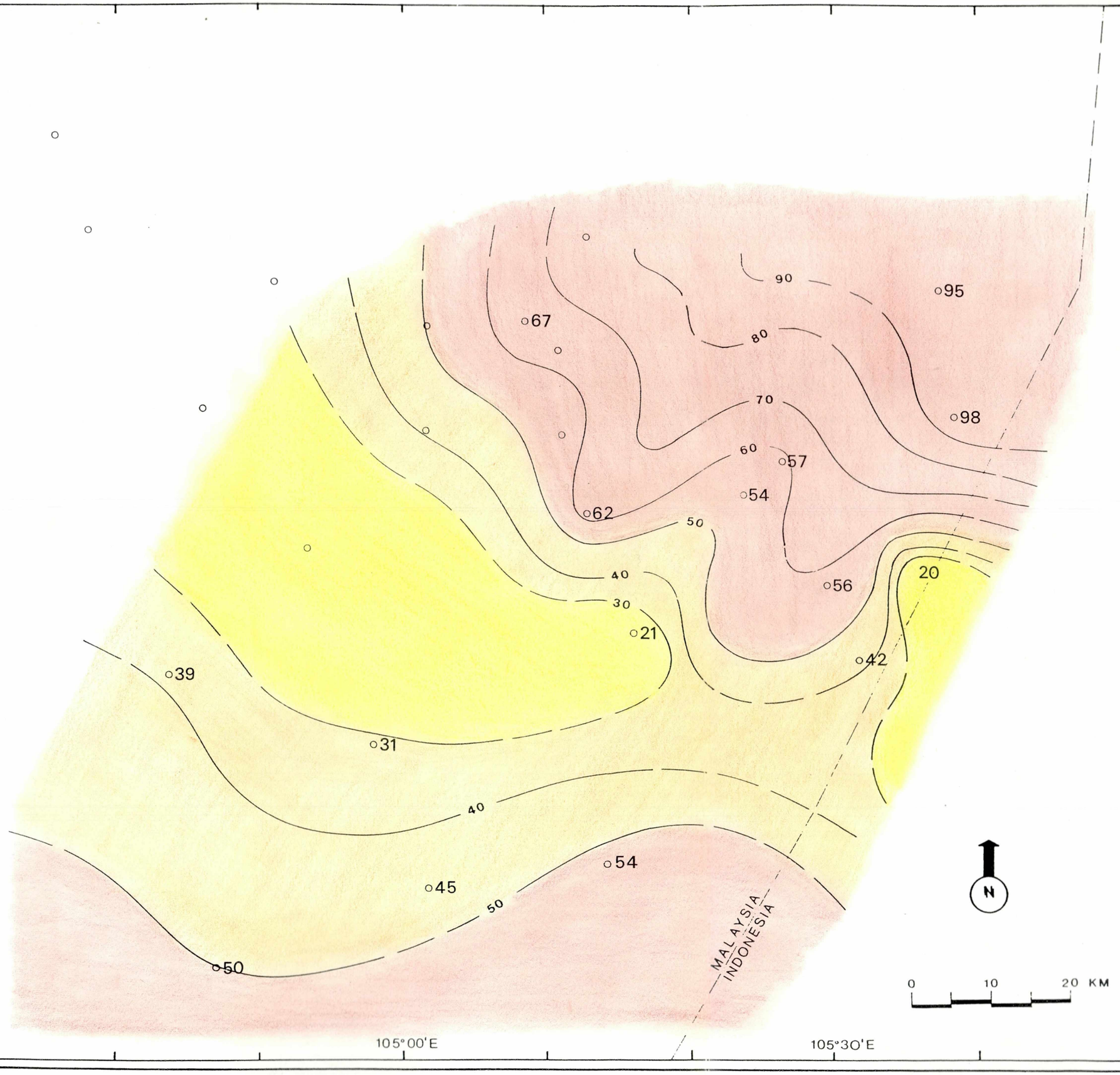
Correlation of this map, Figure 4-24, with the log facies map of the sequence, Figure 4-20, indicates that:

1) Distribution of facies of Motif A correlates generally well with the region of high sand content in the north and northeast, and

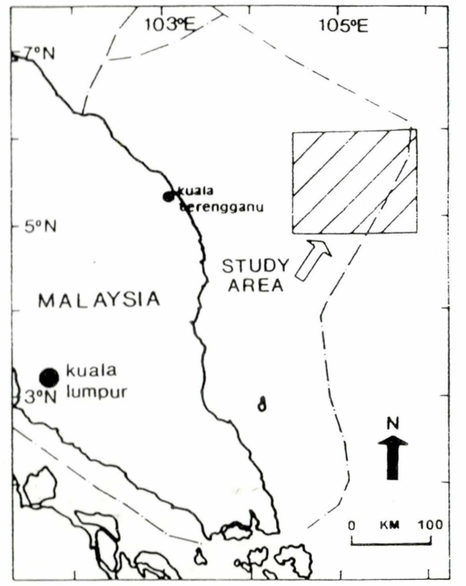
2) Distribution of facies of Motif D correlates with the region of generally moderate sand content (30 to 50 percent) in the southern region of the study area.

4.3.3.3 *Facies and Environments of Deposition*

Based on the cores, gamma-ray log motifs, the ditch cuttings for lithology, and from the study of palaeo-assemblages within the formation at the Palas-1, Duyong Barat-1, Seligi-3, Banggol-1 and Angsi-1 wells (Esso, 1978; Rashidah, et al, 1988; and Carigali, 1986), it is



LOCATION MAP



LEGEND

Low sand content

Moderate sand content

High sand content

o 45 -- control point

C. I. = 10 %

FIGURE 4-24

Net Sandstone Map of the Lower Pulai Sandstones. (Note that high sand content is confined to the northeast and southern regions of the study area).

interpreted that:

1) Sandstone facies of Motif A are alluvial channel deposits. This interpretation is based primarily on the cores at Pulai-1, which display stacked upward-fining sandstone units, and the absence of marine fossils. The facies occur fairly extensively in the north and northeast, extending at least from the Palas-Banggol region in the north to the Pulai-Belanga region in the southeast. Three stratigraphic cross-sections in the region illustrate the extent of the distribution of Motif A facies (Figs. 4-11 to 4-13). The widespread occurrence of the facies and the generally fine to medium grained sandstone of homogeneous texture observed in the core at Pulai-1, Figure 4-21, suggest that the channel sandstones are braided and in parts, consist of reworked sands. Good stratigraphic correlations suggest that these braided channel deposits are sheet-like, and are best developed northwest of Pulai (Fig. 4-20). It is further interpreted that this sandstone sheet constitutes a complex of braided alluvial systems which built out onto:

   i) A lower coastal/delta plain (strand plain/lagoonal/tidal flat) setting in the south, by virtue of its association with facies of Motif D (refer item (2) below), and

   ii) Open shelf in the west. The recent work of Rashidah et al (1988), on some cores and cuttings of the formation indicated a lack of marine faunas. Extensive abundance of *Pediastrum*, a fresh water algae, in the samples at Seligi-3 and Angsi-1, provides strong evidence of deposition and accumulation of the facies in a continental setting.

2) Blocky sandstones and sandstones of interbedded sandstone and shale sequence of Motif D are distributary/tidal channel and tidal flat/strand plain/crevasse splay sandstones respectively. This interpretation is based on the occurrences of:

   i) Interbedded sandstone and shale sequence within the general upward-coarsening log/lithological profile (Johnson and Baldwin, 1986),

   ii) Millimetric vertical burrowings within the interbedded sandstone and shale sequence,

   iii) Coaly fragments and carbonaceous matter in sediments of the interbedded sequence, and

   iv) *Casuarina, Palmae* and *Rhizoporaceae,* spores of coastal and mangrove plants.

   This facies is associated with the distributary/tidal channel sandstones which are massive, exhibiting blocky log profiles. Ripped-off clay clasts are common in the massive sandstones. The occurrence of glauconite in the sandstones is a strong indication of a marine influence (Selley, 1985). Two stratigraphic cross sections, Figures 4-14 and 4-15, indicate that the area covering much of the southern region was probably low-lying and extensive. A "strait" covering the Ophir-Ledang-Duyong region probably constituted an area of intricate channel system, through which open marine waters on the east mixed with the relatively non-marine waters, fresh to probably brackish, in the west during high tides.

4.3.4 Upper Pulai Sandstone Sequence

4.3.4.1 *Characteristic Features*

The Upper Pulai Sandstone sequence consists generally of very thick and massive sandstones, and sandstones interbedded with mudstones and shales. These sandstones are light to dark grey, occasionally carbonaceous and micaceous, and in places contain lignitic fragments and glauconite. The associated shales are firm, light to dark grey, and occasionally tan/buff and greyish brown.

Three types of log facies have been mapped within the sequence (Figs. 3-18 and 4-19). These are:

1) Motif A which consists of sandstones and occasional shale beds. The sandstones are stacked, and measured about 20 to 70 metres thick. Shale beds are usually 3 to 10 metres thick. The sandstones of this motif occur predominantly in the north and north-east of the study area,

2) Motif D which consists essentially of interbedded sandstone, siltstone and shale, and massive sandstones of blocky log profiles. The generally upward-coarsening, sand-silt-shale sequence is cyclic, and the thickness of each cyclic varies from locality to locality, but normally between 10 to 30 metres, and usually the thickness of the sandstone is no greater than 10 metres. However, the thickness of the blocky sandstones is usually between 20 to 25 metres. Motif D facies typify the south and southwestern part of the study area, and

3) Motif B which generally consists of shales and siltstones, with occasional occurrences of thin sandstone beds. The sandstones are

generally less than 1-metre thick. Motif B facies typifies the west and central parts of the study area.

Examination of cores and ditch cuttings indicates the following characteristics of the Upper Pulai Sandstone sequence:

1) Sandstones of Motif A are generally fine to coarse-grained, and in places granulitic, light to medium gray, and slightly micaceous and carbonaceous (Figs. 4-25 and 4-26). Lignitic materials have been observed in some sandstones. The sandstones are generally moderately firm to highly friable, and in places highly friable. The associated shale intervals are medium to dark grey and occasionally brown.

2) Facies of Motif D constitutes interbedded sandstones, siltstones and mudstones and massive sandstone sequences. The massive sandstones are generally very fine to coarse-grained, light to medium gray, carbonaceous with lignitic fragments in parts, and contain traces of glauconite (Fig. 4-27). Ripped-off mudrocks are common within some of the massive units. The sandstones within the interbedded sand-silt-shale sequence are usually less than 10 metres thick, and they generally exhibit upward-fining motif (Figs. 4-28 and 4-29). These sandstones occasionally contain traces of glauconite and lignitic fragments. Millimetric vertical burrows are common in the finer sections of the sandstones. Associated mudstones are usually medium to dark grey and occasionally tan to light brown.

3) Facies of Motif B consists predominantly of shales with occasional occurrences of thin, very fine-grained sandstone beds. These sandstones are usually carbonaceous and slightly glauconitic. The shales are grey to dark grey, and occasionally buff to brown. No

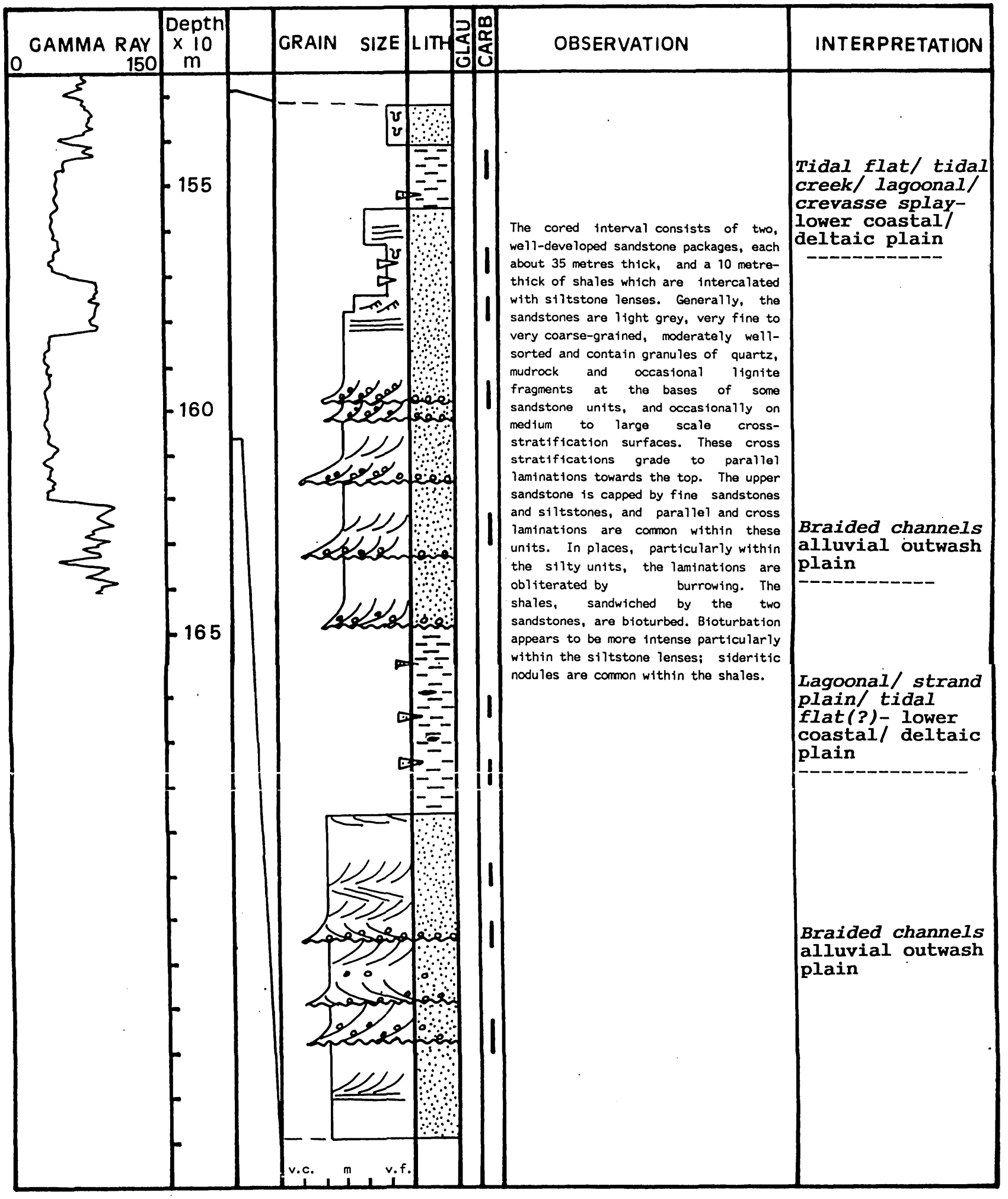


Figure 4-25 - Log responses and core description of facies in the Upper Pulai Sandstones at Seligi-3. (See pocket for core photographs).

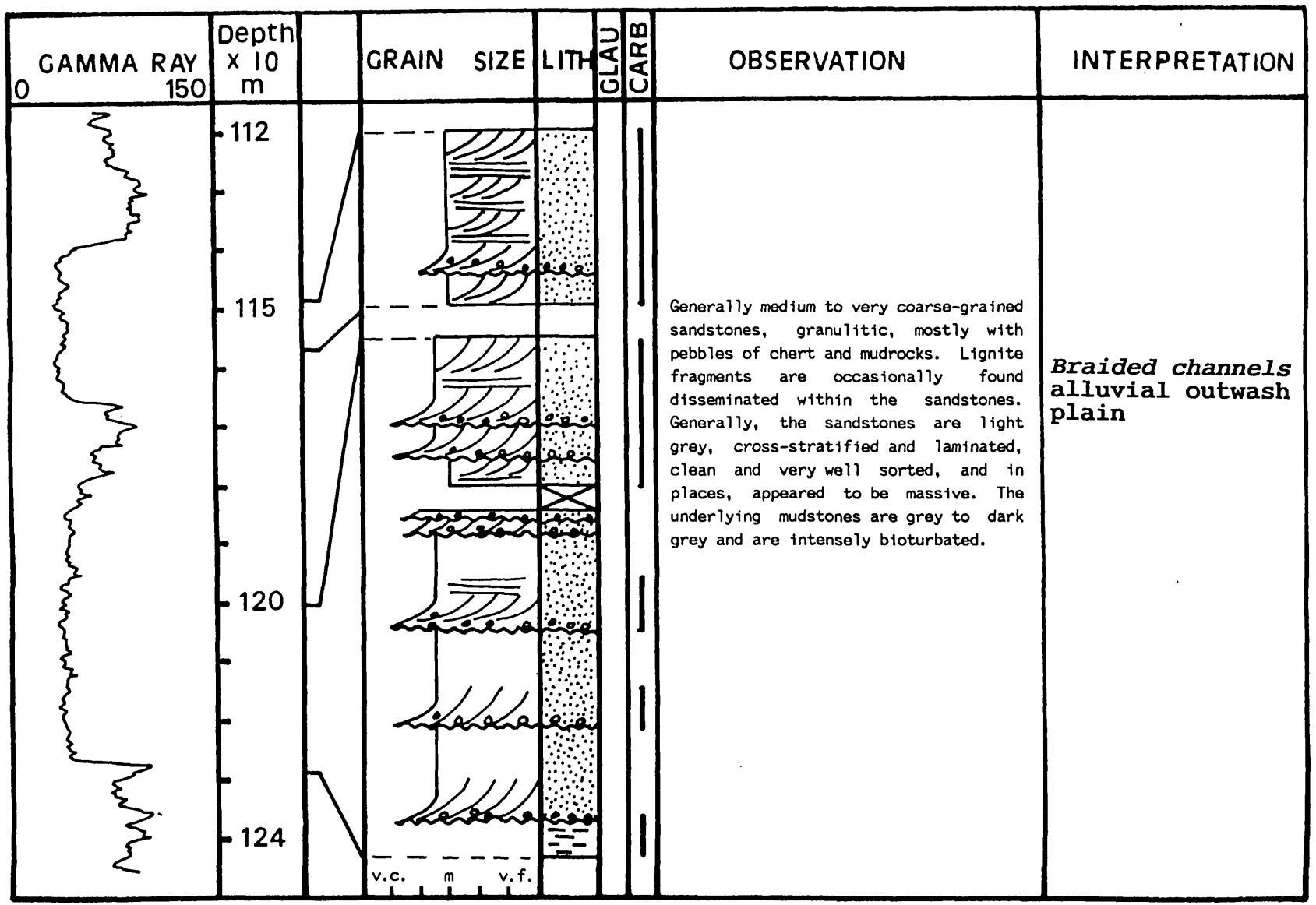


Figure **4-26** - Log responses and core description of facies in the Upper Pulai Sandstones at Pulai-1. (See pocket for core photographs).

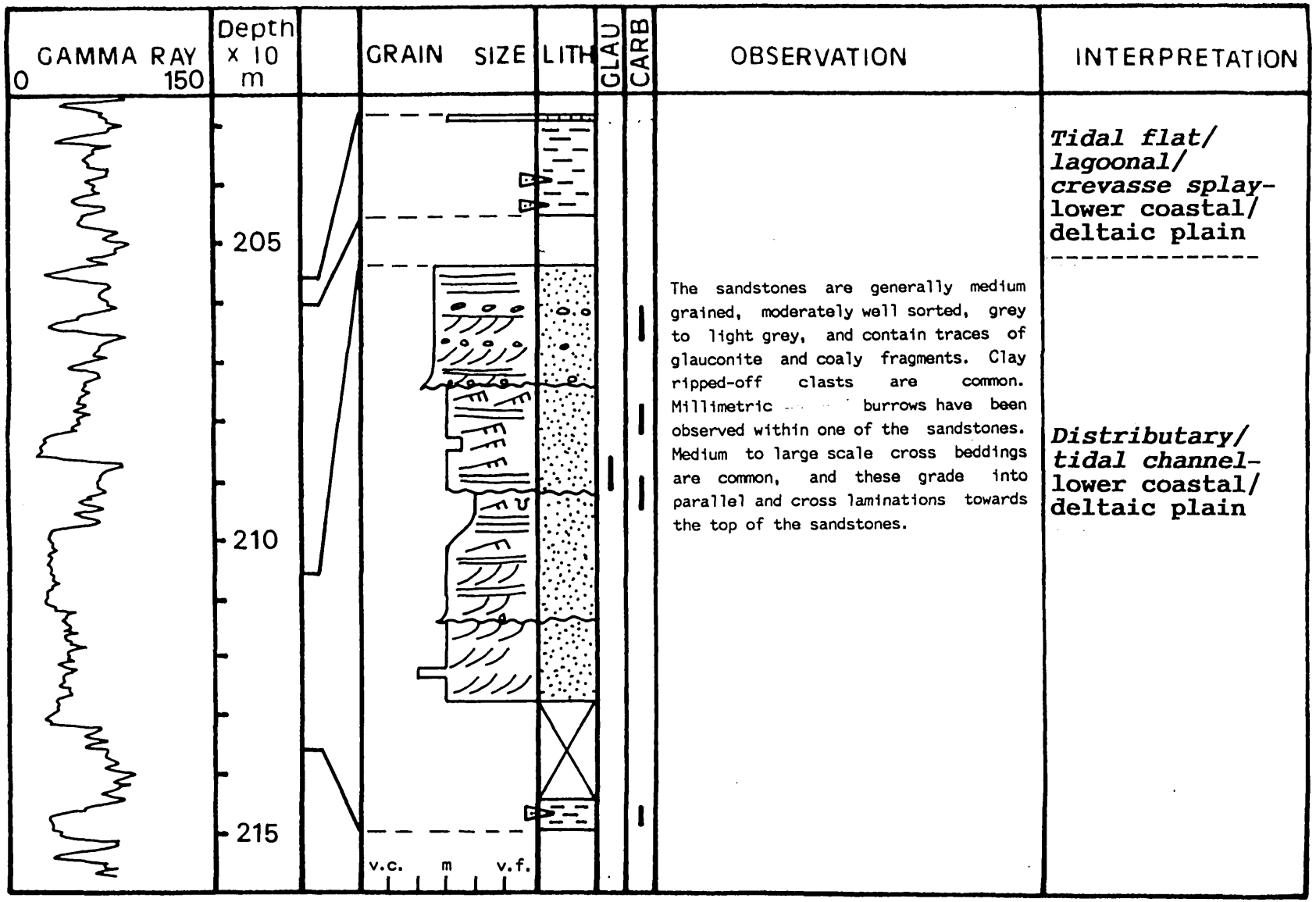


***Figure* 4-27** - Log responses and core description of of facies in the Upper Pulai Sandstones at Besar-1. (See pocket for core photographs).

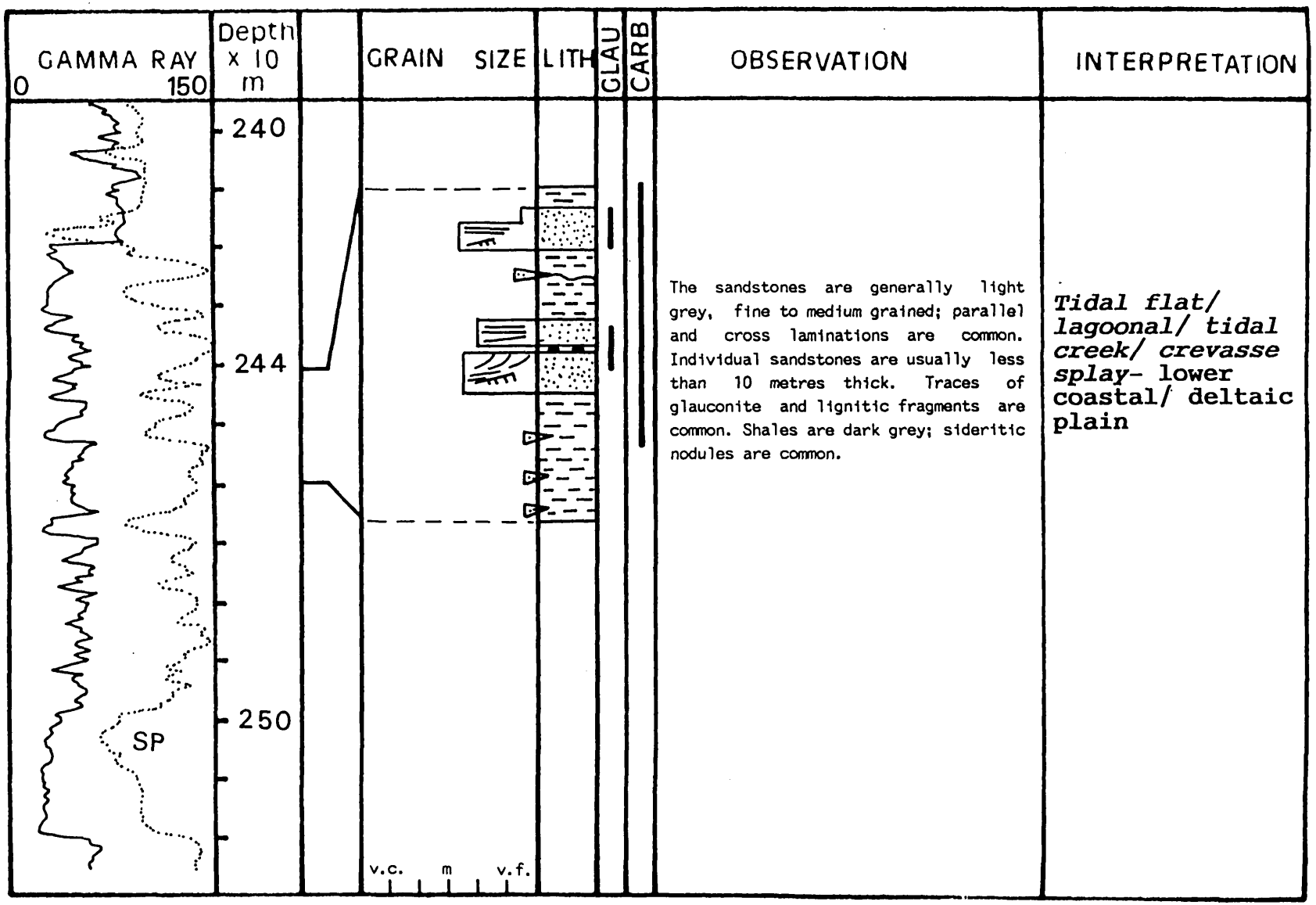


Figure **4-28** - Log responses and core description of facies in the Upper Pulai Sandstones at Angsi-1.

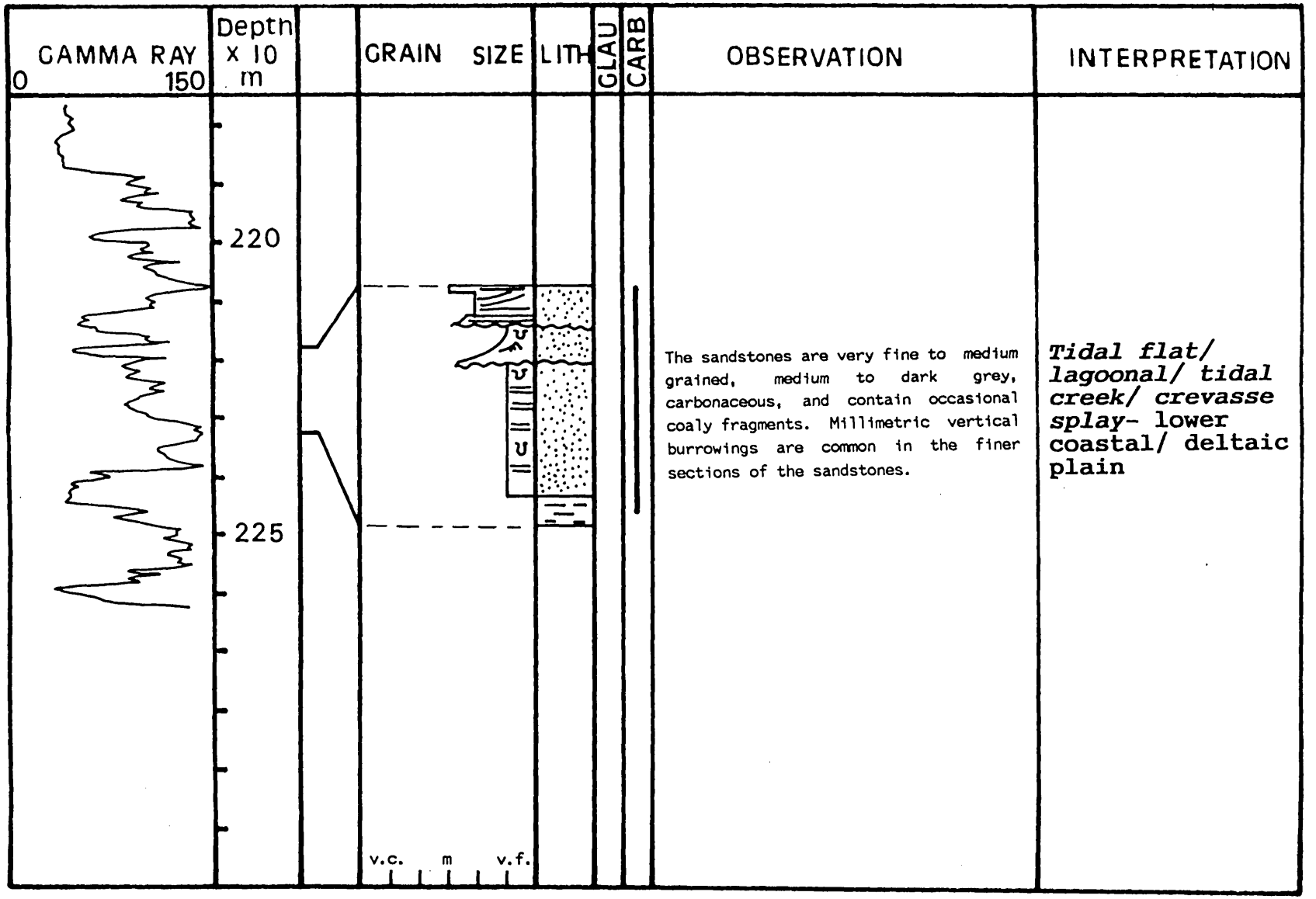


Figure **4-29** - Log responses and core description of facies in the Upper Pulai Sandstones at Sotong 5G-5.1. (See pocket for core photographs).

cores were available for examination, but based on the gamma-ray log, the sandstones are usually less than 1-metre thick.

4.3.4.2. *Facies Distribution*

The net percent sand map of the Upper Pulai Sandstone sequence, Figure 4-30, indicates:

1) An area of relatively low sand content, with sand of less than 30 percent, occurring in the northwestern part of the study area,

2) An area of relatively high sand content, with sand percent exceeding 50 percent, occurring in the northeast of the area, and

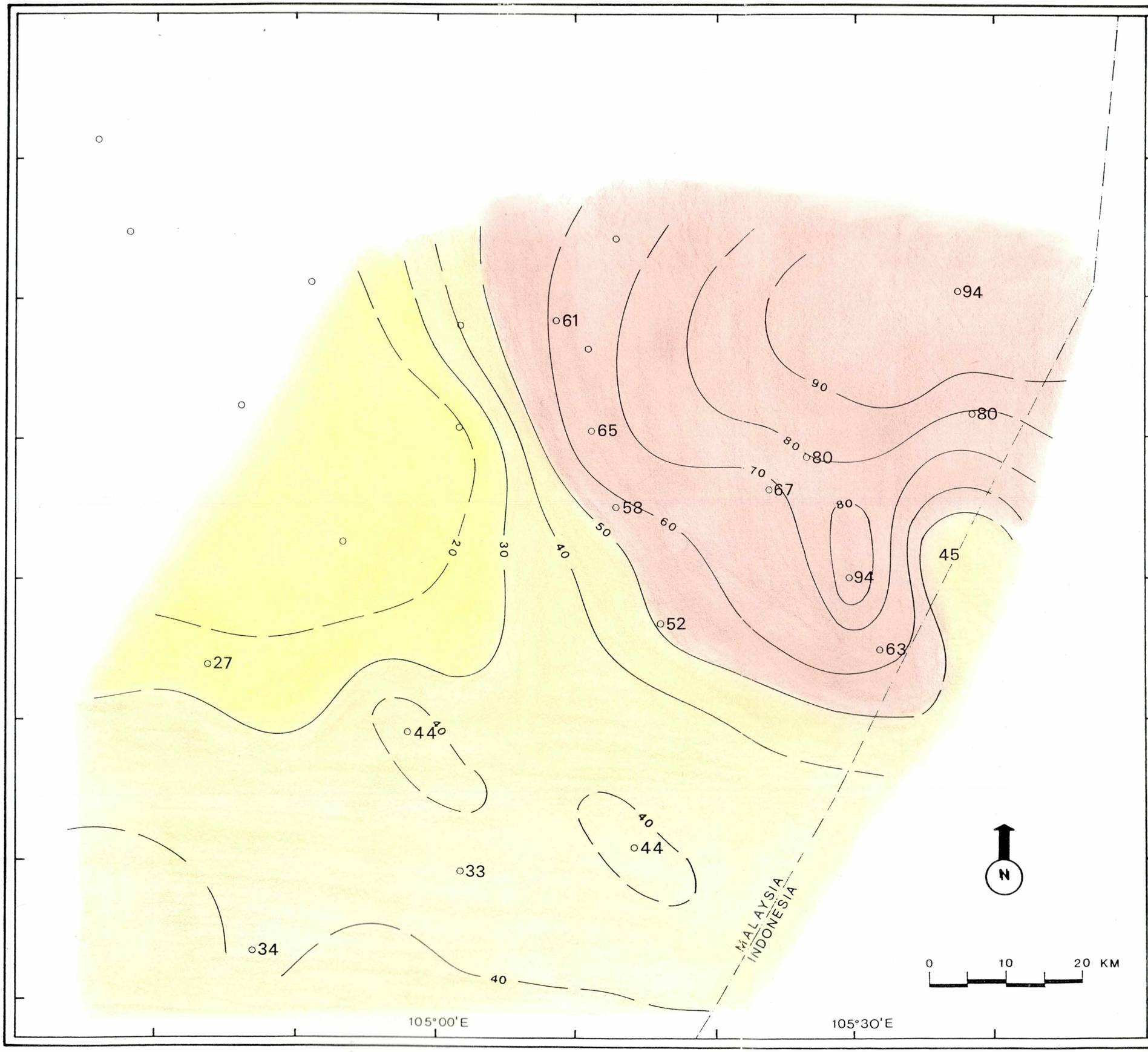
3) Localised occurrences of 40-50 percent sand content within an area of generally moderate sand content, 30-40 percent, in the southern half of the study area.

The results of correlation of the log map of the sequence, Figure 4-19, with the percentage sand map of the same, Figure 4-30, indicate the following relationships:

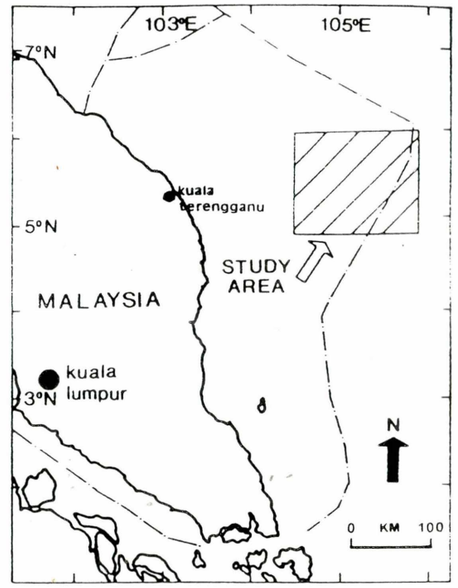
1) That the distribution of Motif A facies correlates with the region of relatively high sand content in the northeast,

2) That the distribution of Motif D facies correlates with the region of moderate sand content. Localised high content of sands within the framework corresponds to the localised occurrences of massive sandstones within the interbedded sands, silts and shales sequence. This facies predominates in the south, and

3) That the distribution of Motif B facies correlates with the area of



LOCATION MAP



LEGEND

Low sand content

Moderate sand content

High sand content

o 45 -- control point

C. I. = 10 %

FIGURE 4-30

Net Sandstone Map of the Upper Pulai Sandstones. (Note that high sand content is confined to the northeastern region of the study area).

low sand content in the west and northwest of the study area.

4.3.4.3 *Facies and Environments of Deposition*

Based on the cores and log motifs, the ditch cuttings for lithology, and from the study of palaeo-assemblages within the formation at the Palas-1, Duyong Barat-1, Seligi-3, Banggol-1 and Angsi-1 wells (Esso, 1978; Rashidah, et al, 1988; and Carigali, 1986), it is interpreted that:

1) Motif A sandstones include fluvial and estuarine channels. This interpretation is based primarily on the blocky log pattern and occasional fining-upward motifs, cut-and-fill structures with sharp erosional bases, medium to large scale cross stratifications which grade into parallel and cross laminations towards the top of the individual units, and on the occurrences of granules of quartz and mudrock as lag deposits. The channel sandstones are considered estuarine when there are burrows within the finer section of the upward-fining sandstone units, mudrock rip up clasts and lignitic fragments, and glauconite. These sandstones are common in the southern area (Figs. 4-14 and 4-15). Those other channel facies which are very coarse-grained and granulitic, especially in the Pulai-Seligi-Tinggi area, and also in areas east and northeast of Palas, are probably fluvial braided channel deposits. The stratigraphic cross-sections of the sequence in these areas, Figures 4-11 to 4-13, show the extent of the channel facies, with the braided channel system predominating in the lower half of the sequence. The correlatable shaly interval, which at Seligi-3 is bioturbated (Fig.4-25), appears to be extensive, and it could well

represent transgressive strand plain/lagoonal sequence. The channel sandstones are sheet-like, and probably constitute parts of delta systems which built out onto:

i) A tidally dominated setting in the south, by virtue of its association with facies of Motif D (refer item (2) below), and

ii) Open shelf in the west.

2) Motif D sandstones are deposits of lower coastal/delta plain, consisting of distributary and tidal channels, and tidal flat/strand plain/crevasse splay sandstones and siltstones. The basis for this interpretation is primarily the occurrences of mottling and burrowing features within the interbedded mudstones, siltstones and sandstones, and occasionally localised burrowing within the massive sandstones; the characteristic upward-fining motif of some interbedded sandstones (Johnson and Baldwin, 1986); medium to large scale cross stratifications which grade into parallel and cross laminations; the occurrences of the mudrock rip up clasts within and at the bases of some of massive sandstone units, and the occurrences of *Casuarina, Palmae* and *Rhizoporaceae*, spores of coastal and mangrove plants. The occurrence of coaly fragments within the channel facies and the coastal and mangrove plant species within the sediments is indicative of the coastal setting, and that of glauconite implies tidal dominance. The distribution of Motif D facies: the interbedded sandstones, siltstones and mudstones in the south and southeastern part of the study area indicates the probable occurrence of extensive and widespread low-lying depositional setting in the region.

3) Minor sandstones of Motif B are probably delta slope sandstones. The predominant shale and minor silt/sandstone sequence, together with the reported occurrence of glauconite within the silt/sandstones, (Tapis-2 Drilling Report), form the basis of this deduction.

4.3.5 Lower Terengganu Shale Sequence

4.3.5.1 *Characteristic Features*

This sequence consists predominantly of shales with intercalated siltstones and sandstones. The sandstones are commonly found at the base of the sequence in the northeastern part of the study area (Fig. 4-18). The sandstones are usually very fine to coarse-grained, light to dark grey and occasionally olive-green, carbonaceous and calcareous. Drilling reports of Bekok-1, Palas-1, Tinggi-1, and Besar-1 indicate the presence of glauconite in the sandstones. Associated shales are generally firm and occasionally fissile, displaying variable colours: dark grey, brownish grey and olive-green.

Log motifs of the sequence, Figure 4-18, fall into three categories:

1) Motif B consists predominantly of shales with occasional occurrences of thin, very fine-grained sandstone beds. The sandstones are generally less than 1-metre thick. Motif B facies typifies the west and a greater portion of the central part of the study area.

2) Motif C comprises coarsening upward sandstones of generally a funnel-shape log motif. Occasionally this log motif is serrated, and, in the upper part of the sequence, the log shape commonly becomes blocky. The thickness of the sequence usually ranges from 25 to about 50 metres, and

3) Motif D consists of cyclic, upward-coarsening log motif, with the thickness of each cyclic sequence not exceeding 10 metres. Occasionally associated with this log facies are sandstones of blocky log motif, with thickness normally not exceeding 40 metres. The occurrence of this facies appears to be localised, and is found at Sotong 5G-5.1 in the extreme southwest, and at Seligi-3, Pulai-1, Ledang-1 and Belanga-1 in the northeast.

Examination of cores and/or ditch cuttings indicates that:

1) Shales of Motif B are grey to dark grey, and occasionally buff to brown in colour, and calcareous. The very minor sandstones intercalated within the shales, are usually grey to dark grey, carbonaceous and slightly glauconitic.

2) Sandstones of Motif C are generally fine to medium grained, and light to dark grey in colour (Fig. 4-31). The sandstones are carbonaceous and glauconitic. Fine cross-laminations and parallel laminations are common features; however, wavy and discontinuous carbonaceous and lignitic laminae are occasionally present within the sandstones. Minor micaceous partings are common. Extensive vertical burrowings have been noted within the cyclic upward-coarsening sequence. The shales and mudstones found intercalated with the sandstones are usually firm, light to dark grey and occasionally tan/buff to greyish brown, and olive green. Occasional bands of brown sideritic lenses are common within the shale interval.

3) Sandstones of Motif D are generally very fine to coarse grained and

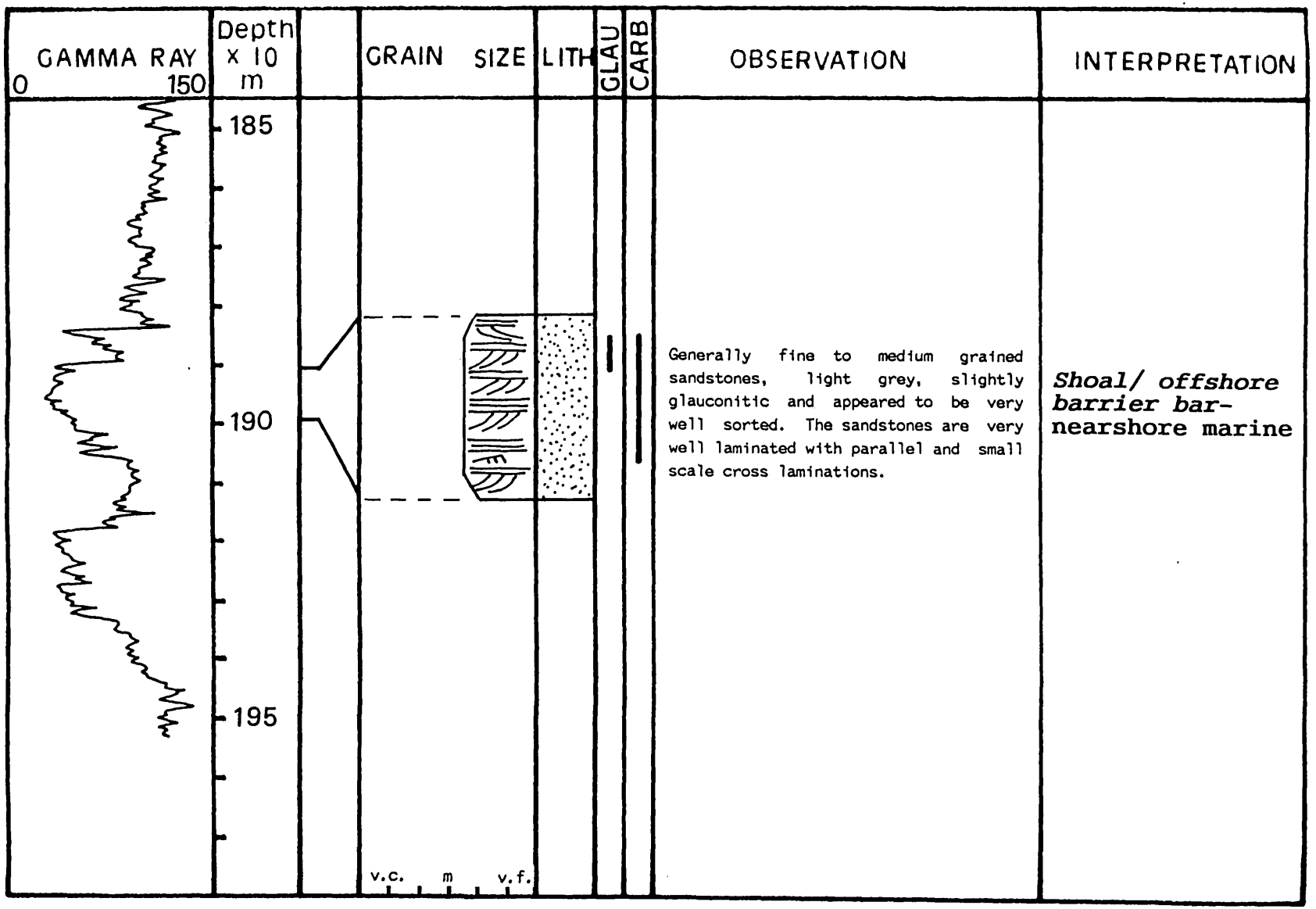


Figure 4-31 - Log responses and core description of facies in the Lower Terengganu Shales at Bekok-1. (See pocket for core photographs).

light to dark gray in colour. The sandstones are carbonaceous, partly calcareous, and contain traces of glauconite. Occasional flaser bedding is common within the interbedded sandstone and shale sequence, although this feature is often obliterated by intense vertical burrowing (Fig. 4-32). On the other hand, the massive sandstones are generally medium to very coarse-grained (Fig. 4-33). Ripped-off mudrock clasts and lignitic fragments are common at the base of the massive sandstones. Small to large scale, trough cross-beddings and finely laminated tops are common sedimentary structures.

4.3.5.2 *Facies Distribution*

The net percent sand map of the Lower Terengganu Shale sequence, Figure 4-34, indicates:

1) That the sequence contains relatively less sand than the underlying Pulai Sandstones sequences. The maximum percent sand in the sequence does not exceed 35 percent.

2) That there are two areas: northeast and extreme southwest, which have sand greater than 10 percent. The sandstones in the northeast are linear and ridge-like and appear to parallel the palaeo setting (Fig. 4-7), and the zone of little sand content (less than 10%). The morphology of sandstones in the extreme southwest is not known for lack of data, but their distribution is probably northwest-southeasterly. This is because the area with 40 percent sand within the Upper Pulai Sandstone sequence in the south lies generally in the east-west direction (Fig. 4-30), and opening up of the Malay basin and the subsequent encroachment of the "sea" from the

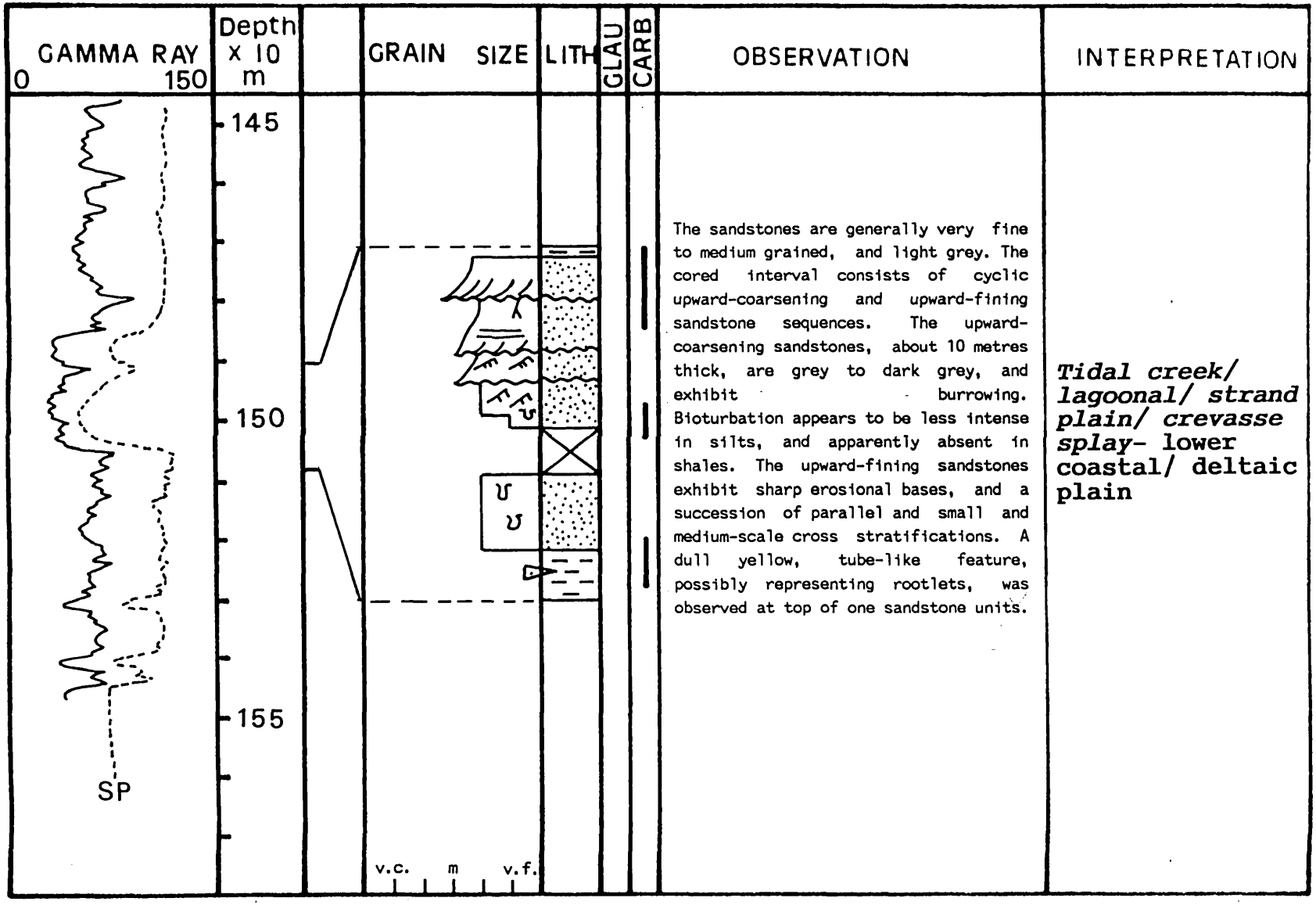


Figure **4-32** - Log responses and core description of facies in the Lower Terengganu Shales at Seligi-3. (See pocket for core photographs).

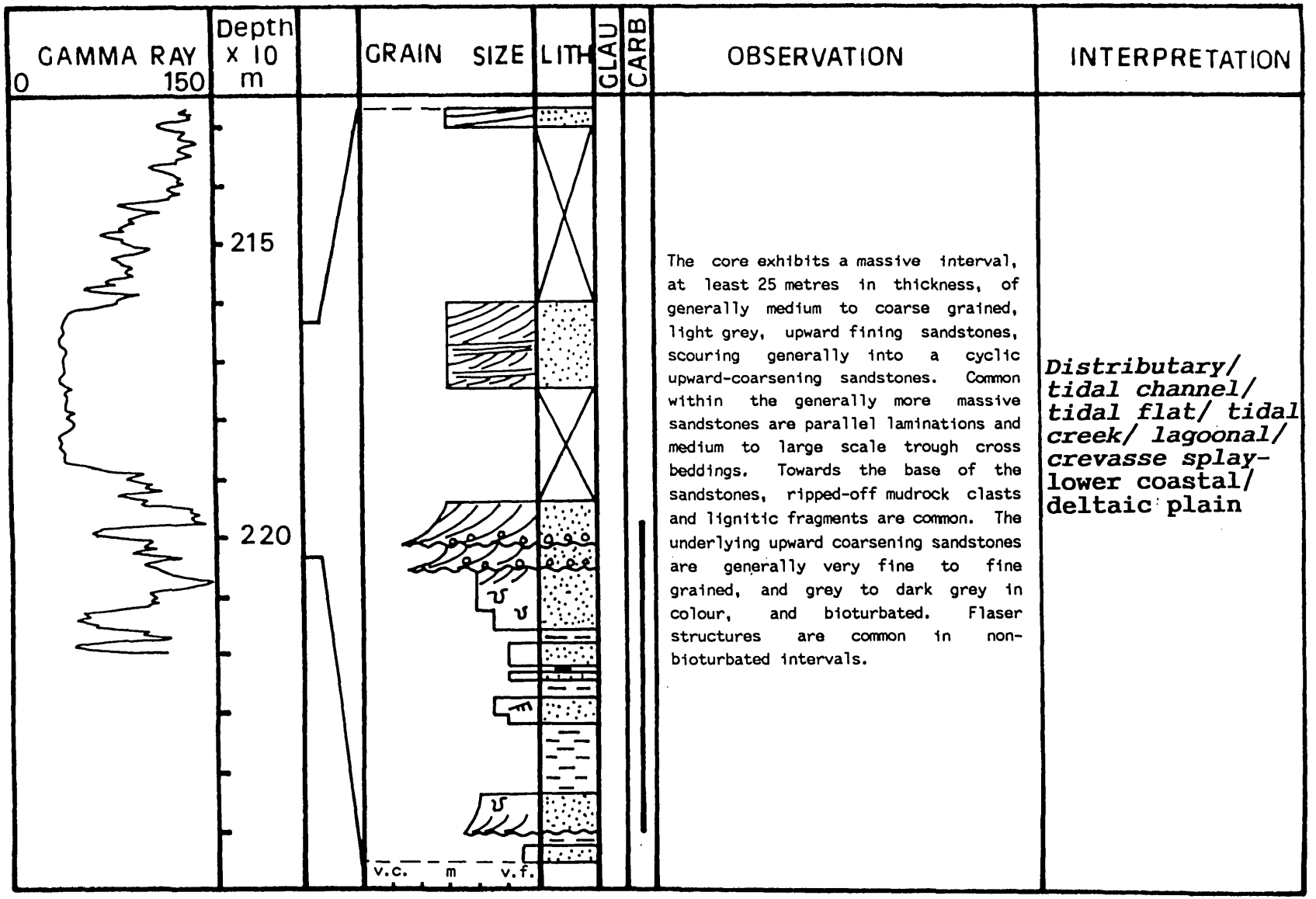


Figure **4-33** - Log responses and core description of facies in the Lower Terengganu Shales at Sotong 5G-5.1. (See pocket for core photographs).

southeast could push the coastline southwestward.

There is a correlative pattern between the percent sandstone map and the log map of the sequence, Figures 4-34 and 4-18. This correlation appears to indicate the following:

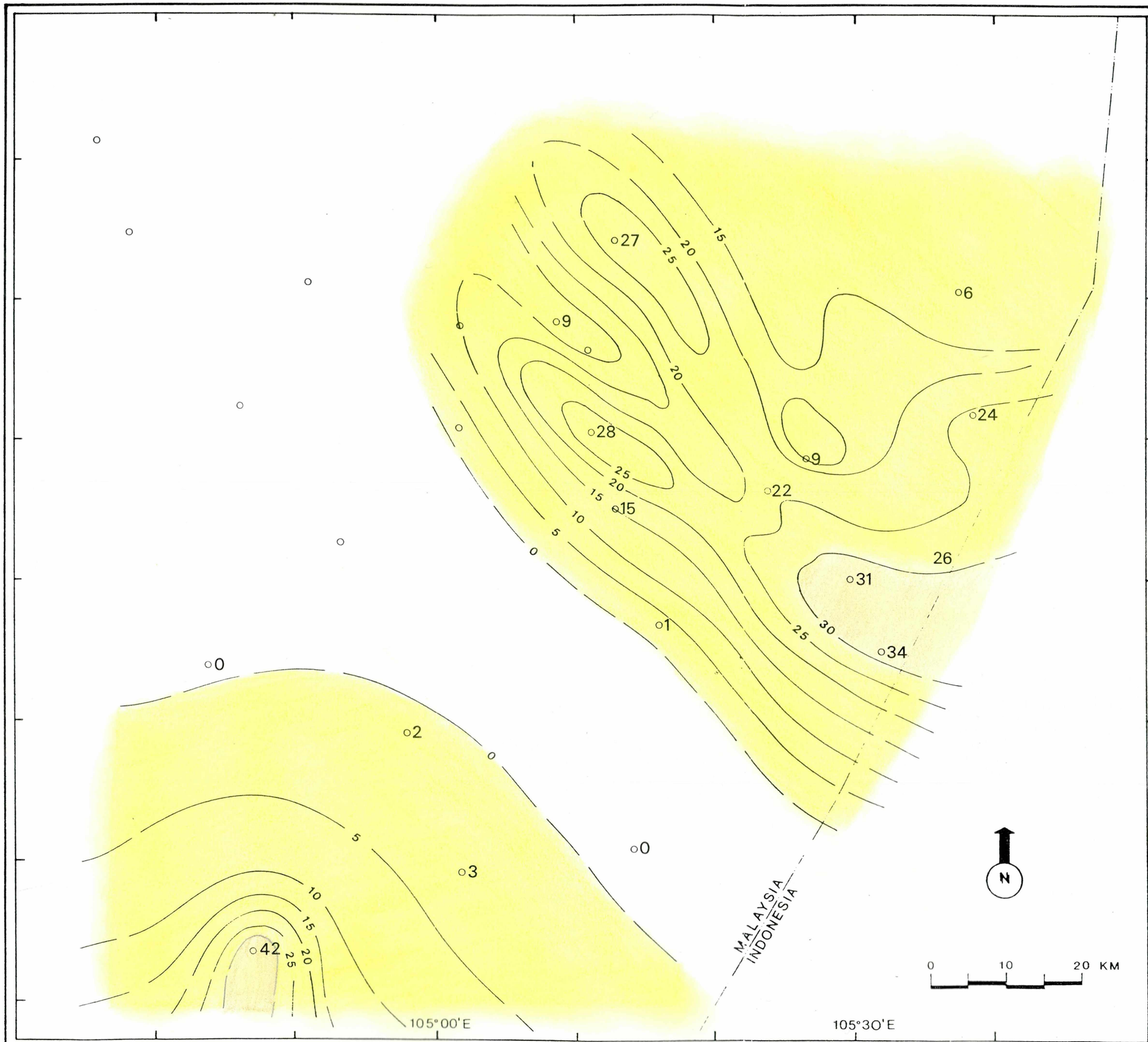
1) That distribution of Motif C facies correlates generally with the region of sand content greater than 10 percent, in the northeast, and

2) That distribution of Motif D facies correlates with the region of sand content generally greater than 20 percent in the northeast covering the Seligi-Pulai-Belanga-Ledang area, and in the extreme southwest around Sotong.

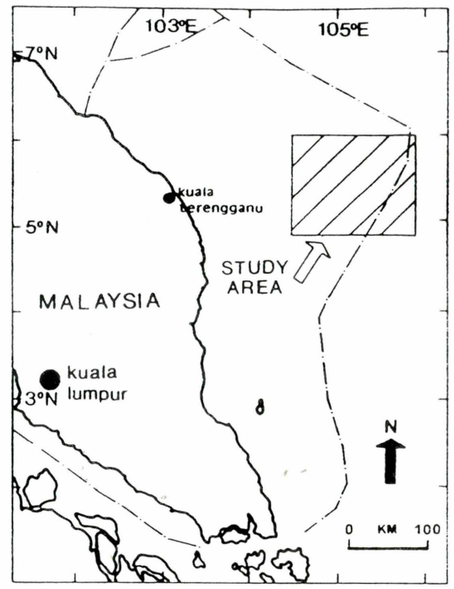
4.3.5.3 *Facies and Environments of Deposition*

Based on the above observations (geometry and lithology) and by inference from the wireline logs, and from the study of palaeo-assemblages within the formation at the Palas-1, Duyong Barat-1, Seligi-3, Banggol-1, and Angsi-1 wells (Esso, 1978; Rashidah, et al, 1988; and Carigali, 1986), it is interpreted that:

1) Sandstones of Motif C are offshore/barrier bars. This interpretation is based primarily on the linear, shoestring and ridge-like morphology, Figure 4-34, which parallels the palaeoslope (Fig. 4-7); and the characteristic overall upward-coarsening lithological/log pattern (Selley, 1985). Other characteristic features common to offshore bars, which have been observed in the sandstones, include very fine to medium grained sandstones, and alternating parallel and



LOCATION MAP



LEGEND

Low sand content

Moderate sand content

o 15 -- control point

C. I. = 5 %

FIGURE 4-34

Net Sandstone Map of the Lower Terengganu Shales. (Note that sandstones are dominant in the northeastern region of the study area).

small to medium-scale cross stratifications. Besides the presence of *Milliammina fusca*, a brackish water fauna, within the Terengganu Shale sequence, the core at Bekok-1 is the prime evidence to corroborate this deduction. Well-sorted, fine grained sand development exhibited in the core probably indicates shoaling where active winnowing and reworking processes were taking place. Dipmeter azimuth within the finer section of the interval at Ledang-1, Figure 4-35, indicates a probable northwest-southeasterly longshore current which assisted in dispersing the sediments. Secondarily, it is interpreted that shales and thin sandstone beds which are on same stratigraphic horizon with the sandstones (Fig. 4-18), in the northeast are lower coastal/delta plain (strand plain/lagoonal/crevasse splay) sediments based primarily on the occurrences of *Casuarina, Palmae* and *Rhizoporaceae*, spores of coastal and mangrove plants, within the sequence, and the colours of ditch cuttings and core at Tinggi-1 (Fig. 4-36), which are light to dark grey and olive green, occurrences of bands of greyish brown sideritic lenses, and on occurrences of vertical burrows. Flaser structures are common in the non-bioturbated intervals. The relationship of the offshore/barrier bar sandstones with these coastal deposits is displayed in Figures 4-11 to 4-13, in which the sandstones transgressively onlap them in the north and northeast.

2) Sandstone facies of Motif D are distributary tidal channels and tidal channel inlets deposited within lower coastal/delta plain settings. The distributary channels are typically massive and blocky, with sharp tops and erosional bases and contain ripped-off mudrock clasts and lignitic fragments. Successions of small, medium, and large-scale cross stratifications and trough cross beddings are

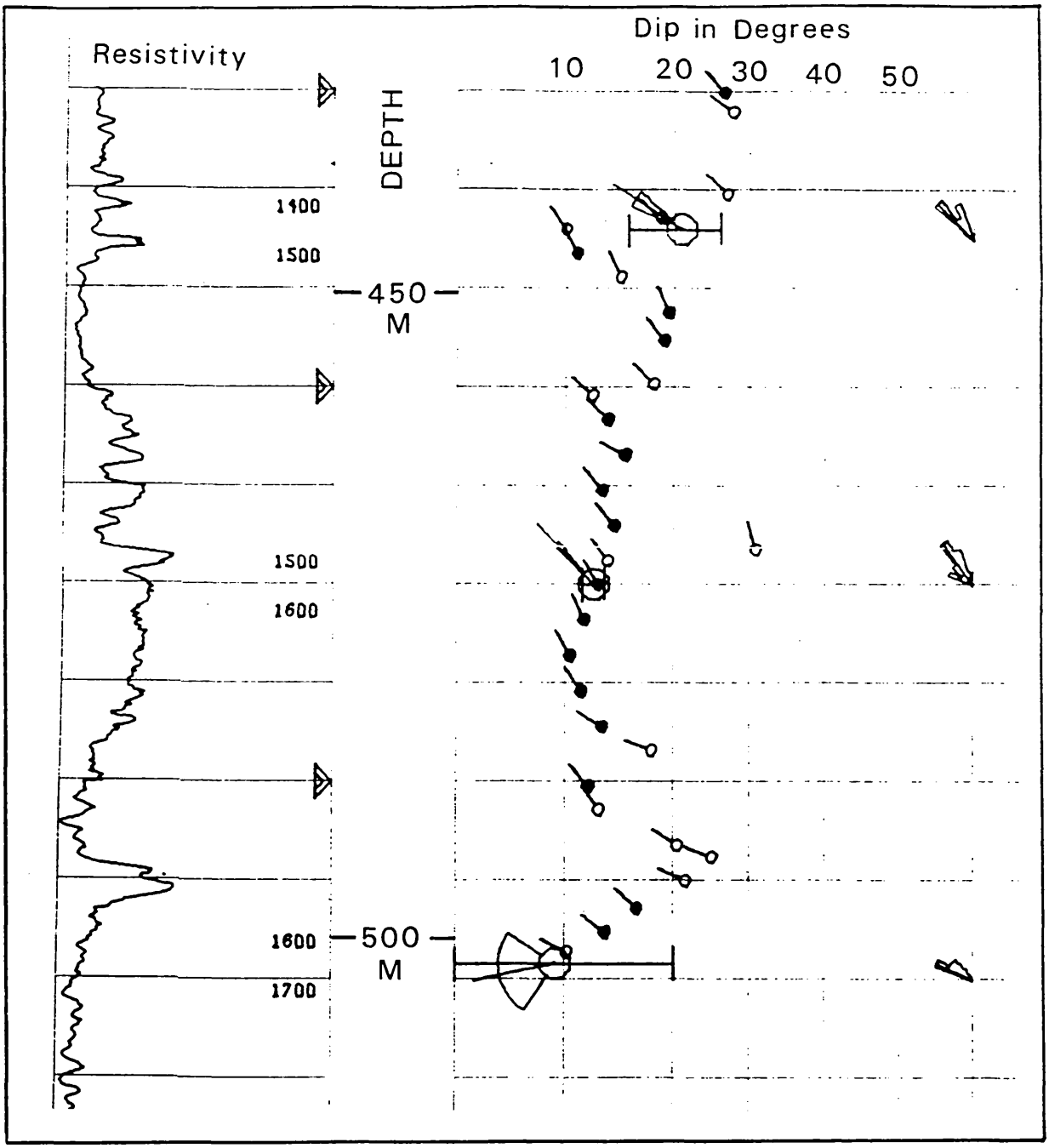


Figure **4-35** - Dipmeter log motif within sediments of the Lower Terengganu Shale interval at Ledang-1, showing the general dip of the sediments in the northwesterly direction.

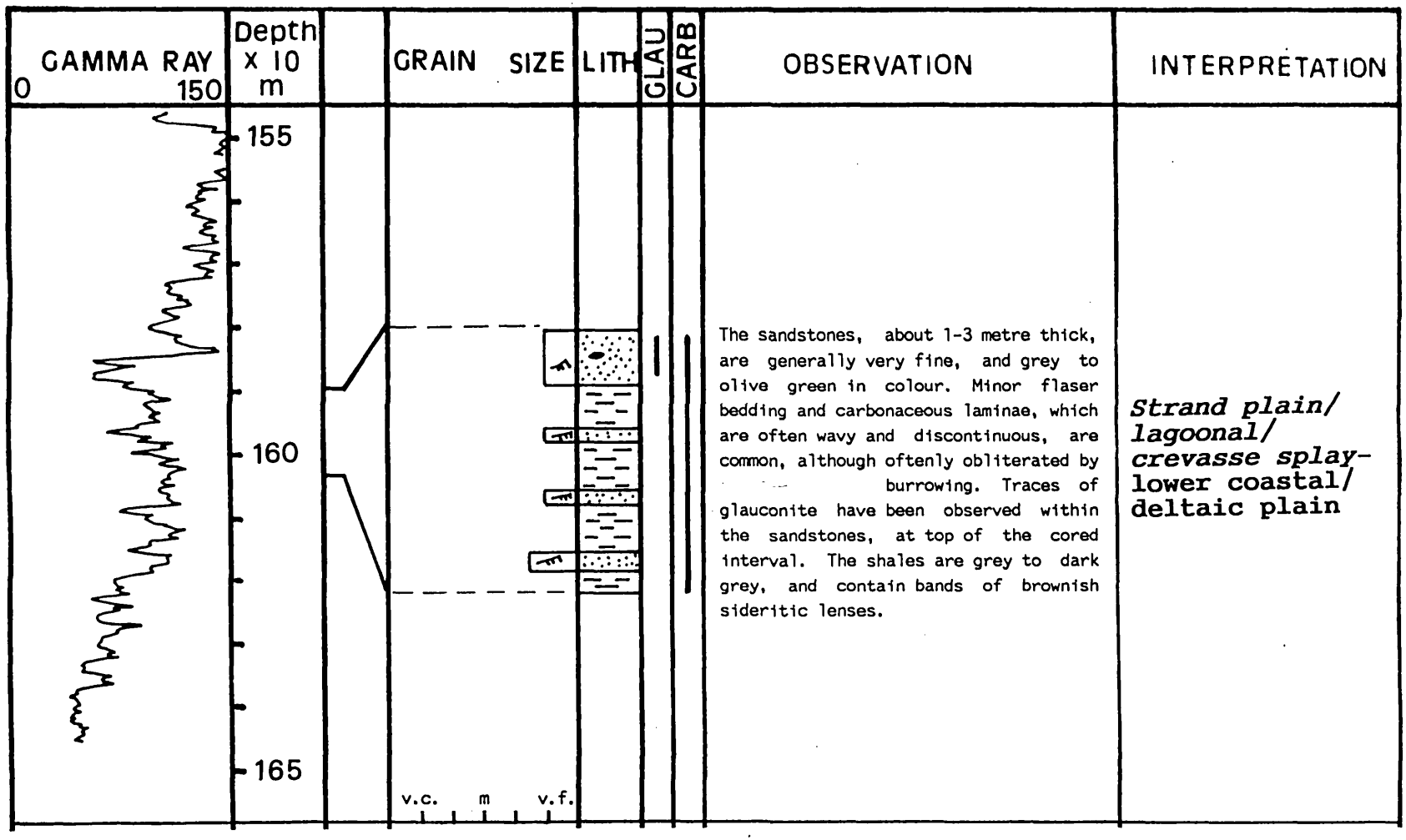


Figure 4-36 - Log responses and core description of facies within the Lower Terengganu Shales at Tinggi-1. (See pocket for core photograph).

common within channel facies. The occurrence of glauconite in the channel facies has led to the belief that the mineral was brought in via tidal processes. Typically associated with these tidal channels are the lagoonal/strand plain shales and silts and crevasse splay sandstones which display cyclic upward-coarsening sequences. The thickness of the sandstones varies, but is generally less than 10 metres.

4.3.6 Upper Terengganu Shale Sequence

4.3.6.1 *Characteristic Features*

Except for minor sandstone occurrences which appear to develop around Belanga-Pulai-Tinggi region in the east-northeast, the Upper Terengganu Shale sequence consists primarily of shales (Fig. 4-16). No cores were cut within this sequence, but by inference from ditch cuttings and log responses, the sandstones within the sequence generally have the following characteristics:

1) The sandstones comprise of one log facies of Motif C. These sandstones have varying thickness, from about 5 metres at Tinggi-1 to about 10 metres at Pulai-1 and 40 metres at Belanga-1 (Fig. 4-17),

2) The sandstones are generally light grey to olive-green, very fine-grained and "dirty", with high concentration of silt and clay, and

3) Traces of glauconite have been reported to have occurred within the sandstones (Drilling Reports).

4.3.6.2 *Facies Interpretation and Distribution*

Both the log and net percent sandstone maps, Figures 4-17 and 4-37, suggest that the sandstones developed only in the northeastern region of the study area. Outside this region the sandstones occur as very thin and minor intercalations within the predominant shale sequence.

It is interpreted that the sandstones are delta front/offshore barrier bars. These sandstones display generally the following characteristics:

1) An upward-coarsening log motif,

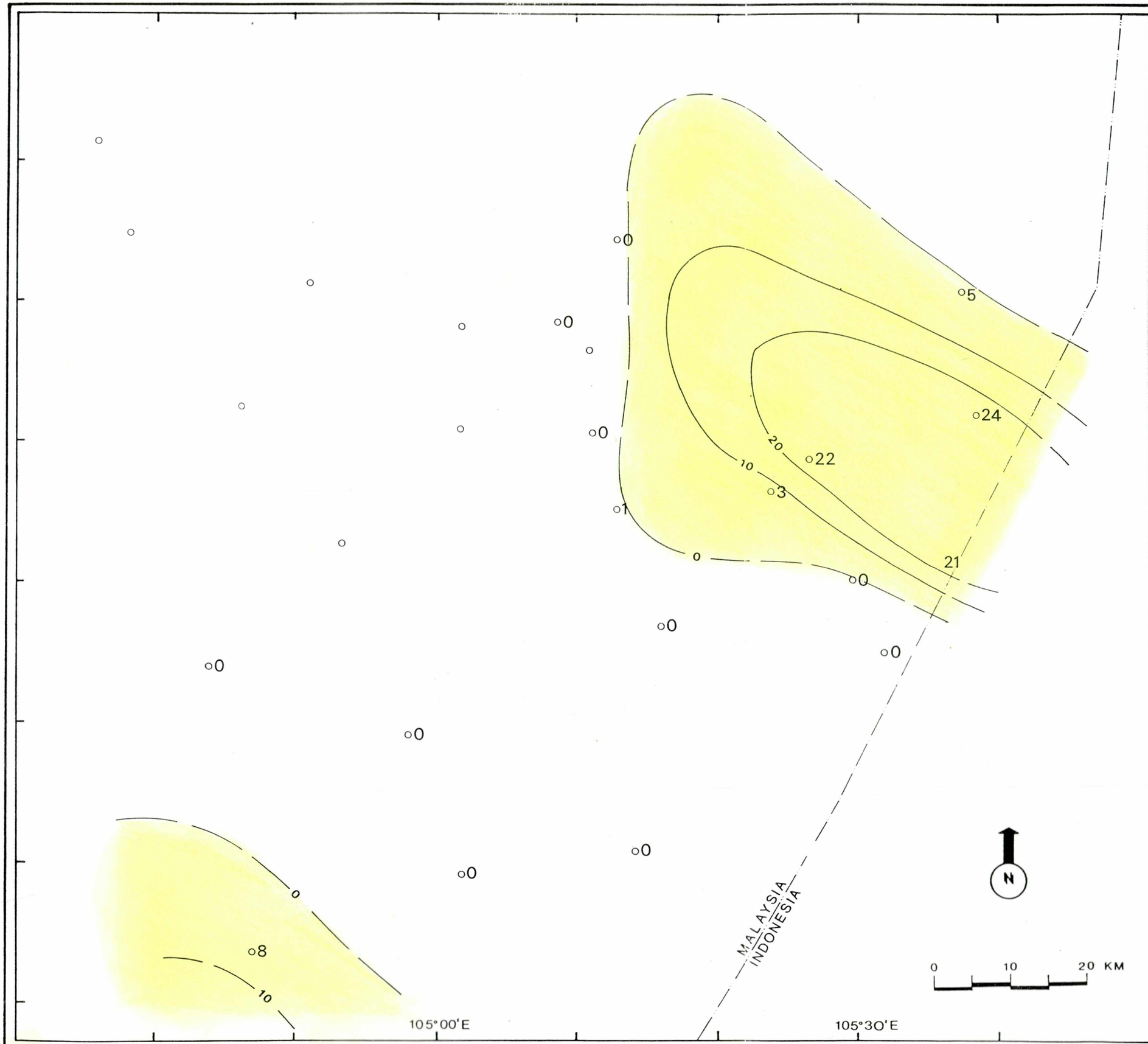
2) Cuspate-like and strike-elongated morphology, with a general orientation in a northwesterly direction (Fig.4-37). Sandstone morphology of this nature probably indicates an active interaction of waves and possibly long-shore currents (Weise, 1980), which provided a mechanism for a widespread distribution of the sediments,

3) Occurrences of glauconite in the sediments, indicating a marine environmental setting (Selley, 1985), and

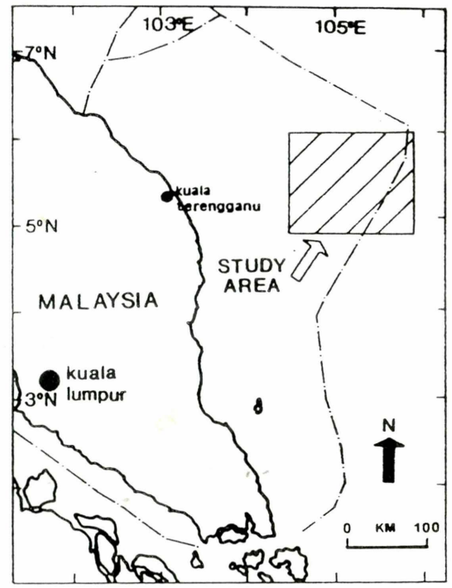
4) Occurrences of *Milliamina fusca*, a brackish water fauna, within the interval at five well locations: Palas-1, Duyong Barat-1, Seligi-3, Banggol-1 and Angsi-1.

4.4 *SEISMIC-LITHOLOG FACIES INTEGRATION*

Correlation of seismic facies map of R-B seismic sequence (Fig. 4-8), with the log maps of Upper and Lower Terengganu Shale sequences (Figs. 4-17 and 4-18), and similarly seismic facies map of B-P sequence



LOCATION MAP



LEGEND

Low sand content

o 5 -- control point

C. I. = 10 %

FIGURE 4-37

Net Sandstone Map of the Upper Terengganu Shales.

(Fig. 4-16), with Upper and Lower Pulai Sandstone sequences (Figs. 4-19 and 4-20), indicate that one facies type can be used to "read" or infer the other. It follows therefore that:

1) Seismic facies of Type I correlates with litho-log facies of Motif A (Figs. 4-16, 4-19 and 4-20),

2) Seismic facies of Type II correlates with litho-log facies of Motif B (Figs. 4-8 and 4-18),

3) Seismic facies of Type III correlates with litho-log facies of Motif C (Figs. 4-8 and 4-17), and

4) Seismic facies of Type IV correlates with litho-log facies of Motif D (Figs. 4-16, 4-19 and 4-20).

The significance of these relationships is most apparent, particularly in predicting facies distribution (Fig. 4-38 and 4-39). For example, in the Lower Terengganu Shale sequence, seismic mapping predicts the northwestward occurrence of Type III facies (Fig. 4-8), where well data in the area northwest of Palas-Banggol is lacking. Likewise, litholog facies predicts the southeastward extension of Motif C facies (Figs. 4-17), where the area southeast of Bekok-Seligi, is complicated by tectonics (Fig. 2-5), in which in this area, it was difficult to decipher the seismic characters.

4.5 *PALAEOGEOGRAPHY*

Interpretation of the depositional environments for the Pulai-II Formation was based on the premise that the Late Oligocene to Early Miocene marked the beginning of a marine invasion which transgressed

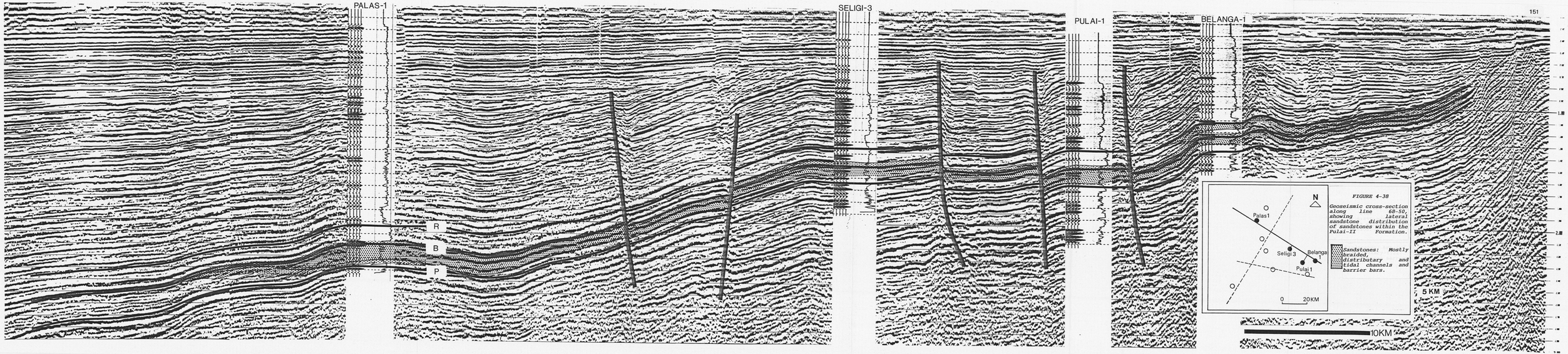


FIGURE 4-38

Geoseismic cross-section along line 68-50, showing lateral sandstone distribution of sandstones within the Pulai-II Formation.

Sandstones: Mostly braided, distributary and tidal channels and barrier bars.

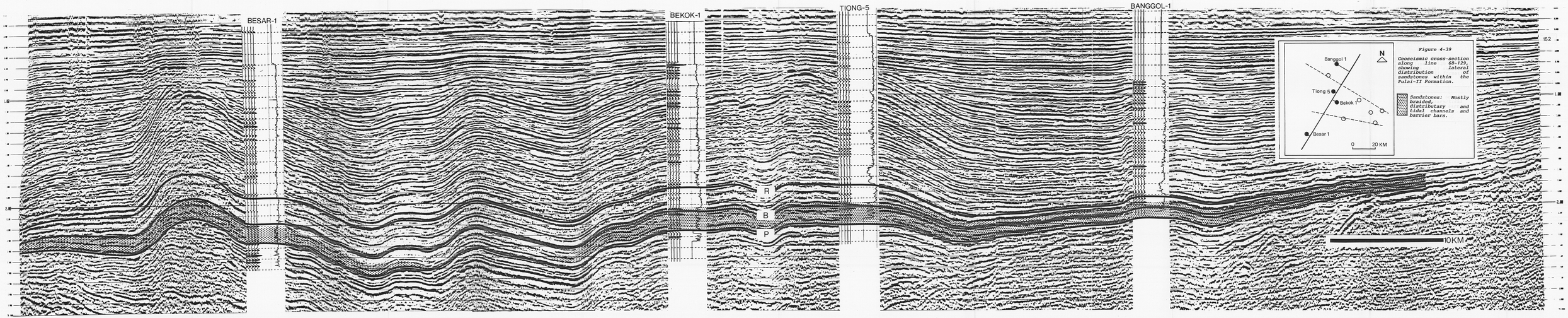


Figure 4-39

Geoseismic cross-section along line 68-129, showing lateral distribution of sandstones within the Pulai-II Formation.

Sandstones: Mostly braided, distributary and tidal channels and barrier bars.

into and onto the Malay basin via a strait in the southeastern part of the study area. The bases for arriving at this premise are:

1) Glauconite, a mineral generally believed to form in a marine environment (Selley, 1985), began to appear in the stratigraphic section in the early Late Oligocene. Its appearance in the sandstones during this period is restricted to the region in the extreme southeastern part of the study area. By the early Early Miocene, it became relatively widespread and increasingly more abundant,

2) *Pediastrum*, a fresh water alga, has been found in relative abundance within the Pulai Sandstones in five wells: Palas-1, Seligi-3, Banggol-1, Duyong Barat-1 and Angsi-1 (Esso, 1978, Carigali, 1986 and Rashidah et al, 1988),

3) Marine foraminifera and nannofossils have not been observed in the Pulai Sandstone sequence at the above five well locations and also at Pulai-1 (Esso, 1978; Carigali, 1986; Rashidah et al, 1988; and Armitage et al, 1977). The non-diagnostic *Milliamina fusca* found within the Terengganu Shales has been interpreted to indicate that the sediments were deposited generally in a brackish environment (Carigali, 1986; Rashidah et al, 1988), and

4) *Casuarina, Palmae* and *Rhizoporaceae* spores found in most of the wells indicate a possible widespread lower coastal/deltaic plain setting, particularly in the south.

4.5.1 Late Oligocene-Early Early Miocene

It is envisaged therefore that during the Late Oligocene, the Malay basin was an inland sea, or near-enclosed body of water measuring 150 to 300 km in width and exceeding 500 km in length. A strait in the extreme southeastern part of the study area, some 30 to 50 km in width, initially formed a communication between the apparently non-marine inland sea in the northwest and the open sea in the southeast. The sandstones of the Pulai-II Formation are interpreted to have been deposited within three predominant environmental settings. These are:

1) Transitional environment of lower coastal/delta plains, with tidal influence in the south and southeastern regions of the study area. The topographic setting in these regions was probably flat, with the region in the southeast relatively flatter. The region in the southeast constituted the strait which provided a linkage between the marine conditions in the southeast and the non-marine condition on the west and northwest.

2) Continental environment in the north and northeastern half of the study area. The braided channel facies of the Pulai Sandstones constitute alluvial outwash plain deposits.

3) Non-marine shelf environment, a freshwater lake(?), in the region west of the Tapis-Ophir area and north of Angsi, during the earlier part of the period. The upward-coarsening sequence observed at the base of the Lower Pulai sandstones at Palas-1, Figure 4-38, probably constituted a prodelta-delta front facies.

The relationship of the three environments in the study area is that the braided streams of the alluvial outwash plain in the northeast,

scoured through and reworked sediments of abandoned channels and flood plain deposits, and discharged their sediment loads to the west into the non-marine shelf, lake(?). A similar alluvial system prograded and lapped onto the low-lying, lower coastal/delta plain sediments in the south.

4.5.2 Early Early Miocene-Late Early Miocene

Marine encroachment, most likely related to basinal subsidence due to faulting (refer to Section 4.1), during the late Late Oligocene to Early Miocene caused the strait to the inland sea to be opened up and widened. Extending from Sotong to Peta, the widened strait permitted free mixing of the inland sea with the open sea waters. The condition in the southeastern Malay basin was therefore very much more marine. Sandstone packages contained within the Terengganu Shales are therefore believed to have been deposited primarily within the marine environment. A minor delta system from the east, around the Pulai-Belanga area, probably contributed much of the offshore and barrier bar sandstones in the region. The distributary tidal channels in the far southwest at Sotong are within the low-lying lower coastal/deltaic plain environment.

4.6 *STRATIGRAPHIC MODELLING*

Results of the stratigraphic modelling exercises along three stratigraphic cross-sections which orientate roughly in dip-direction, indicate generally a good correlation between:

1) Stratigraphic cross-sections and resultant seismic modelling (synthetic) sections (Figs. 4-40 to 4-42), and

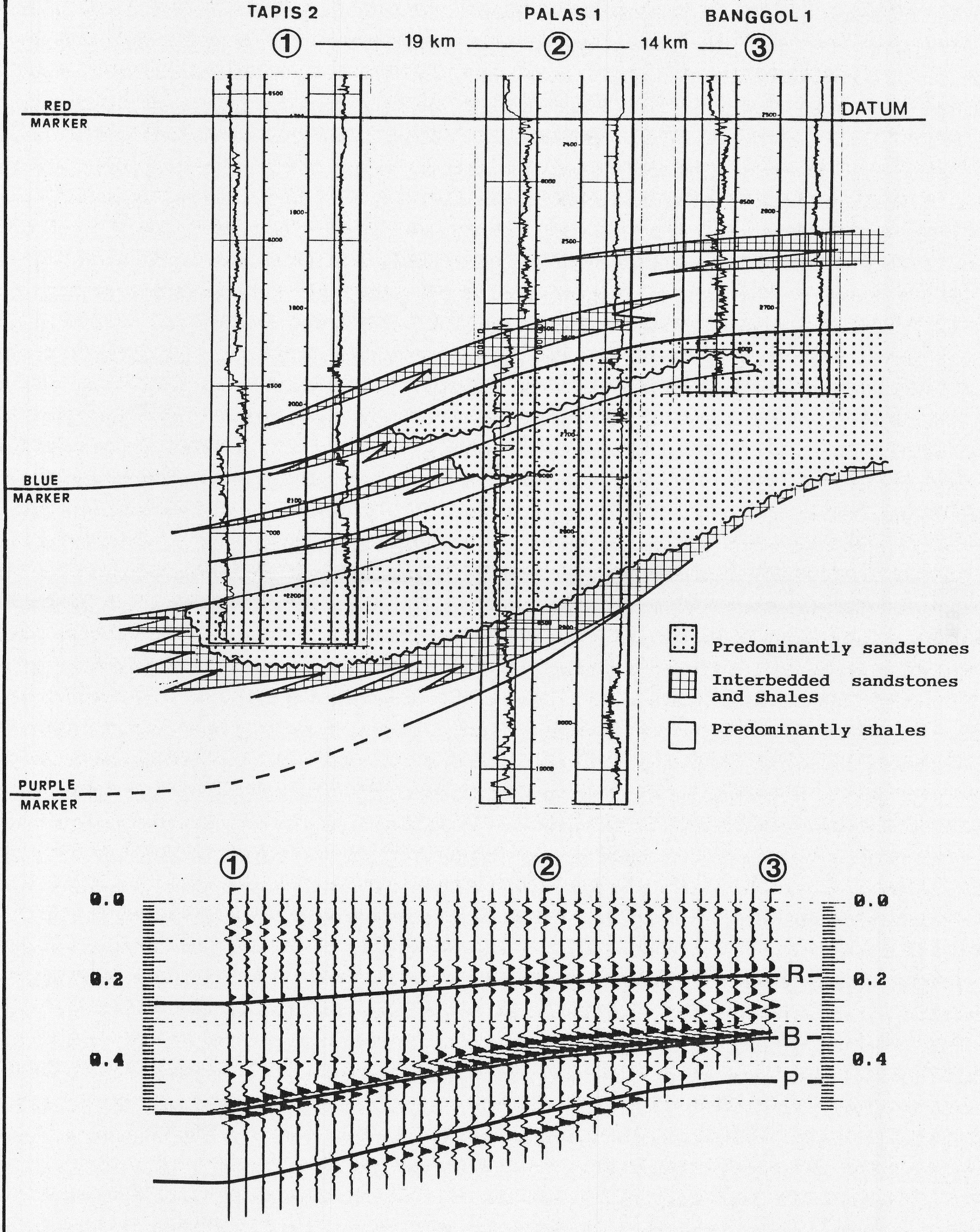


FIGURE 4-40

Section A--Stratigraphic Model along Tapis, Palas and Banggol.

Ophir 1 — Bekok 1 — Tiong 5 — Palas 1

⑤ —— 16 KM —— ④ — 11 KM — ③ —— 15 KM —— ②

RED MARKER

DATUM

BLUE MARKER

PURPLE MARKER

Predominantly sandstones

Interbedded sandstones and shales

Predominantly shales

⑤ ④ ③ ②

0.0

0.2 — R

0.4 — B

0.6 — P

0.8

SAMPLE INTERVAL = 1 Ms.
WAVELET = RICKER 30Ms 0 Phase

AC. IMP. =Sonic
MULTIPLES =None
NOISE = 0 %

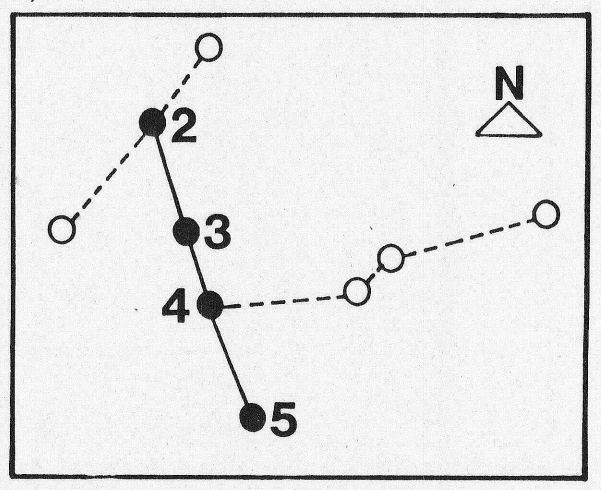


FIGURE 4-41

Section B--Stratigraphic Model along Ophir, Bekok, Tiong and Palas.

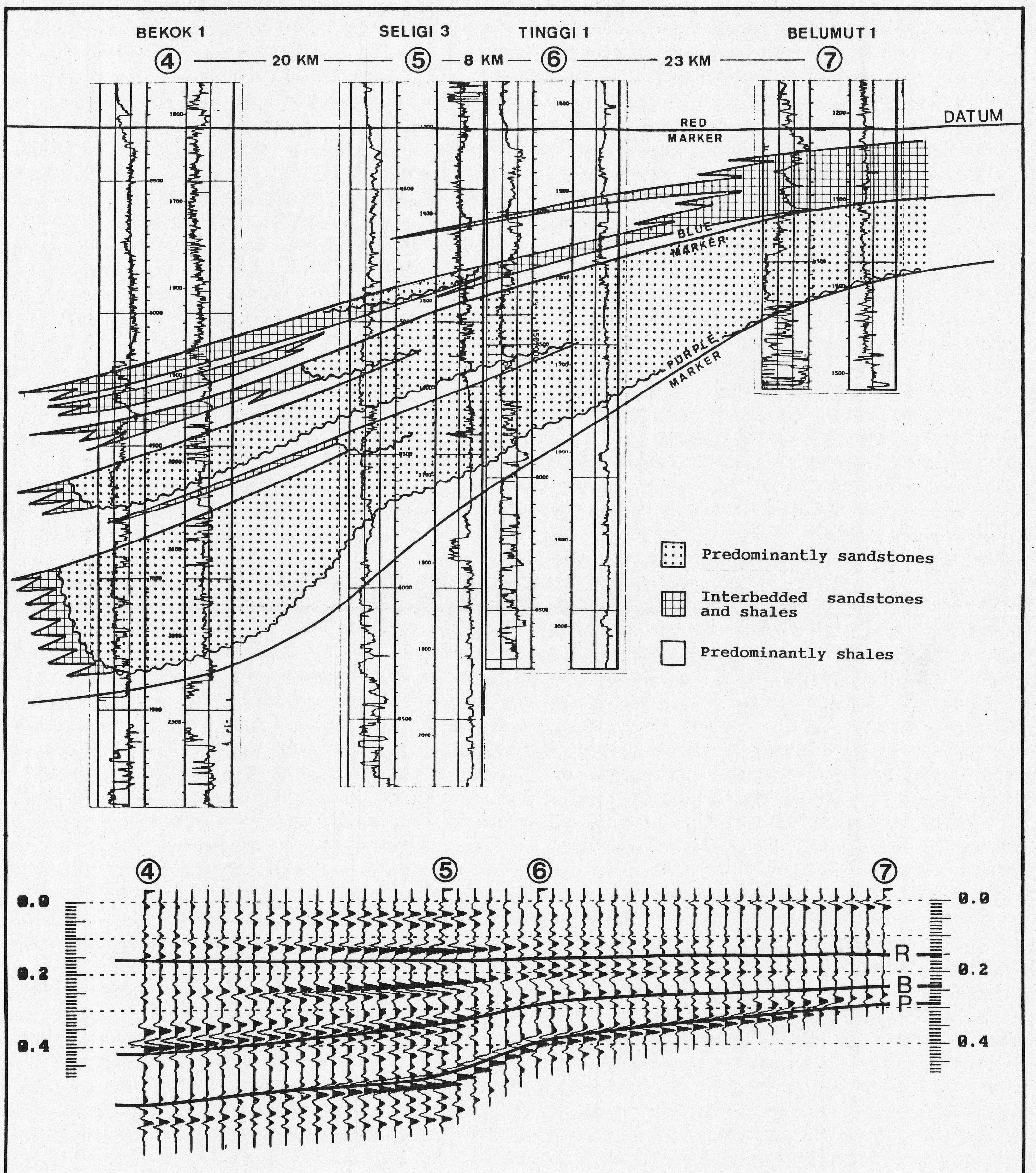


FIGURE 4-42

Section C--Stratigraphic Model along Bekok, Seligi, Tinggi and Belumut.

2) Synthetic section of Section A, Figure 4-40, and part of seismic line 68-121 (Fig. 4-43).

The results also indicate that:

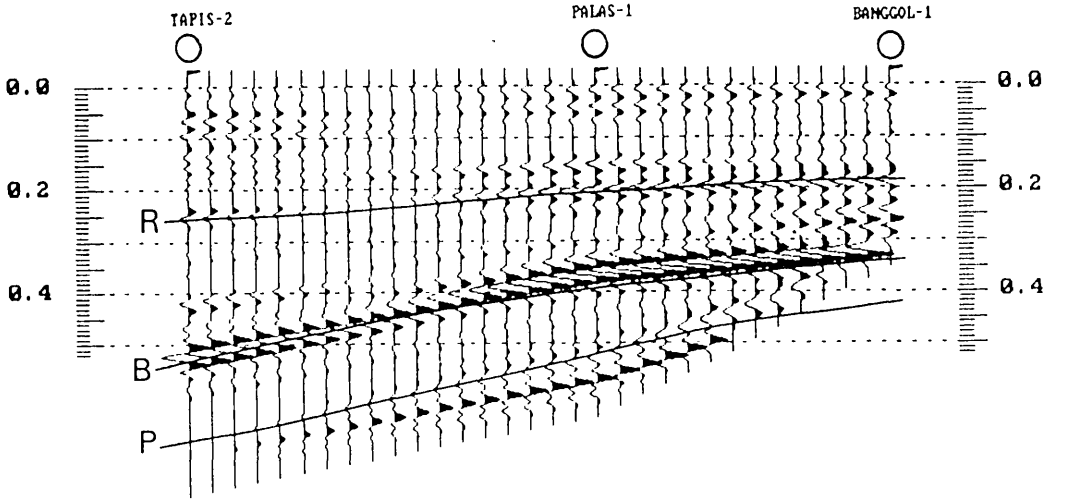
1) The boundary which separates the Terengganu Shale and the Pulai Sandstone sequences is marked by a very clear high amplitude and laterally continuous signature, the Blue (B) seismic marker, and

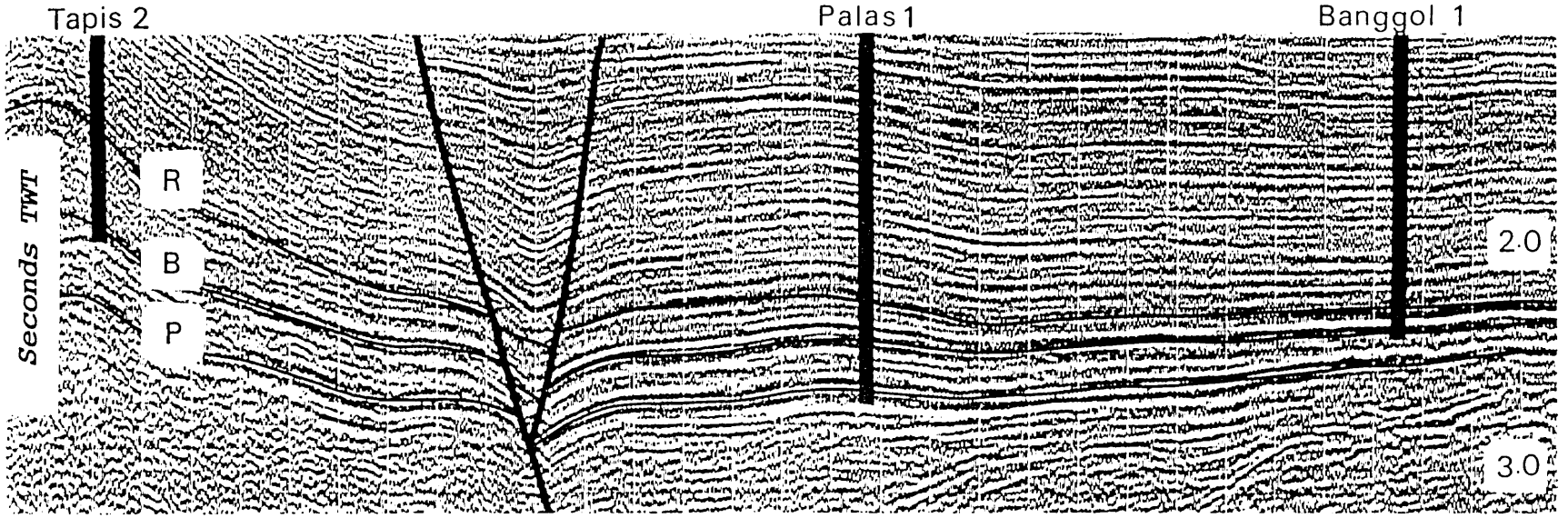
2) In the synthetic stratigraphic sections, the R-B and B-P intervals representing the Terengganu Shale and Pulai Sandstone sequences respectively, are commonly clear and noiseless, and are generally free from high amplitude signatures. But where high amplitude signatures are present, they are localised and appeared to die out laterally. On seismic section, Figure 4-39, this gradual lateral change of amplitude is usually related to shaling out of the lithofacies of Motif C basinward. But the occurrence of hard calcareous siltstones within the predominantly shale section can also generate high amplitude signatures, and within the R-B sequence, occurrences of such hard, calcareous siltsones are common (Figs. 4-38 and 4-39). Within the B-P seismic sequence this lateral amplitude change is caused by a 10-20 metre-thick shale bed within the monotonous sandstone interval. It is also noted within this sequence, that the disappearance of high amplitude signatures east of Tiong-5 in Figure 4-41, and east of Tinggi-1 in Figure 4-42, marks the end of the occurrences of shale beds within the interval, and the beginning of the homogeneity and predominance of sandstone facies.

The seismically generated stratigraphic cross-section along the Banggol-Palas-Tapis line was compared with the seismic data in the

Figure 4-43

Comparative illustration of part of line 68-121 and stratigraphic model along Section A. (see Fig. 4-41 for comparison).





vicinity of the section (Fig. 4-43). It is observed generally that:

1) There is a comparable similarity of the seismic facies within the R-B seismic sequence of the model and the seismic section, where the transgressive-regressive couplets of Type III are present, but

2) The seismic facies within the B-P sequence are less obvious and difficult to recognise. There is no comparision between the synthetic and normally processed seismic sections. Whereas in the synthetic sections, the B-P interval which consists dominantly of Motif A facies, shows a monotonously clear and noiseless section, the same interval on seismic sections shows the sequence to consist generally of discontinuous high amplitude signatures of Type I. This difference is probably expected because:

   i) the synthetic section is the result of computer integration of velocity data between two points, and the integration assumes no velocity variation between the points. The more data points there are within the section, the closer the synthetic section would be to the normally processed seismic section; the normally processed seismic section is the result of data sampling at an infinite number of points along the line, and

   ii) the synthetic section is a noise-free section. No multiples were introduced.

5. PETROGRAPHY AND DIAGENESIS

5.1 *INTRODUCTION*

The clastic facies of the Pulai-II Formation were interpreted, in Chapter 4, as having been deposited in a wide range of environments: continental, transitional, and marine, with deposits of the continental environment constituting the dominant facies. The blanket-like sandstones of braided channel and fluvial / distributary deposits of Motif A, the tidal channel deposits of Motif D and the offshore barrier bar deposits of Motif C comprise the main reservoir package. The thickness of each of these sandstone packages varies considerably, from about 25 metres in some sandstones of Motifs C and D, to as thick as 130 metres in Motif A. Other less important reservoirs are tidal flat sandstones in Motif D, which are generally less than 10 metres thick.

5.2 *PETROGRAPHY*

5.2.1 Sandstone Composition

A total of 135 samples were examined for their mineralogical composition through an optical petrographic microscope. Of these, 88 samples were from the Upper Pulai Sandstones, 49 from the Lower Pulai Sandstones and 8 from the Lower Trengganu Shales. These sandstones are generally fine to medium and coarse-grained, and only a small proportion comprises very fine to fine-grained sandstones. The results of the analyses indicate that:

1) The primary detritals or framework grains of the sandstones consist of quartz, feldspars and rock fragments, with accessory micas and

zircon. Trace amounts of glauconite have also been found within some sandstones of the Upper Pulai Sandstone and Lower Trengganu Shale sequences (Plate 5-1),

2) The matrix and the cementing materials consist primarily of carbonates, clay minerals and quartz overgrowth (Plates 5-2 to 5-4). Traces of barytes and pyrite have also been detected.

3) Quartz, Q, comprises the dominant framework grains, about 50-80 percent; feldspars, F, constitute 15-30 percent, and rock fragments, RF, 10-35 percent. The average mode of the 135 sandstone samples is $Q_{50}F_{20}RF_{30}$. Based on Folk's classification (1968), the sandstones are classified generally as feldspathic litharenites (Fig. 5-1).

4) There was very little difference in composition between:

   i) the sandstones of Facies A , C and D (Fig. 5-2), and

   ii) the Pulai Sandstone and the Terengganu Shale Members of the Pulai-II Formation (Fig. 5-3).

This similarity in composition is believed to reflect the granitic, metamorphic and sedimentary rock terrains which flank the basin (Chung, 1968; Haile, 1970 and 1973; and Achalabhuthi, 1974).

5.2.1.1 *Framework Quartz*

Quartz is the most common framework mineral in all of the three sandstone facies of the Pulai-II Formation. It appears to predominate in coarser grained sandstones more than in the finer grained sandstones. Three varieties of quartz have been distinguished in the samples: unstrained monocrystalline, strained monocrystalline and polycrystalline

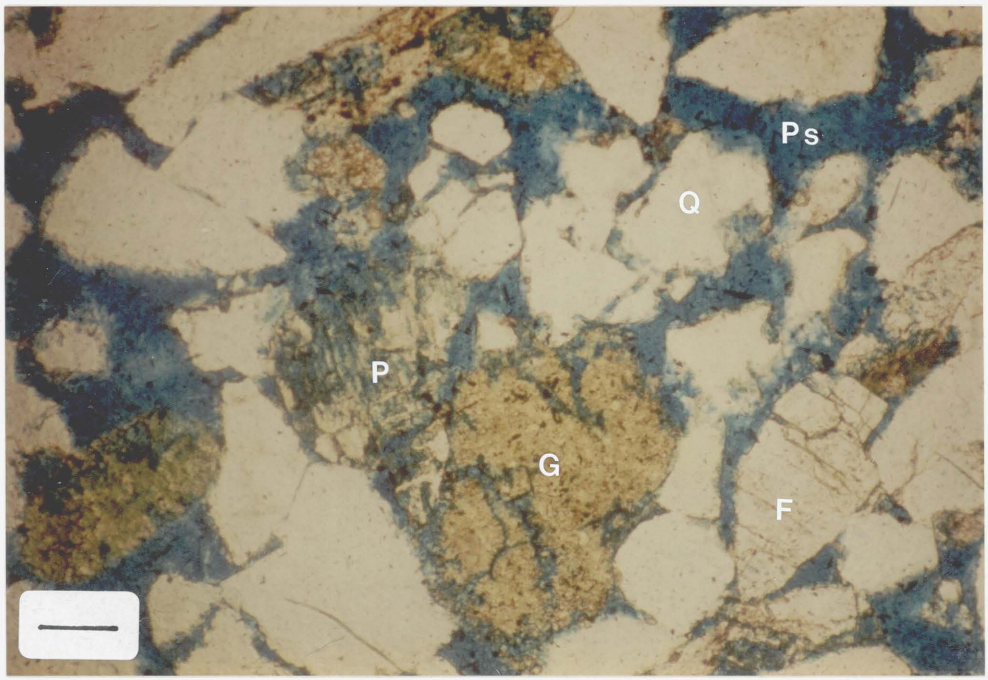


Plate 5-1 - Photomicrograph of thin section showing framework grain composition of Pulai-II sandstones. Q-quartz, F-K-feldspar, P-plagioclase, G-glauconite, and Ps-pore space (blue epoxy). Sample from Bekok-1 at depth of 1890.1 m msl. Scale bar = 0.10 mm.

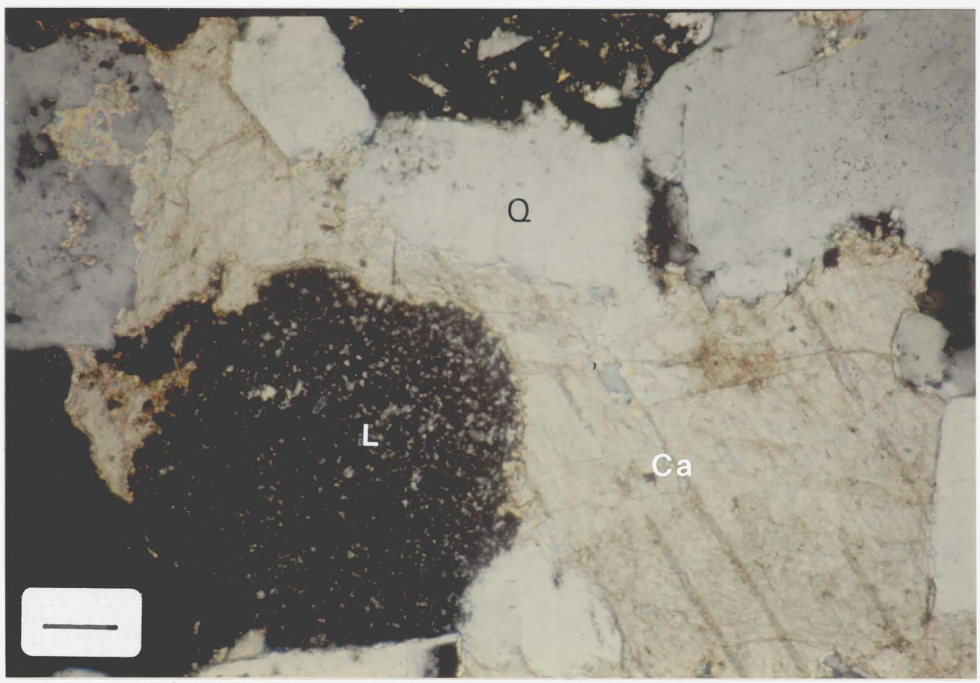


Plate 5-2 - Photomicrograph of thin section showing framework grains cemented by calcite (Ca). Note framework grains have corrugated outlines, indicative of replacement by calcite. The sandstone appears to be very well cemented, with virtually no visible porosity (Q-quartz and L-lithic). Sample from Duyong 6H-32.1 at depth of 2370.1 m msl. Scale bar = 0.05 mm.

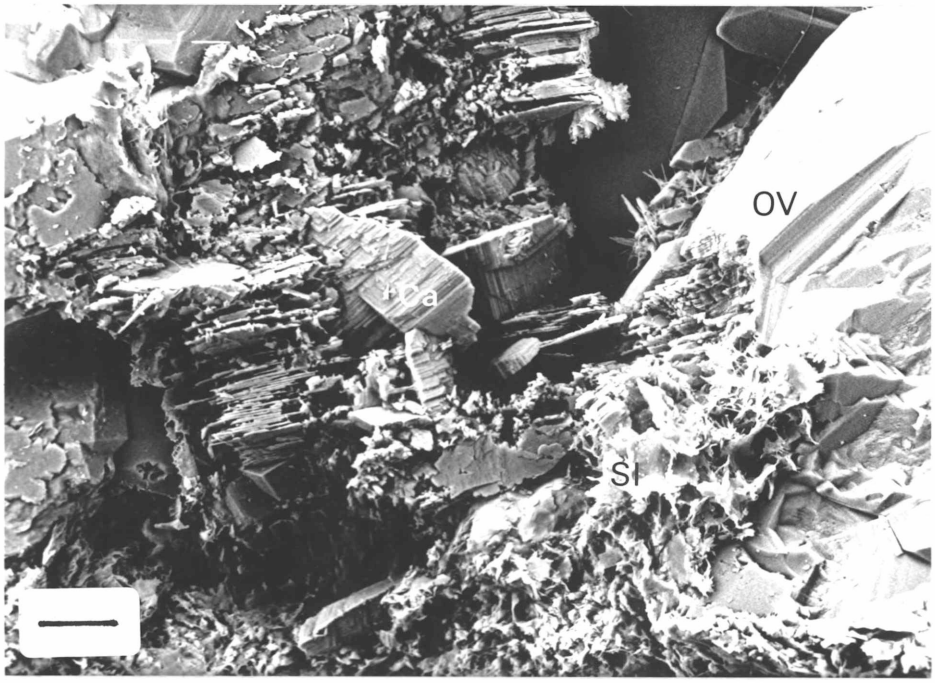


Plate 5-3 - SEM Photomicrograph of pore-filling calcite (Ca), smectite-illite (SI) and overgrowth quartz (OV). Sample from Tapis-2 at depth of 2227.4 m msl. Scale bar = 25 microns.

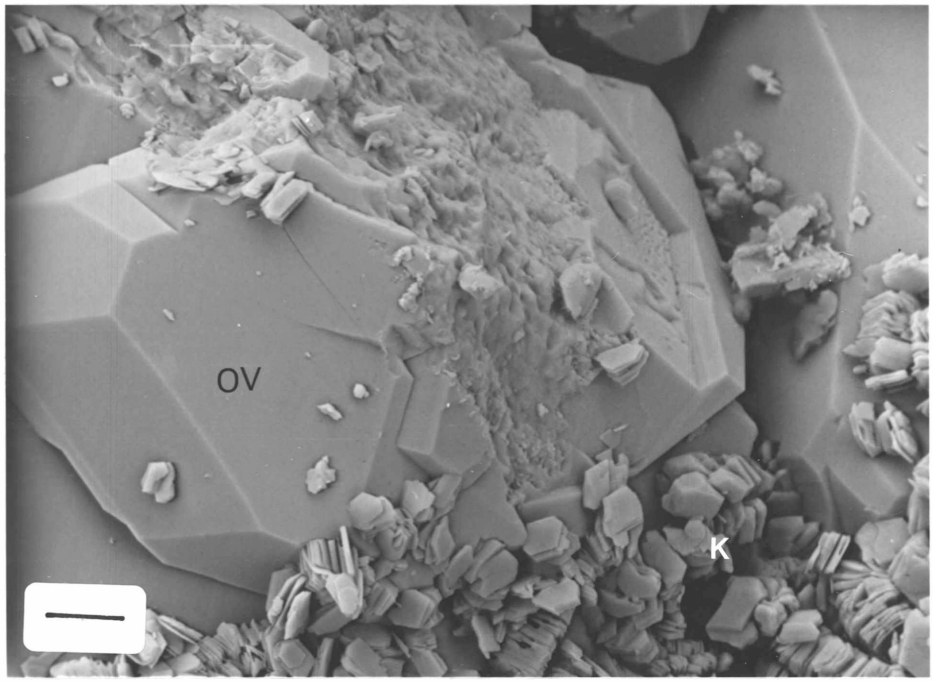


Plate 5-4 - SEM Photomicrograph showing well-developed quartz overgrowth (OV) and kaolinite crystals (K). Note that some kaolinite crystals appear to intergrow with quartz overgrowth. Sample from Angsi-1 at depth of 2450.6 m msl. Scale bar = 15 microns.

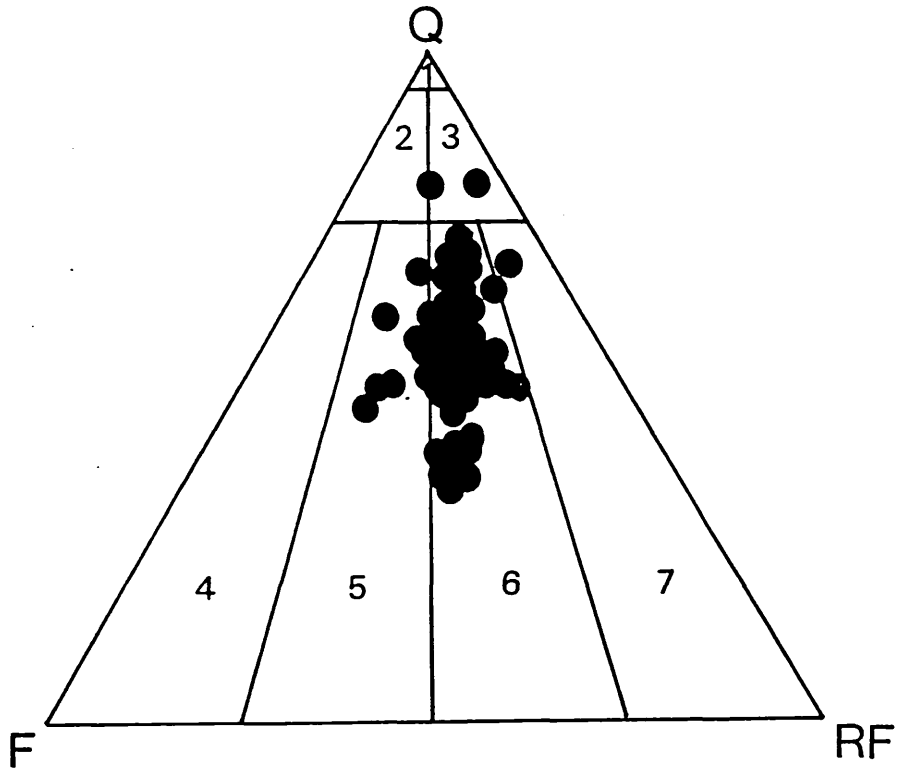


Figure 5-1 - Average sandstone composition, Pulai-II Formation. Data from Pulai-1, Bekok-1, Tiong-5, Besar-1, Sotong 5G-5.1, Duyong 6H-32.1, Seligi-3, Tapis-2, Tinggi-1 and Belumut-1. (Q-quartz; F-total feldspars; RF-lithic fragments; 1-quartzarenite, 2-subarkose, 3-sublitharenite, 4-arkose, 5-lithic arkose, 6-feldspathic litharenite and 7-litharenite) (after Folk, 1968).

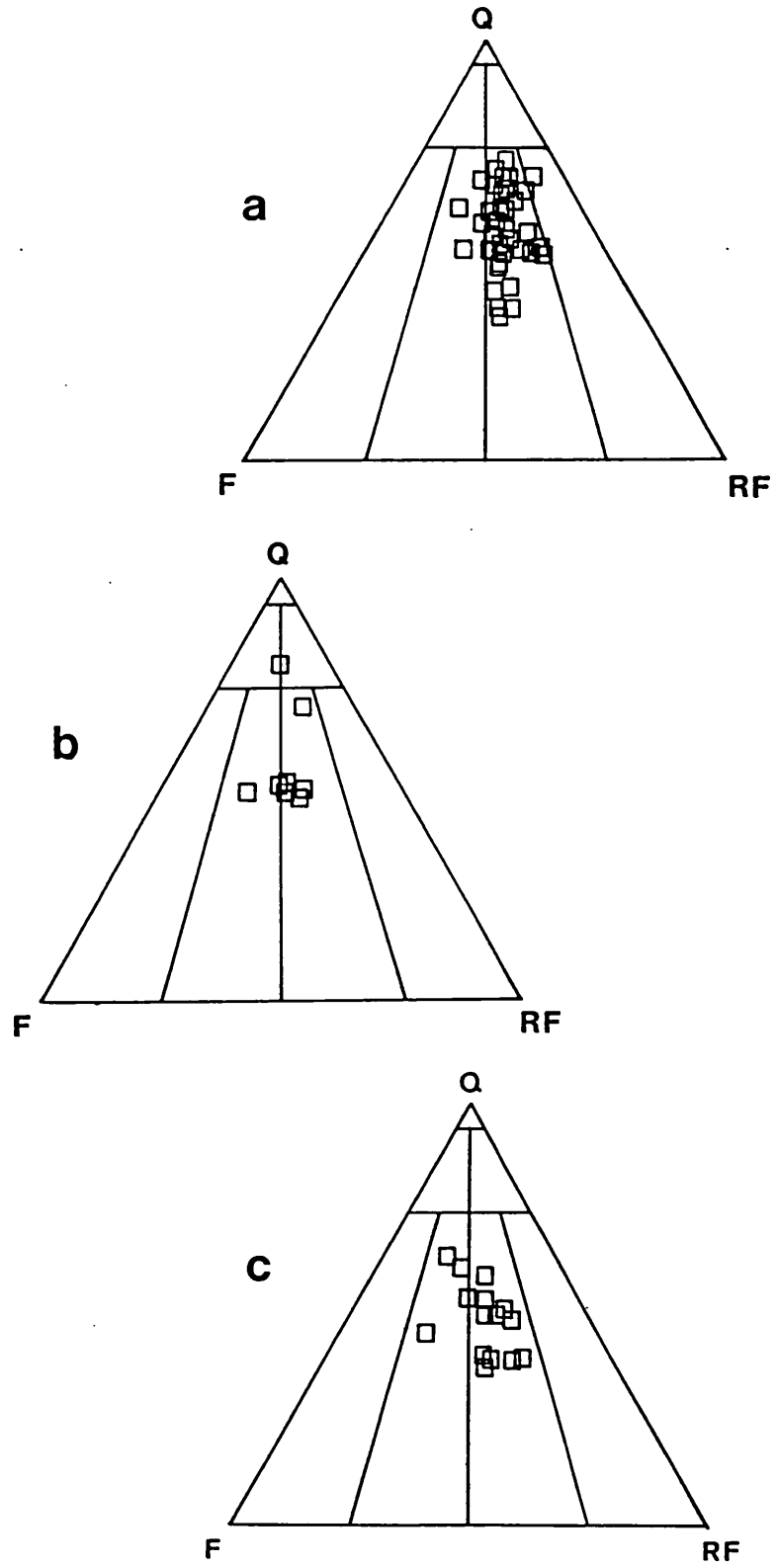


Figure 5-2 - Sandstone compositions in a) Motif A, b) Motif C and c) Motif D. (Q-quartz; F-total feldspars; RF-lithic fragments).

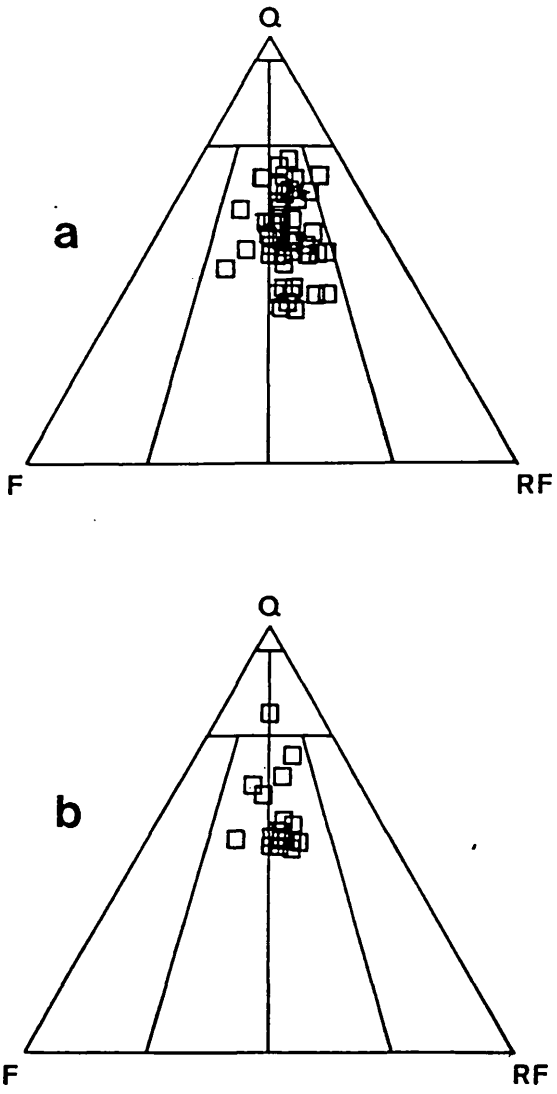


Figure 5-3 - Sandstone compositions in a) Pulai Sandstone Member and b) Terengganu Shale Member. (Q-quartz; F-total feldspars; RF-lithic fragments).

quartz; the unstrained monocrystalline variety appears in abundance. Authigenic quartz overgrows mainly on monocrystalline grains. These quartz overgrowths usually exhibit distinctly straight facets (Plate 5-4). In other cases, no overgrowth was found on monocrystalline framework quartz, and usually these grains are either highly angular with corrugated outlines and occasionally low sphericity; some exhibiting "floating" textures within pores (Plate 5-5), or they are closely packed together, together with the other quartz grains, to produce occasionally sutured contacts (Plate 5-6). Plates 5-7 and 5-8 show a pitted feature on a quartz surface. This feature probably indicates:

1) Molds caused by unobstructed quartz overgrowth around druse-lined detrital quartz grain,

2) Grain contact caused by suturing, or

3) Etches caused by replacive calcite.

5.2.1.2 *Framework Feldspar*

Feldspar grains are plagioclase and K-feldspars (orthoclase with occasional micro-perthite), and are present in variable proportions throughout the sandstones (Fig. 5-1).

Plagioclase appears to be the most common feldspar. The plagioclase framework grains are usually altered and some almost completely dissolved (Plates 5-1 and 5-9). Frequently, alteration of plagioclase resulted in the formation of albite, with kaolinite and/or illite as associated by-products (Plate 5-10). Alteration of plagioclase in some tightly packed sandstones appears to be less intense. Authigenic albite

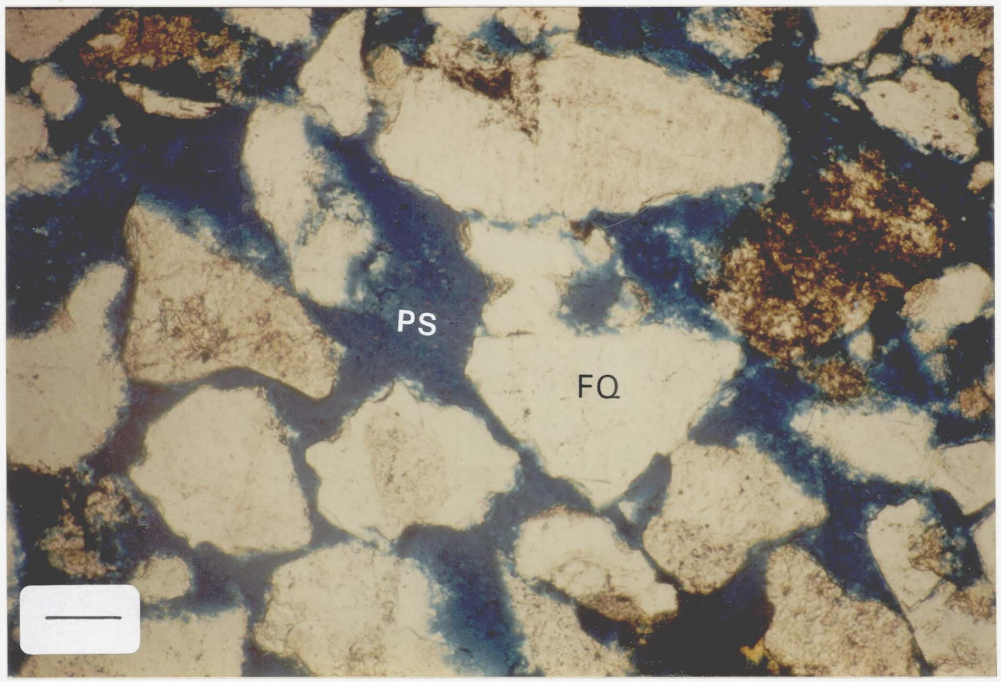


Plate 5-5 - Photomicrograph of thin section showing corrugated framework quartz (FQ) virtually floating in blue epoxy pore spaces (PS). Sample from Peta-1 at depth of 1364.3 m msl. Scale bar = 0.10 mm.

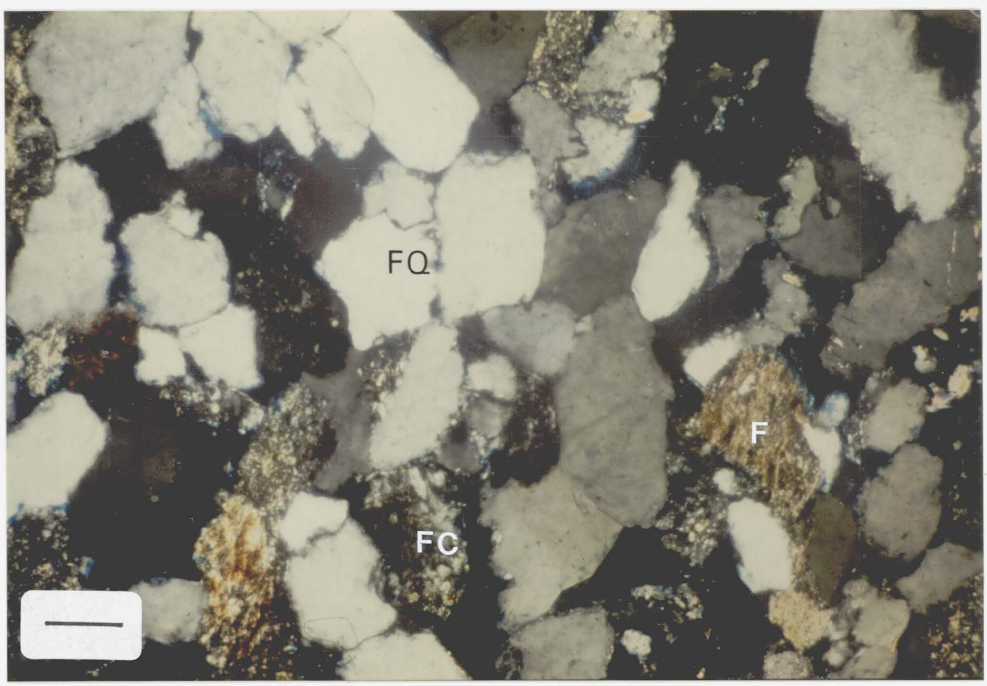


Plate 5-6 - Photomicrograph of thin section showing closely packed framework grains: quartz (FQ), chert (FC) and highly altered feldspar grains (F). Note close packing led to grain boundary suturing (pressure solution). Sample from Duyong 6H-32.1 at depth of 2219.8 m msl. Scale bar = 0.10 mm.

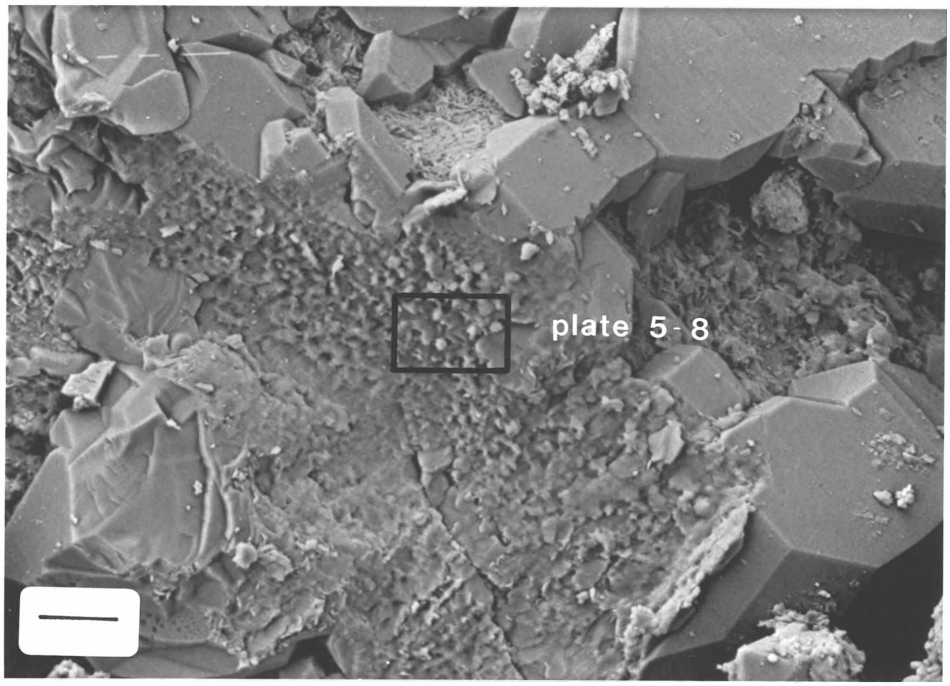


Plate 5-7 - SEM Photomicrograph showing pitted/etched surface on framework quartz. (See plate 5-8 for details). Sample from Sotong 5G-5.1 at depth of 2175.0 m msl. Scale bar = 15 microns.

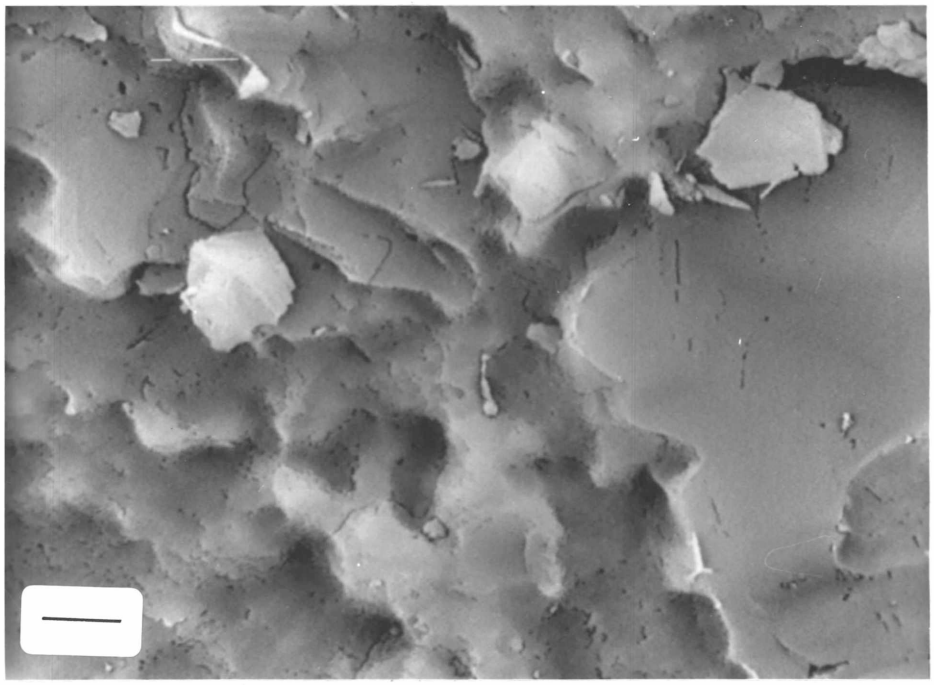


Plate 5-8 - SEM Photomicrograph showing pitted/etched surface on framework quartz. Sample from Sotong 5G-5.1 at depth of 2175.0 m msl. Scale bar = 1.5 microns.

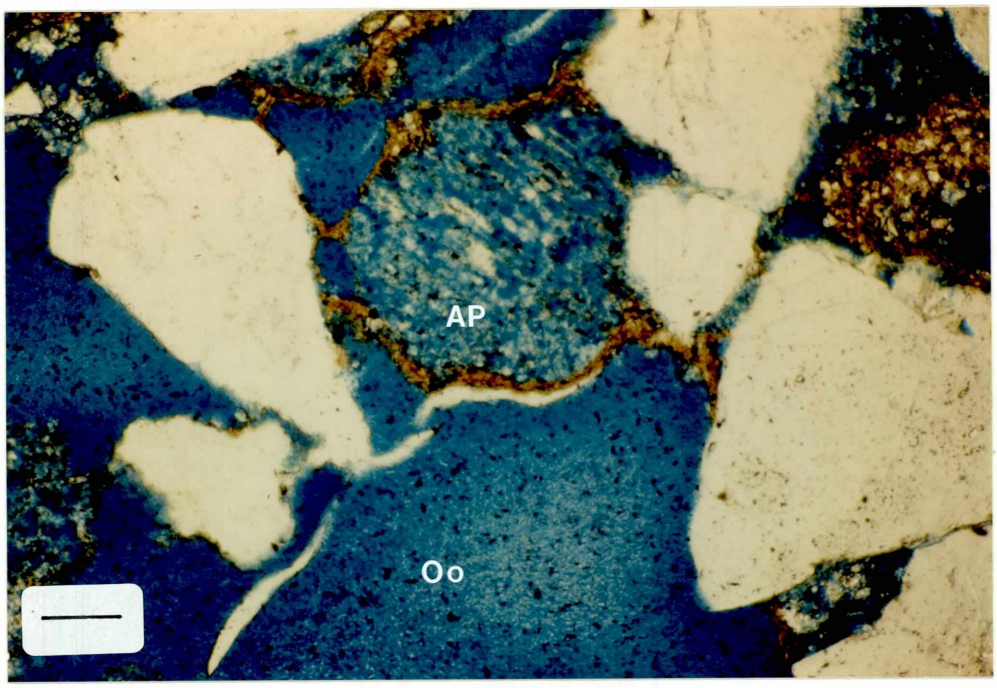


Plate 5-9 - Photomicrograph of thin section showing enlarged pores (Oo) and almost completely dissolved plagioclase framework grain (AP) rimmed by brownish material. Sample from Seligi-3 at depth of 1584.1 m msl. Scale bar = 0.05 mm.



Plate 5-10 - SEM Photomicrograph showing albite (Al) and illite (I) as by-products of plagioclase alteration. Sample from Tinggi-1 at depth of 1602.7 m msl. Scale bar = 10 microns.

overgrowths have also been seen in some samples (Plate 5-11).

The K-feldspar grains also exhibit variable degrees of alteration and dissolution. Untwinned framework orthoclase often has a brown clouded appearance, and many grains show partial to almost complete alteration (Plate 5-12).

5.2.1.3 *Framework Rock Fragments*

Rock fragments are predominantly grains of poly-microcrystalline chert. Lithic fragments are generally rare. Like most framework feldspars, the framework chert also have undergone varying degrees of alteration and dissolution (Plate 5-13); and in general in thin sections, partially altered grains exhibit a brown cloudy appearance. Alteration within the framework chert appears to be selective, with the microscopically fine crystals apparently more susceptible to dissolution, leaving the more stable and coarser poly-microcrystalline grains encased usually by brown materials (Plate 5-13).

5.2.1.4 *Other Accessory Framework Minerals*

Accessory framework minerals include glauconite (Plate 5-1), micas which consist of biotite and muscovite, and zircon. Both glauconite and biotite show signs of alteration, but muscovite appears to be relatively more stable. Glauconite are invariably clouded by brownish dust, possibly limonite, while the biotite flakes are darkened by opaque and dark layers of iron and/or titaniferous(?) oxides. The high birefringence zircon grains are usually more rounded, and are probably reworked.

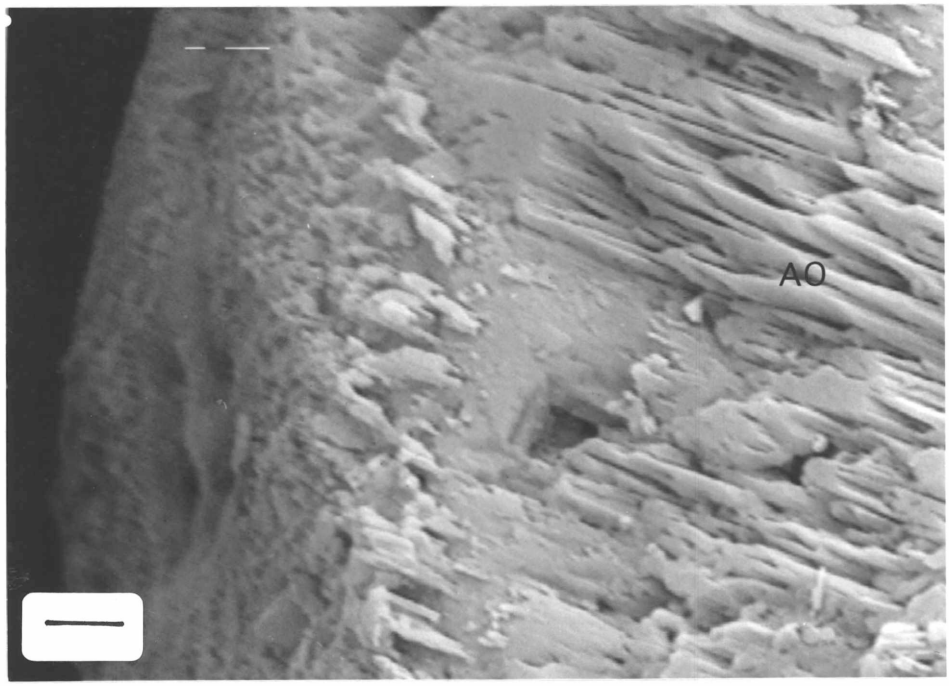


Plate 5-11 - SEM Photomicrograph showing albite overgrowth (AO) on plagioclase framework grain. Sample from Pulai-1 at depth of 1149.7 m msl. Scale bar = 1.5 microns.

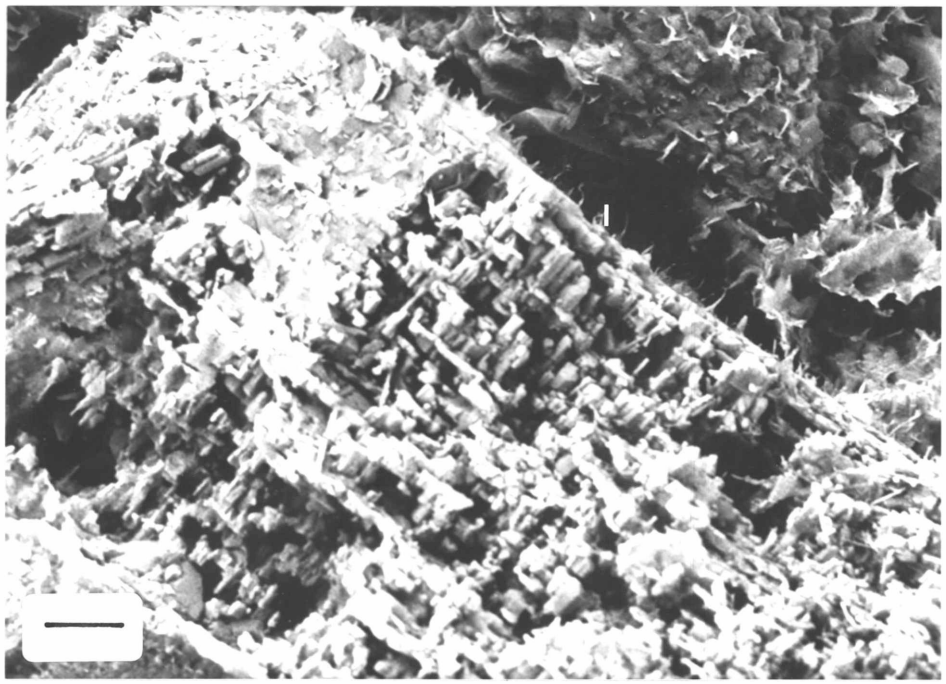


Plate 5-12 - SEM Photomicrograph showing partially dissolved K-feldspar framework grain. Note illite "hairs" (I) on the surface of altered grain. Sample from Sotong 5G-5.1 at depth of 2188.1 m msl. Scale bar = 10 microns.

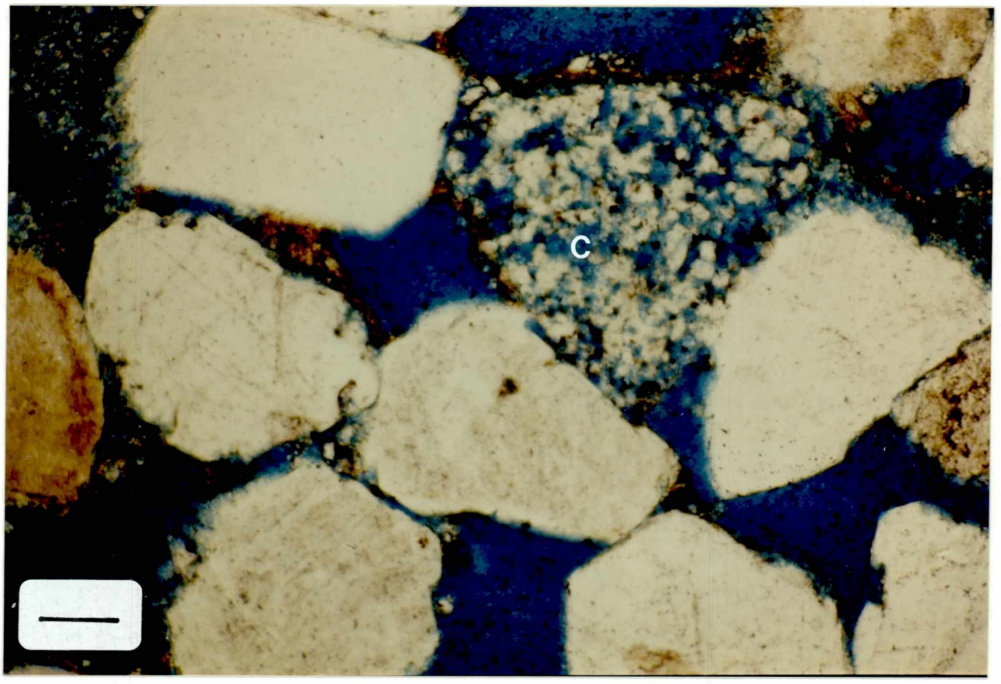


Plate 5-13 - Photomicrograph of thin section showing partially dissolved chert framework grain (C), partially encased by brownish material. The remaining encased "material" consists of micro-crystalline grains. Straight boundaries of some framework quartz are caused by quartz overgrowth. Sample from Seligi-3 at depth of 1584.1 m msl. Scale bar = 0.10 mm.

5.2.2 Authigenic Minerals

The authigenic materials found within the Pulai-II sandstones consist of:

1) Overgrowths: primarily of quartz and secondarily of albite and barytes on framework quartz, feldspars and rarely on lithic grains (Plates 5-4, 5-11 and 5-14 to 5-16),

2) Clay minerals: primarily kaolinite, smectite-illite, illite and chlorite (Plates 5-3, 5-4 and 5-17 to 5-20),

3) Carbonate minerals: calcite, ferroan-calcite, siderite and ankerite (Plates 5-2, 5-3, 5-21 and 5-22), and

4) Pyrite (Plate 5-23), and occasional colloidal iron(?) oxide.

Semi-quantitative XRD analyses of some selected samples (Table 5-1), indicate that:

1) Quartz comprises 71-91 percent of the total rock. (These values include both the framework and authigenic quartz, as XRD cannot differentiate the two).

2) Total feldspars comprise up to 6 percent. This is substantially less than the estimates from thin sections analysis by about 15 percent (average total feldspars is about 20 percent (Fig. 5-1)). This difference was expected because most of the framework feldspars show various degrees of alteration. The relatively small proportions of the total feldspar within the sandstones, as determined by XRD, are the residue of the partially dissolved grains and the authigenic

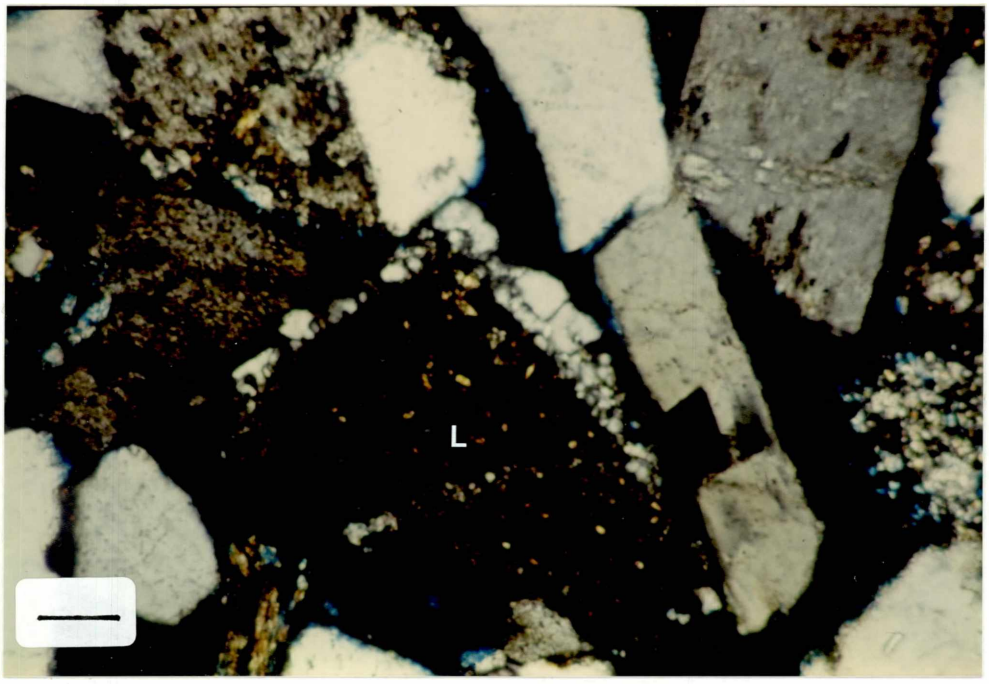


Plate 5-14 - Photomicrograph of thin section showing drusy authigenic quartz overgrowth on lithic framework grain (L). Note two stages of overgrowth on the grain. Sample from Pulai-1 at depth of 1157.6 m msl. Scale bar = 0.05 mm.



Plate 5-15 - SEM Photomicrograph showing quartz overgrowth (OV) on feldspar framework grain (F). Sample from Tapis-2 at depth of 2214.9 m msl. Scale bar = 15 microns.

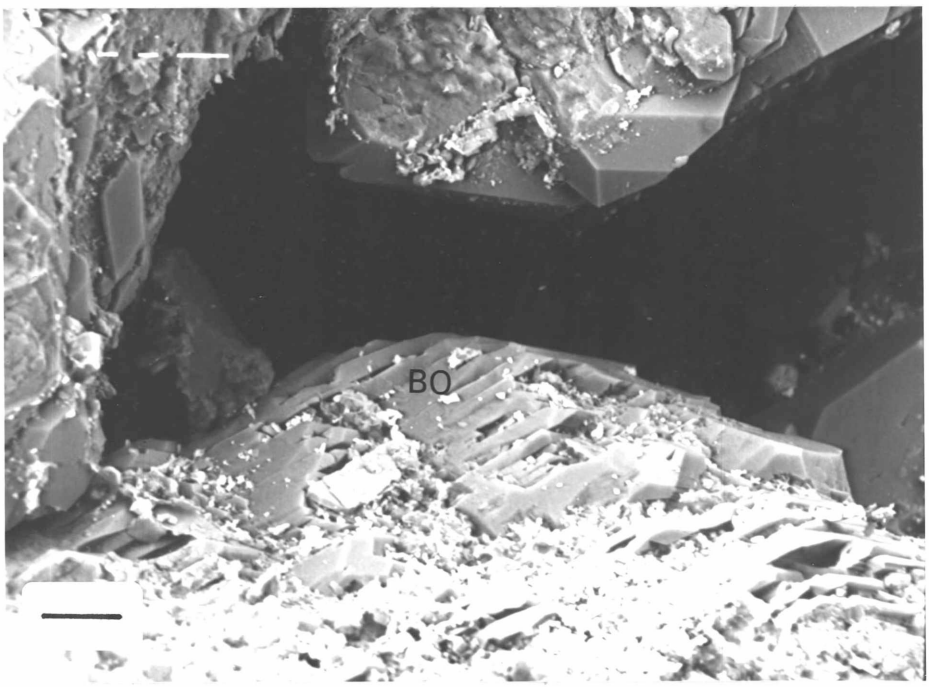


Plate 5-16 - SEM Photomicrograph showing barytes overgrowth (BO) on feldspar(?) framework grain. (See also plate 5-42). Sample from Besar-1 at depth of 2106.1 m msl. Scale bar = 15 microns.

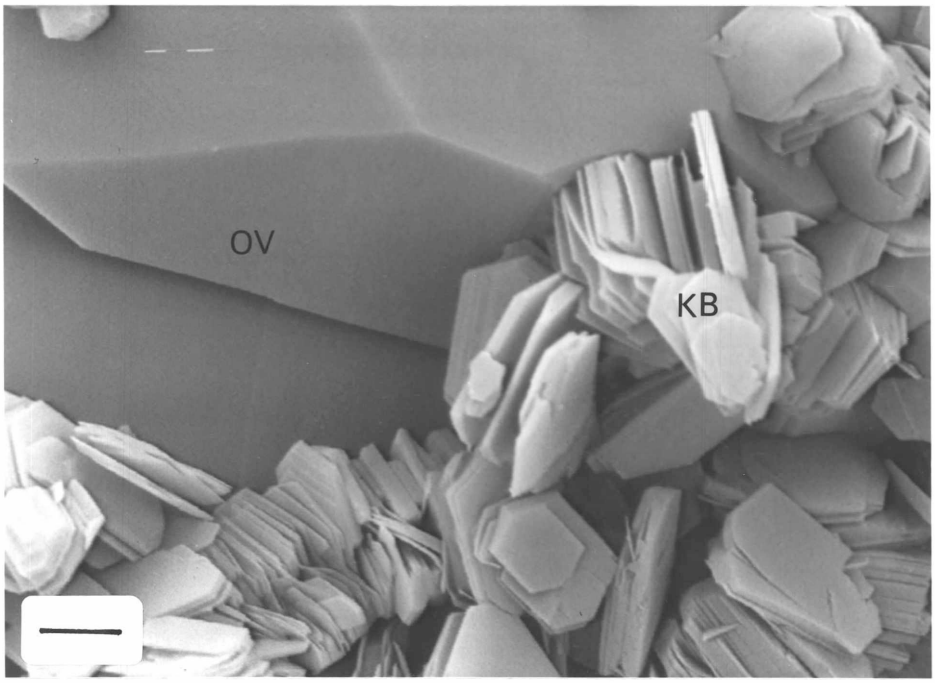


Plate 5-17 - SEM Photomicrograph showing kaolinite "booklets" (KB) and quartz overgrowth (OV). Some of kaolinite crystals appear to intergrow with quartz. Sample from Angsi-1 at depth of 2450.6 m msl. Scale bar = 3 microns.

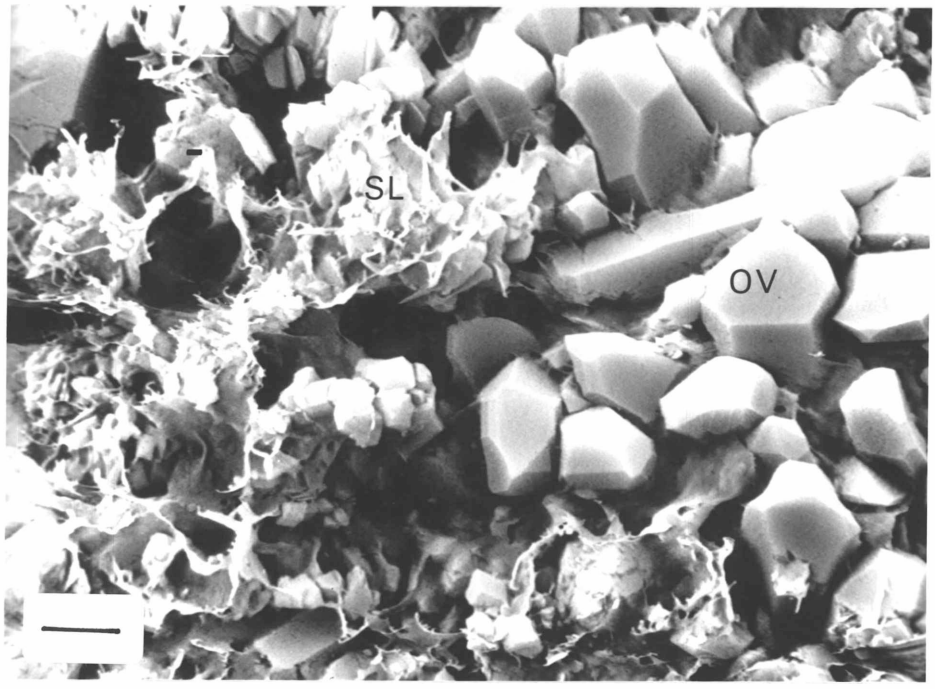


Plate 5-18 - SEM Photomicrograph showing smectite-illite (SL) and quartz overgrowth (OV). Note that some of smectite-illite intergrown with quartz. Sample from Tiong-5 at depth of 2312.8 m msl. Scale bar = 3 microns.

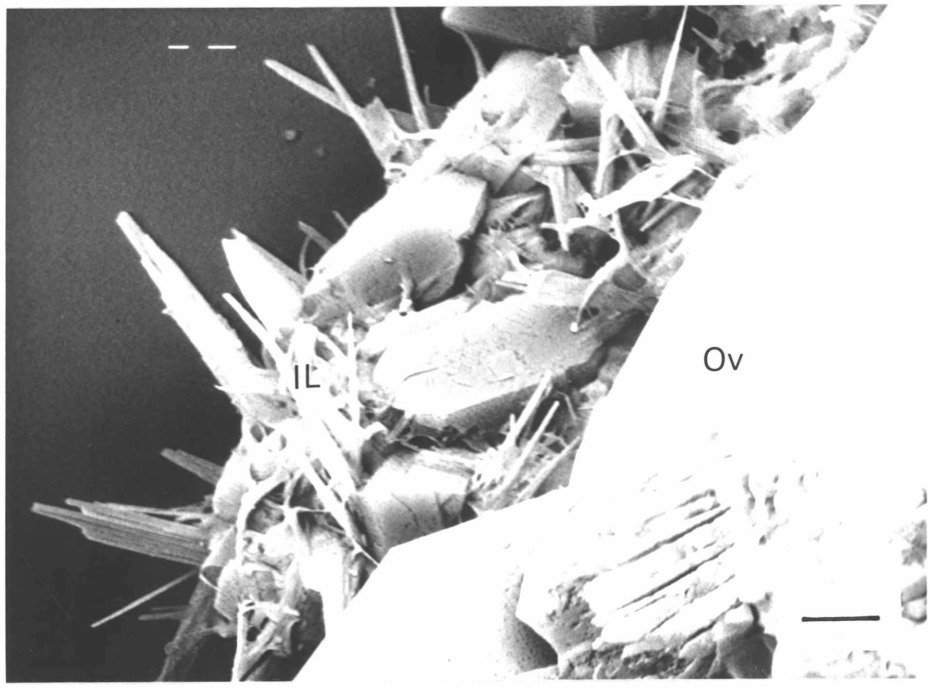


Plate 5-19 - SEM Photomicrograph showing illite (IL) and quartz overgrowth (Ov). Note that some of illite crystals appear to intergrow with quartz. Sample from Tapis-2 at depth of 2227.4 m msl. Scale bar = 3 microns.

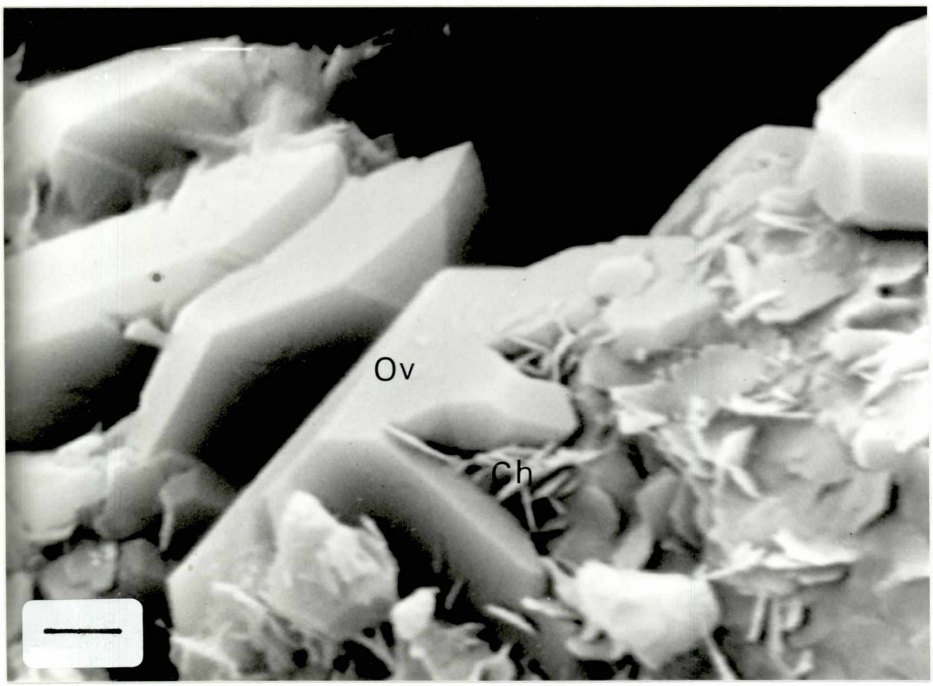


Plate 5-20 - SEM Photomicrograph showing idiomorphic chlorite (Ch). Note authigenic quartz (Ov) overgrowing on chlorite. Sample from Besar-1 at depth of 2121.3 m msl. Scale bar = 1.5 microns.

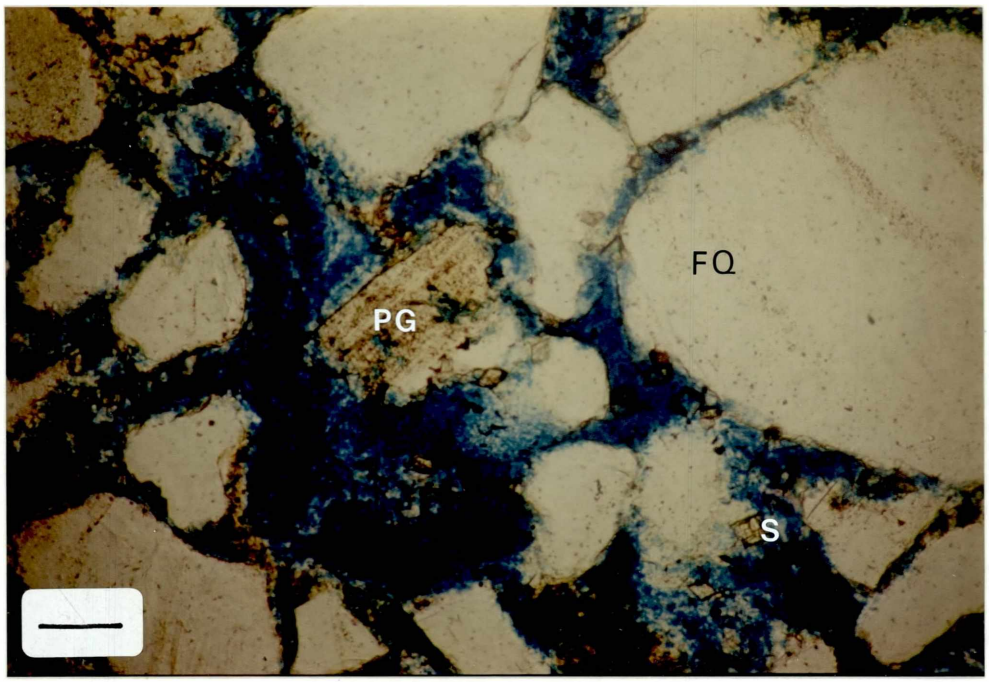


Plate 5-21 - Photomicrograph of thin section showing siderite rhombs (S) rimming pore walls. Note corrugated framework grains: quartz (FQ) and plagioclase (PG). The slightly murky pores are due to clay minerals. The murky appearance in plagioclase grain is caused by illitic clay. (See plate 5-10). Sample from Sotong 5G-5.1 at depth of 2188.1 m msl. Scale bar = 0.1 mm.

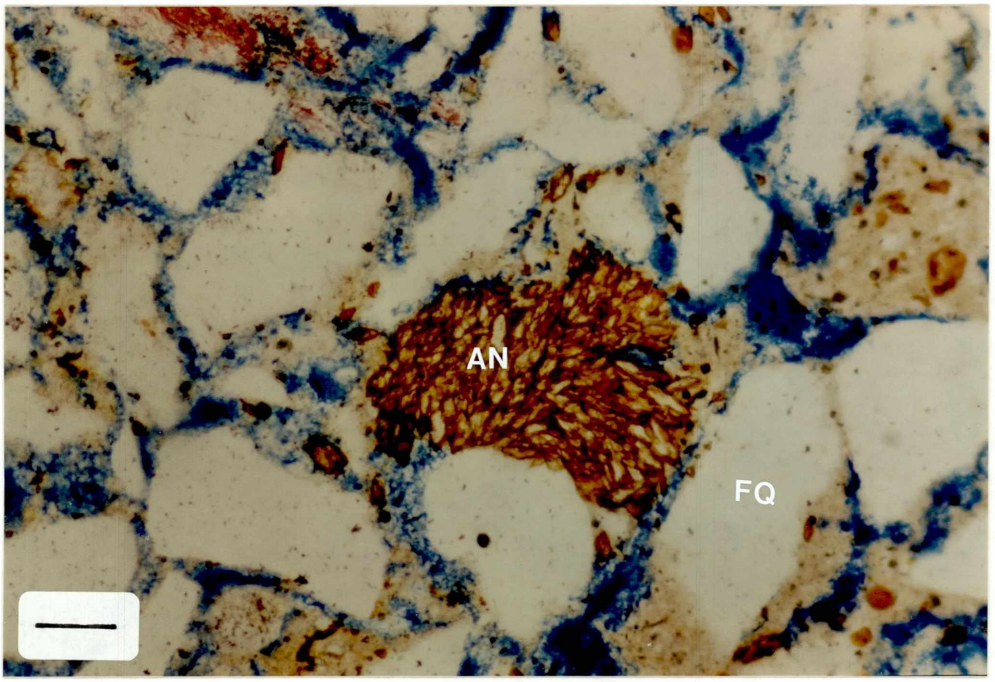


Plate 5-22 - Photomicrograph of thin section showing ankerite clusters (AN) within generally very fine grained sandstones. Note that most of framework quartz grains (FQ) are coated with light brown, clayey materials. Sample from Seligi-3 at depth of 1539.0 m msl. Scale bar = 0.05 mm.

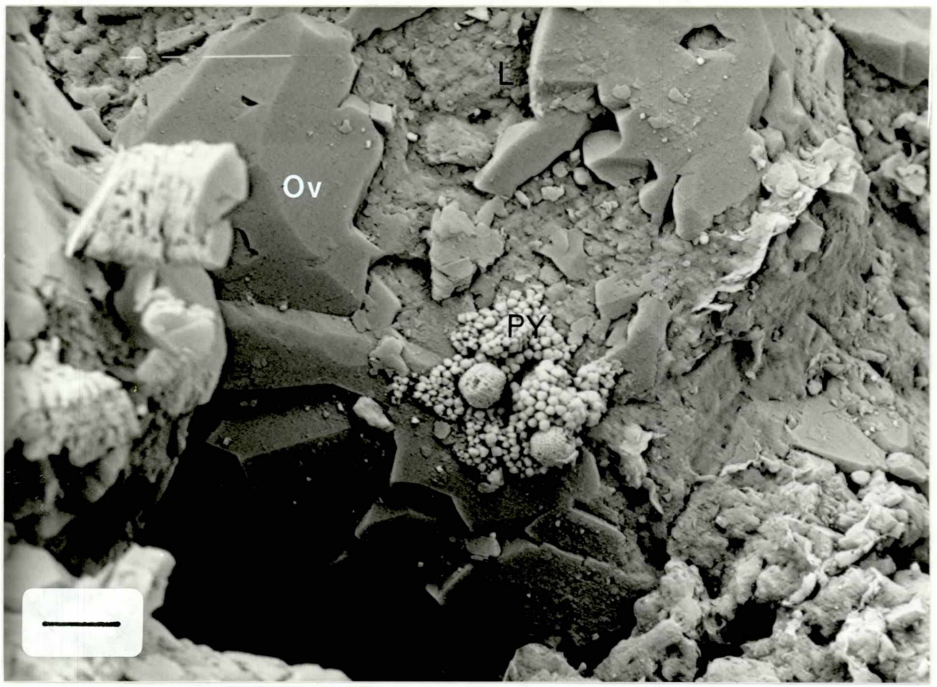


Plate 5-23 - SEM Photomicrograph showing framboid pyrite (PY). Note that pyrite appears to develop on the framework grain, pre-dating quartz overgrowth (Ov). Sample from Seligi-3 at depth of 1590.1 m msl. Scale bar = 10 microns.

Table 5-1 - Sandstone composition determined from XRD on the whole rock samples. Depth in metres m.s.l.

WELL	SAMPLE DEPTH	Total Percentage QTZ	ORTH[1]	PLAG[2]	CLAY[3]	CARB[4]	OTHERS
Bekok-1							
	1890	84	1	0	14	1	0
	1896	84	1	3	11	1	0
Tapis-2							
	2215	87	2	3	7	1	0
	2228	80	2	4	9	4	0
Angsi-1							
	2442	81	0	2	9	8	0
	2444	83	0	3	6	8	0
	2451	87	0	3	4	5	0
	2454*	66	0	3	12	19	0
Seligi-3							
	1493	91	1	1	5	2	0
	1499	79	2	1	7	9	2x
	1505	84	1	1	7	3	0
	1539*	70	1	0	10	17	2x
	1546	91	2	1	4	2	0
	1565	86	0	1	8	4	1b
	1578*	68	2	4	22	4	0
	1584	78	0	0	6	7	4b,5p
	1590	88	0	0	6	0	4b,2p
	1601	90	0	1	7	0	2b,1p
Belumut-1							
	1340	90	2	0	6	0	1b,1p
	1469	81	1	0	15	0	3x
	1471	75	1	0	21	3	0
Tinggi-1							
	1595*	66	0	3	28	3	0
	1596	79	0	6	15	0	0
	1603	71	1	4	16	7	0
Tiong-5							
	2298	73	0	3	8	16	0
	2306	81	0	3	10	6	0
	2313	83	0	2	10	5	0
Pulai-1							
	1150	83	3	2	5	3	4b
	1154	88	2	3	4	2	1b
	1191	87	2	3	6	2	0

cont. Table 5-1

Besar-1						
	2056	64	0	3	29	4	0
	2107	92	1	3	4	0	0
	2121	85	1	2	9	3	0
	2128	76	2	4	16	3	0
Sotong-5G-5.1						
	2175	85	1	4	8	2	0
	2188	91	0	4	4	1	0

1 - orthoclase, microcline, perthite
2 - mostly albite
3 - kaolinite, illite, smectite-illite)

and chlorite) see Table 5-2
4 - siderite, calcite and ankerite)
b - barytes; p - pyrite; x - limonite
* - silt to very fine-grained sandstones

feldspars. Albite forms the dominant plagioclase feldspar. K-feldspar is present, but in trace quantities. Because most of the albite seen under the SEM are associated with clay minerals, it would be most reasonable to assume that most albite detected through XRD are the product of plagioclase albitization (Plate 5-10), in addition to albite overgrowth (Plate 5-11).

3) Clay minerals are present in all the samples. They comprise about 4 to 29 percent of the total composition (Table 5-2). Kaolinite makes up 10 to 90 percent, illite with mixed-layer smectite-illite about 10 to 30 percent, and chlorite up to 23 percent (Fig. 5-4). It is observed that:

i) Chlorite is absent in sandstones with water saturation, S_w, of less than 35 percent. Otherwise, chlorite is found in varying amounts, particularly in sandstones adjacent to thick shale

Table 5-2 - Percentage clay and carbonate minerals in some selected sandstone samples. Depth in metres m.s.l.

Well	Sample Depth	Clay Minerals			Carbonate Minerals		
		Ch	I+S	K	Ca	Fe	CFM
Bekok-1							
	1890	3	6	6	1	0	0
	1896	3	4	4	1	0	0
Tapis-2							
	2215	1	4	2	0	1	0
	2228	2	6	1	1	3	1
Angsi-1							
	2442	0	1	4	0	6	2
	2444	0	3	3	0	3	5
	2454*	2	6	4	3	4	12
Seligi-3							
	1493	0	1	4	2	0	0
	1499	0	3	4	1	2	6
	1505	0	3	4	0	2	1
	1539*	0	5	5	0	9	17
	1565	0	4	4	0	2	2
	1578*	0	7	15	0	0	4
	1584	0	1	5	0	6	1
	1590	0	0	6	0	0	0
	1601	1	2	4	0	0	0
Belumut-1							
	1340	0	1	5	0	0	0
	1469	4	4	7	0	0	0
	1471	3	10	8	0	2	1
Tinggi-1							
	1595*	8	12	8	3	0	0
	1596	3	7	5	0	0	0
	1603	3	6	7	0	3	4
Tiong-5							
	2298	0	3	5	2	0	14
	2306	0	5	5	0	1	5
	2313	0	5	5	0	3	2
Pulai-1							
	1150	0	2	3	0	3	0
	1154	0	1	3	0	2	0
	1191	0	2	4	0	2	0

cont. Table 5-2

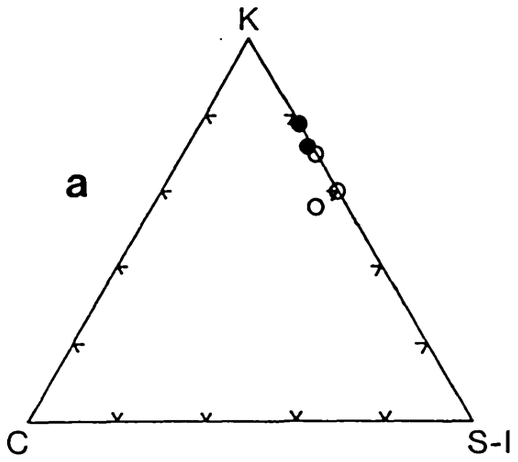
Besar-1						
2056	8	12	9	2	0	2
2107	1	1	2	0	0	0
2121	3	3	3	0	0	3
2128	5	6	5	3	0	0
Sotong-5G-5.1						
2175	2	3	3	1	1	0
2188	0	2	2	1	0	0

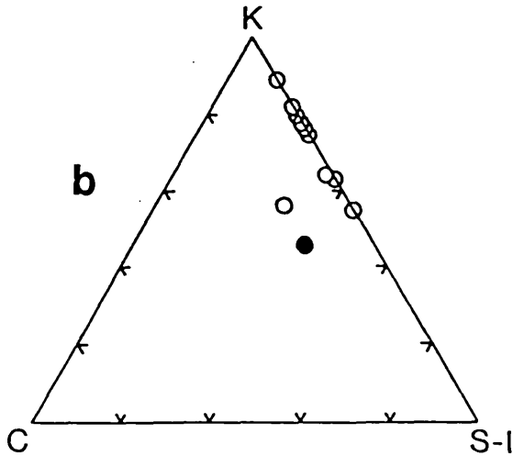
Ch - Chlorite; I+S - Illite-smectite; K - Kaolinite;
Ca - Calcite; Fe - Siderite; CFM - Ankerite.
* - silt to very fine grained sandstones

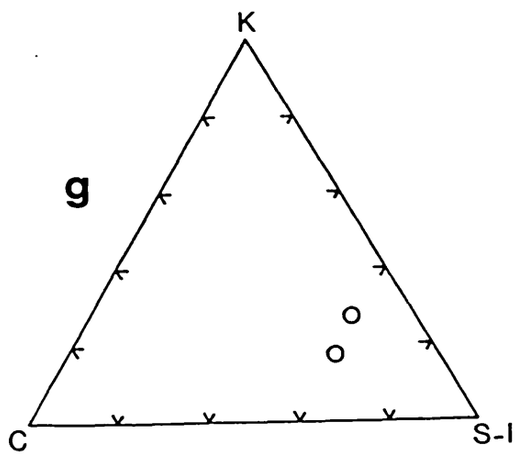
beds,

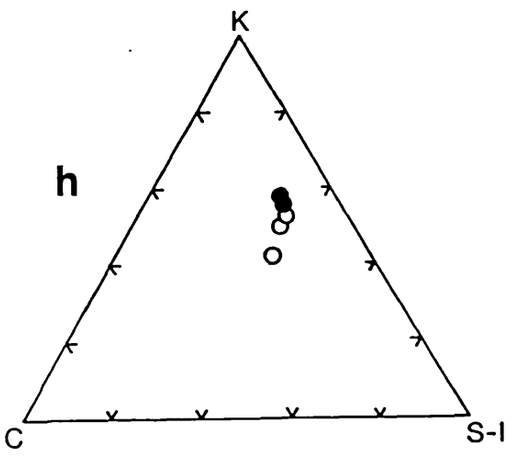
ii) There is no apparent relationship between sandstone grain size and clay mineral species. However, it appears that the more compacted sandstones, for example at Tiong-5 where the porosity is about 12 percent (Fig. 5-4f), contain a relatively higher proportion of smectite-illite than the less compacted sandstones, for example Bekok-1 where the porosity is about 20 percent (Fig. 5-4e), and

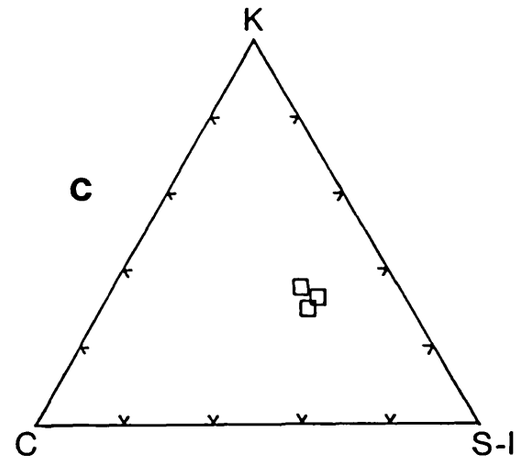
iii) Composition of clays in Facies A sandstones varies significantly: from predominantly kaolinite, K, with no trace of chlorite, C, and small amount of smectite-illite, S+I, ($C_0S+I_{10}K_{90}$), to a mixture of smectite-illite, chlorite and kaolinite, with kaolinite generally predominating ($C_{23}S+I_{17}K_{60}$) (Fig. 5-5a). In the case of Motif C sandstones, based on two samples, the average composition is 62 percent kaolinite, 28 percent smectite-illite and 10 percent chlorite ($C_{10}S+I_{28}K_{62}$) (Fig. 5-5b) and, within the Facies D, the average composition

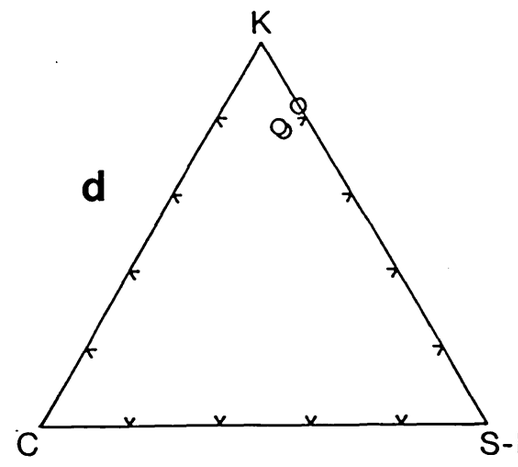


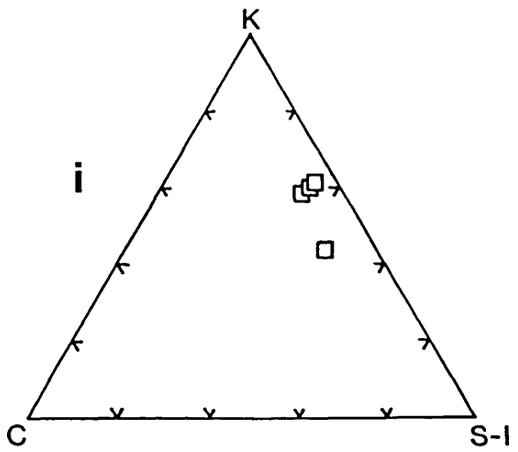


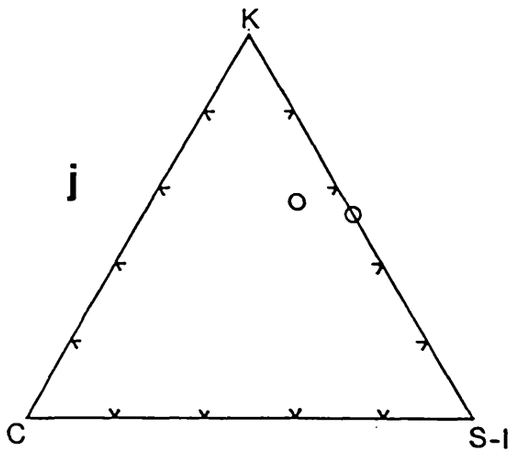


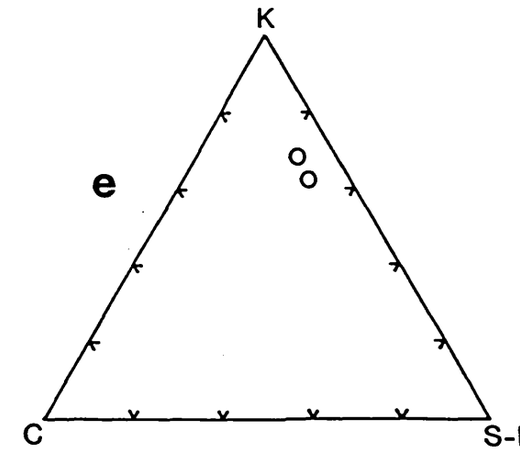












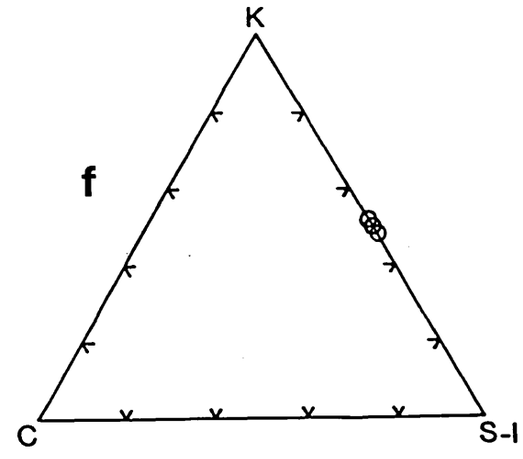


***Figure* 5-4** - Clay mineral compositions in sandstones at a) Pulai-1, b) Seligi-3, c) Tinggi-1, d) Belumut-1, e) Bekok-1, f) Tiong-5, g) Tapis-2, h) Besar-1, i) Angsi-1 and j) Sotong 5G-5.1 and Duyong 6H-32.1. (K-kaolinite; C-chlorite; S-I-smectite-illite).

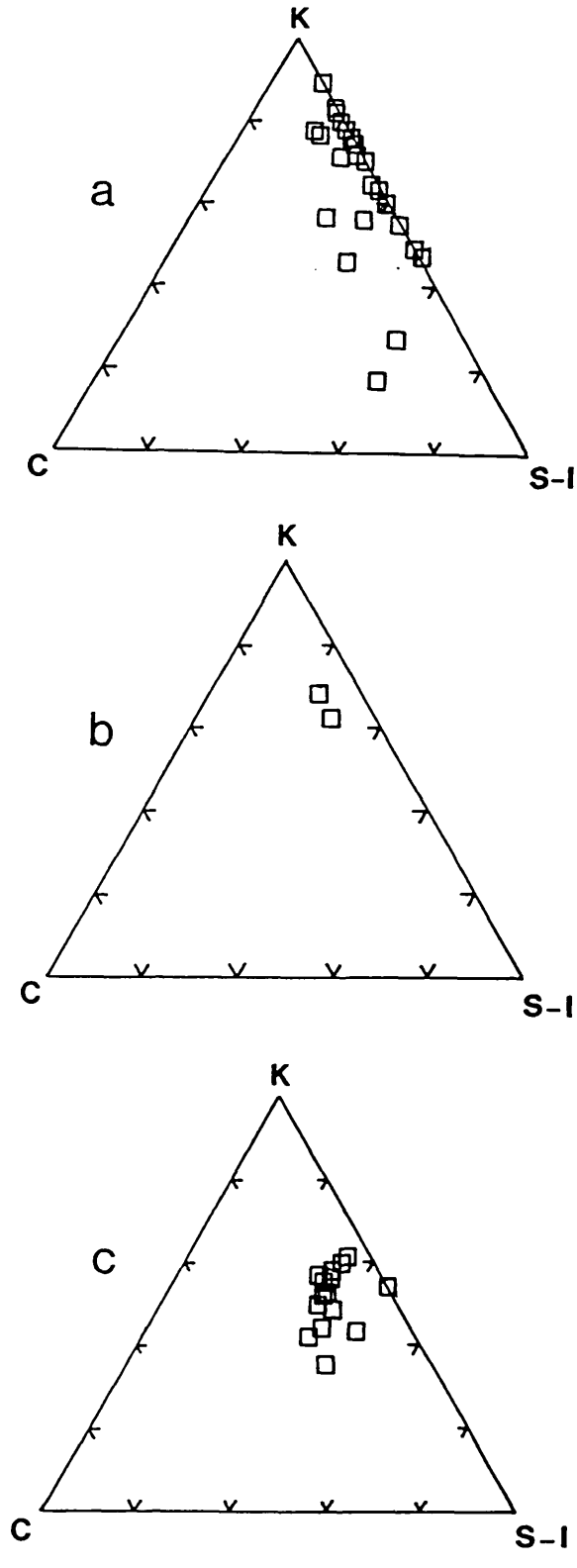


Figure 5-5 - Clay mineral composition in sandstones of a) Motif A, b) Motif C and c) Motif D. (K-kaolinite; C-chlorite; S-I-smectite-illite).

is 62 percent kaolinite, 33 percent smectite-illite and 5 percent chlorite ($C_5S+I_{33}K_{62}$) (Fig. 5-5c).

4) Carbonate minerals are found in most of the samples. They comprise up to 25 percent of the total composition (Table 5-1). Ankerite appears to be dominant in the generally finer-grained sandstones, whereas siderite and ferroan-calcite are common in the relatively coarser-grained sandstones. Medium to coarse-grained hydrocarbon bearing sandstones did not seem to contain calcite or ferroan-calcite.

5) Pyrite and barytes are less common secondary authigenic minerals, and only at Seligi-3 do both pyrite and barytes occur together. They constitute up to 9 percent of the total rock (Table 5-1). The other secondary, but generally rare authigenic mineral is colloidal iron oxide/limonite.

5.2.2.1 *Authigenic Quartz*

Authigenic quartz forms one of the dominant cementing components. It usually occurs as:

1) Pore-lining and pore-filling syntaxial overgrowths (Plates 5-4, 5-7, 5-15 and 5-20),

2) Microcrystalline, drusy overgrowths (Plate 5-18), and

3) Euhedrally well-developed quartz crystals (Plate 5-24).

The authigenic quartz is commonly intergrown with pore-filling kaolinite, illite and chlorite (Plates 5-4, 5-18 and 5-20). It usually overgrows around framework quartz grains; however, framework feldspars

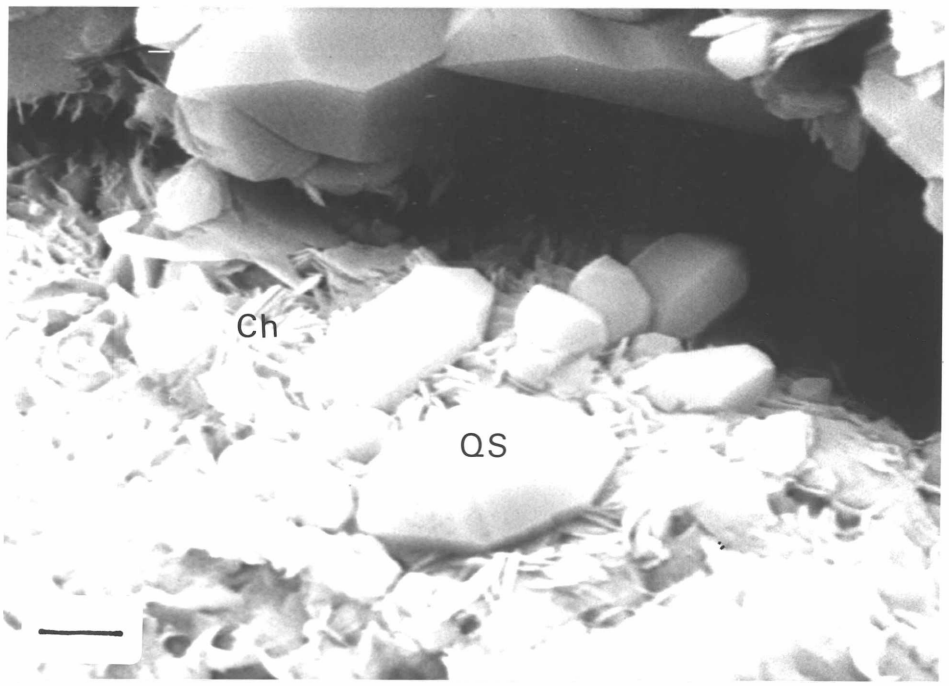


Plate 5-24 - SEM Photomicrograph showing euhedral quartz druse (QS) settling on chlorite (Ch) coated framework grain. Sample from Duyong 6H-32.1 at depth of 1799.4 m msl. Scale bar = 2 microns.

and lithic fragments have also been observed to provide the platforms for growth (Plates 5-14 and 5-15). Smectite-illite, chlorite and occasionally ferroan-calcite have also been observed to inhibit quartz overgrowths. Smectite-illite and chlorite prevent overgrowing by coating the overgrowths and quartz nucleation sites, and ferroan-calcite by occupying pore sites. However, overgrowth continues in places where there are gaps in the framework coating. In some instances, it appears that illitic coating could not prevent quartz from forming new nucleation and re-establishing new overgrowths (Plate 5-25).

The environmental conditions favouring quartz precipitation probably persisted in the system for quite some time. It appears, in places, that authigenic quartz continued growing to the extent that some overgrowths interlock (Plate 5-26). A common explanation for continued quartz overgrowth involves the presence of and the continued supply of silica-rich pore waters to the system, and this silica enrichment has been linked to smectite-illite transformation and dissolution of unstable feldspar grains (Eberl and Hower, 1977 and Boles and Franks, 1979). As observed in this study, the dissolution of framework chert could also contribute to the enrichment of silica content in pore waters.

5.2.2.2 *Authigenic Kaolinite*

Kaolinite is the most common authigenic clay mineral (Table 5-2), and is found in varying quantities in the sandstones. Kaolinite exhibits a very sharp peak on XRD spectrum, indicating its high crystallinity (Figs. 3-22 and 3-23). The SEM microphotographs show well-developed kaolinite crystals ranging in size from a few microns to several tens of microns and are found:

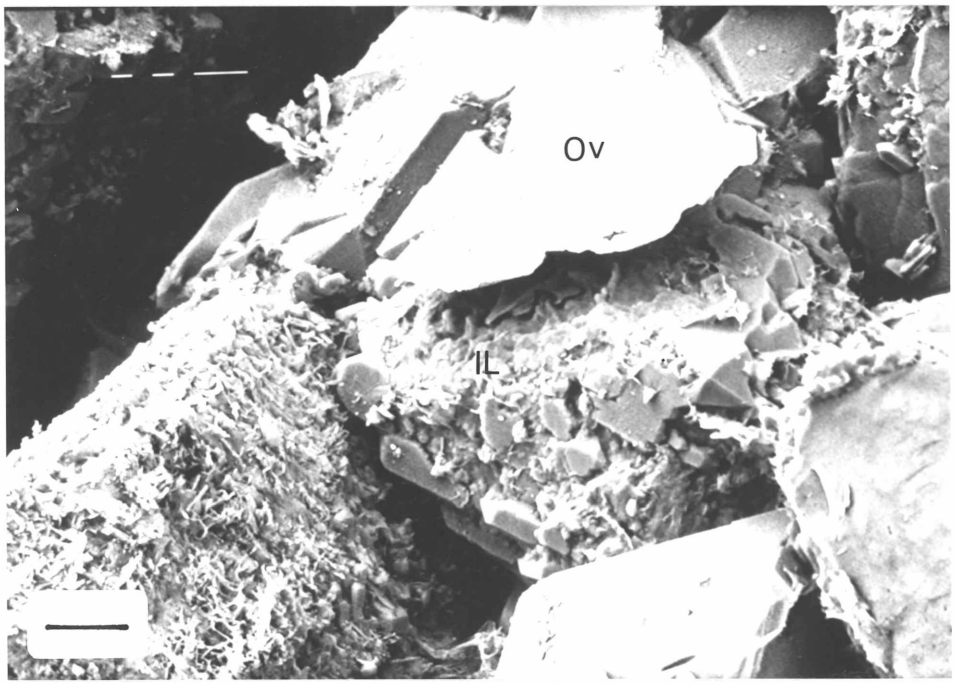


Plate 5-25 - SEM Photomicrograph showing authigenic quartz (Ov) overgrowing on illite (IL) coated framework grain. Sample from Sotong 5G-5.1 at depth of 2188.1 m msl. Scale bar = 15 microns.

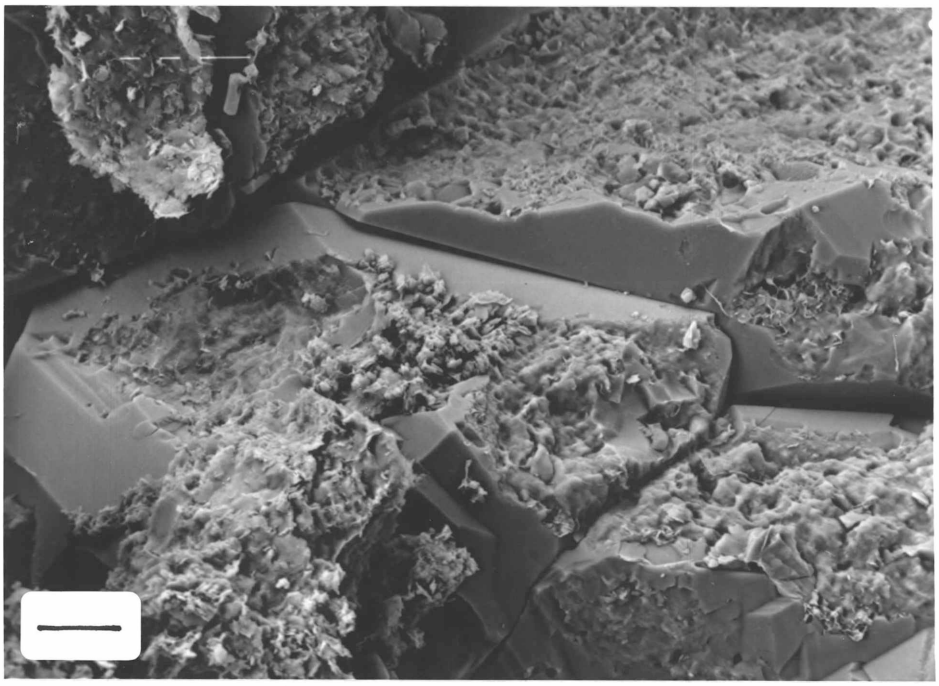


Plate 5-26 - SEM Photomicrograph showing interlocking syntaxial quartz overgrowth. No primary porosity visible. Sample from Besar-1 at depth of 2128.1 m msl. Scale bar = 15 microns.

1) As a by-product of feldspar alteration (Plate 5-27). Kaolinite "booklets" are very fine, usually about 1 to 3 microns in diameter.

2) As booklets or aggregates of fine crystals, about 5 microns in diameter, congregating around and/or occluding pore throats and/or "resting" on framework grain surfaces (Plates 5-4, 5-17 and 5-28). They are frequently found to be associated with authigenic quartz, and

3) As coarse-grained crystals, often vermicular, measuring about 10 to 20 microns in diameter (Plate 5-29).

The kaolinites in cases 2) and 3) above are believed to have formed through precipitation, whereas case 1) appears to be the direct product of feldspar alteration. Because the morphologies of the kaolinites in cases 2) and 3) are different, they are believed to have been precipitated at different times, with the coarse-grained vermicules comprising early stage species, and the fine-grained booklets either a later stage kaolinites or early stage kaolinites which were deprived from growing due to changes of circumstances, such as emplacement of hydrocarbons into the system.

5.2.2.3 *Authigenic Illite and Smectite-Illite*

Illite and smectite-illite collectively are very common authigenic clay minerals, and they comprise up to 12 percent of some sandstones (Table 5-2). The minerals occur as pore-linings, pore-filling and occasionally as pore bridging materials. Six illite and smectite-illite morphologies have been observed. These are:

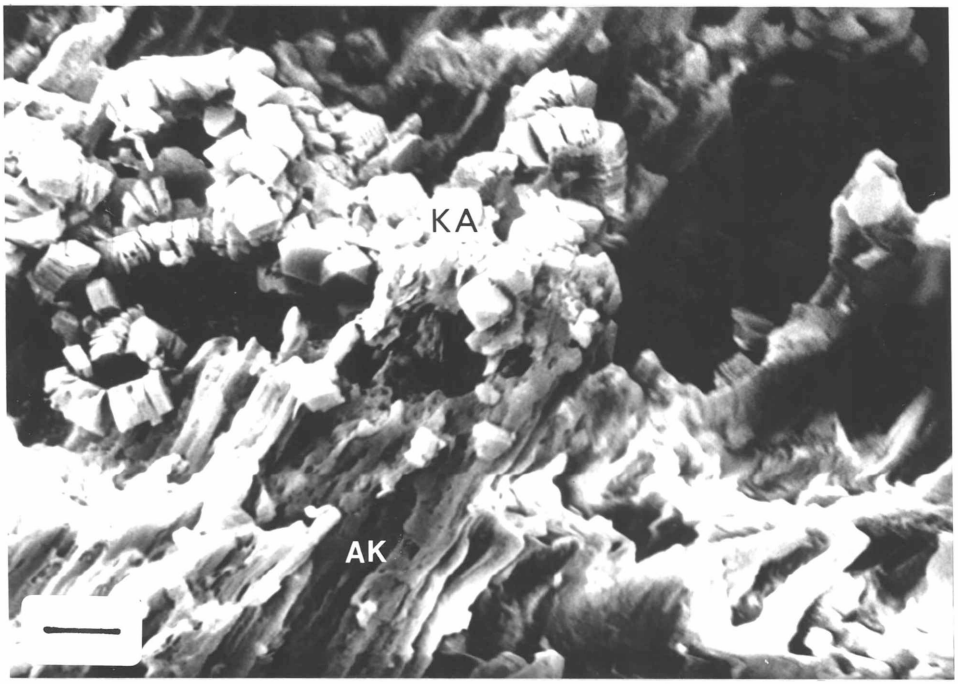


Plate 5-27 - SEM Photomicrograph showing 1 micron kaolinite "booklets" (KA), in association with altered K-feldspar (AK). Sample from Seligi-3 at depth of 1492.7 m msl. Scale bar = 3 microns.



Plate 5-28 - SEM Photomicrograph showing 5 micron kaolinite "booklets" (KA), on smectite-illite (SL) coated framework grain. Sample from Tiong-5 at depth of 2312.8 m msl. Scale bar = 10 microns.



Plate 5-29 - SEM Photomicrograph of accordian-like kaolinite vermicules. Sample from Seligi-3 at depth of 1498.5 m msl. Scale bar = 3 microns.

1) Matty illite layers which normally coat the framework grains. These illites probably represent either detrital illite, or illite formed from smectite-illite transformation (Plates 5-25 and 5-30),

2) Ragged and occasionally flake-like aggregates which commonly are found associated with albite, the by-products of plagioclase alteration (Plates 5-10),

3) Whiskery aggregates (Plate 5-31),

4) Thin membranes which cover and at the same time bridge framework grains and authigenic minerals (Plate 5-32),

5) Ribbon and filamentous laths which occasionally also bridge crystals or framework grains (Plate 5-33), and

6) Lath, blade-like clusters which developed apparently freely in pore spaces (Plate 5-19), and in one sample, intergrown with ferroan-calcite (Plate 5-34).

Probably, with the exception of cases 1) and 2) above, illite and smectite-illite were precipitated from pore waters. Their different morphological features seen in cases 3) to 6) probably indicate a progressive increase in crystallinity, reflecting different depth, temperature and/or time, at which each was developed; the more crystalline blady illite was precipitated last, between 95°-135°C (Lee, *et al*, 1989).

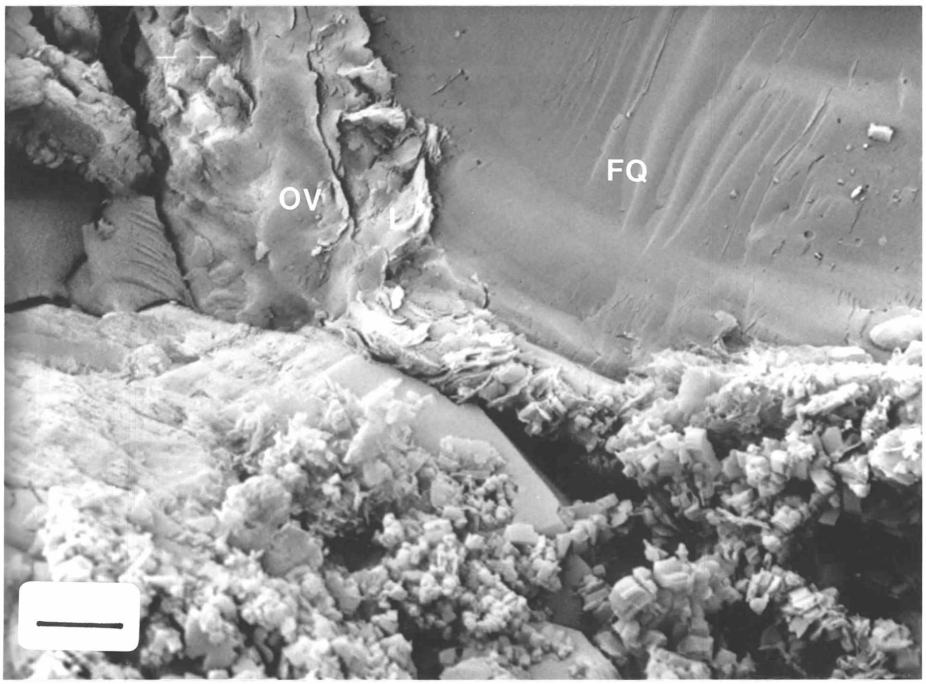


Plate 5-30 - SEM Photomicrograph of fractured framework quartz grain (FQ), showing illitic line (L) around the framework grain, which is then covered by overgrowth quartz (OV). This line probably represents the "dust-line" on framework grains viewed in some thin section. Sample from Sotong 5G-5.1 at depth of 2175.0 m msl. Scale bar = 3 microns.

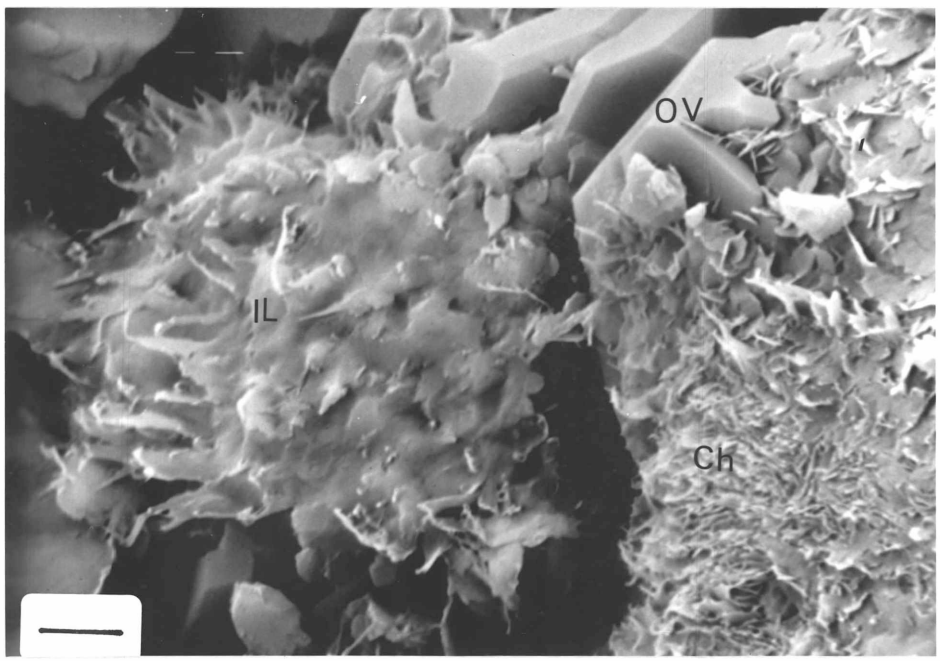


Plate 5-31 - SEM Photomicrograph of whiskery illite (IL). Note that illite is closely associated with quartz overgrowth (OV) and chlorite (Ch). Sample from Besar-1 at depth of 2121.3 m msl. Scale bar = 2.5 microns.

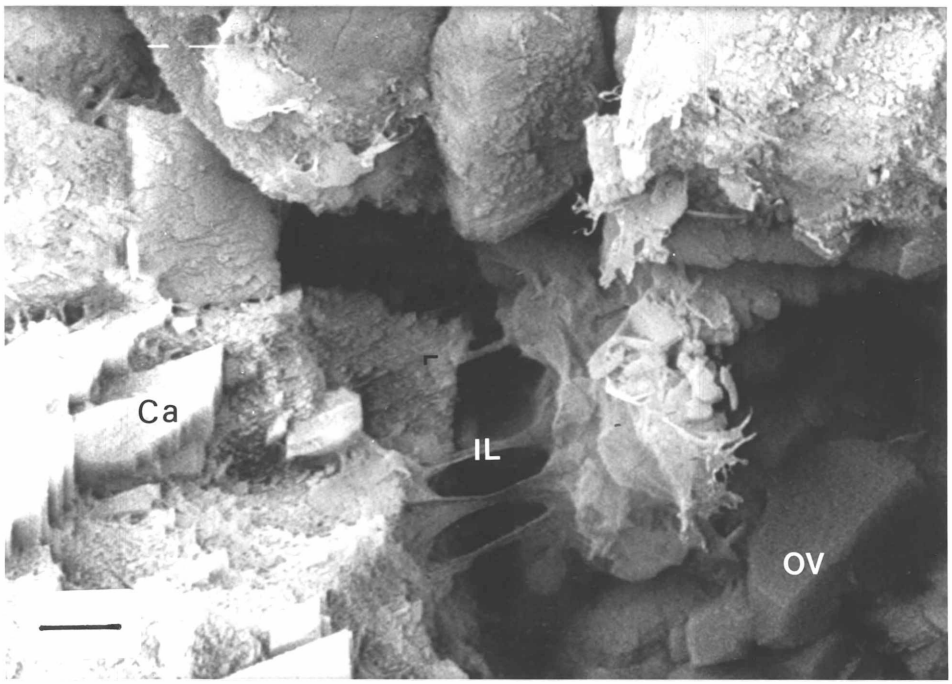


Plate 5-32 - SEM Photomicrograph of bridging illite (IL). Note that illite appears to consist of very thin membrane which covers most of the framework grains and authigenic calcite (Ca) and quartz (OV). Some illite is whiskery. Sample from Sotong 5G-5.1 at depth of 2175.0 m msl. Scale bar = 3 microns.

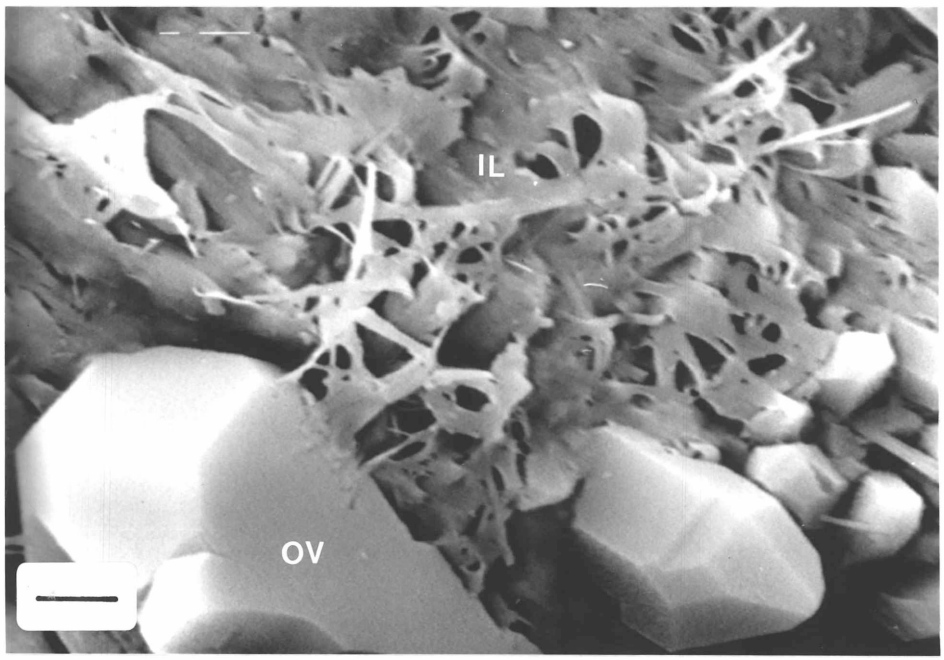


Plate 5-33 - SEM Photomicrograph of illite (IL). Note that illite consists of interwoven laths, which coats in part the framework grain covered by drusy quartz overgrowth (OV). Sample from Tapis-2 at depth of 2227.4 m msl. Scale bar = 1.5 microns.

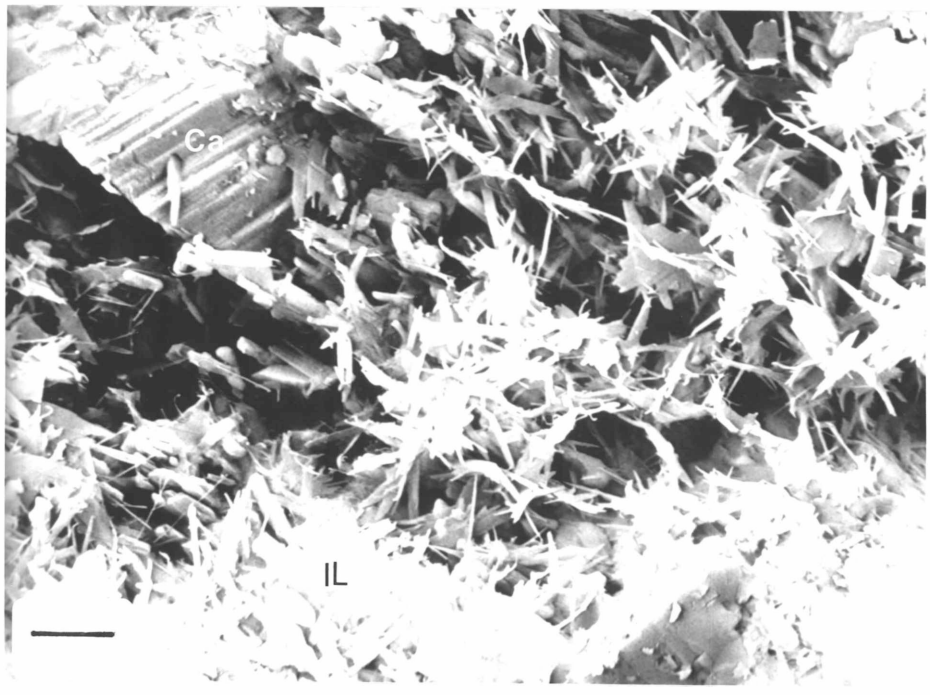


Plate 5-34 - SEM Photomicrograph of illite (IL). Note that illite consists of cluster, blade-like laths. In the top left corner of the plate, ferroan-calcite (Ca) "swallows" partly an illite lath. Sample from Tiong-5 at depth of 2312.8 m msl. Scale bar = 3 microns.

5.2.2.4 *Authigenic Chlorite*

Authigenic chlorite is a less common clay mineral than kaolinite, illite and smectite-illite (Table 5-2), and is found in relatively small quantities in sandstones of Motifs C and D, and generally absent in most sandstones of Motif A (Fig. 5-5a). Pore-lining chlorite occurs as thin occasionally discontinuous coats rimming framework grains. This chlorite rim, viewed through the SEM, consists of well-developed platelets, about 1 to 2 microns in size, seated randomly on crystal edges perpendicular to framework grains (Plate 5-35). This idiomorphic chlorite is often found intergrown with and predating authigenic quartz (Plate 5-20 and 5-31).

In analysing the XRD results, it was found that the absence of chlorite in the sandstones of Motif A (e.g. at Seligi-3), and also from some channel facies of Motif D (e.g. at Sotong 5G-5.1), relates to the presence of hydrocarbons. However, chlorite was also found in Motif A sandstones which are water-bearing. Chlorite was found in the sandstones of Motif C and in some sandstones of Motif D which contain glauconite, even if the sandstones contain hydrocarbons. These observations have led to the conlusion that:

1) Glauconite, seen in thin sections as altered framework grains (Plate 5-1), probably consists of minute chlorite crystals, and these were transformed from glauconite during burial diagenesis. Because chlorite occurs within the hydrocarbon-bearing sandstones, the transformation probably occurred prior to hydrocarbon emplacement, and

2) Idiomorphic chlorite crystals found intergrown with authigenic

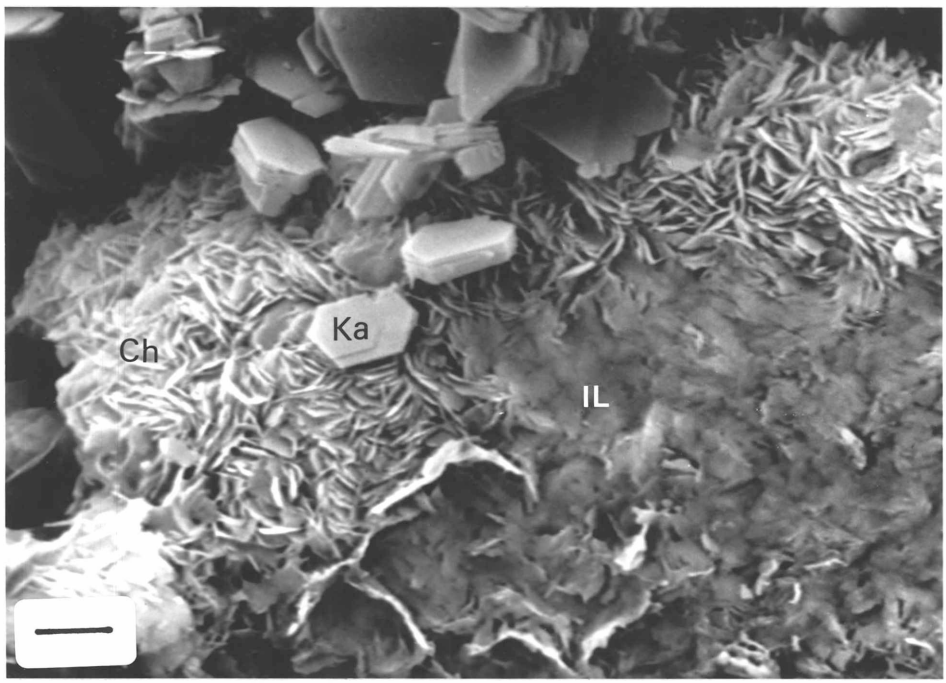


Plate 5-35 - SEM Photomicrograph of chlorite (Ch). Note its idiomorphic morphology, and its relation with other authigenic minerals: kaolinite (Ka) resting on it and so also illite membrane (IL) coating it. Sample from Besar-1 at depth of 2121.3 m msl. Scale bar = 3 microns.

quartz (Plate 5-31), were precipitated after the entrapment of hydrocarbons, within water-bearing sandstone interval. This is because no chlorite was detected within the hydrocarbon-bearing zone of genetically related sandstones.

5.2.2.5 *Authigenic Calcite and Ferroan-calcite*

Authigenic calcite was found primarily as pore-filling and occasionally as replacive cement, and it occurs in two forms:

1) As isolated patches within generally very fine-grained sandstones. It appears to replace quartz and imparts corrugated outlines to the adjacent framework quartz (Plates 5-2 and 5-36). Calcite found in these fine-grained sandstones is probably an early stage calcite which escaped dissolution. Calcite of similar morphology was not seen in medium to coarser-grained sandstones, and

2) As highly crystallized grains which, in some sandstones, apparently completely occupy pore spaces, leaving no visible porosity, indicating of its late "arrival" in relation to authigenic quartz overgrowth (Plate 5-37), and possibly illite (Plate 5-34). EDAX analyses of these late stage calcite crystals often show the presence of Fe cations: in one particular sample, it shows Fe-Ca zonations, in which the more intense Fe peaks were registered on the edges rather than on the inside of the crystals (Fig. 5-6 and Plate 5-38).

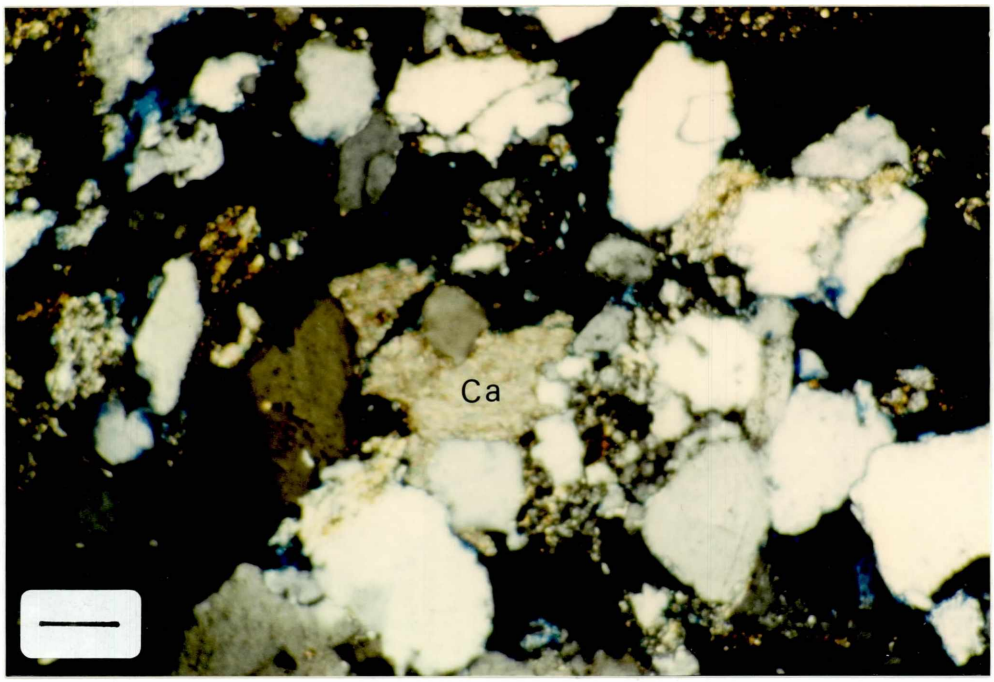


Plate 5-36 - Photomicrograph of thin section showing calcite (Ca) within generally very fine grained sandstone. Note corrugated outline of the framework quartz grains surrounding it. Sample from Duyong 6H-32.1 at depth of 2163.4 m msl. Scale bar = 0.1 mm.

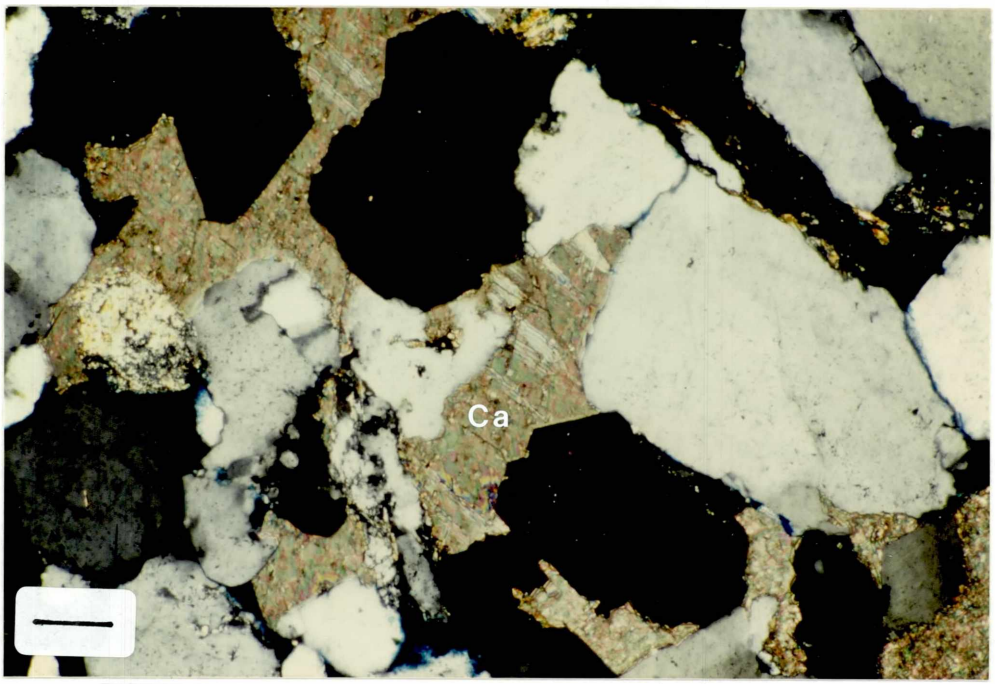


Plate 5-37 - Photomicrograph of thin section showing calcite (Ca) within generally medium grained sandstone. Note that calcite cementation post-dated quartz overgrowth. Sample from Duyong 6H-32.1 at depth of 2370.1 m msl. Scale bar = 0.1 mm.

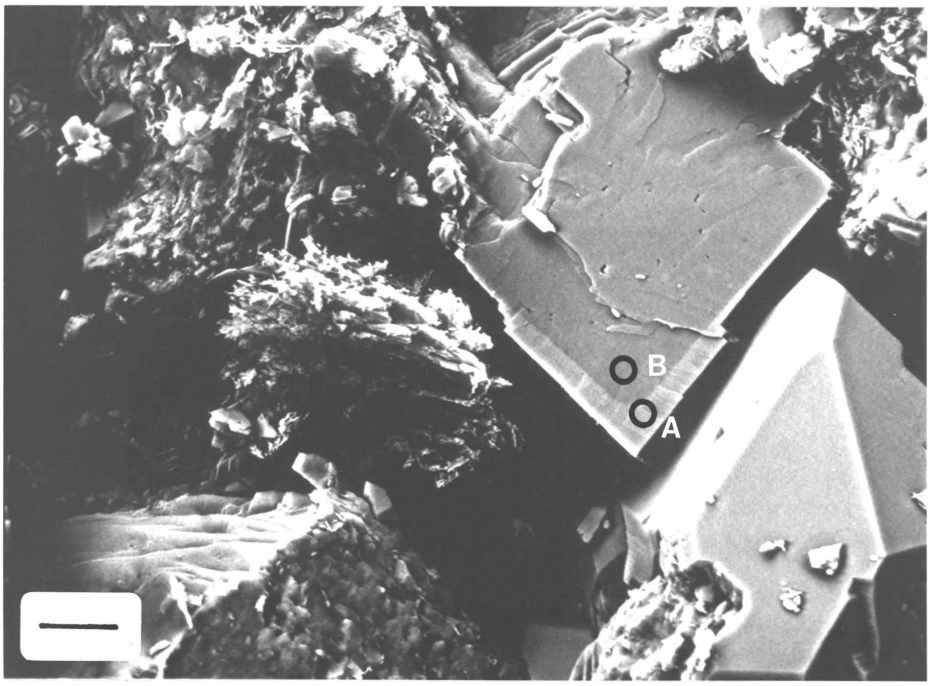


Plate 5-38 - SEM Photomicrograph showing EDAX locations on calcite crystal. Sample from Besar-1 at depth of 2121.3 m msl. Scale bar = 10 microns.

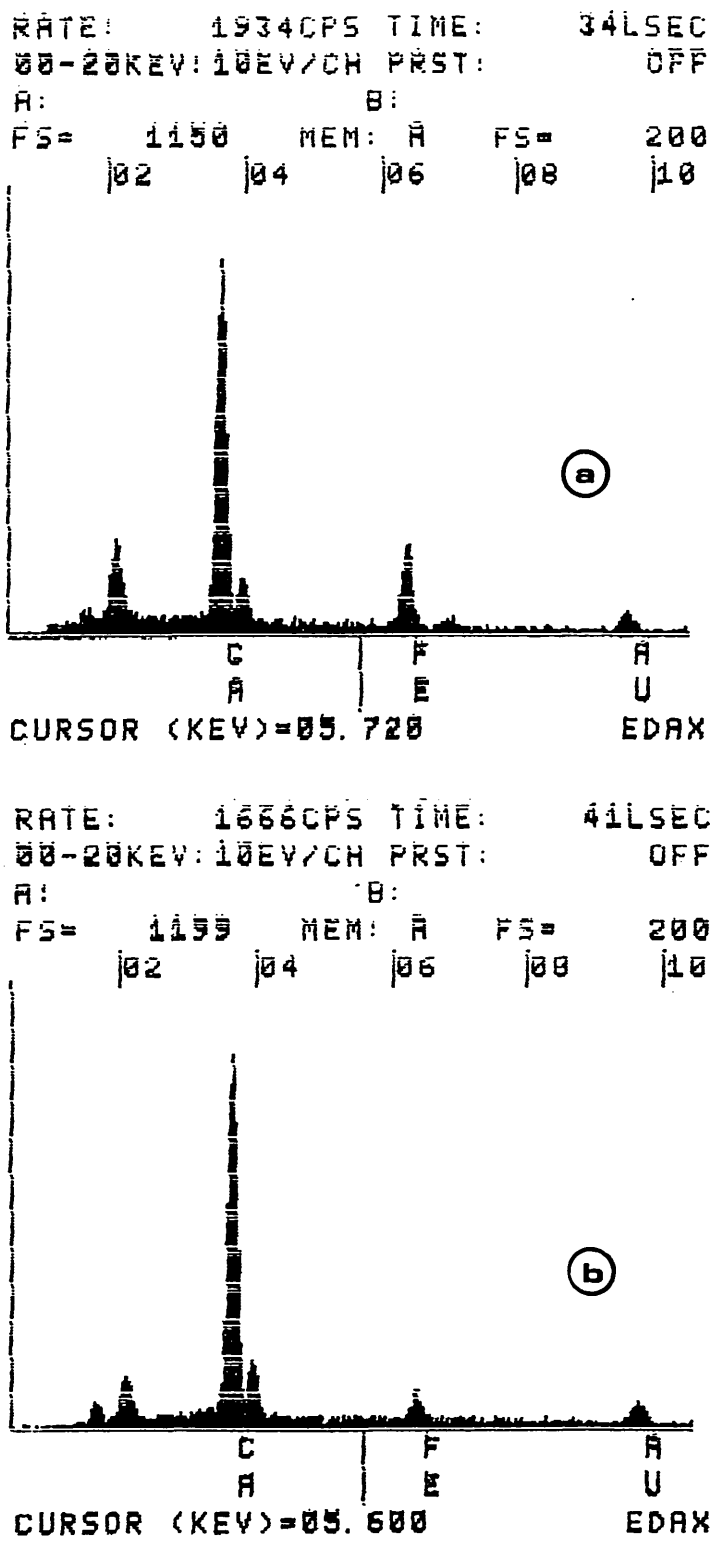


Figure 5-6 - EDAX spectra of ferroan-calcite showing relative intensity of Fe peak with respect to Ca peak, taken at two seperate locations on a "calcite" crystal (see accompanying plate). The spectra show higher Fe intensity in outer side of the crystal than from the inside, indicating higher Fe/Ca ratio on the outside the crystal.

5.2.2.6 *Authigenic Siderite and Ankerite*

Authigenic siderite and ankerite occur in most of the sandstones, and comprise up to 14 percent of the total carbonates (Table 5-2).

Siderite shows its predominance generally in coarser-grained sandstones. Pore-filling siderite usually occurs as isolated and occasionally cross-twinned euhedral rhombs (Plate 5-39), which adhere or attach to framework grains (5-21).

Authigenic ankerite, on the other hand, usually occurs as pore-filling clusters or aggregates of microcrystalline rhombs in generally fine-grained sandstones (Plate 5-22).

5.2.2.7 *Authigenic Pyrite*

Authigenic pyrite crystals occur both as pore-lining and pore filling mineral, and are found disseminated sporadically through the sandstones. Pyrite have been observed to occur:

1) As framboids consisting of round and occasionally oval-shaped aggregates of small closely packed crystals, which pore-line framework grains (Plate 5-23), or which "cling" to pore walls, plugging pore spaces, by means of an illitic membrane (Plate 5-40). Framboid pyrite has always been thought to have been formed as a by-product of sulphate reduction during early stages of sediment diagenesis (Curtis, 1978). The observations made in some sandstones of the Pulai-II Formation suggest that framboidal pyrite formed at the same time as, or slightly later than authigenic quartz overgrowth (Plate 5-23) but predating illite membrane precipitation (Plate 5-40). However, the fact that pyrite was detected in relative

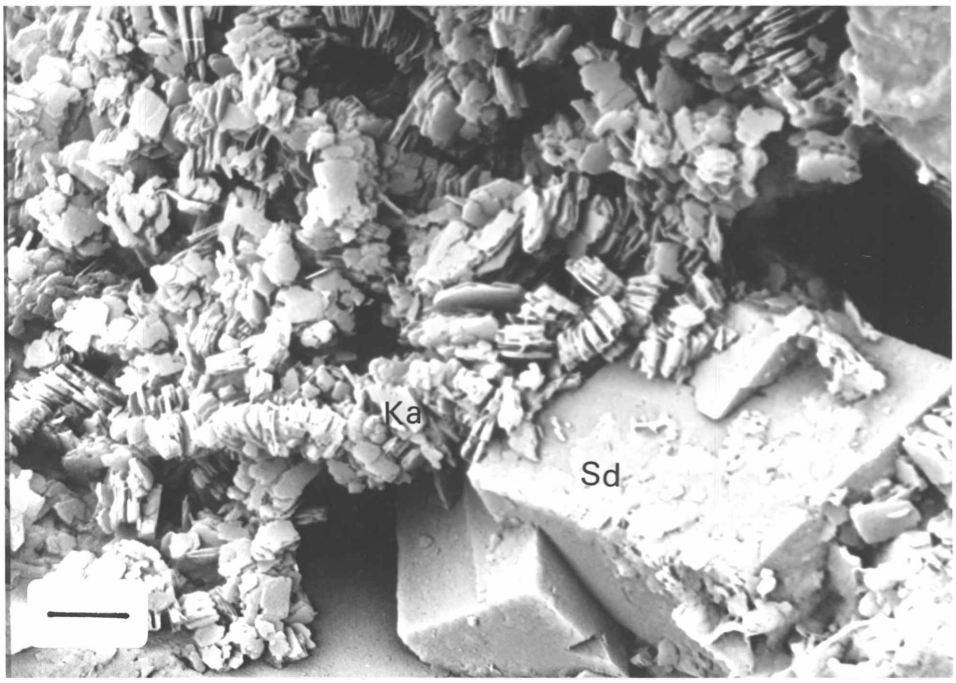


Plate 5-39 - SEM Photomicrograph of intertwinning siderite (Sd). Kaolinite booklets appear to have been formed at the same time or immediately after formation of siderite rhombs. Sample from Angsi-1 at depth of 2454.0 m msl. Scale bar = 3 microns.

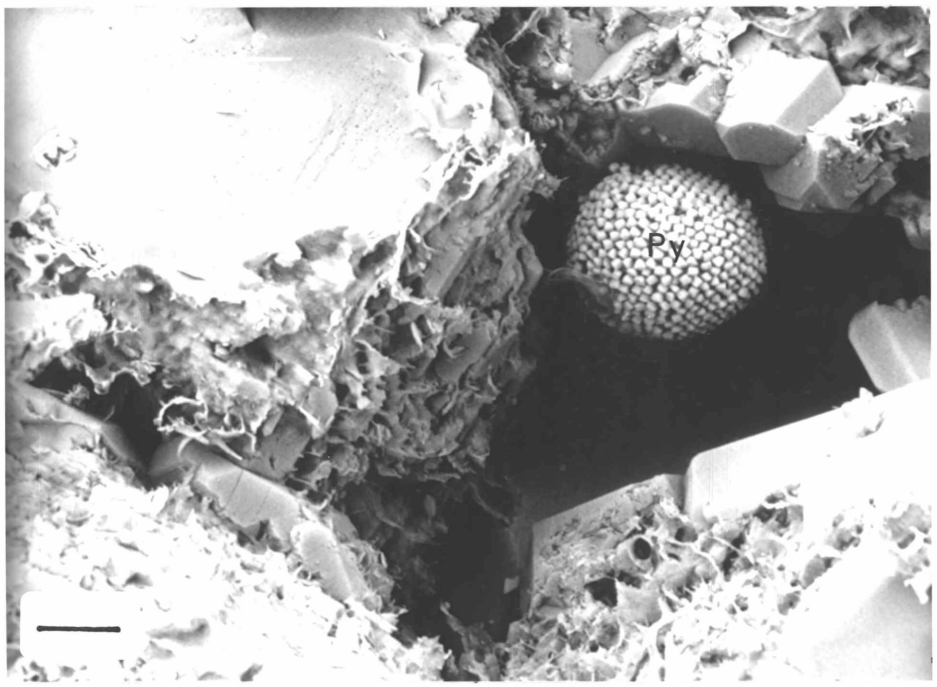


Plate 5-40 - SEM Photomicrograph of framboid pyrite (Py) pore-filling the pore space. Note that the framboid hangs onto the pore wall by means of an illitic membrane. Sample from Sotong 5G-5.1 at depth of 2188.1 m msl. Scale bar = 10 microns.

abundance in fine to very fine sandstones of Motif D, together with some calcite believed to have escaped dissolution, could well represent early stage pyrite, compatible with the observations made other workers (e.g. Curtis, 1978), and

2) As euhedrally octahedral pyrite crystals. These are individual crystals which settled on illite-covered pore walls (Plate 5-41). Edman et al (1984) and Market et al (1984) indicated that euhedral pyrites are last phase authigenic minerals.

The XRD results on the whole rock XRD samples show that pyrite is generally lacking in fine to coarse-grained sandstones of Motif A. However, at Seligi-3, up to 5 percent of the total rock consists of pyrite and, coincidently(?), this pyrite occurs with barytes (Table 5-1).

5.2.2.8 *Authigenic Barytes*

Authigenic barytes appears to occur only within fine to medium grained sandstones of Motif A. The XRD analyses show that it occurs with pyrite, and constitutes up to 4 percent of the total rock (Table 5-1). SEM microphotographs indicate that barytes overgrows framework feldspar (Plates 5-16 and 5-42). The timing of its development is very difficult to establish, but it could have formed after illite formation. Its growth on the framework feldspar appears to be interrupted by the occurrences of the whiskery illite aggregates. However, the relationship of barytes with pyrite in the sandstones at Seligi-3 is not very clear. It probably can be explained as follows either:

1) Barytes as a primary material which precipitated out in sulphate-

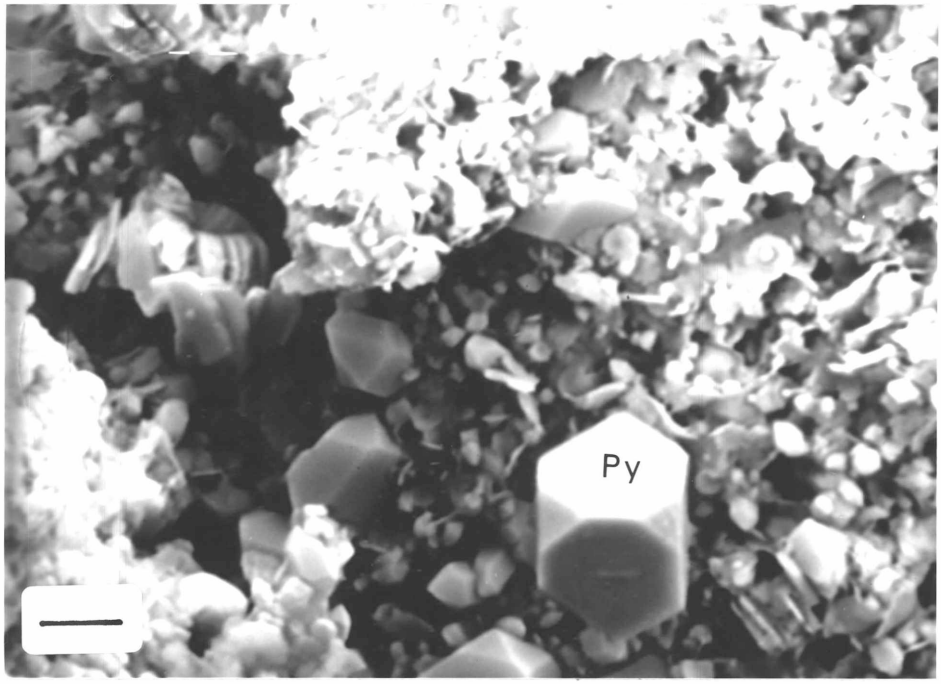


Plate 5-41 - SEM Photomicrograph of cubic pyrite (Py) pore-filling the pore space. Note that the cube rests on illite coated framework grain. Sample from Tapis-2 at depth of 2227.4 m msl. Scale bar = 3 microns.

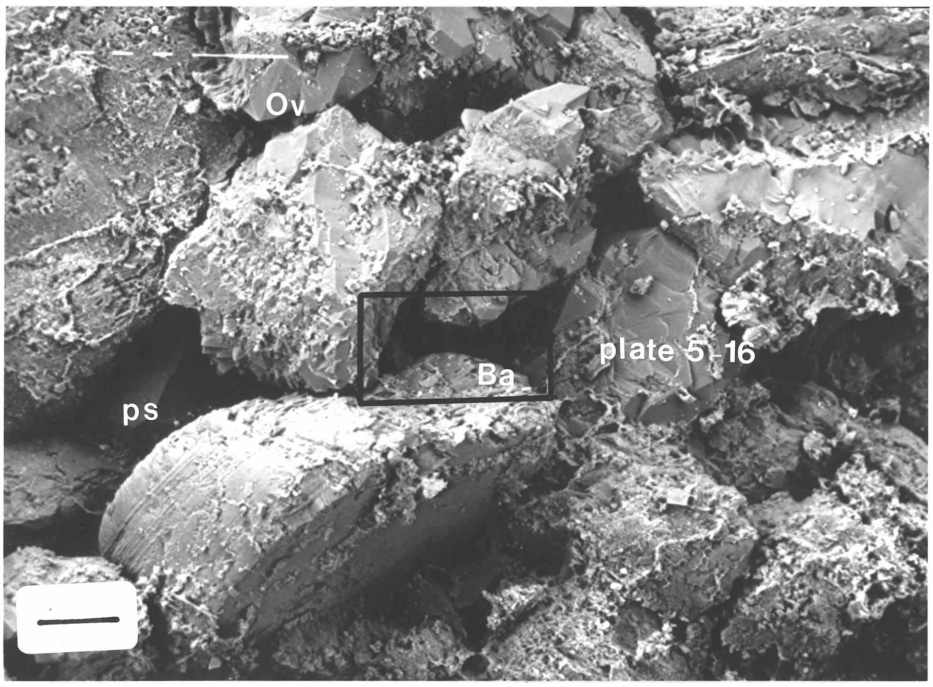


Plate 5-42 - SEM Photomicrograph showing development of overgrowths: barytes (Ba) and quartz (Ov). Note the primary connecting pores (ps) within this generally coarse-grained sandstone. (See also plate 5-16 for details of barytes overgrowth). Sample from Besar-1 at depth of 2106.1 m msl. Scale bar = 75 microns.

saturated pore waters, prior to redox reactions of kerogen, in which both Fe^{+3} and SO_4^{-2} ions were reduced to Fe^{2+} and S^{-2} ions respectively, and subsequently under high Eh-low pH conditions allowing pyrite to precipitate, or

2) Barytes as a newly introduced material during drilling.

5.2.2.9 *Authigenic Albite*

Authigenic albite is common in most sandstones, particularly in the very fine to medium grained sandstones (Table 5-1). It occurs in two forms:

1) As a replacement mineral or a by-product of albitization of framework plagioclase (Plate 5-10). The murky brown appearance in thin section (Plate 5-21), indicates the nature of plagioclase alteration, and on the SEM, this murky appearance represents illite (Plate 5-10), and

2) As overgrowths (Plates 5-11 and 5-43). The parallelism of the overgrowths on host framework plagioclase and the apparent texture of the host grain probably indicate that they are in optical continuity.

The XRD results show that plagioclase constitutes up to 6 percent of the total rock (Table 5-1). Compositionally, it consists entirely of albite, suggesting that the plagioclase in the sandstones is largely authigenic.

The different modes of albite occurrences in the sandstones probably relate to the ways in which albite was formed. Albite as an alteration

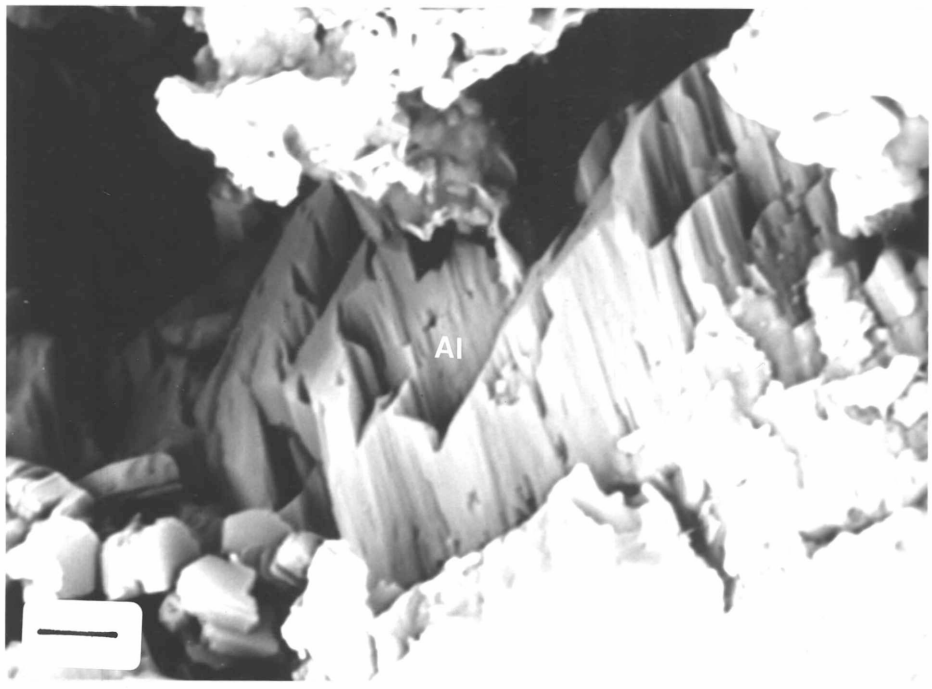


Plate 5-43 - SEM Photomicrograph of albite overgrowth (Al). Sample from Besar-1 at depth of 2106.1 m msl. Scale bar = 3 microns.

product of plagioclase is probably early formed, as compared with the late albite which occurs as overgrowths. The sequence of albitization may be similar to that observed by Helmold et al (1984), in Paleogene shales of Santa Ynez, California. They noticed that the disappearance of smectite in the mixed-layer smectite-illite corresponds to interval of albitization, and Boles (1982) suggested that albitization window ranges from 100° to 150°C.

5.3 *PARAGENETIC SEQUENCE*

A simplified diagenetic sequence of events and porosity evolution of the Pulai-II sandstones and their relationship to the hydrocarbon generation and entrapment, is illustrated in Figure 5-7. This sequence was developed from observations of the occurrences and relationships of the authigenic minerals with each other, and with the conditions of the pores and the framework grains. All features do not occur in all the samples. The common authigenic minerals are quartz, kaolinite, illite, smectite-illite, chlorite, ferroan-calcite, siderite, ankerite, calcite and albite, with the less common pyrite and barytes. The following chemical reactions have probably occurred within the sandstones, resulting in the formation and/or precipitation of the minerals (Kaiser, 1984):

1) $CaCO_3 + H^+ + Fe^{+2}$ = Ferroan calcite and/or Siderite + Ca^{+2}

2) $CaCO_3 + H^+ + Mg^{+2} + Fe^{+2}$ = Ankerite

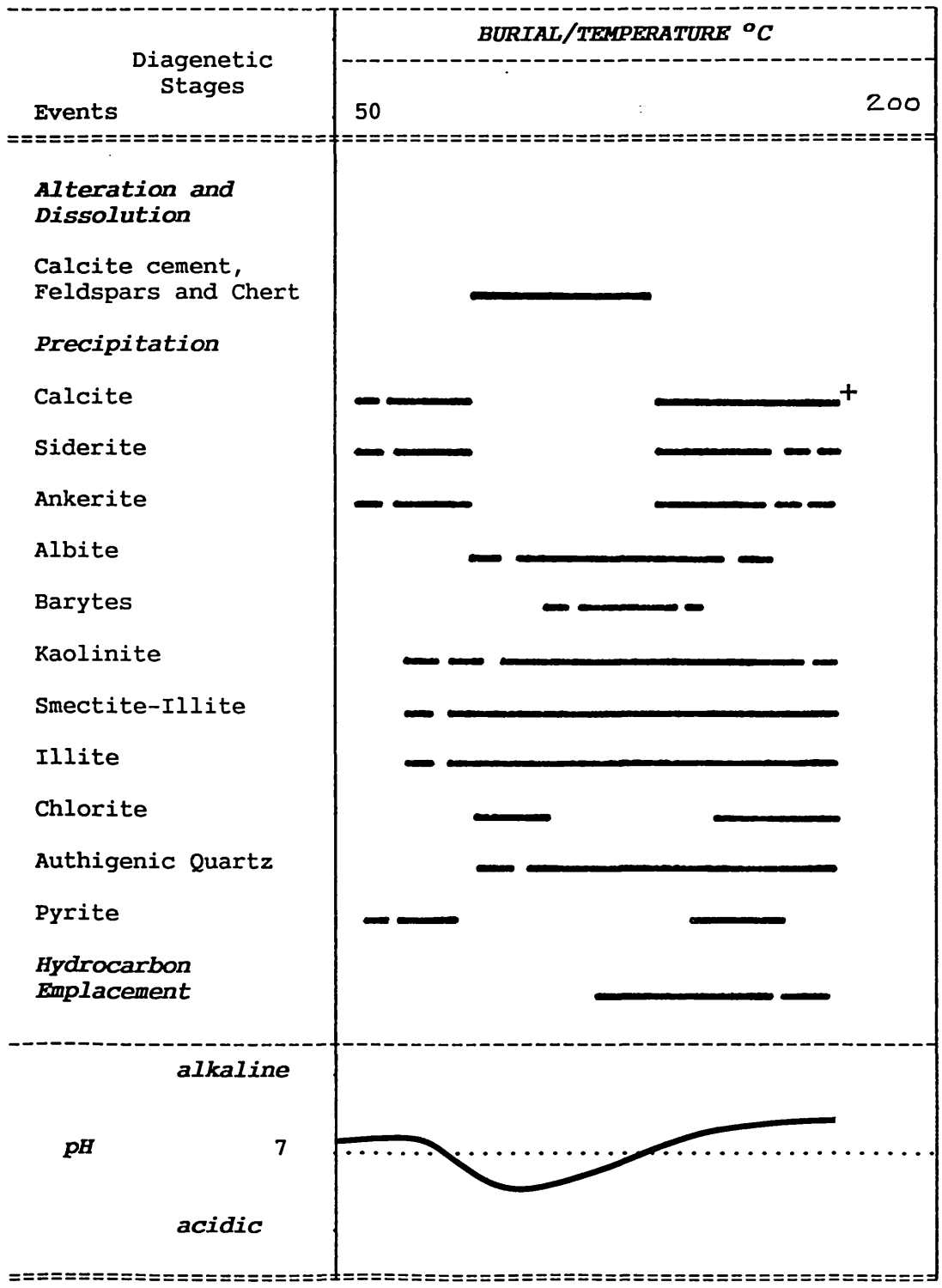
3) $Ba^{+2} + SO_4^{-2}$ = Barytes

4) Plagio + $H^+ + H_2O$ = Kaolinite + $Ca^{+2} + Na^{+1} + H_4SiO_4 + Al^{+3}$

5) Plagio + $Na^+ + H_4Sio_4$ = Albite + $Ca^{+2} + H_2O + Al^{+3}$

6) K-feld + $H^+ + H_2O$ = Kaolinite + $K^+ + H_4SiO_4 + Al^{+3}$

Figure 5-7 - Paragenetic Sequence of Diagenetic Events in Pulai-II Sandstones. Temperature inferred from Surdam et al, 1989.



\+ ferroan-calcite

7) Chert + H^+ + H_2O = H_4SiO_4

8) H_4SiO_4 = Quartz overgrowth + H_2O

9) Smectite + K^+ + Al^{+3} = Illite + Mg^{+2} + Fe^{+2} + Fe^{+3} + Ca^{+2} + H_4SiO_4 + Na^+ + H_2O

10) Fe^{+2} + Mg^{+2} + Al^{+3} + SiO_4^{-4} + H_2O = Chlorite

11) Fe^{+2} + HS^- = Pyrite

12) Ca^{+2} + Fe^{+2} + HCO_3^- = Ferroan-calcite

Many workers (Schmidt and McDonald, 1979, and Surdam et al , 1989, to mention a few) have stressed the importance of pore water pH in contributing to the destruction and generation of porosity. Accordingly, reactions 1) to 9) occur mostly under acidic pore water conditions, usually at pH between 4.0 and 6.0, both at shallow near surface and in subsurface environments at a temperature below 105°C; reactions 10) to 12) occur generally in subsurface under relatively more alkaline conditions (Schmidt and McDonald, 1979, Kaiser, 1984 and Surdam et al, 1989).

Acidity of pore waters is caused by dissolved carbon dioxide, carboxylic acids and phenols. In shallow, near surface conditions, acidity of pore waters is caused primarily by the dissolved carbon dioxide through surface run-off (Shanmugam, 1985); on the other hand, in subsurface, thermal and/or oxidative cracking of kerogen between 80° and 105°C generate carboxylic acids and phenols (Carothers et al, 1984), and these are dissolved in pore waters derived from shale compaction and smectite-illite transformation (Burst, 1969; Colten-Bradley, 1987). These organically-derived acids are accordingly unstable above 100°C (Surdam et al, 1984) (Fig. 5-8), and they undergo decarboxylation, a process of thermal destruction mostly of carboxylic acids to form

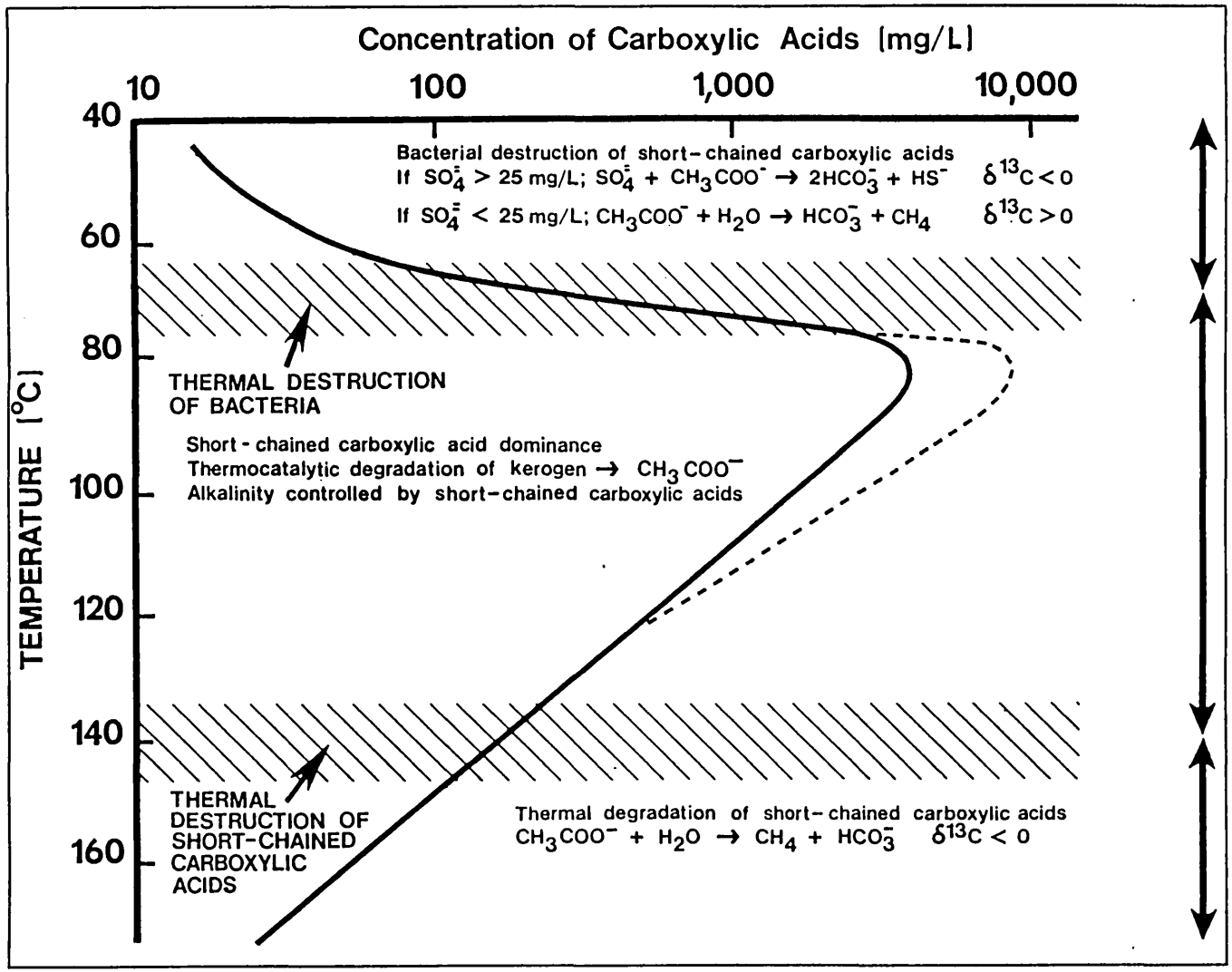


Figure 5-8 - Concentration of carboxylic acids in oil-field waters verses temperature (from Surdam, et al, 1989). The diagram shows the maximum concentration of carboxylic acids between 80° to 100°C.

methane and carbon dioxide (Carothers et al, 1984). Continued process of decarboxylation eventually results in a gradual increase in pore water alkalinity.

Under acidic conditions (near-surface and in subsurface prior to decarboxylation), both calcite cement and framework feldspar and lithic grains are unstable, and consequently undergo alteration and dissolution. Ions are released into solution. Some of the "released" ions, for example Al^{+3}, complex with organic acids and stay in solution (Surdam et al, 1989), but those not complexed combine to form and precipitate such minerals as siderite and/or ankerite, kaolinite, quartz, smectite-illite, albite, and barytes. With increasing depth of burial (and subsequently temperature), chlorite, ferroan-calcite and pyrite are precipitated, in addition to the formation and precipitation of more kaolinite, illite, and quartz overgrowth. These processes occurred in the Pulai-II sandstones, in the southern Malay basin.

5.4 *POROSITY*

The results of porosity analyses of the Pulai-II sandstones, based on petrographic examination of thin sections and geological log analysis for direct and indirect porosity measurement, and on the XRD and SEM analyses for the identification of minerals and pore characteristics, indicate that:

1) The porosity is predominantly intergranular, although intragranular pores are also common. The intergranular pores were differentiated into three groups:

   i) Intergranular pores between framework grains, evidently not

subsequently completely filled with cement (Plates 5-13, 5-42 and 5-44),

ii) Intergranular pores between corrugated framework grains, evidently generated as a result of cement dissolution (Plate 5-5), and

iii) Intergranular pores which evidently resulted from complete dissolution of unstable framework grains. These pores are oversized, and occasionally encased by a brownish material (Plates 5-9 and 5-45).

Similarly, two intragranular pore textures have been recognised:

i) Partial alteration and incomplete dissolution of framework grains (Plates 5-12, 5-13, 5-46), and

ii) Pore spaces created by framework grain fracturing (Plate 4-47); however these are uncommon.

2) The porosity varies widely, from 8 to 18 percent in relatively very fine to fine-grained sandstones and occasionally in fine to medium-grained sandstones, to more than 35 percent in apparently loose, medium to coarse-grained sandstones (Fig. 5-9). This porosity appears to be related to the total cement (carbonate and clay) content: higher cement content is found in the generally very fine to fine-grained sandstones than in medium to coarse-grained sandstones (Figs. 5-10 and 5-11), with:

i) relatively highest percentage of total carbonate minerals, 8-18 percent, within very fine to fine-grained sandstones, and lowest carbonate mineral content, 0-8 percent, within medium to

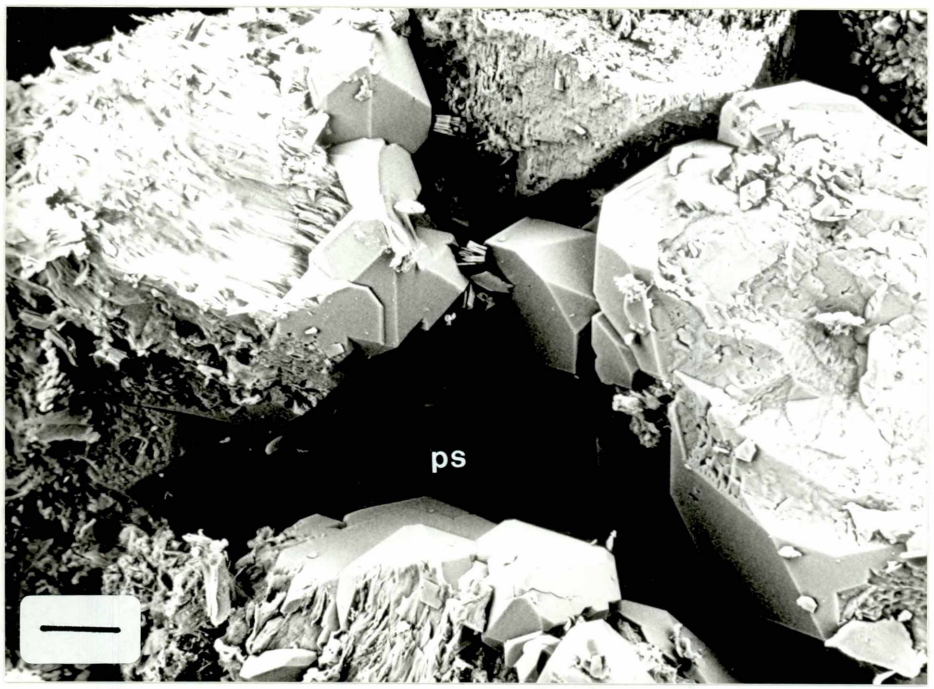


Plate 5-44 - SEM Photomicrograph showing intergranular, primary porosity (ps). Sample from Tapis-2 at depth of 2214.9 m msl. Scale bar = 30 microns.

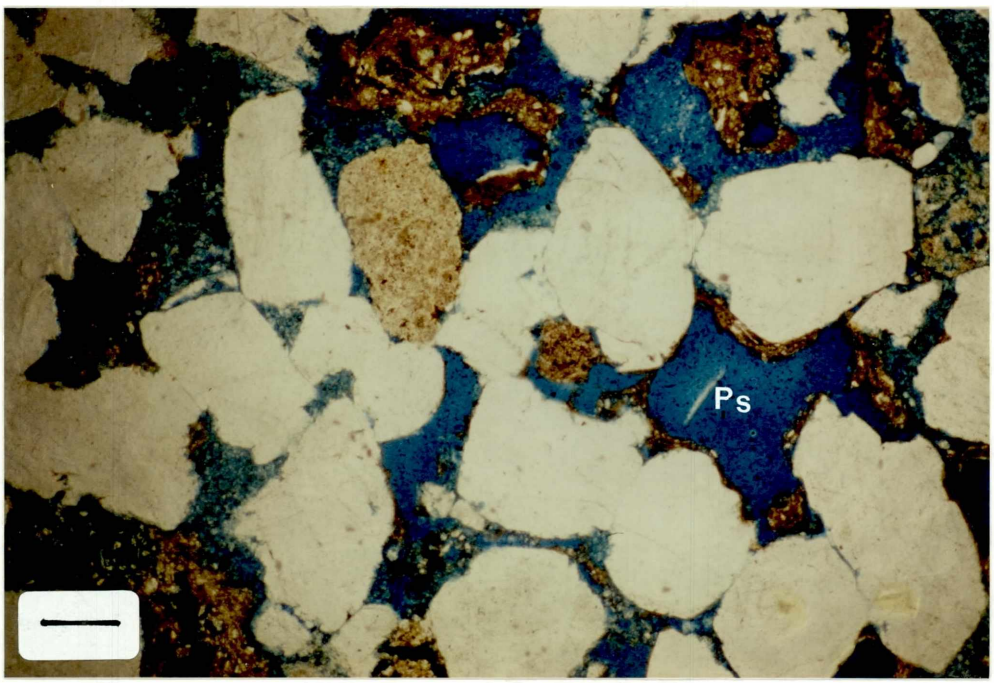


Plate 5-45 - Photomicrograph of thin section showing blue epoxy pores (Ps) caused by the dissolution of unstable framework grains. Sample from Seligi-3 at depth of 1589.0 m msl. Scale bar = 0.20 mm.

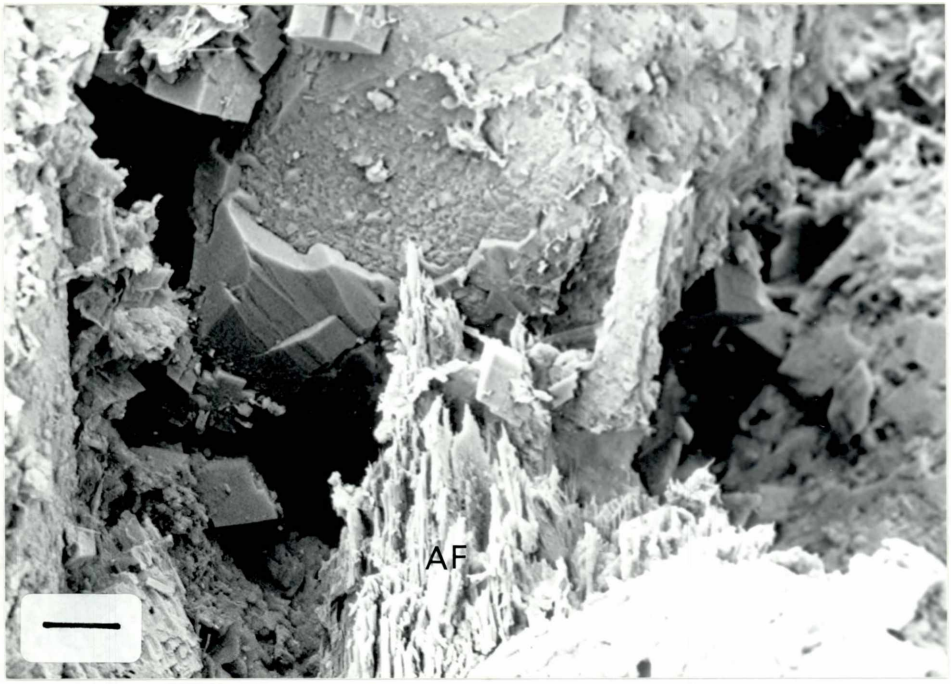


Plate 5-46 - SEM Photomicrograph showing additional porosity to the sandstone caused by partial dissolution of framework feldspar grain (AF). Note late phase siderite rhombs (Sd) on framework grain. Sample from Sotong 5G-5.1 at depth of 2188.1 m msl. Scale bar = 20 microns. (See also Plate 5-21 for comparison).

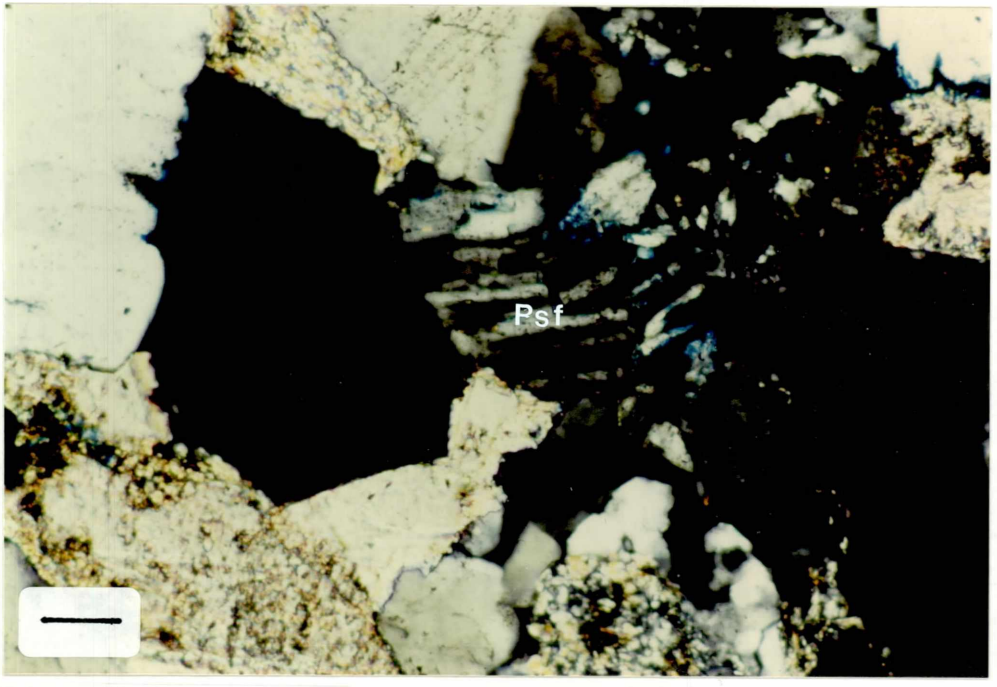


Plate 5-47 - Photomicrograph of thin section showing intragranular pores caused by grain fracturing (Psf). Note poor porosity resulting from compaction and cementation. Sample from Duyong 6H-32.1 at depth of 2370.1 m msl. Scale bar = 0.05 mm.

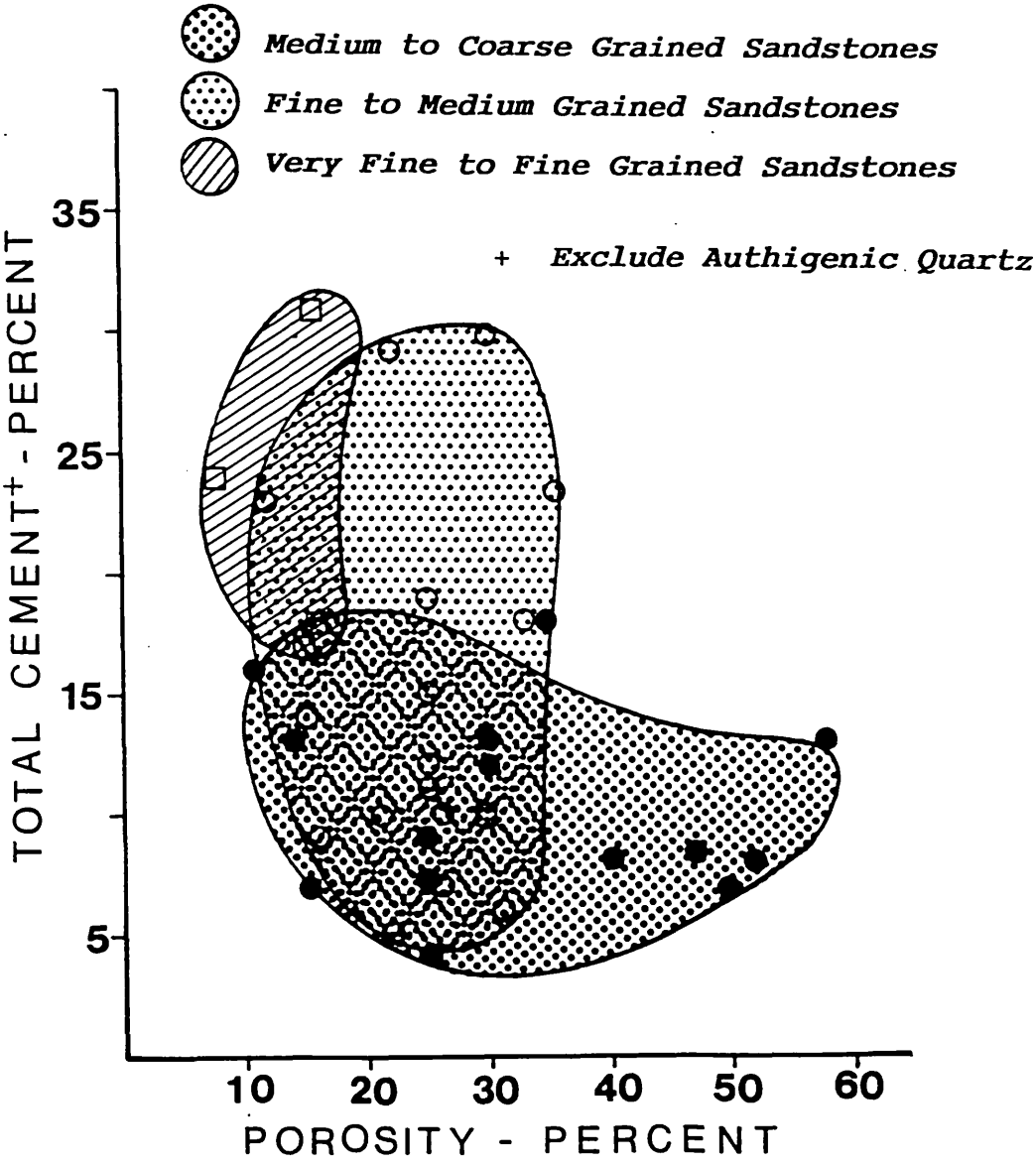


Figure 5-9 - An illustration showing relationship of total porosity with total cement (clay and calcite minerals). Note generally that the coarser is the sandstones, the higher is the porosity and the lower is the cement content.

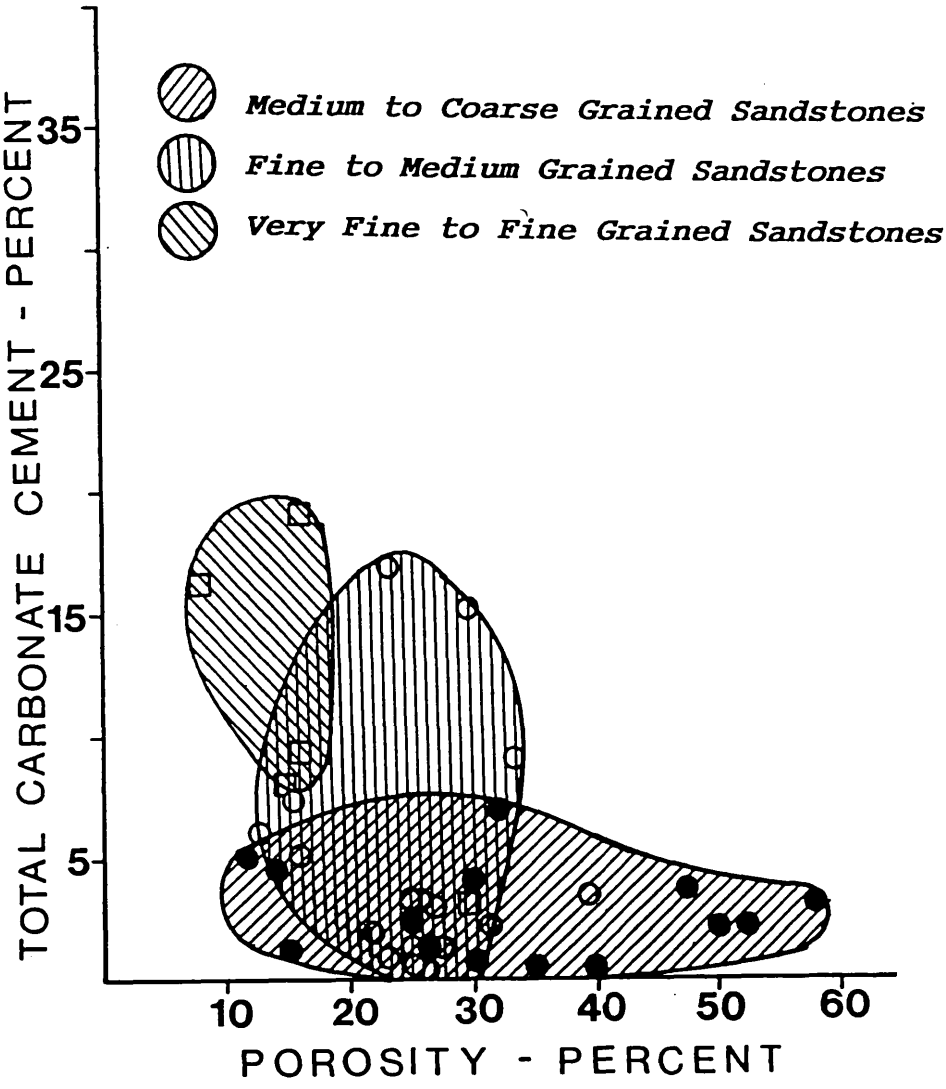


Figure 5-10 - An illustration showing relationship of total porosity with total carbonate minerals in sandstones of different grain sizes. Generally low carbonate cement content within coarser grained sandstones; but low porosity values and low carbonate content in some coarse grained sandstones probably due to compaction and also to cementation primarily by quartz overgrowth and clay minerals.

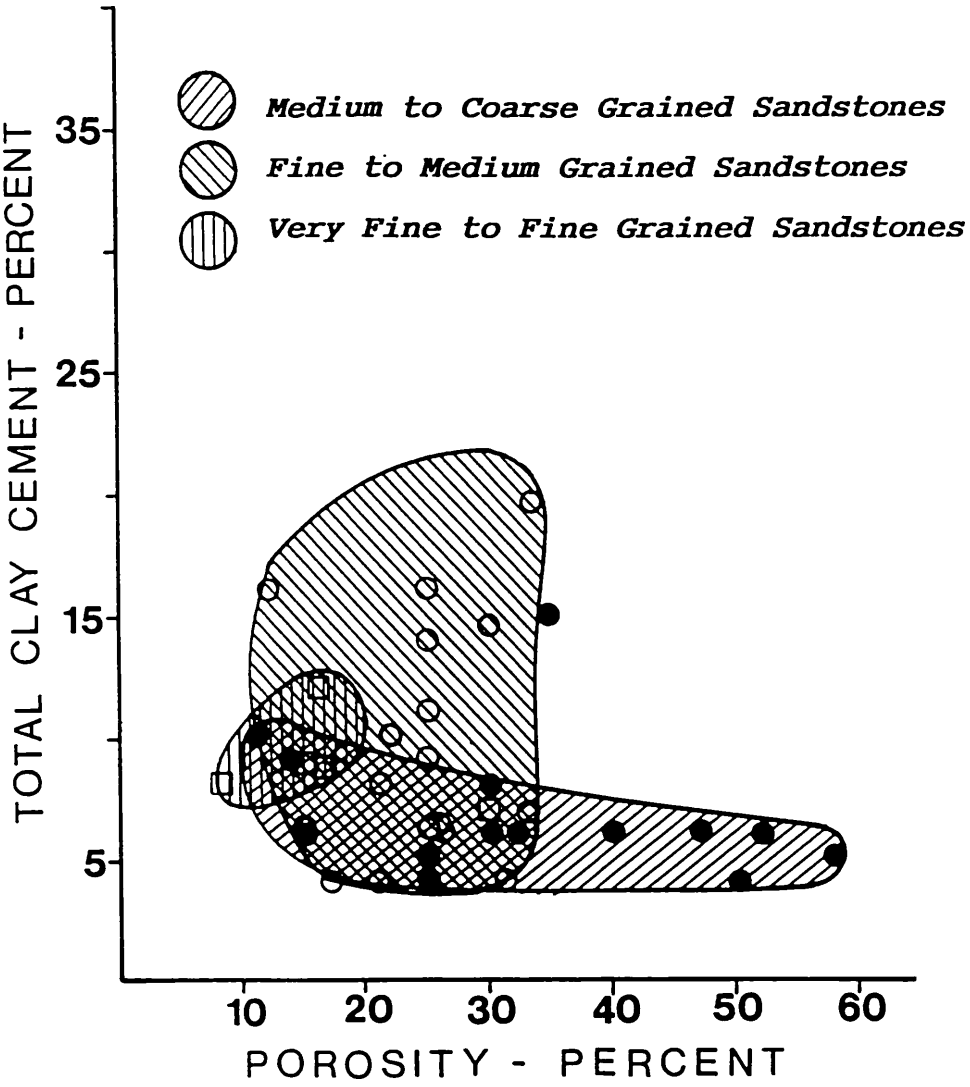


Figure 5-11 - An illustration showing relationship of total porosity with total clay minerals in sandstones of different grain sizes. The relationship of grain sizes with porosity and clay mineral content within the sandstones is not very clear, but generally lower total clay mineral content within coarser grained sandstones than in finer grained sandstones. Low porosity values and low clay mineral content in some coarse grained sandstones probably due to compaction and also to cementation primarily by quartz overgrowth and carbonate minerals.

coarse-grained sandstones (Tables 5-1 and 5-2 and Fig. 5-10), and

ii) generally higher total clay mineral content in very fine to medium grained sandstones than in medium to coarser grained sandstones (Tables 5-1 and 5-2 and Fig. 5-11). Kaolinite appears to be relatively more abundant than smectite-illite in fine to medium-grained sandstones with porosity of 10 to 35 percent, and in medium to coarse-grained sandstones with porosity ranging from 10 to more than 50 percent (Figs. 5-12 and 5-13).

3) Porosity generally decreases exponentially with depth (Fig. 5-14). A porosity greater than 30 percent occurs generally shallower than 2000 metres, and a porosity of less than 15 percent in some sandstones deeper than 2200 metres. If it is assumed that the "eyeball" best fit porosity deterioration trend, obtained by averaging porosity values in the sandstones which have S_w greater than 60 percent, represents a normal porosity destruction trend in the Pulai-II sandstones for the study area, then a sandstone porosity of 15 percent would be reached at a depth of about 2700 metres (Fig. 5-14). (A 15-percentage porosity cut-off is normally used by PETRONAS as the lower porosity limit for oil exploitation in the Malay basin). Consequently, it would probably be reasonable to suggest that deviations to the right of the normal porosity destruction trend represent sandstones having enhanced or secondary porosity, whilst deviations to the left of the line represent the sandstones undergoing early cementation.

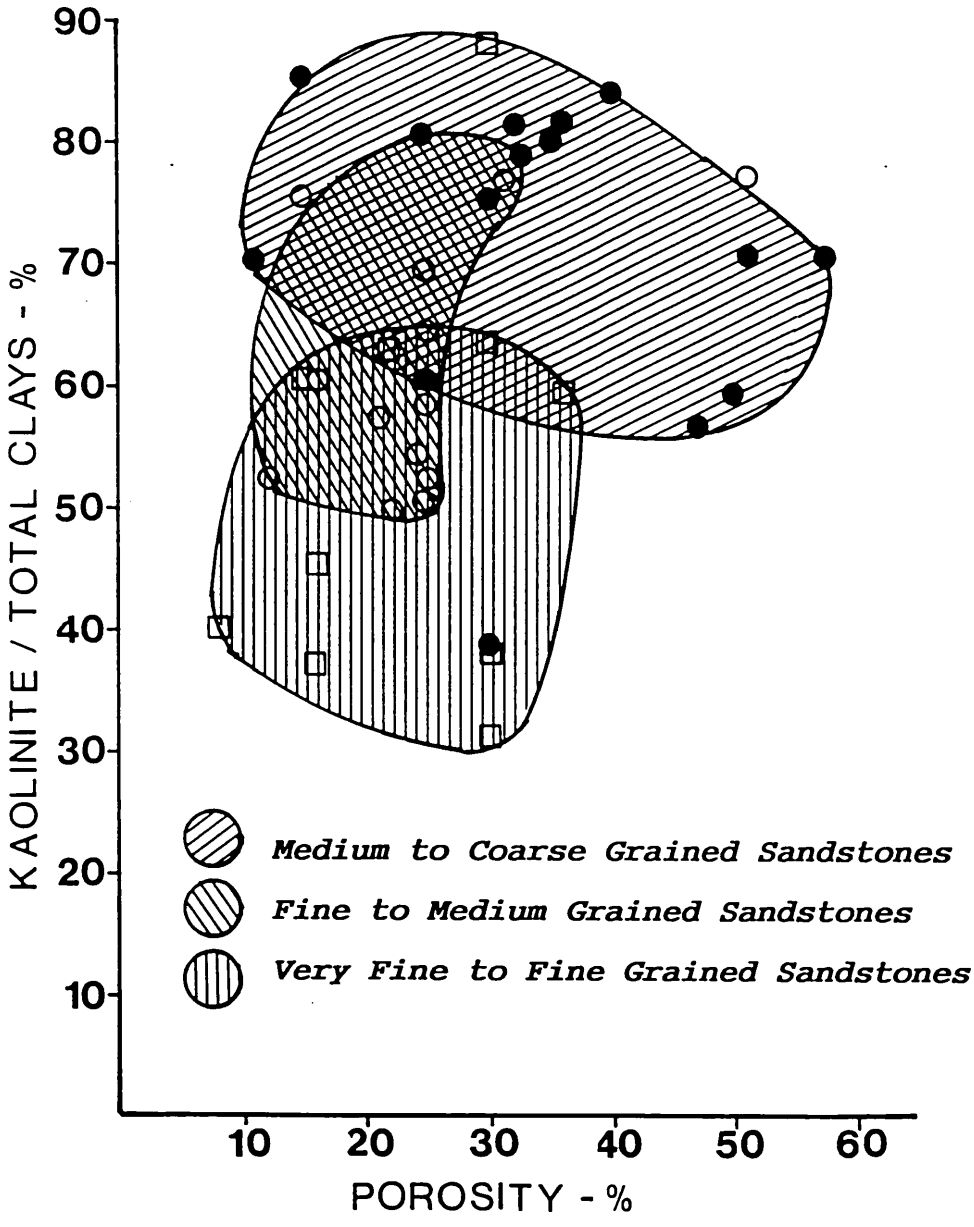


Figure 5-12 - An illustration showing relationship of total porosity with kaolinite/total clay minerals in sandstones of different grain-sizes. Coarser-grained sandstones generally have higher kaolinite/total clays ratios and relatively better porosities than the finer grained sandstones.

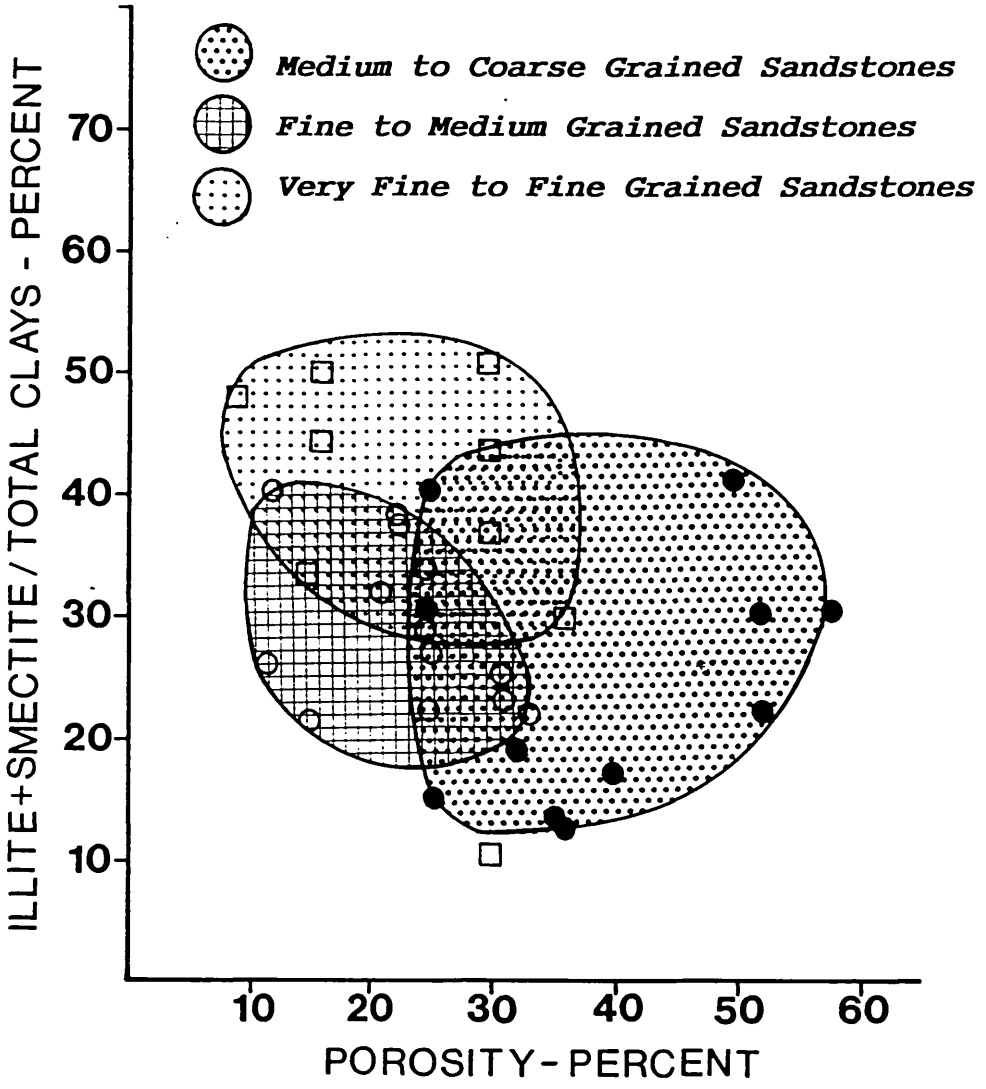


Figure 5-13 - An illustration showing relationship of total porosity with smectite-illite/total clay minerals in sandstones of different grain sizes. Smectite-illite are found in most samples, but relatively higher smectite-illite/total clay rations in finer grained sandstones than in coarser-grained sandstones.

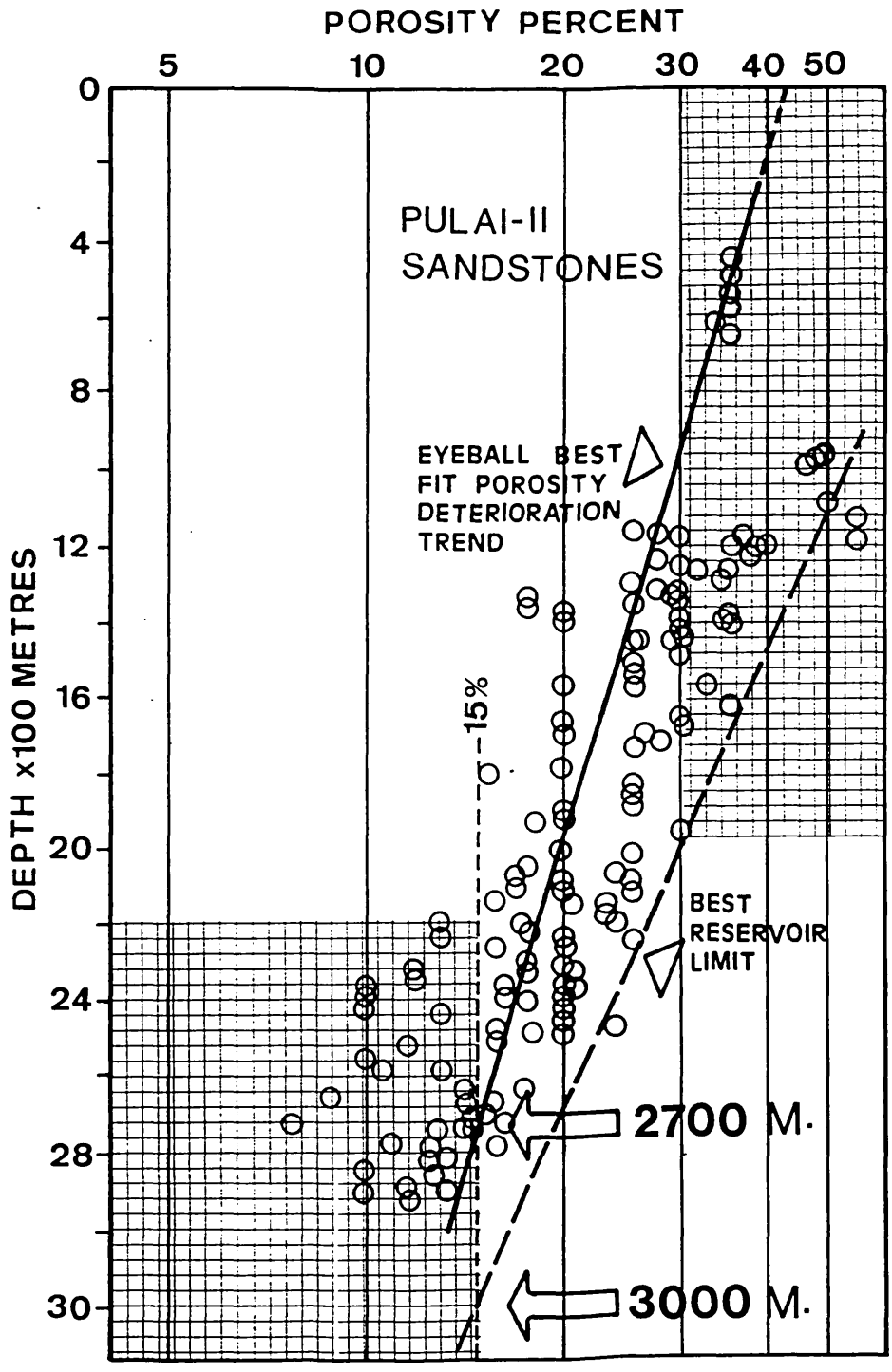


Figure 5-14 - Average porosity-depth trend in the Pulai-II sandstones. Porosity of more than 30 percent is found in sandstones buried at depths shallower than 2000 m, and less than 15 percent at depth deeper than 2200 m. Normally compacted sandstones would not have porosities greater than 15 percent below 2700m. In over-pressured reservoirs, this porosity is maintained upto a depth of 3000m.

4) The authigenic materials which were precipitated in pores and pore throats are primarily authigenic quartz and clay and carbonate minerals, with as much as 29 percent of estimated clay and carbonate minerals present in the sandstones (Table 5-1 and Fig. 5-9). The relative amount of authigenic quartz in the sandstones is difficult to assess but, based on the XRD results, is probably substantial, because in most of the analysed samples total quartz is more than 75 percent of the total composition (Table 5-1). This is generally higher than the amount of quartz petrographically estimated, which averages about 50 percent (see Section 5.2).

5.5 *POROSITY DISTRIBUTION*

In this study, the following porosity definitions were used:

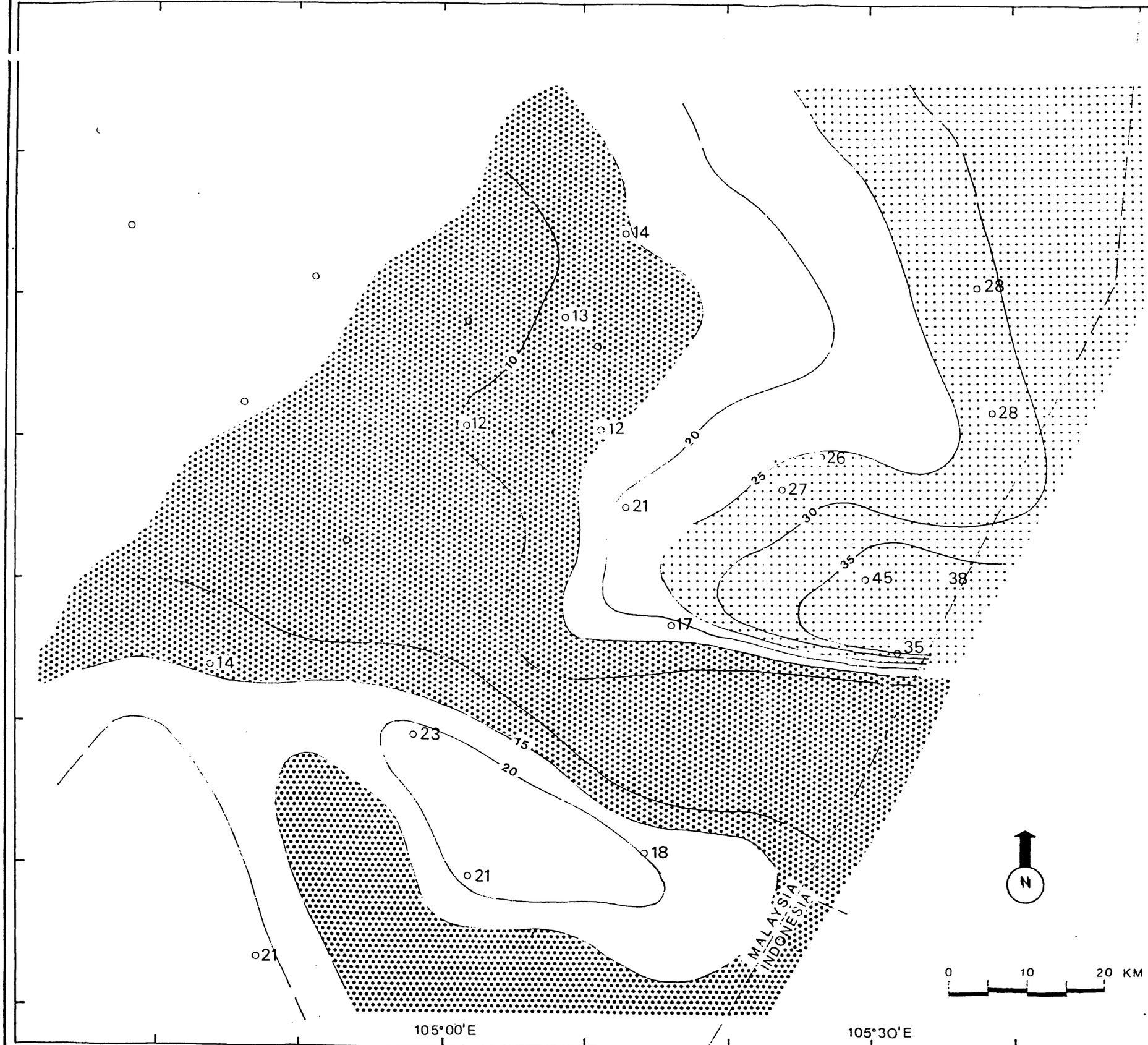
1) Poor reservoir quality - less than 15 percent,

2) Fair to good quality - between 15 to 25 percent, and

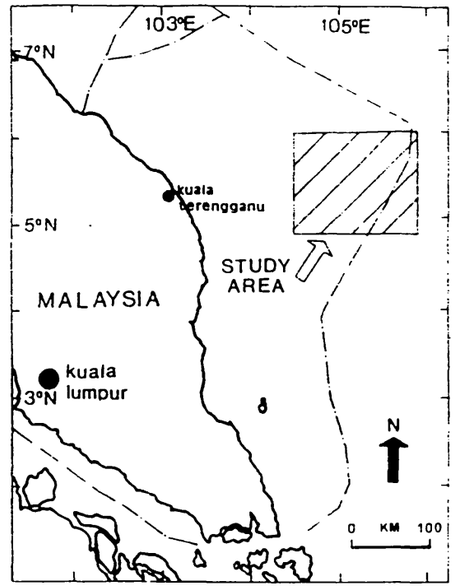
3) Good to excellent quality - greater than 25 percent.

The objective of this simplified classification was to isolate areas having a porosity of less than 15 percent where, under the current circumstances, any hydrocarbon discovery in the areas would not be likely to receive immediate attention for development.

Distribution of average total porosity within the Pulai-II sandstones is shown in Figure 5-15. Generally, there are two regions in the study area where porosity of the sandstones is better than fair to good: the east and northeast and the south and southwestern regions. A zone of poor porosity, some 15 to 30 km in width, separates the two



LOCATION MAP



LEGEND

Less than 15 percent.

15 - 25 percent.

Greater than 25 percent.

o 25 -- control point.

C. I. = 5 percent

FIGURE 5-15

Average Porosity Distribution Map, Pulai-II Sandstones, Southern Malay Basin.

regions. The occurrence of poor porosity sandstones to the south of the Besar-Duyong trend is somewhat interpretive, and was deduced from the extrapolation of the structural map (Fig. 2-5), and the porosity-depth plot (Fig. 5-14).

5.5.1 East and Northeastern Region

The sandstones with fair to excellent porosity occur in area covering Bekok, Ledang, Seligi, Tinggi, Pulai, Belumut, Belanga and Peta: porosity of about 20 percent occurs at Bekok and greater than 45 percent in some sandstones at Pulai (Table 5-3, Fig. 5-15). Much of this porosity is intergranular of primary and secondary origins. Based on porosity-depth plots of some wells in the region (Fig. 5-16), it would appear that between 10-40 percent of the total porosity in the sandstones is of secondary origin.

Porosity appears to deteriorate very rapidly to the west and south of the region (Fig. 5-15). A sharp porosity break in the south of the region relates to an abrupt sandstone discontinuity caused by a major east-west trending fault with a throw exceeding 1500 metres (Figs. 2-5 and 4-5 Section D-D'). To west of this region, the sandstones occur at much greater depths (Fig. 2-5, Table 5-3), and generally the porosity is much reduced. Thin section photomicrographs show that these substantially low porosity values are caused by compaction and cementation (see Section 5.6).

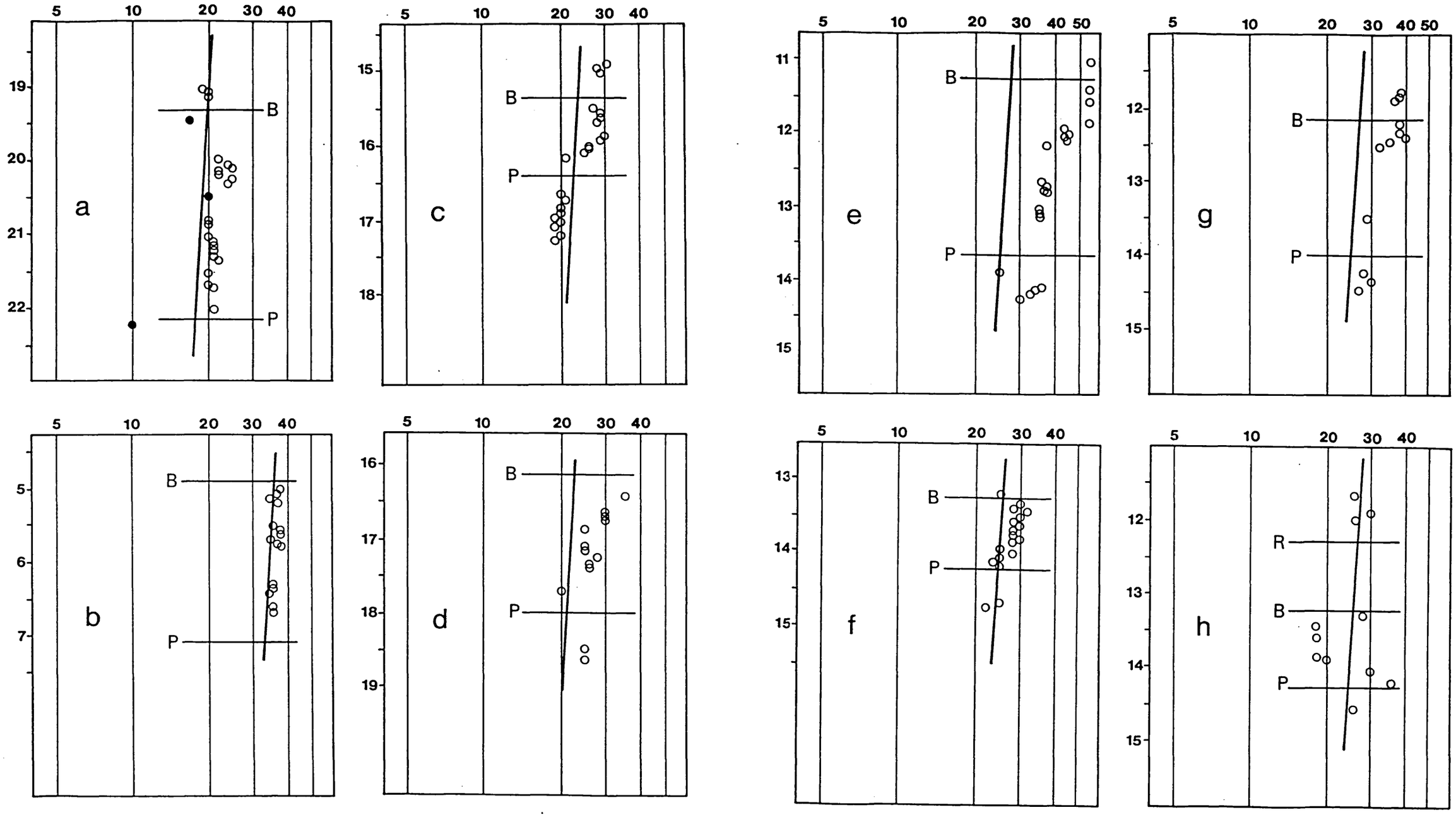


Figure 5-16 - Porosity-depth trend in Motif A sandstones at a) Bekok-1, b) Ledang-1, c) Seligi-3, d) Tinggi-1, e) Pulai-1, f) Belumut-1, g) Belanga-1 and h) Peta-1. Note that except in h), most porosity-depth points are to the right of the normally compacted trend-line, suggesting that much of these sandstones have secondary porosity. Circles indicate values taken within sandstones usually greater than 10 metres in thickness (see Fig. 3-14).

Table 5-3 - Computed porosity of Pulai-II sandstones at eighteen well locations. Depth in metres m.s.l.

Well Name	Depth Range metres	Porosity Range (Average) Percent
Bekok-1	1860 - 2260	20 - 25 (21)
Pulai-1	1090 - 1340	30 - 52 (45)
Seligi-3	1460 - 1770	15 - 30 (27)
Tinggi-1	1580 - 1800	18 - 35 (26)
Ledang-1	0430 - 0720	32 - 36 (35)
Belanga-1	1160 - 1400	20 - 39 (38)
Belumut-1	1220 - 1430	20 - 35 (28)
Peta-1	1280 - 1480	18 - 35 (28)
Banggol-1	2620 - 2780	11 - 18 (14)
Palas-1	2560 - 2960	10 - 18 (13)
Tiong-5	2200 - 2480	10 - 20 (12)
Tapis-2	2050 - 2250	12
Ophir-1	1950 - 2240	15 - 30 (17)
Besar-1	2010 - 2290	20 - 24 (23)
Angsi-1	2380 - 2640	12 - 20 (14)
Sotong 5G5.1	2230 - 2350	14 - 22 (21)
Duyong 6H32.1	2134 - 2330	13 - 19 (18)
Dy. Barat-1	2390 - 2590	7 - 22 (21)

5.5.2 South and Southwestern Region

Porosity within the sandstones in area covering Angsi, Besar, Duyong, Duyong Barat and Sotong, varies with facies and diagenesis. A porosity range of 7 to 27 percent is found generally in thin sandstone beds (less than 10 metres in thickness), and a range of 14 to 24 percent in thicker channel sandstones (Fig. 5-17). Much of the porosity is intergranular. Any porosity loss appears to be due to compaction and cementation mainly by quartz overgrowth and ferroan-calcite cementation (see Section 5.6).

Except at Sotong, most of the sandstones in the south and southwestern area are overpressured (Table 5-4), and most of the

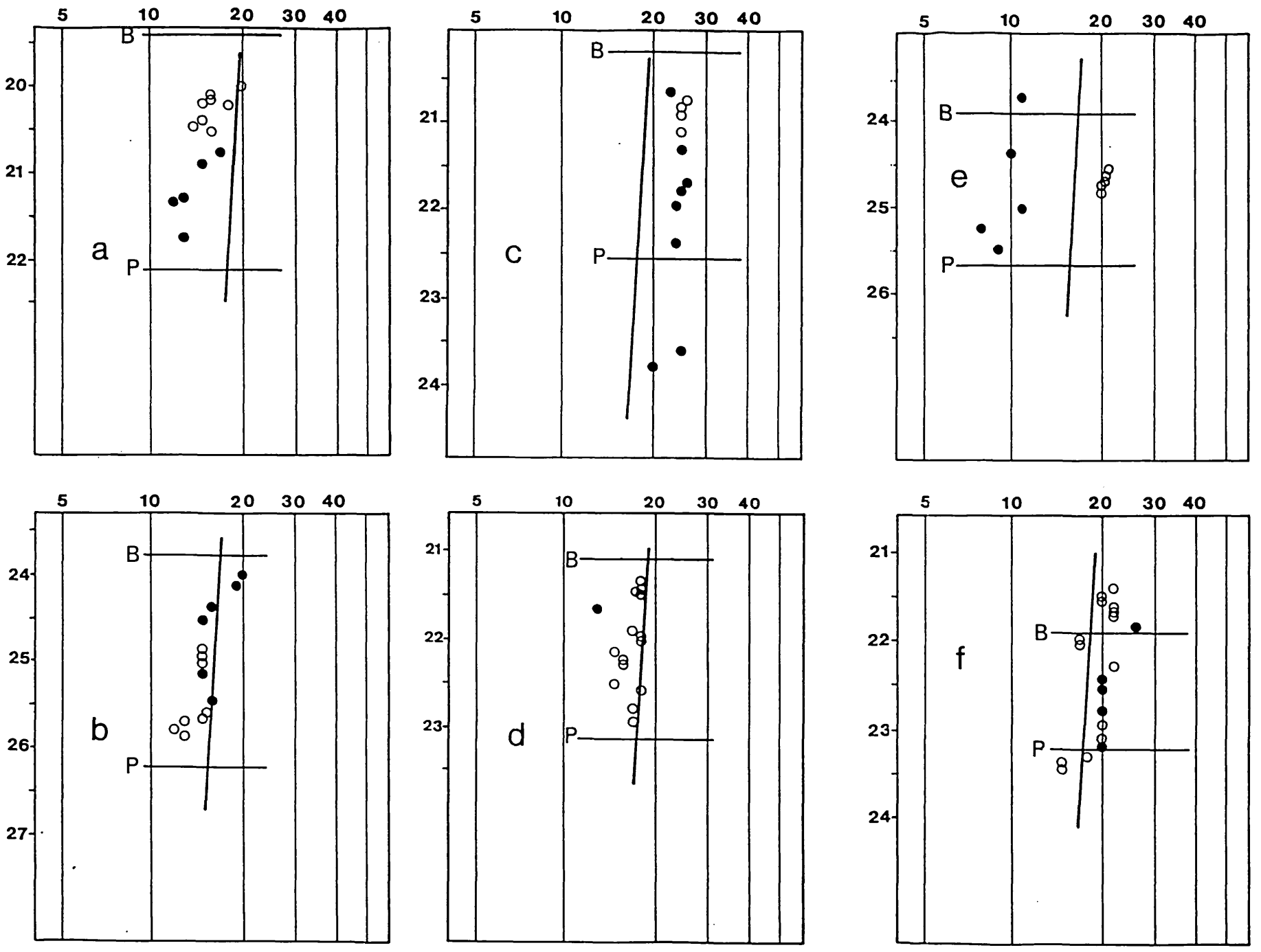


Figure 5-17 - Porosity-depth relationship in Motif D sandstones at a) Ophir-1, b) Angsi-1, c) Besar-1, d) Duyong Barat-1, e) Duyong Barat-1 and f) Sotong 5G-5.1. Note that except in c), e) and f), most porosity-depth points are to the left of the normally compacted trend-line, and these sandstones have porosities less than 20 percent. Compaction and cementation are the causes of porosity reduction. Good porosity occurrences in some sandstones relate to hydrocarbon occurrences, and usually these are over-pressured. Circles indicate values taken within sandstones greater than 10 metres thick, and dots indicate values within sandstones normally less than 10 metres thick (see Fig. 3-14).

overpressured sandstones have fair to good porosity. Hydrocarbons have been found within some of them (e.g. some channel sandstones at Sotong, Besar and Duyong Barat). Where no hydrocarbons were found, for example in channel sandstones at Duyong 6H-32.1, porosity is usually poor. The association of fair to good porosity sandstones in the vicinity of generally poor porosity sandstones, Figure 5-15, appears to imply, among others, that the emplacement of hydrocarbons in the sandstones inhibited cementation, and subsequently porosity reduction.

Table 5-4 - Average pressures: (final shut-in pressure (FSIP) and hydrostatic pressure (HP) and temperature in Pulai-II sandstones.

Well Name	Depth Range in metres	FSIP in p.s.i.*	HP	Ave. Temp. Deg. C
Angsi-1	2384-2625	4500	3750	152
Besar-1	2015-2266	5200	3260	133
Dy. Barat-1	2398-2566	?	3800	116
Duyong 6H-32.1	2088-2302	5530	3460	133
Sotong 5G-5.1	2277-2311	3200++	3460	138
Ophir-1	1937-2220	4530	3200	116
Ledang-1	0480-0699	1000	1000	046
Pulai-1	1129-1356	2200	1860	064
Bekok-1	1922-2230	4270	3200	122
Tapis-2	2048-2378**	5330	3400	120?
Seligi-3	1506-1762	3100	2460	099
Tinggi-1	1586-1787	2900	2600	101
Tiong-5	2263-2581**	4330	3660	138
Palas-3	2606-2909+	4600	4140	147+
Palas-1	2617-2928	-	-	-
Banggol-1	2690-2866**	4460	4200	140
Belanga-1	1199-1341	2130	2000	072
Belumut-1	1308-1430	2340	2000	076
Peta-1	1308-1414	2200	2100	065

* current industry standard
++ initial shut-in pressure (ISIP)
** estimated base limit of reservoirs
\+ projected value
? value questionable
\- no data

5.6 *POROSITY DESTRUCTION*

Sediment compaction and cementation are probably the main causes for the destruction of porosity in the Pulai-II sandstones.

5.6.1 Compaction

Both primary and secondary porosity show a destruction trend with increasing overburden (depth) (Fig. 5-14). By extrapolating porosity trend within the best reservoir limit downwards, a porosity of 15 percent would be reached at a depth of about 3000 metres, which is about 300 metres below the depth at which, under present-day circumstances, the sandstones would have attained the porosity had it undergone a normal compaction burial. However, porosities between 10-13 percent, were recorded at depths of 2150-2250 metres at Tapis-2 and 2250-2450 metres at Tiong-5 (Fig. 5-18). One possible explanation for the occurrence of low porosity values at depths shallower than predicted is that the depths at which these sandstones were encountered are not the maximum depths to which they had originally been buried.

Analyses of maximum depth of burial for the Pulai-II Formation indicate that the sandstones at many well locations in the study area appeared to have been buried to depths much greater than at the present-day (Table 5-5), and the maximum depths to which the sandstones at Tapis-2 and Tiong-5 had been buried, have been extrapolated to be 2950 and 2650 metres respectively, some 400 to 800 metres deeper than today (Figs. 5-19 to 5-21). Based on average geothermal gradient, which is 3.80 °C per 100 metres for the study area (Figs. 3-24 and 5-22), the sandstones at Tapis-2 and Tiong-5 had most likely been subjected to a temperature window of 125°-135°C. The sutured framework quartz

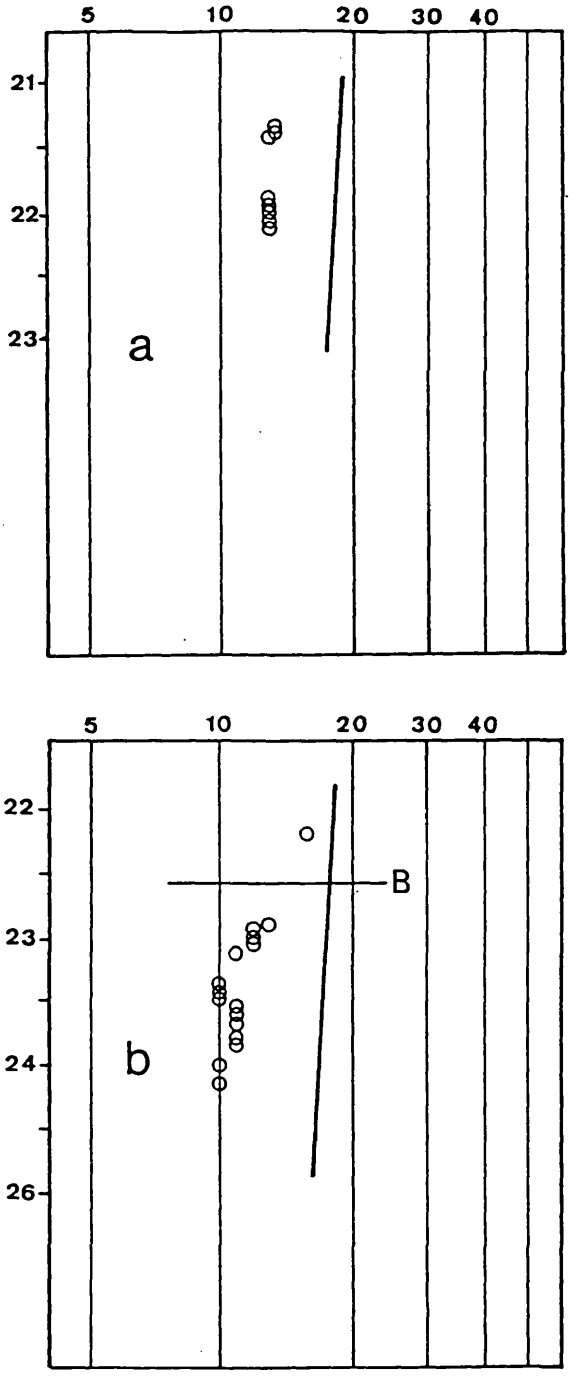


Figure 5-18 - Porosity-depth relationship in the Pulai-II sandstones at a) Tapis -2 and b) Tiong-5. Note that most porosity-depth points are to the left of the normally compacted trend-line. These sandstones have porosities less than 15 percent. Circles indicate values taken within sandstones greater than 10 metres thick (see Fig. 3-14).

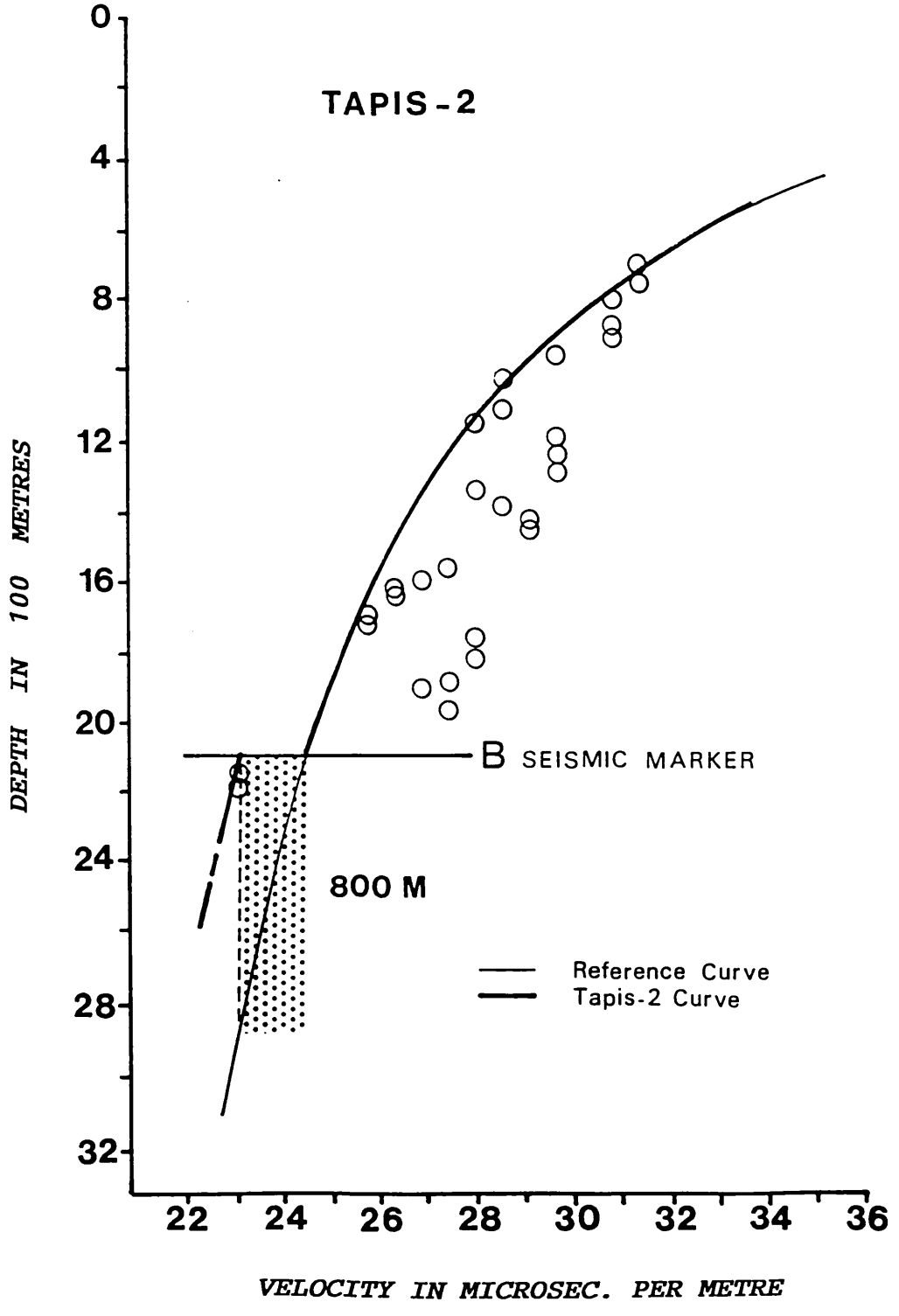


Figure 5-19 - Depth-velocity plot at Tapis-2. Tapis curve is compared with Banggol curve (see Fig. 3-25). Note that section above B-seismic marker was never buried relatively deeper than its present depth. Some 800 m of the section below the marker was eroded, and that section below B was buried at least 800 m below its present depth.

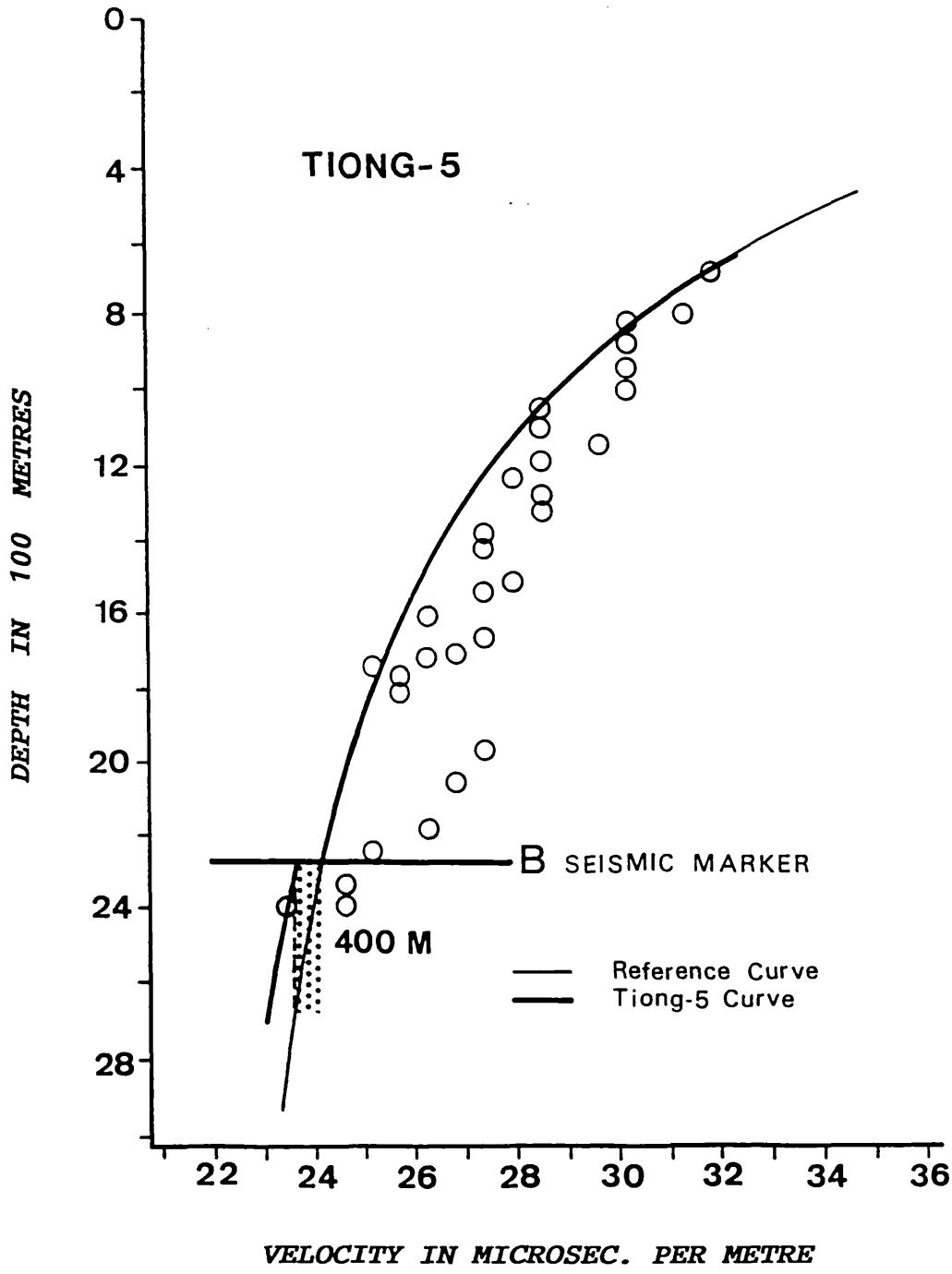


Figure 5-20 - Depth-velocity plot of Tiong-5. Tiong curve is compared with Banggol curve (see Figure 3-25). Note that section above B-seismic marker was never buried relatively deeper than its present depth. Some 400 m of the section below the marker was eroded, and that section below B was buried at least 400 m below its present depth.

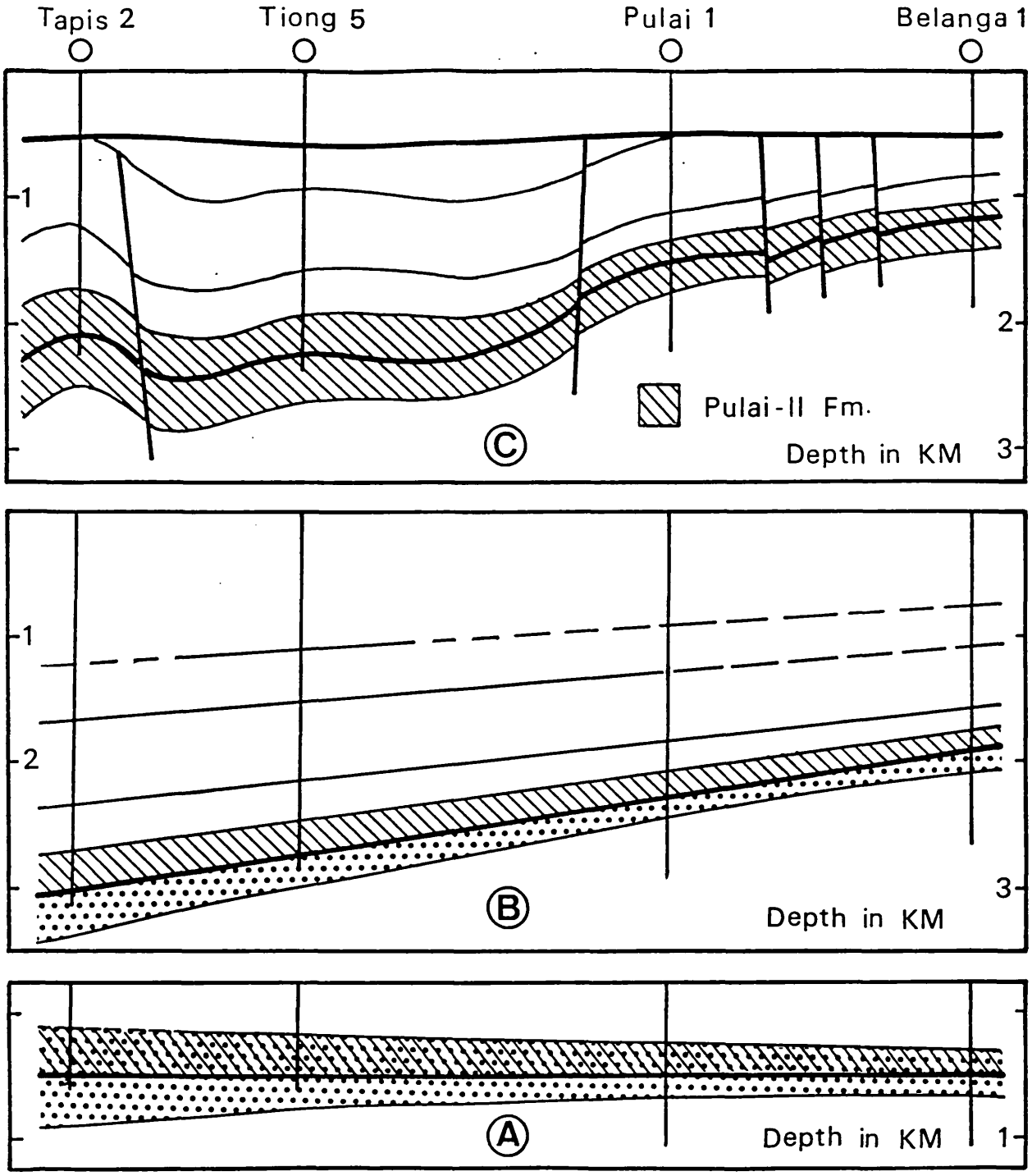
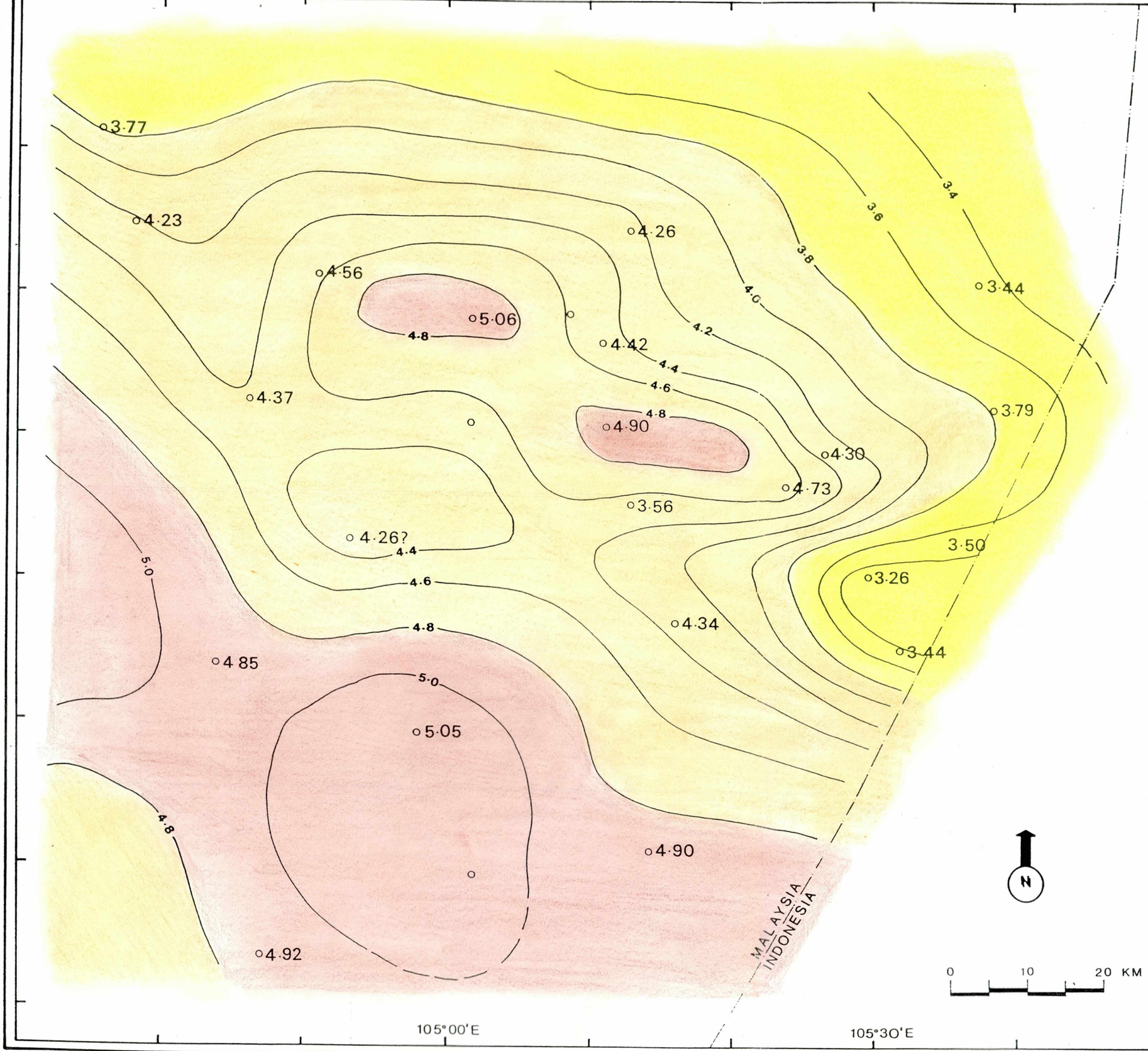
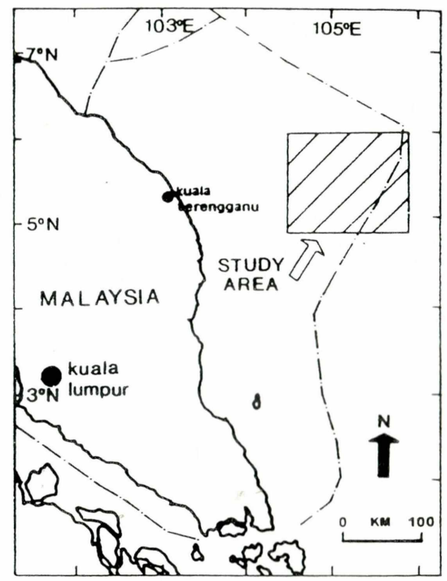


Figure 5-21 - Schmetic cross-section through Tapis-2, Tiong-5, Pulai-1 and Belanga-1 illustrating present-day and palaeo settings and the relative amounts of overburden removed during late Late Oligocene to Early Miocene and Late Miocene. A- shows initial thickness of the Pulai sandstone sequence prior to erosion in late Late Oligocene-Early Miocene (Table 5-5 indicated estimated amounts eroded). B- Deposition of the Terengganu Shale sequence and the subsequent sedimentation and burial. It shows maximum depths of burial at each location. C- Present-day setting showing structures related to Late Miocene-Pliocene tectonics.



LOCATION MAP



LEGEND

Less than 3.80°C per 100 metres.

3.80°C - 4.80°C per 100 metres.

Greater than 4.80°C per 100 metres.

o 3.45 -- control point

C. I. = 0.20°C/100 m

FIGURE 5-22

Geothermal Gradient Map, Southern Malay Basin.

Table 5-5 - Estimated maximum depths of burial of Pulai-II sandstones at each well location. Measurement in metres m.s.l.

WELL NAME	TOP OF B MARKER	ESTIMATED LOSS +50	RESTORED DEPTH
Banggol-1	2690	reference well	
Angsi-1	2384	0	2384
Besar-1	2015	op	2015?
Dy. Barat-1	2398	op	2398?
Duyong 6H-32.1	2088	op	2088?
Sotong 5G-5.1	2277	op	2277?
Ophir-1	1937	400	2337
Pulai-1	1129	300	1429
Ledang-1	480	400	880
Belanga-1	1199	250	1449
Tinggi-1	1586	300	1886
Seligi-3	1508	300	1808
Belumut-1	1308	150	1458
Bekok-1	1922	150	2072
Tiong-5	2263	400	2663
Tapis-2	2048	800	2848
Palas-1	2617	100	2717

op = overpressured

boundaries observed in some sandstones of the formation probably explain the combined effects of burial (compaction) and subsequent temperature which led to porosity destruction.

5.6.2 Cementation

Authigenic quartz and ferroan-calcite are the major cementing minerals. Extensive occurrence of these minerals in some sandstones which have porosities of less than 15 percent, and which are presently buried deeper than 2200 metres, suggests that these sandstones have been subjected to a temperature greater than 105°C and probably not exceeding 140°C (Fig. 5-23 and Table 5-4). According to Surdam et al (1989) (Fig. 5-8), a temperature range of 110°-140°C places the Pulai-II sandstones

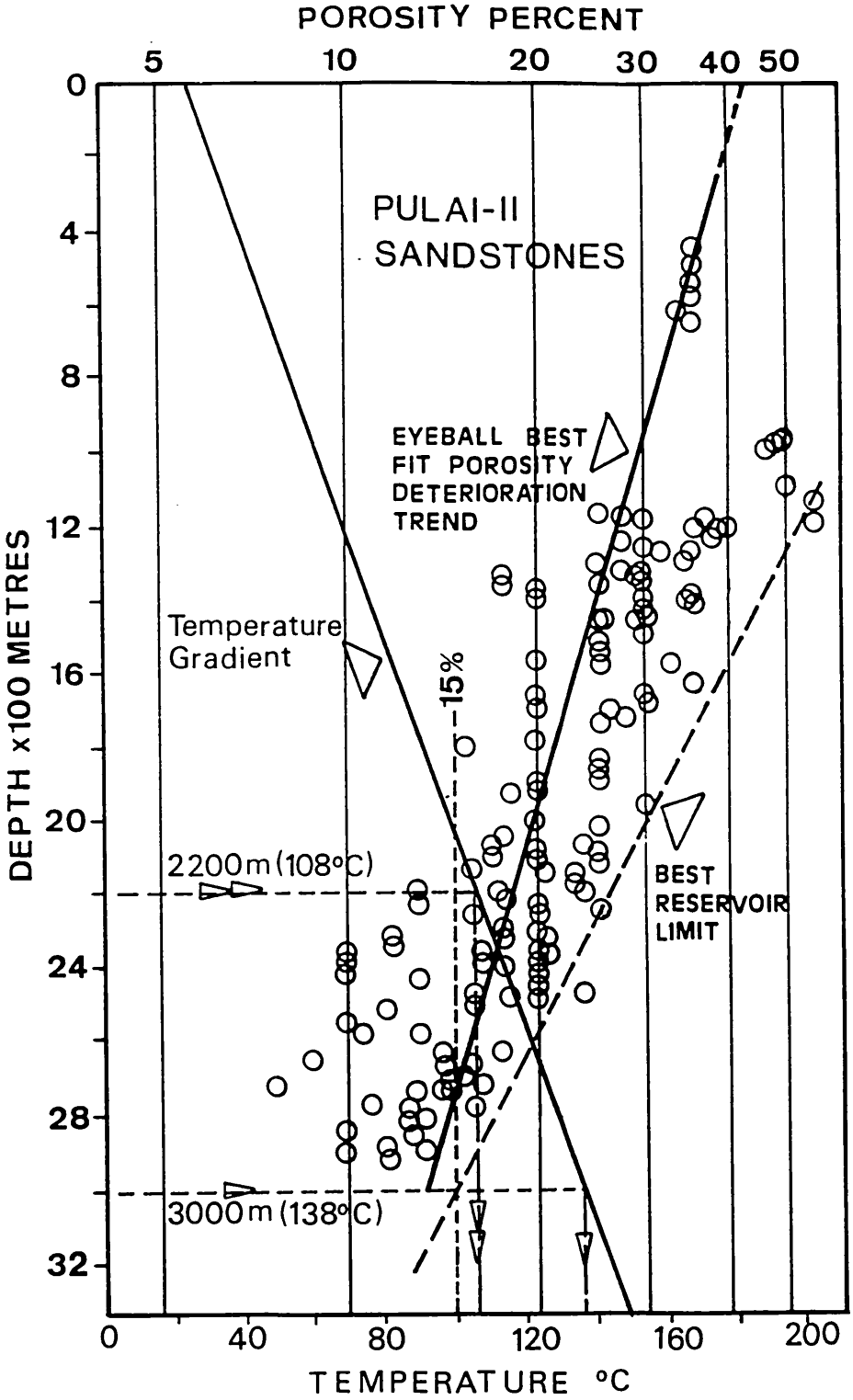


Figure 5-23 - Depth-porosity-temperature diagram illustrating that loss in porosity is related to increase in depth and temperature. Most sandstones with porosity of less than 15 percent are within temperature exceeding 108°C. From Fig. 5-8, it probably suggests Fe-calcite precipitation occurring at 100°C; lack of sandstones with porosity of more than 15 percent below 3000m, suggests intense Fe-calcite precipitation, and also precipitation of other cementing materials, such as quartz, between 108°-138°C.

within the range of vigorous precipitation of quartz and ferroan-calcite, as well as continued precipitation of chlorite, pyrite, kaolinite and smectite-illite. Based on the examination of the sandstone samples through the SEM and thin sections, it would appear that the clay minerals do not appear to cause such a severe porosity reduction as that caused by authigenic quartz and ferroan-calcite.

5.7 *POROSITY ENHANCEMENT*

The photomicrographs from the thin sections and SEM indicate that porosity enhancement of the Pulai-II sandstones is primarily through the dissolution of calcite and unstable framework grains (Plates 5-5, 5-9, and 5-13). Volume of pore space caused by dissolution is difficult to assess; however, based on the porosity-depth relationship (Fig. 5-14), and visual assessment from the thin sections, it probably constitutes up to 40 percent of total porosity.

Based on the porosity distribution within the sandstones in the study area (Fig. 5-15), and its relationship with:

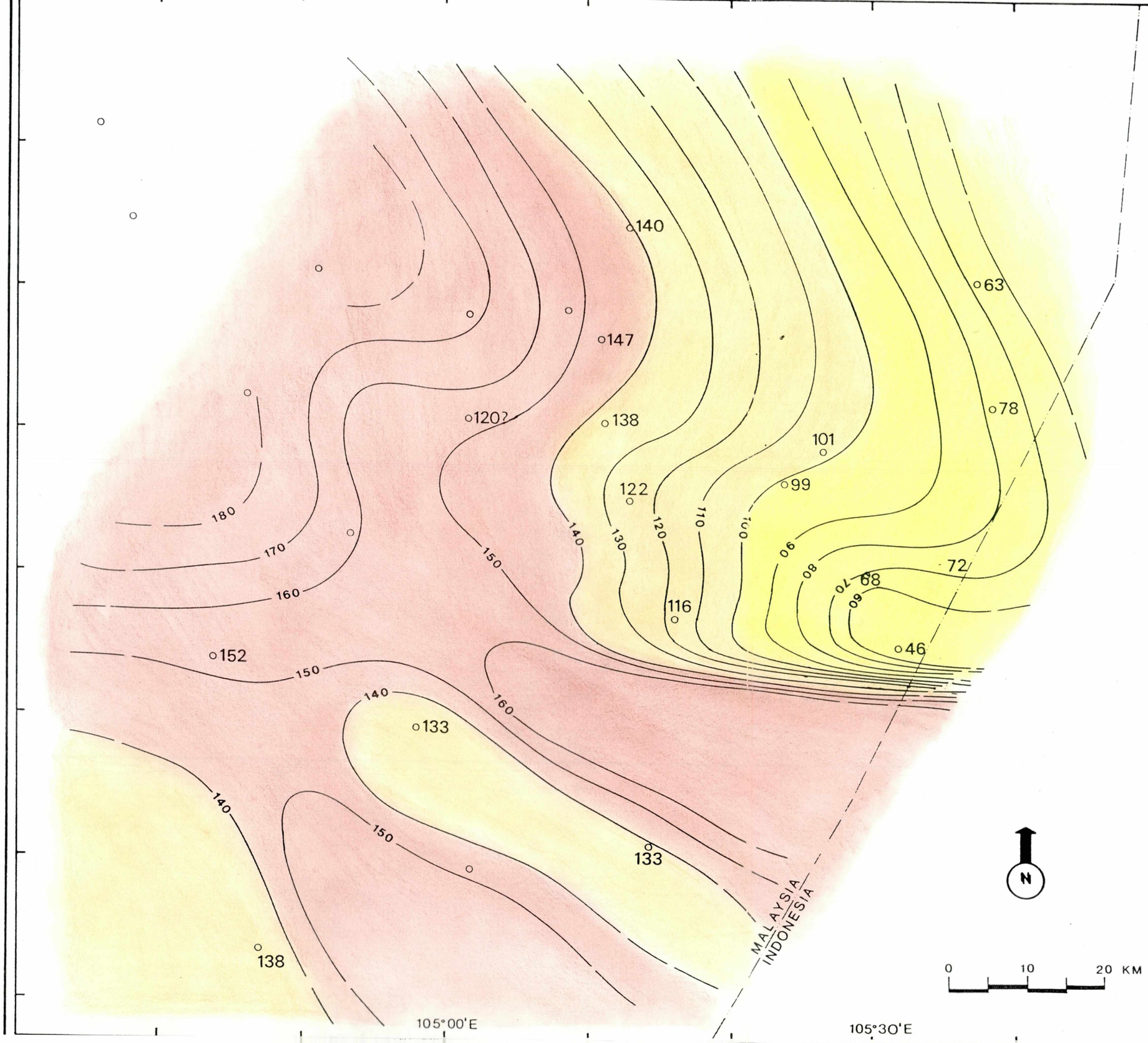
1) The depth of burial and subsequently temperature of the formation (Figs. 2-5 and 5-24),

2) The structural styles or tectonics of the area (Fig. 2-5),

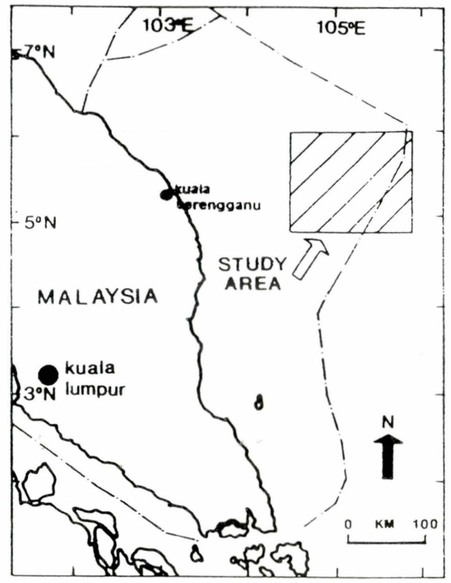
3) The distribution of facies within the Pulai-II Formation (Figs. 4-18 to 4-20), and

4) The salinity (total chloride) distribution in the formation waters (Fig. 5-25),

Where it was observed that the 15-percent porosity contour, Figure 5-15,



LOCATION MAP



LEGEND

Less than 100°C

100° - 140°C

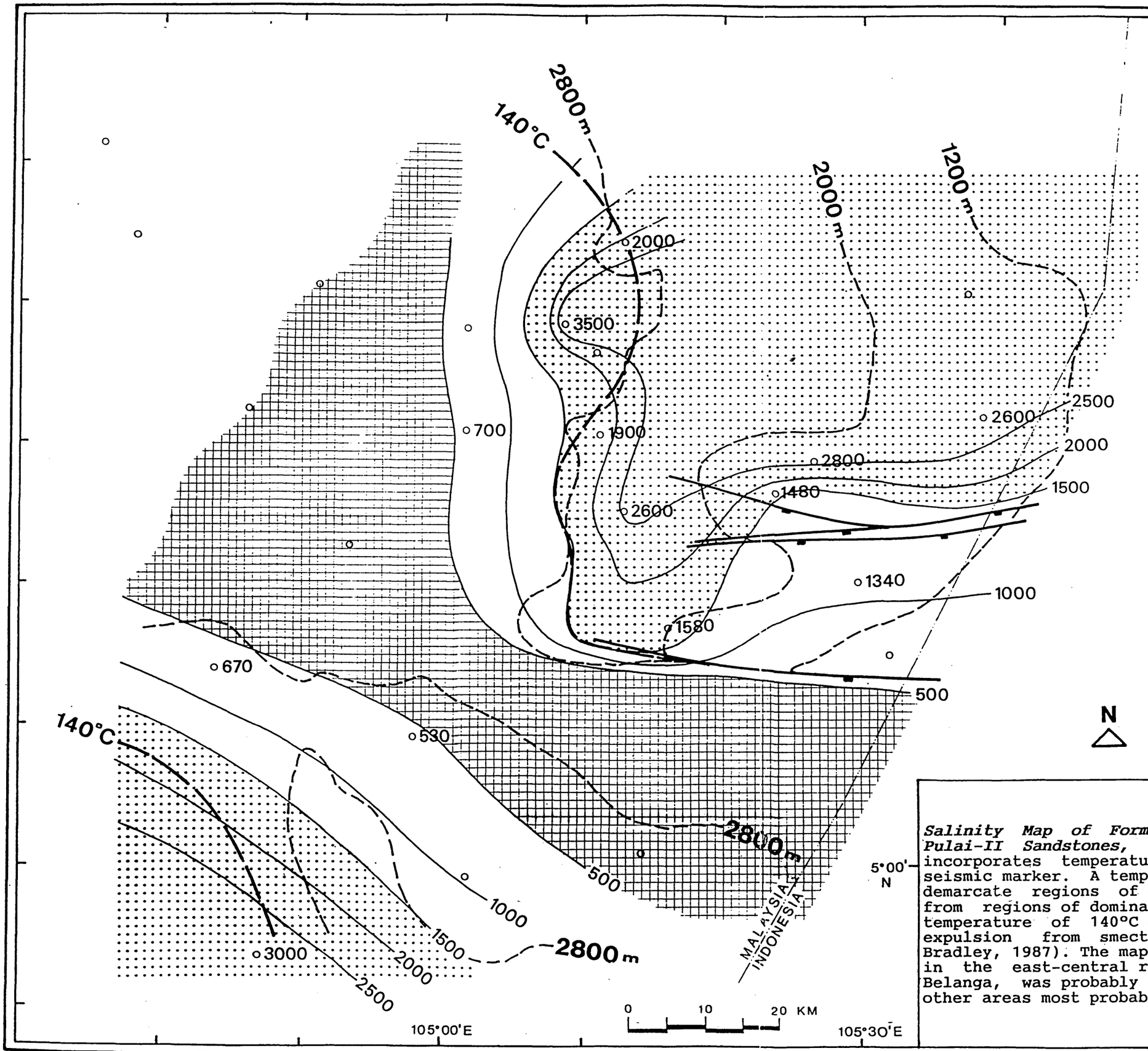
Greater than 140°C

o 145 -- control point

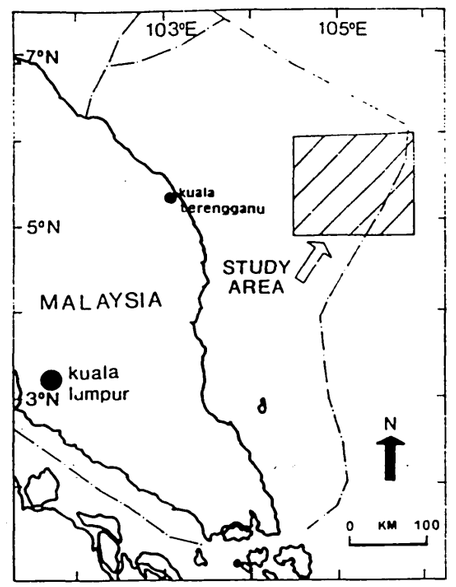
C. I. = 10°C

FIGURE 5-24

Average Formation Temperature Map, Pulai-II sandstones, Southern Malay Basin.



LOCATION MAP



LEGEND

Less than 500 ppm total chloride.

500 - 1500 ppm total chloride.

Greater than 1500 ppm total chloride.

o 1245 -- control point

C. I. = 500 ppm Cl^-

Figure 5-25

Salinity Map of Formation Waters (ppm total chloride), Pulai-II Sandstones, Southern Malay Basin. (The map incorporates temperature and structural contouring on B-seismic marker. A temperature contour of 140°C was used to demarcate regions of dominant subsurface water influence from regions of dominant meteoric water influence, as the temperature of 140°C marks the begining of maximum water expulsion from smectite-illite transformation (Colten-Bradley, 1987). The map suggests that porosity in sandstones in the east-central region covering Seligi-Pulai-Ledang-Belanga, was probably caused dominantly by meteoric waters; other areas most probably by subsurface waters.

corresponds generally to:

1) The present-day structural contour of 2800 metres (Fig. 2-5),

2) The formation temperature contour of 140°C (Fig. 5-24), and

3) The salinity contour of 1500 ppm total chloride west of Bekok-1 and Ophir-1 (Fig. 5-25),

It is believed that porosity enhancement in the Pulai-II sandstones was caused most likely by:

1) Combined effect of acidic meteoric and subsurface waters in the east and northeastern region of the study area, with acidic meteoric water being more dominant than subsurface water, and

2) Predominant effect of acidic subsurface waters in other areas (Fig. 5-25).

The above deductions were made from the observations that:

1) The porosity values greater than 25 percent in the east and northeastern region, Figure 5-15, appear to be confined to the region:

    i) Which is structurally more tectonised, consisting of numerous east-west faulted horsts and grabens (Fig. 2-5). The faults which originated at depth (Figs. 2-3 and 2-4), and fractures, probably have provided evenues for subsurface waters, liberated from shale compaction and smectite-illite transformation, to migrate into the sandstones, and

    ii) which was truncated and sub-aerially exposed to erosion during

Late Miocene (Fig. 2-10). Sub-aerial exposure provided the mechanism for meteoric waters to react with the cement and unstable framework grains as the waters infilterated and permeated through the sandstones.

Because the sandstones in this region are predominantly of Motifs A and C sandstones, they probably had a very high initial permeability. Development of good to excellent porosity was probably the results of influx and the continuing reactions of pore waters with the cement and the unstable framework grains. Where infiltration and flushing were more intense and efficient, particularly in the coarse-grained sandstones, dissolution of the cement and the unstable framework grains became more complete, with the result that the remaining framework grains consisted dominantly of quartz. Precipitation of cementing materials probably occurred when the pore waters became over-saturated with Al^{+3}, Fe^{+2}, Ca^{+2}, Mg^{+2}, Na^{+}, and SiO_4^{-4} ions (Kaiser, 1984).

2) Areas west of Bekok-1, and the south Ophir-1, with porosity of less than 15 percent, Figure 5-15, are generally within the seismic facies of Type II and Type IV (Figs. 4-8 and 4-15). Generally, Type II and Type IV facies contain a high proportion of shales which, when compacted discharged a large volume of water. This water and the water from the smectite-illite transformation were acidic (Surdam et al, 1989), making cementing calcite and feldspar and chert grains unstable and eventually, if the supply of the acidic waters was sustained, both the cement and the unstable framework grains would completely be dissolved. Because these areas underwent relatively rapid burial, and consequently the sediments

were subjected to higher temperature regimes, much of the enhanced porosity was probably lost due to compaction and subsequent cementation.

6. FINDINGS AND CONCLUSIONS

6.1 *FINDINGS*

This study involved the examination of seismic, well and core data, from a megascopic scale to a microscopic scale. The results of the study have led to the following principal findings:

1) The Puali-II Formation, which consists of the Terengganu Shale and Pulai Sandstone Members, can be mapped regionally by two bounding principal seismic markers; arbitrarily, these are called the Red(R) and Purple (P). A third marker, Blue(B), divides the formation, with the R-B interval representing the Terengganu Shales and the B-P interval the Pulai Sandstones. The B-marker is a regional unconformity.

2) Lithologically, as the name implied, the Terengganu Shales consist predominantly of shales, with minor sandstone development. The sandstones within this sequence are best developed at the base of the sequence in the east and northeast of the study area. On the other hand, the Pulai Sandstones are a sequence dominated by massive sandstones in the northeast, and interbedded sandstones, siltstones and shales in the south and southwest.

3) On the basis of log data, each member of the formation can be sub-divided into sub-members. From top to bottom, these are:

   i) Upper Terengganu Shales,

   ii) Lower Terengganu Shales,

   iii) Upper Pulai Sandstones, and

iv) Lower Pulai Sandstones.

4) Generally, the formation is best developed in the west and west-central parts of the study area, with thickness exceeding 1000 metres. It thins towards the south and southwest to about 300 metres, and north and northeast to about 200 metres. The isopach maps of the Terengganu Shales and the Pulai Sandstones suggest that the Pulai-II sandstones in the study area were derived primarily from the northeast, east and south.

5) There are four lithological/log facies, and similarly four correlatable seismic facies in the Pulai-II Formation. The log facies are Motif A, Motif B, Motif C and Motif D; the seismic facies are Type I, Type II, Type II and Type IV. Using log-seismic character correlation, facies distribution and morphology matching, Type I facies correlates with Motif A facies, Type II with Motif B, Type III with Motif C and Type IV with Motif D. The characteristics of these facies are:

   i) Type I consists of discontinuous high and low amplitude seismic signatures in generally low amplitude seismic background. The geological logs show that the facies consist of massive sandstones, generally of blocky patterns, sharp bases and either sharp or upward-fining tops. Thicknesses vary from about 25-130 metres.

   ii) Type II consists of continuous low amplitude signatures in generally low amplitude seismic background. Continuous, high-amplitude signatures occur occasionally within the R-B

interval, forming an excellent marker for regional correlation. Lithologically, the facies comprise shales, with thin calcareous sandstone/siltstone beds and lenses which are usually less than 10 metres thick. It is these calcareous beds which generate the continuous seismic events within the predominantly shale interval.

iii) Type III consists of one- or two-cycle, high amplitude signatures which diffuse laterally into a low amplitude medium and/or terminate against high amplitude signatures. This facies corresponds lithologically to upward-coarsening sandstone sequences. The thickness of these sequences is usually between 25-50 metres, and

iv) Type IV facies consists of discontinuous low and continuous high amplitude signatures. Lithologically, the facies consists of interbedded sandstones, siltstones and shales, and massive sandstones of blocky log patterns. Usually the interbedded sandstones exhibit an overall upward-coarsening profiling. The thickness of the sandstones varies from 3 metres in interbedded sequence to as thick as 25 metres in massive sandstones.

Significant sandstone development is found within facies of Motifs A, C and D (Type 1, Type III and Type IV).

6) The Lower Pulai Sandstone sequence consists of facies of Motifs A and D. The sandstones of these facies are fine to very coarse grained, light to dark grey, occasionally carbonaceous. Glauconite was observed in some sandstones of Motif D in the southeast. The facies of Motif A are more dominant in the north and northeast,

whereas Motif D typifies the south and south-central part of the study area.

7) The Upper Pulai Sandstone sequence consists of the facies of Motifs A, B, and D. The sandstones of these facies are fine to very coarse grained, light to dark grey, occasionally carbonaceous and lignitic. Glauconite was observed in some sandstones of Motif D. The facies of Motif A are dominant in the north and northeast, Motif B in the west and Motif D in the southern parts of the study area.

8) The Lower Terengganu Shale sequence consists primarily of the facies of Motif B, with secondary occurrences of the facies of Motif C and D. The sandstones of Motifs C and D are very fine to occasionally coarse grained, light grey to olive green, glauconitic, and are found mostly in the northeast.

9) The Upper Terengganu Shale sequence comprises dominantly the facies of Motif B, but minor occurrences of Motif C sandstones, which usually are very fine to fine grained, are found in the northeastern region of the study area.

10) The sandstones of the Lower and Upper Pulai Sandstone sequences display a morphological framework of fan systems with braided fluvial channel deposits, which are prominently developed in the north and northeast; and a flat, low-lying setting with lower coastal/deltaic plain deposits, including distributary and tidal channel and crevasse splay sandstones, and lagoonal and strand plain sandstones, and shales, in the south and southwest.

11) The sandstones of the Lower and Upper Terengganu Shale sequences display a morphological framework of delta front/offshore barrier bar systems, which are well developed principally in the northeast, and lower coastal plain in the extreme southwest.

12) The sandstones of Motifs A, C and D consist primarily of quartz, feldspars and chert, with occasional occurrences of lithic fragments and other accessory minerals, micas and zircon, and trace amounts of glauconite in some sandstones of Motifs C and D. These sandstones are compositionally feldspathic litharenites, with an average mode of $Q_{50}F_{20}RF_{30}$.

13) Framework feldspars, chert and lithic grains constitute the more unstable minerals. These are invariably altered and dissolved and some, particularly in the coarse-grained sandstones, have been completely dissolved, with the result that the remaining framework grains consist mainly of quartz. Ancillary framework grains of glauconite and biotite show signs of alterations, but muscovite appears to be relatively more stable. Glauconite grains are invariably clouded by brownish limonitic dust.

14) The cementing materials are primarily quartz overgrowths and clay and carbonate minerals, and secondarily albite and trace amounts of barytes and pyrite.

15) Authigenic quartz occurs as pore-lining and pore-filling syntaxial overgrowths, as microcrystalline and drusy overgrowths on framework grains (quartz, feldspar and lithic grains, although overgrowth on lithic grains is rare), and occasionally as euhedrally well-developed quartz crystals. Some of the quartz overgrowths are

occasionally intergrown with pore-filling clay minerals: kaolinite, smectite-illite, illite and chlorite.

16) The clay mineral composition varies considerably. Within the sandstones of Motif A, the compositions are from 0 percent chlorite (C), 10 percent smectite-illite (S+I) and 90 percent kaolinite (K) ($C_0S+I_{10}K_{90}$) to 23 percent chlorite, 17 percent smectite-illite and 60 percent kaolinite ($C_{23}S+I_{17}K_{60}$); within Motif C, the composition is $C_{10}S+I_{28}K_{62}$; and within Motif D, the composition is $C_5S+I_{33}K_{62}$.

17) Kaolinite occurs generally as a pore-filling mineral, in different crystal forms. The very fine-grained crystals, about 1 to 3 microns in diameter, appear to be the product of feldspar alteration; whereas the coarser-grained crystals, larger than 5 microns, are precipitates and occur as booklets or aggregates of well-developed crystals, and occasionally as vermicules. Kaolinite is relatively more abundant in the coarser-grained and less compacted sandstones than in finer-grained and relatively more compacted sandstones. Usually, the coarser-grained sandstones are braided fluvial channel facies of Motif A.

18) Illite and smectite-illite occur as pore-lining, pore-filling and occasionally as pore bridging minerals, and also as by-products of plagioclase alteration, and are generally more common in the more compacted and in low porosity sandstones. Illite and smectite-illite, which coat the framework grains, generally inhibit quartz overgrowth.

19) Chlorite occurs generally as a pore-lining mineral, and is found in small quantities in sandstones of Motifs C and D, and in some sandstones of Motif A. Chlorite is absent from sandstones with S_w less than 35 percent, but is present in hydrocarbon bearing sandstones of Motifs C and D which contain glauconite. Chlorite also appears to inhibit quartz overgrowth.

20) In some sandstones carbonate minerals comprise up to 25 percent of the total sandstone composition, with pore-filling ankerite forming the dominant species in finer-grained sandstones, and siderite and ferroan-calcite in relatively coarser-grained sandstones. Calcite occurs as a pore-filling mineral, and frequently is found as a replacive cement in generally very fine-grained sandstones. Late phase pore-filling calcite is ferroan, and ferroan-calcite is generally absent in hydrocarbon bearing sandstones.

21) Albite is common in most sandstones, but relatively more abundant in very fine to medium grained sandstones than in coarse grained sandstones, and it occurs both as a product of albitization of framework plagioclase and as overgrowths.

22) Pyrite occurs both as a pore-lining and pore filling mineral, and is found disseminated sporadically in the sandstones, with framboidal pyrite occuring both as a pore-lining and pore-filling and euhedral pyrite as a pore-filling mineral.

23) Barytes occurs only in fine to medium-grained sandstones of Motif A. XRD analyses show that barytes occurs with pyrite, and constitutes up to 4 percent of the total rock.

24) The pores of the sandstones are dominantly intergranular. The intergranular pores are of primary and secondary origins, of which up to 40 percent of the pores are secondary. The porosity generally decreases exponentially with the increase in depth, and consequently with temperature. A porosity greater than 30 percent generally occurs in sandstones buried shallower than 2000 metres, and a porosity of less than 15 percent deeper than 3000 metres.

25) Porosity greater than 25 percent is found in the northeastern part of the study area, in an area which is structurally more elevated and tectonised. This area also corresponds to the region which has formation water salinity between 500-1500 ppm chloride. Meteoric waters seeping through faults and fractures, are thought to be responsible for diluting the formation waters, and most importantly the dissolution of calcite cement and unstable framework grains.

26) Secondary porosity appears to have been formed by the dissolution of the unstable framework feldspars, chert and lithic grains and of the early-stage calcite cement. In some braided sandstone facies a porosity of more than 45 percent was achieved. In the northeastern area, where the Pulai-II sandstones occur at shallower depths, it would appear that the role of meteoric waters in enhancing the secondary porosity outweighs that of subsurface waters. The predominance of framework quartz and general lack of albite in the sandstones of Motif A probably indicate an effective dissolution process of the unstable framework grains by acidic waters.

27) Low porosity values are generally found in very fine to fine-grained, and sometimes in fine to medium-grained, sandstones which are, or have been, buried to great depths. Medium to coarse-grained

sandstones usually have good to excellent porosities.

28) Authigenic quartz and ferroan-calcite occur extensively in some sandstones which are buried deeper than the present-day of 2200 metres. It would appear that the Pulai-II sandstones at most studied locations have been buried to much greater depths than at the present-day: for example at Tapis-2, the sandstones were at least 800 metres and, at Pulai-1 about 400 metres, deeper than at present. Although the quality of the reservoir is generally depth related, porosity appears to have been preserved in some sandstones which contain hydrocarbons.

29) The majority of the wells drilled into over-pressured sandstones contain hydrocarbons. Porosity is generally fair to good. Where no hydrocarbons were found, the porosity is usually poor.

30) Much of the area south of the major east-west fault, Fault A (Fig. 2-5), and west of Banggol-Palas-Tiong-Bekok-Ophir line, except in the extreme southwest, is within a temperature zone exceeding 140°C. Within this area, the porosity of most sandstones is less than 15 percent.

6.2 *CONCLUSIONS*

Based on the integration of the above findings, it is concluded that:

1) The sandstones of the Pulai-II Formation were deposited during the initial period of marine incursion into the Malay basin, in three broad environmental settings: continental, transitional and shelf.

The early part of the Late Oligocene-Early Miocene saw the deposition of the Pulai Sandstone sequence in a continental setting in the northeast, and in low-lying coastal/deltaic conditions in the south. Marine transgression during the later part of the Late Oligocene-Early Miocene allowed the deposition of barrier bar sandstones of the Terengganu Shale sequence.

2) Generally, the braided fluvial channel sandstones form the dominant facies. These sandstones comprise several complexly developed alluvial outwash plain systems which overlap, superimpose and coalesce to form a blanket covering at least 100 km in length and 30-40 km in width. The less dominant facies are the barrier bar and the distributary and tidal channel sandstones. The distributary and tidal channel sandstones are laterally discontinuous.

3) The braided fluvial channel and the barrier bar sandstones, developed in the northeast, form the best reservoirs. These sandstones have average total porosities generally exceeding 15 percent (between 15 to 45 percent). Good initial permeability within the coarser sandstones, particularly within the braided fluvial channel facies, probably contributed to a more complete dissolution of calcite cement and unstable framework feldspars and chert. The distributary and tidal channels in the south also form good reservoirs, with average total porosity ranging from 15 to 23 percent; but their distribution, particularly the massive units, is difficult to map and therefore their continuity less easy to predict.

4) The porosity in the Pulai-II sandstones is governed by:

i) Facies distribution and grain size variations within each sandstone facies. The finer-grained sandstones generally contain a higher percentage of authigenic minerals than the coarser-grained sandstones,

ii) Depth of burial and temperature. Usually an increase in depth of burial is accompanied by an increase in degree of compaction and cementation. It is apparent that poor porosity is found in the Pulai-II sandstones where they are, or have been, buried relatively to great depths. This poor porosity development is caused primarily by the precipitation of authigenic quartz and ferroan-calcite. Precipitation of other authigenic minerals does not appear to create any significant porosity reduction. Except possibly under highly overpressured conditions, porosity greater than 15 percent is not likely to be found in the sandstones at depth below 3000 metres,

iii) Hydrocarbons. Timely emplacement of hydrocarbons into the reservoirs inhibits precipitation of authigenic minerals, and

iv) Structure. Adjustment of fault blocks and subsequent faulting in the Late Miocene-Pliocene, particularly in the northeastern part of the study area, have caused exposure of the Pulai-II sandstones to the continuous invasion of acidic meteoric waters. Much of the secondary porosity generated in this area was the result of the reactions of these waters on the unstable framework feldspars and chert.

5) The northeastern quadrant of the study area is probably the area that will continue to give highest exploration success, with a better

chance of encountering liquid hydrocarbons than the rest of the study area. The generally high temperatures within the sandstones in the south and west are likely to degrade any of trapped liquid hydrocarbons into gas and condensate, and possibly also pyrobitumen.

6.3 *FUTURE WORK*

Because this study is an overview of the deposition and diagenesis of the Pulai-II sandstones in the southern part of the Malay basin, the conclusions are inevitably broad. Several in-depth studies of a similar nature ought to be undertaken on a smaller scale, for example on a field by field basis where more data can be used for all the prospective formations, and where recent seismic data are available. Nevertheless, the following studies may corroborate the findings and conclusions of this thesis:

1) The structural evolution of the Malay basin, particularly the southern part of the basin where the area is known to be relatively oil-prone. It is essential to relate the findings of this study to the timing of generation and migration of hydrocarbons. The availability of new seismic data acquired during 1988-89, will make this study more meaningful. Similarly, the use of these seismic data for the direct detection of facies and their distribution would be significant, particularly in delineating potential reservoirs which have not previously been penetrated by wells.

2) Source rock maturation analysis. Until now, because hydrocarbons are found in the area, the need to know their sources has been of secondary importance. Company reports have suggested that some of the hydrocarbons trapped in the Pulai-II sandstones in some fields

in the northeast, were sourced from the sequences underlying the Pulai-II Formation (Fig. 1-6). If it can be proven that these sequences sourced some of the hydrocarbons, it could re-activate interest in deep drilling. Except for some wells drilled before 1975, most wells were terminated before reaching the Seligi Formation.

3) Pore/formation pressure and pressure distribution analysis. It is known that some of the over-pressured sandstones in the study area contain hydrocarbons, and that a porosity greater than 15 percent is preserved. Again, the understanding of pressure regimes and pressure dynamics, in conjunction with the burial history and diagenetic history of the sandstones, among others, could assist further exploration.

4) Sediments of the Gagau Group, Jurassic-Cretaceous in age, have been mapped onshore on the Peninsula, and are not described as metamorphosed. Because the Gagau Group appears to occur at depth in the study area, it is essential to assess and establish its petroleum significance by examining the outcrops on the Peninsula in more detail.

SELECTED BIBLIOGRAPHY

Achalabuthi, C., 1974, Petroleum geology of Gulf of Thailand (abs.): Am. Assoc. Petroleum Geologists Bull., v. 58, p. 1430.

Armitage, J. H., and C. Viotti, 1977, Stratigraphic nomenclature, southern end Malay basin: Indonesian Petroleum Association, Sixth Annual Conv., Jakarta, Preprint 43 p.

Ayers, W. B., 1986, Lacustrine and Fluvial-deltaic depositional systems, Fort Union Formation (Paleocene), Powder River basin, Wyoming and Montana: Am. Assoc. Petroleum Geologists Bull., vol. 70, p. 1651-1673.

Baldwin, B., and C. D. Butler, 1985, Compaction curves: Am. Assoc. Petroleum Geologists Bull., vol. 69, p. 622-626.

Ballay, A. W. (Editor), 1987, Atlas of Seismic stratigraphy. In Am. Assoc. Petroleum Geologists Studies in Geology, No. 27, vol. 1, 124 p.

Blanche, B. J., and J. H. M. Whittaker, 1978, Diagenesis of part of the Brent Sand Formation (Middle Jurassic) of the northern North Sea basin: Geological Society of London Journal, vol. 135, p. 73-82.

Boles, J. R., 1982, Active albitization of plagioclase, Gulf Coast Tertiary: American Journal of Science, vol. 282, p. 165-180.

----------, 1984, Secondary porosity reactions in the Stevens Sandstones, San Joaquin Valley, California. In: Am. Assoc. Petroleum Geologists Memoir 37 - Clastic Diagenesis (Ed. by D. A. McDonald and R. C. Surdam), p. 217-224.

----------, and S. G. Franks, 1979, Clay diagenesis in Wilcox sandstones of southwest Texas: implications of smectite diagenesis on sandstones: Journal of Sedimentary Petrology, vol. 49, p. 55-70.

Brami, J. B. and M. Y. Muhhaiyuddin, 1984, History and geology of the Tinggi field, offshore Peninsular Malaysia: 5th Offshore South East Asia Conference, Singapore, Preprint 14 p.

Brown, L. F., and W. L. Fisher, 1982, Seismic stratigraphic interpretation and petroleum exploration: Am. Assoc. Petroleum Geologists Continuing Education Course Notes Series No. 16, 125 p.

Bulling, T. P., and J. A. Breyer, 1989, Exploring for subtle traps with high-resolution palaeogeographic maps: Reklaw 1 Interval (Eocene): Am. Assoc. Petroleum Geologists Bull., vol. 73, p. 24-39.

Burley, S. D., and J. D. Kantorowicz, 1986, Thin section and SEM textural criteria for the recognition of cement-dissolution porosity in sandstones: Sedimentology, vol. 33, p. 587-604.

Burst, J. F., 1969, Diagenesis of Gulf Coast clayey sediments and its possible relation to petroleum migration: Am. Assoc. Petroleum Geologists Bull., vol. 53, p. 73-93.

Cant, D. J., 1982, Fluvial facies models and their application. In: Am. Assoc. Petroleum Geologists Memoir 31 -- Sandstone Depositional Environments (Ed. by P. A. Scholle and D. Spearing), p. 115-137.

----------, 1986, Diagenetic traps in sandstones: Am. Assoc. Petroleum Geologists Bull., vol. 70, p. 155-160.

Carothers, W. W., and Y. K. Kharaka, 1978, Aliphatic acid anions in oil-field waters-- implication for origin of natural gas: Am. Assoc. Petroleum Geologists Bull., vol. 62, p. 2441-2453.

CARIGALI, 1985, Structures in PM 12 Operating Area: unpublished company report.

--------, 1986, Stratigraphic scheme for hydrocarbon exploration in Carigali's operating areas, offshore Peninsular Malaysia: unpublished company report.

Chung, S, K., and E. H. Yin, 1968, Brief outline of the geology of West Malaysia: Geological Survey Malaysia, p. 53-67.

Coleman, J. M., and D. B. Prior, 1982, Deltaic environments of deposition. In: Am. Assoc. Petroleum Geologists Memoir 31 - Sandstone Depositional Environments (Edited by P. A. Scholle and D. Spearing), p. 139-189.

Collinson, J. D., 1986, Alluvial sediments. In: Sedimentary environments and facies (Edited by H. G. Reading, Second Edition), Blackwell Scientific Publications, p. 20-62

Colten-Bradley, V. A., 1987, Role of pressure in smectite-to-illite transformation: Am. Assoc. Petroleum Geologists Bull., vol. 71, p. 1414-1427.

Curtis, C. D., 1978, Possible links between sandstone diagenesis and depth related geochemical reactions occurring in enclosed mudstones: Quarterly Journal of the Geology Society of London, v. 135, p. 107-117.

Damanti, J. F., and T. E. Jordan, 1989, Cementation and compaction history of synorogenic foreland basin sedimentary rocks from Huaco, Argentina: Am. Assoc. Petroleum Geologists Bull., vol. 73, p. 858-873.

DeWitt, R. J., 1984, Well log responses to environmental facies: Esso Workshop on clastic facies school, Kuala Lumpur.

Dixon, S. A., D. M. Summers, R. C. Surdam, 1989, Diagenesis and preservation of porosity in Norphlet Formation (Upper Jurassic), Southern Alabama: Am. Assoc. Petroleum Geologists Bull., vol. 73, p. 707-728.

Eberl, D. D., and J. Hower, 1977, The hydrothermal transformation of sodium and potassium smectite into mixed-layer clay: Clay and Clay Minerals, vol. 25, p. 215-227.

Edman, D. D., and R. C. Surdam, 1984, Diagenetic history of the Phosphoria, Tensleep and Madison Formations, Tip Top field, Wyoming: Am. Assoc. Petroleum Geologists Memoir 37 - Clastic Diagenesis (Ed. by D. A. McDonald and R. C. Surdam), p. 317-345.

Elliot, T., 1986, Deltas. In: Sedimentary environments and facies (Ed. by H. G. Reading, Second Edition), Blackwell Scientific Publications, p. 155-228.

ESSO, 1976, Structural development of the Malay basin: unpublished contractor's report to PETRONAS.

----, 1978, Palaeontological analysis of selected sidewall cores from EPMI Palas-1, Peninsular Malaysia Contract Area--unpublished rpt. No. EPR.30ES.78.

Eynon, G., 1981, Basin development and sedimentation in the Middle Jurassic of the northern North Sea. In: Petroleum Geology of the continental shelf of northwest Europe (Ed. by L. V. Illing and G. D. Hobson), p. 196-204.

Folk, R. L., 1968, Petrology of sedimentary rocks: Austin, Texas, Hemphill Publishing Company, 182 p.

Franks, S. G., and R. W. Forester, 1984, Relationships among secondary porosity, pore-fluid chemistry and carbon dioxide, Texas Gulf Coast. In: Am. Assoc. Petroleum Geologists Memoir 37 - Clastic Diagenesis (Edited by D. A. McDonald and R. C. Surdam), p. 63-80.

Galloway, W. E., 1974, Deposition and diagenetic alteration of sandstones in northeastern Pacific arc-related basins: implications for greywacke genesis: Bull. Geological Society of America, vol. 85, p. 379-390.

----------, and D. K. Hobday, 1983, Terrigenous clastic depositional systems: Springer, New York, 433 p.

Garrels, R. M., and C. L. Christ, 1965, Solutions, minerals and equilibria: New York, Harper and Row, 450 p.

Gobbette, J. D., and C. S. Hutchison, (Eds.), 1973, The geology of the Malay Peninsula: New York, John Wiley-International, 438 p.

Gretener, P. E., 1981, Pore pressure: Fundamentals, general ramifications and implications for structural geology. Am. Assoc. Petroleum Geologists, Continuing Education Course Note Series No. 4, 87 p.

Haile, N. S., 1970, Notes on the geology of the Tambelan, Anambas, and Natuna islands, Sunda Shelf, Indonesia: United Nations ECAFE-CCOP Tech. Bulletin, vol. 3, p. 55-75.

----------, 1973, The geomorphologyand geology of the northern part of the Sunda Shelf and its place in the Sunda mountain system: Pacific Geology, vol. 6, p. 73-90.

Hamilton, W., 1979, Tectonics of the Indonesian region: U. S. Geological Survey Professional Paper no. 1078, 345 p.

Helmold, K. P., and P. C. van de Kamp, 1984, Diagenetic mineralogy and controls on albitization and laumontite formation in Paleogene arkoses, Santa Ynez Mountains, California. In: Am. Assoc. Petroleum Geologists Memoir 37 - Clastic Diagenesis (Ed. by D. A. McDonald and R. C. Surdam), p. 239-276.

----------, and E. H. Snider, 1981, Geothermal gradients, organic metamorphism, and mineral diagenesis in Tertiary rocks, Santa Ynez Mountain, California: Am. Assoc. Petroleum Geologists Bull., vol. 65, p. 937.

Hubbard, R. J., J. Pape, and D. G. Roberts, 1985, Depositional sequence mapping as a technique to establish tectonic and stratigraphic framework and evaluate hydrocarbon potential on a passive continental margin. In: Am. Assoc. Petroleum Geologists Memoir 39 - Seismic Stratigraphy II (Ed. by O. R. Berg and D. G. Woolverton), p. 79-93.

Hutchison, C. S., 1973, Tectonic evolution of Sundaland-- a Phanerozoic synthesis: Geol. Soc. Malaysia Bull., vol.6, p. 61-86.

Johnson, H. D. and C. T. Baldwin, 1986, Shallow siliciclastic seas. In: Sedimentary environments and facies (Ed. by H. G. Reading, Second Edition), Blackwell Scientific Publications, p. 229-282.

Kaiser, W. R., 1984, Predicting reservoir quality and diagenetic history in the Frio Formation (Oligocene) of Texas. In: Am. Assoc. Petroleum Geologists Memoir 37 - Clastic Diagenesis (Ed. by D. A. McDonald and R. C. Surdam), p. 195-215.

Kingston, D. R., C. P. Dishroon, and P. A. Williams, 1983, Global basin classification system: Am. Assoc. Petroleum Geologists Bull., vol.67, p. 2175-2193.

Klemme, H. D., 1972, Geothermal gradients: Part 1, Oil Journal, vol. 69, p. 136, p.115-123.

Land, L. S., 1984, Frio sandstone diagenesis, Texas Gulf Coast: A regional isotopic study. In: Am. Assoc. Petroleum Geologists Memoir 37-- Clastic Diagenesis (Ed. by D. A. McDonald and R. C. Surdam), p. 47-62.

Leder, F., and W. C. Park, 1986, Porosity reduction in sandstones by quartz overgrowth: Am. Assoc. Petroleum Geologists Bull., vol. 70, p. 1713-1728.

Lee, M., J. L. Aronson, and S. M. Savin, 1989, Timing and conditions of Permian Rotliegende Sandstone diagenesis, southern North Sea: K/Ar and oxygen isopopic data: Am. Assoc. Petroleum Geologists Bull., vol. 73, p. 195-215.

Loucks, R. G., M. M. Dodge, and W. E. Galloway, 1984, Regional controls on diagenesis and reservoir quality in Lower Tertiary sandstones along the Texas Gulf Coast. In: Am. Assoc. Petroleum Geologists Memoir 37 - Clastic Diagenesis (Ed. by D. A. McDonald and R. C. Surdam), p. 15-45.

Lundegard, P. D., and A. S. Trevena, 1987, Influence of fluid chemistry and high geothermal gradient on sandstone diagenesis (abs.): Am. Assoc. Petroleum Geologists Bull., vol. 71, p. 586.

Magara, K., 1975, Reevaluation of montmorillonite dehydration as cause of abnormal pressure and hydrocarbon generation: Am. Assoc. Petroleum Geologists Bull., vol. 59, p. 292-302.

----------, 1976, Water expulsion from clastic sediments during compaction-- directions and volume: Am. Assoc. Petroleum Geologists Bull., vol. 60, p. 543-553.

Markert, J. C., and Z. Al-Shaieb, 1984, Diagenesis and evolution of secondary porosity in Upper Minnelusa sandstones, Powder River basin, Wyoming. In: Am. Assoc. Petroleum Geologists Memoir 37 - Clastic Diagenesis (Ed. by D. A. McDonald and R. C. Surdam), p. 367-389.

McBride, E. F., 1980, Importance in secondary porosity in sandstones to hydrocarbon exploration. In: Am. Assoc. Petroleum Geologists Bull. vol.64, p. 742.

--------------, L. S. Land, and L. E. Mack, 1987, Diagenesis of eolian and fluvial feldspathic sandstones, Norphlet Formation (Upper Jurassic), Rankin County, Mississippi, and Mobile County, Alabama: Am. Assoc. Petroleum Geologists Bull., vol. 71, p. 1019-1034.

McCubbin, D. G., 1982, Barrier-island and strand plain facies. In: Am. Assoc. Petroleum Geologists Memoir 31 - Sandstone Depositional Environments (Ed. by P. A. Scholle and D. Spearing), p. 247-279.

McGovney, J. E., and B. J. Radovich, 1985, Seismic stratigraphy and facies of the Frigg Fan Complex. In: Am. Assoc. Petroleum Geologists Memoir 39 - Seismic Stratigraphy II (Ed. by O. R. Berg and D. G. Woolverton), p. 139-156.

Meckel, L. D., 1975, Holocene sand bodies in the Colorado Delta area, northern Gulf of California: Deltas-- models for exploration, M. L. Broussard (Editor), p. 239-265.

Miall, A. D., 1988, Reservoir Heterogeneities in fluvial sandstones: lessons from outcrop studies: Am. Assoc. Petroleum Geologists Bull., vol. 72, p. 682-697.

Mitchum, R. M.,Jr., P. R. Vail, and J. B. Sangree, 1977, Seismic stratigraphy and global changes in sea level, Pt. 6: Stratigraphic interpretation of seismic reflection patterns in depositional sequences. In: Seismic Stratigraphy-- applications to hydrocarbon exploration (Ed. by C. E. Payton), Am. Assoc. Petroleum Geologists Memoir 26, Tulsa, p. 117-133.

Murphy, R. W., 1974, Structural evolution of Tertiary basins of Southeast Asia (abs.): Am. Assoc. Petroleum Geologists Bull., v. 58, p. 1451-1452.

Nagtegaal, P. J. C., 1978, Sandstone framework instability as a function of burial diagenesis: Journal Geological Society, vol. 135, p. 101-105.

----------, 1980, Clastic reservoir rocks: origin, diagenesis and quality: Proceedings International Meeting on Petroleum Geology, Beijing, China, 23 p.

Neidell, N. S., 1980, Stratigraphic modelling and interpretation--geophysical principles and techniques: Am. Assoc. Petroleum Geologists Continuing Education Course Notes Series No. 13, 145 p.

Nik Ramli, 1988, Humid tropical fan-delta sedimentation: An ancient model from the K sandstones (Late Oligocene-Early Miocene), southeastern part of the Malay basin, offshore West Malaysia. In: Fan Deltas and Related Systems: Sedimentology and Tectonic Settings (Ed. by W. Nemec and R. J. Steel), Blackie Publication Co., p. 341-353.

Nilsen, T. H., 1982, Alluvial fan deposits. In: Am. Assoc. Petroleum Geologists Memoir 31-- Sandstone Depositional Environments (Edited by P. A. Scholle and D. Spearing), p. 49-86.

Ngah, K., 1975, Stratigraphic and structural analyses of the Penyu basin, Malaysia: unpublished M.Sc. thesis, Oklahoma State University, Stillwater, Oklahoma, 52 p.

Parke, M. L., K. O. Emery, R. Szymankiewiez, and L. M. Ronalds, 1971, Structural framework of continental margin in South China Sea: Am. Assoc. Petroleum Geologists Bull., vol. 55, p. 723-751.

Paul, L., 1975, Offshore Tertiary basins of Southeast Asia, Bay of Bengal to South China Sea: Proceeding of 9th World Petroleum Congress: Panel Discussion no. 7-- Exploration in the Far East outside Japan, p. 1-15.

Payton, C. E. (Editor), 1977, Seismic Stratigraphy--applications to hydrocarbon exploration: Am. Assoc. Petroleum Geologists Memoir 26, Tulsa, 516 p.

Pollastro, R. M., 1985, Mineralogical and morphological evidence for the formation of illite at the expense of illite/smectite: Clay and Clay Minerals, vol. 33, p. 265-274.

Pupilli, M., 1973, Geological evolution of South China Sea area--Tentative reconstruction from borderland geology and well data: Second Indonesisn Petroleum Assoc. Conv., Jakarta, Preprint, 22 p.

Pusey, W. C., 1973, Paleotemperatures in Gulf Coast using the ESR-Kerogen method: Gulf Assoc. of Geological Societies Transaction, vol. 23, p. 195-202.

Rashidah, A. K., C. K. Ho, and C. K. Razak, 1988, Biostratigraphy of selected wells from the Malay basin: Seminar, Geological Society Malaysia, Kuala Lumpur, Malaysia, Preprint 33 p.

Ray, R. R., 1982, Seismic stratigraphic interpretation of the Fort Union Formation, western Wind River basin: example of subtle trap exploration in a nonmarine sequence. In: Am. Assoc. Petroleum Geologists Memoir 32 - The Deliberate Search for the Subtle Trap (Ed. by M. T. Halbouty), p. 169-180.

Rishworth, D. E. H., 1974, The Upper Mesozoic terrigenous Gagau Group of Peninsular Malaysia: Geological Survey Malaysia Special Paper 1, 78 p.

Schmidt, V., D. A. McDonald, and R. L. Platt, 1977, Pore geometry in the course of sandstone diagenesis: Bull. Canadian Petroleum Geologists, vol. 25, p. 271-290.

Selley, R. C., 1978, Porosity gradients in North Sea oil-bearing sandstones: Geological Society of London Journal, vol. 135, p. 119-132.

----------, 1985, Ancient sedimentary environments (3rd. Edition): Chapman and Hall, 317 p.

----------, 1989, Subsurface facies analysis: Joint Assoc. For Petroleum Exploration Courses (UK), Course Notes no. 89, 150 p.

Senathirajah, S., 1969, Younger Mesozoic sedimentary rocks, State of Johore, West Malaysia: Am. Assoc. Petroleum Geologists Bull., vol. 53, p. 2187-2194.

Serra, O., 1985, Sedimentary environments from wireline logs: Schlumberger, 211 p.

Shanmugam, G., 1985, Significance of secondary porosity in interpreting sandstone composition: Am. Assoc. Petroleum Geologists Bull., vol. 69, p. 378-384.

----------, and K. A. Alhilali, 1988, Parameters influencing porosity in sandstones: A model for sandstone porosity prediction: Discussion: Am. Assoc. Petroleum Geologists Bull., vol. 72, p. 852-853.

----------., and J. B. Higgins, 1988, Porosity enhancement from chert dissolution beneath Neocomian unconformity: Ivishak Formation, North Slope, Alaska: Am. Assoc. Petroleum Geologists Bull., vol. 72, p. 523-535.

Shaw, H. F, 1987, Clays and their effects in source and reservoir rocks: Joint Assoc. For Petroleum Exploration Courses (UK), Course Notes no. 61, 165 p.

Shell Oil Company, 1987, Seismic sequences as applied to basin-fill analysis: Taranki basin, New Zealand: In Ballay, A. W. (Editor), 1987, Atlas in Seismic stratigraphy, Am. Assoc. Petroleum Geologists Studies in Geology, No. 27, vol. 1, 124 p.

Shelton, J. W., 1973, Models of sand and sandstone deposits: a methodology for determining sand genesis and trends: Oklahoma Geological Survey Bull., 119 p.

Surdam, R. C., S. W. Boese, and L. J. Crossey, 1984, The chemistry of secondary porosity. In: Am. Assoc. Petroleum Geologists Memoir 37 - Clastic Diagenesis (Edited by D. A. McDonald and R. C. Surdam), p. 127-150.

----------, L. J. Crossey, E. S. Hagen, H. P. Heasler, 1989, Organic-inorganic interactions and sandstone diagenesis: Am. Assoc. Petroleum Geologists Bull., vol. 73, p. 1-23.

Tapponnier, P., G. Peltzer, A. Y. LeDain, R. Amijo, and P. Cobbold, 1982, Propogating extrusion tectonics in Asia-- new insights from simple experiments with plasticine: Geology, vol. 10, p. 611-616.

Terry, R. D., and G. V. Chilingar, 1955, Summary of "Concerning some additional aids in studying sedimentary formations" by M. S. Shvetsov: Journal Sedimen. Petrol., vol. 25, no. 3, p. 229-234.

Trevena, A. S., and R. A. Clark, 1986, Diagenesis of sandstones reservoirs of Pattani basin, Gulf of Thailand: Am. Assoc. Petroleum Geologists Bull., vol. 70, p. 299-308.

Tyler, N, and W. A. Ambrose, 1986, Facies architecture and production characteristics of strand-plain reservoirs in North Markham-North bay City field, Frio Formation, Texas: Am. Assoc. Petroleum Geologists Bull., vol. 70, p. 809-829.

Vail, P. R., R. M. Mitchum, Jr., and S. Thompson, III, 1977, Seismic stratigraphy and global changes in sea level, Part 4: Global cycles of relative changes of sea level. In: Seismic Stratigraphy--applications to hydrocarbon exploration (Ed. by C. E. Payton), Am. Assoc. Petroleum Geologists Memoir 26, Tulsa, p. 83-97.

----------, R. G. Todd, and J. B. Sangree, 1977, Seismic stratigraphy and global changes in sea level, Part 5: Chronostratigraphic significance of seismic reflections. In: Seismic Stratigraphy--applications to hydrocarbon exploration (Ed. by C. E. Payton), Am. Assoc. Petroleum Geologists Memoir 26, Tulsa, p. 99-133.

Weimer, R. J., J. D. Howard, and D. R. Lindsay, 1982, Tidal flats and associated tidal channels. In: Am. Assoc. Petroleum Geologists Memoir 31 - Sandstone Depositional Environments (Ed. by P. A. Scholle and D. Spearing), p. 191-245.

Weise, B. R., 1980, Wave-dominated delta systems of the Upper Cretaceous San Miguel Formation, Maverick basin, south Texas, Report of investigation, 107: Bureau of Economic Geology, University of Texas, Austin.

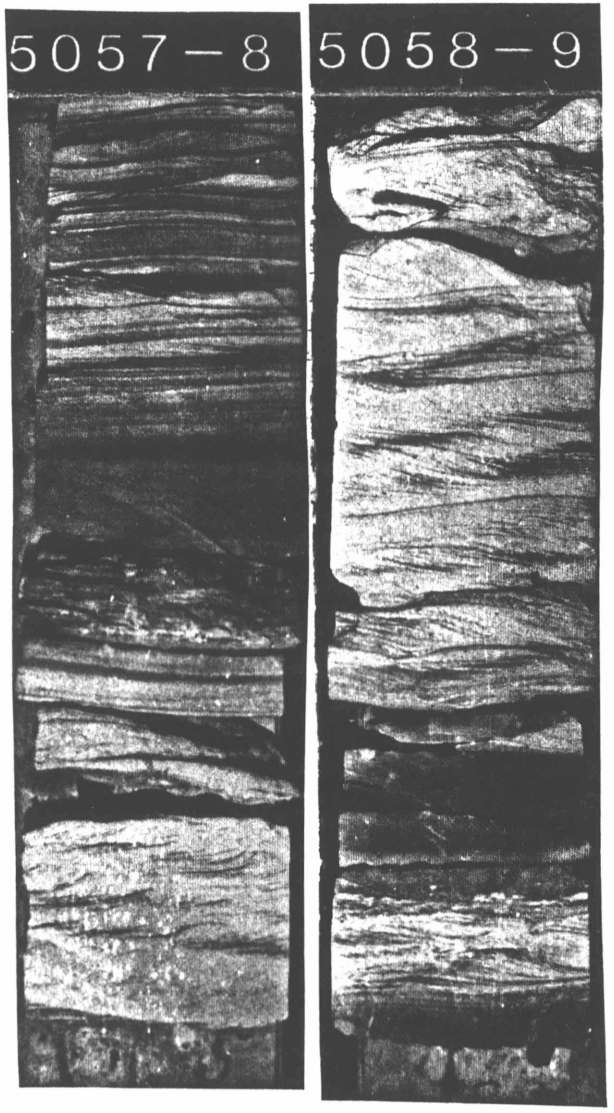
Wilson, J. C., and E. F. McBride, 1988, Compaction and porosity evolution of Pliocene sandstones, Ventura basin, California: Am. Assoc. Petroleum Geologists Bull., vol. 72, p. 664-681.

Wilson, M. D. and E. D. Pittman, 1977, Authigenic clays in sandstones--recognition and influence on reservoir properties and palaeoenvironmental analysis: Journal of Sedimentary Petrology, vol. 47, p. 3-31.

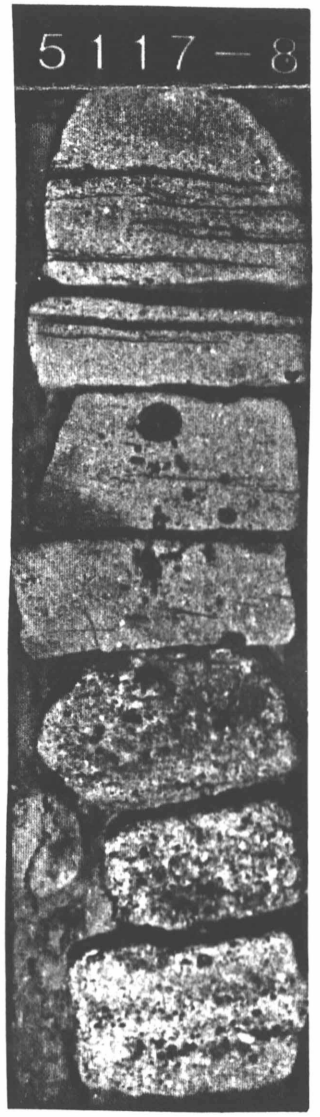
Well Name - Seligi-3
Unit - Upper Pulai Sandstones
Depth - 1531 m.; 1541 m.; 1560 m. and 1580 m..



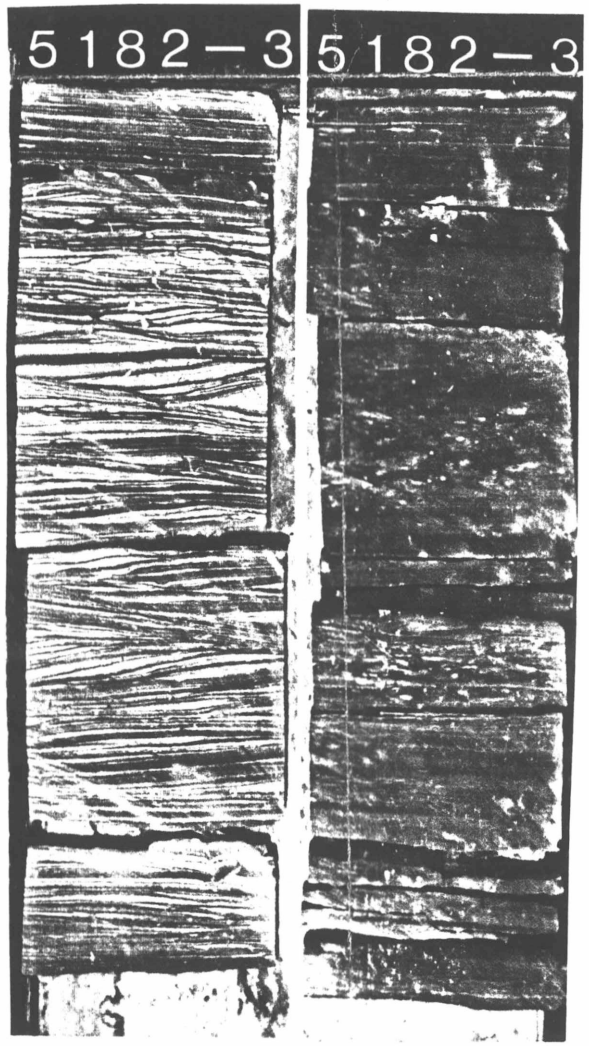
1531 m.



1541 m.



1560 m.

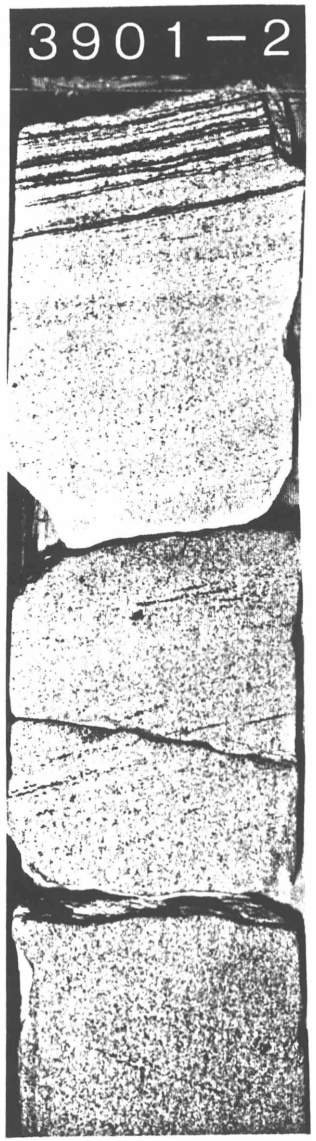


1580 m.

Well Name – Pulai-1
Unit – Upper Pulai Sandstones
Depth – 1152 m.; 1158.5 m.; 1212.5 m. and 1216 m..



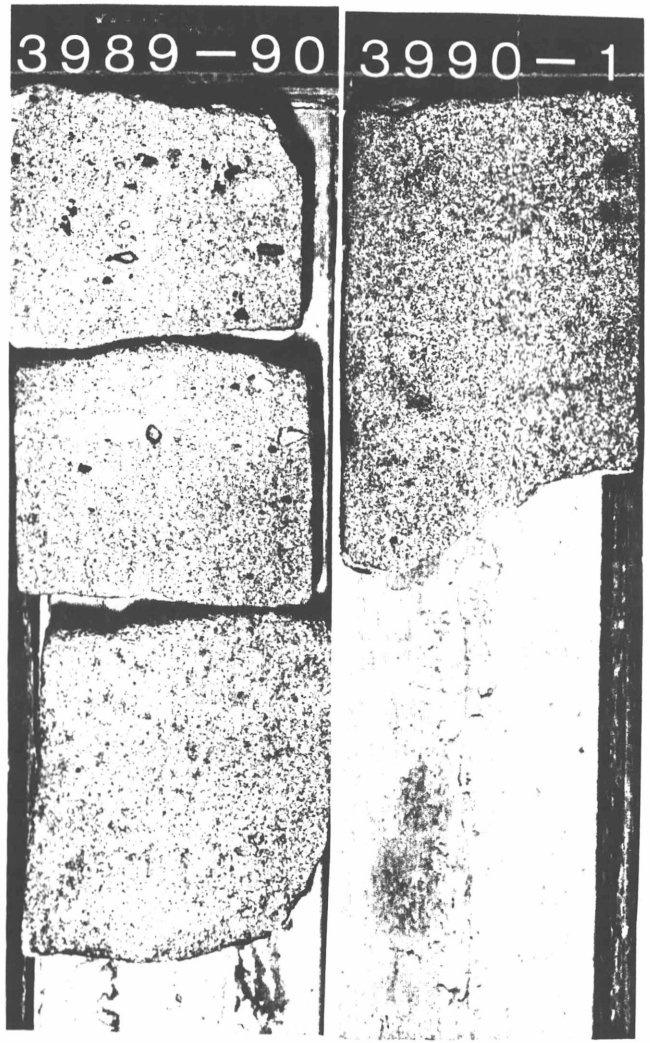
1152 m.



1158.5 m.



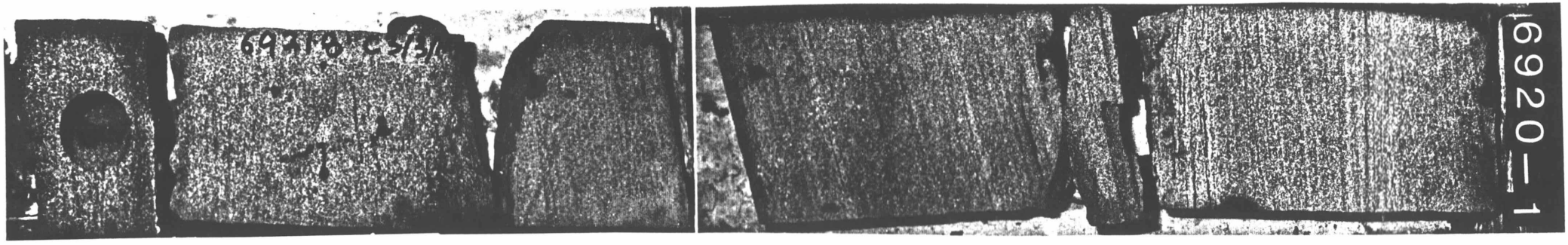
1212.5 m

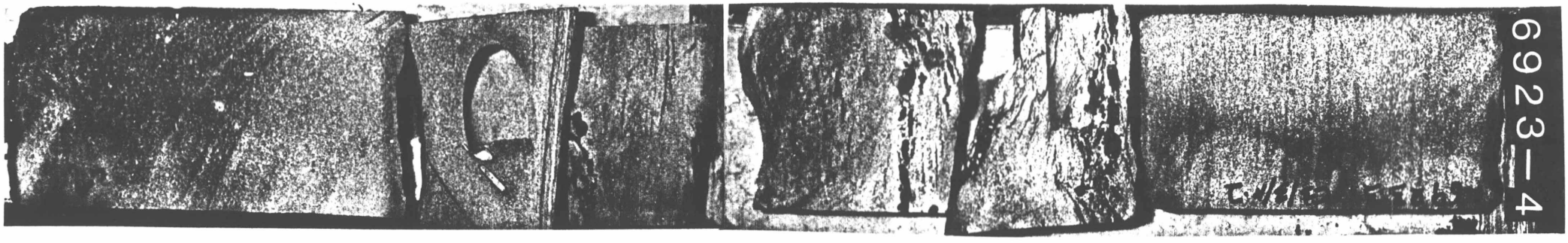


1216 m.

CORE PHOTOGRAPHS - Reference Page in Text ... 129

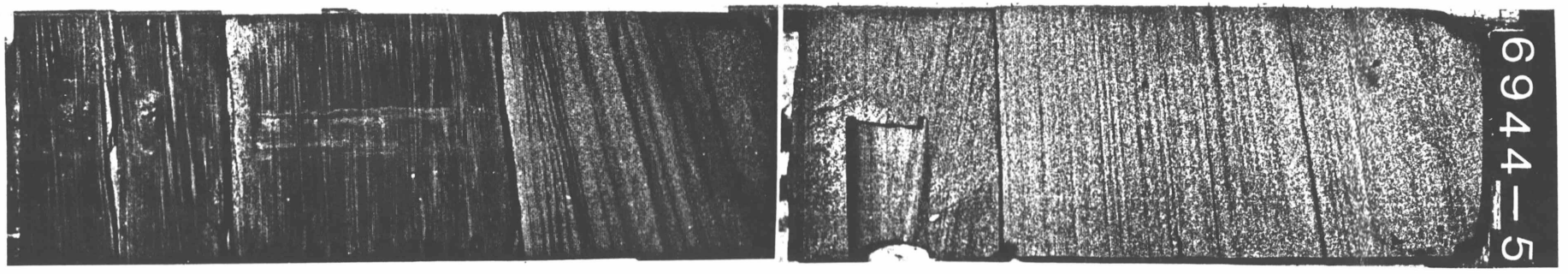
Well Name - Besar-1
Unit - Upper Pulai Sandstones
Depth - 2109.7 m.; 2117 m. and 2126.5 m.



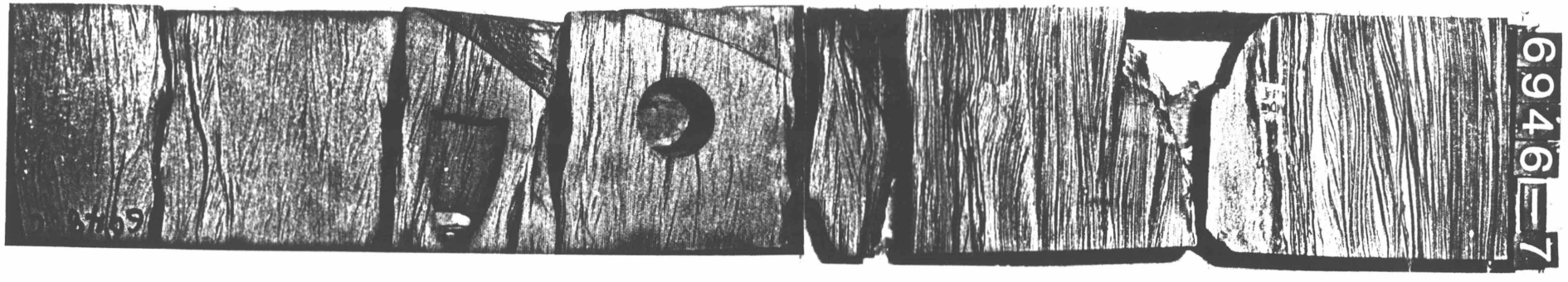


2109.7 m.

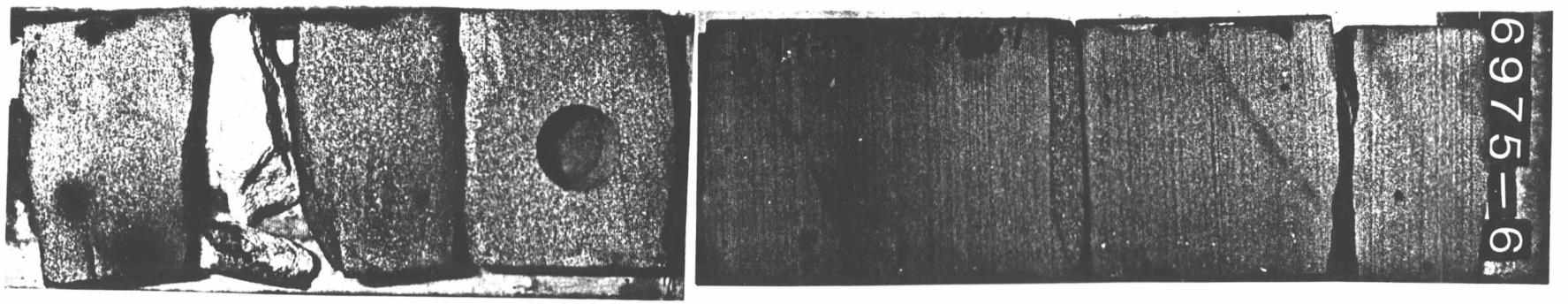
Well Name – Besar-1
Unit – Upper Fulai Sandstones
Depth – 2109.7 m.; 2117 m. and 2126.5 m.



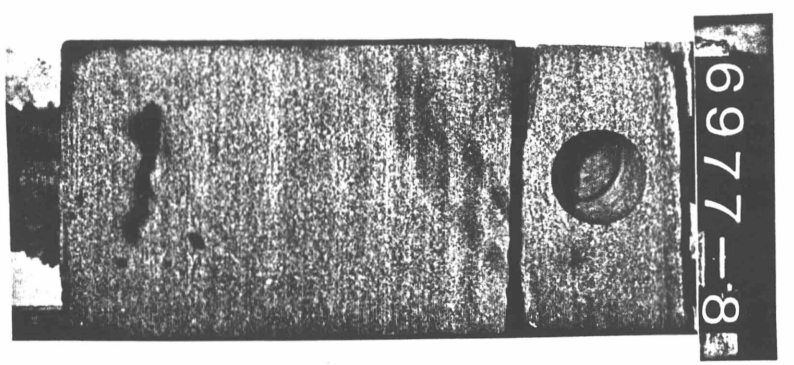
2117 m.



Well Name - Besar-1
Unit - Upper Pulai Sandstones
Depth - 2109.7 m.; 2117 m. and 2126.5 m.

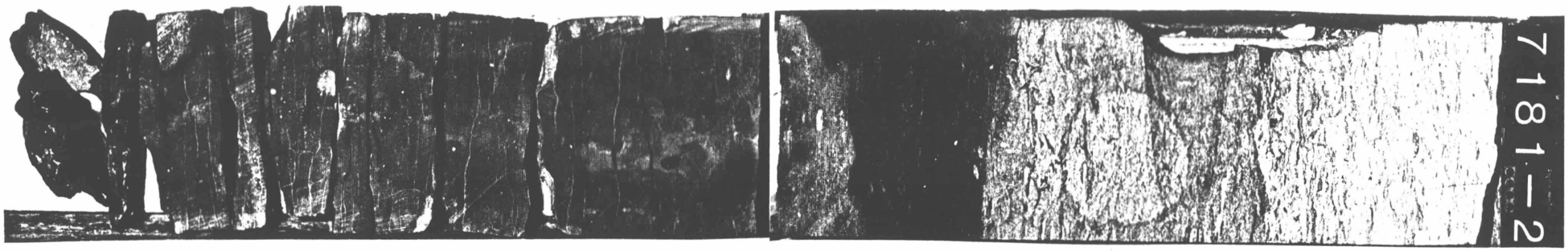


2126.5 m.



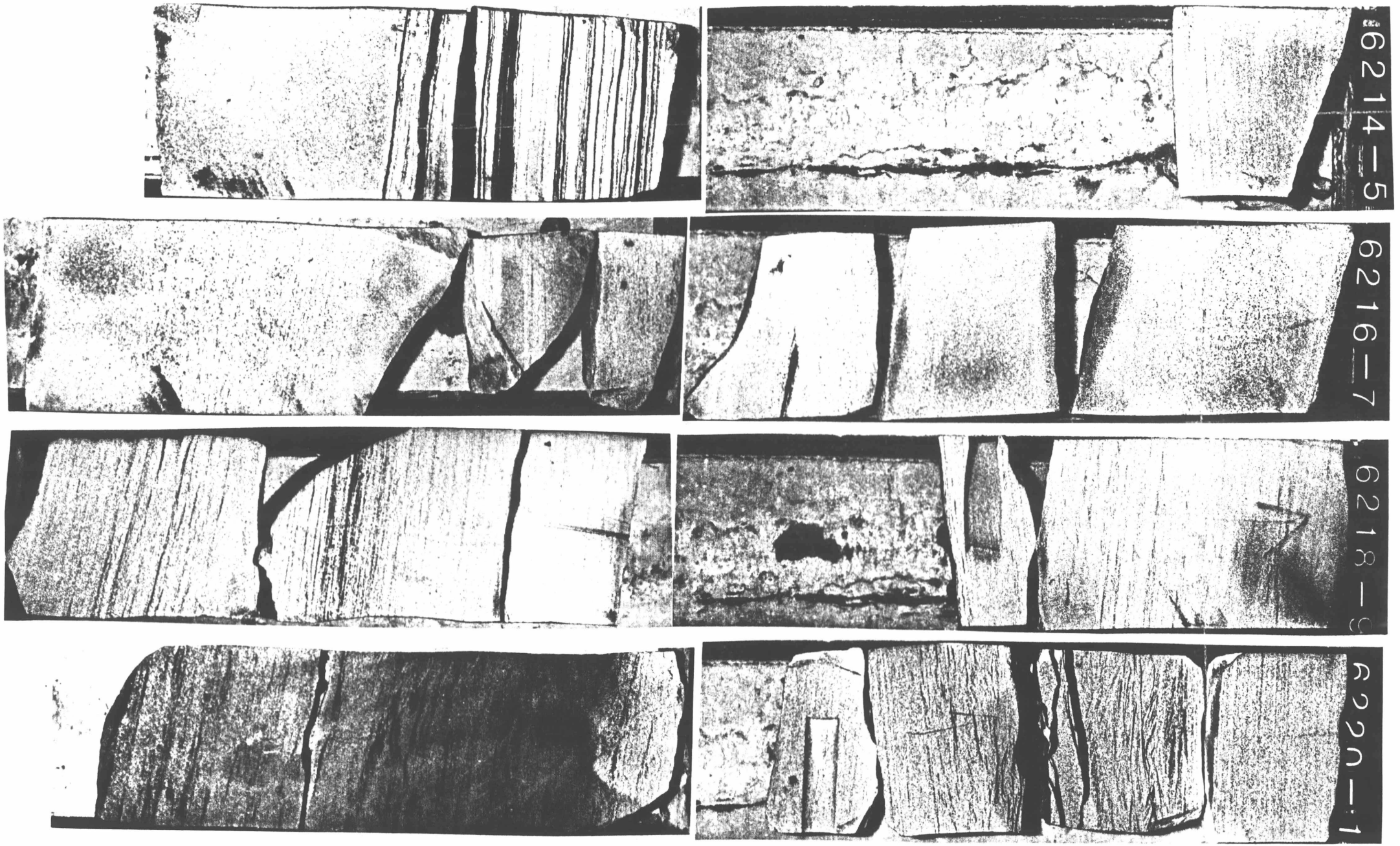
Well Name - Sotong 56-5.1
Unit - Upper Pulai Sandstones
Depth - 2189 m.





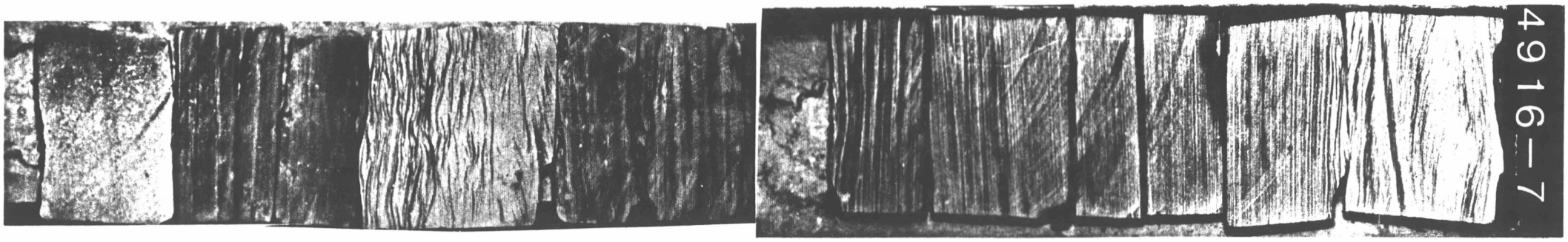
CORE PHOTOGRAPHS - Reference Page in Text ... 138

Well Name - Bekok-1
Unit - Lower Terengganu Shales
Depth - 1894.5 m. - 1896.6 m.



CORE PHOTOGRAPHS - Reference Page in Text ... 140

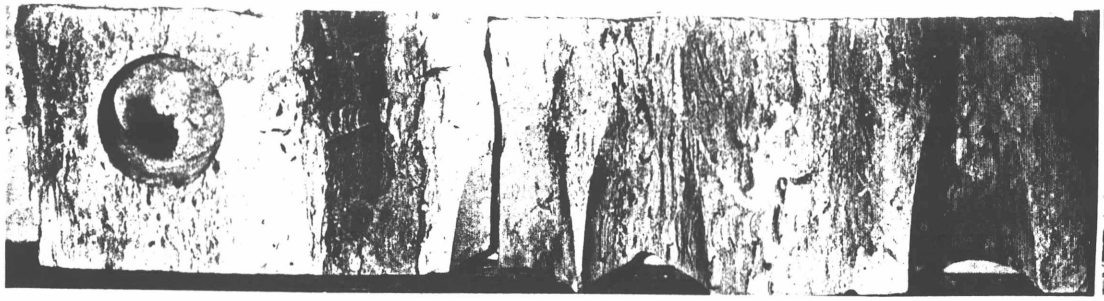
Well Name - Seligi-3
Unit - Lower Terengganu Shales
Depth - 1498.8 m.

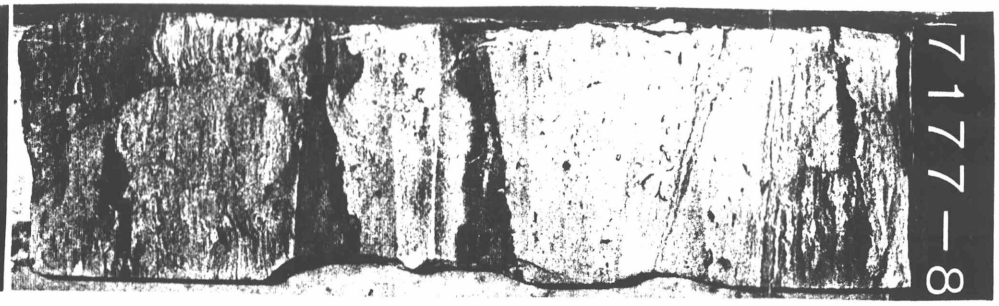


Well Name - Sotong 56-5.1
Unit - Lower Terengganu Shales
Depth - 2186. 2 m. and 2188.1 m..









CORE PHOTOGRAPH - Reference Page in Text ... 140

Well Name - Tinggi-1
Unit - Lower Terengganu Shales
Depth - 1599.5 m.

